Toward Catalytic Antibodies Capable of Ergopeptine Hydrolysis

A thesis submitted
in partial fulfilment of the
requirements for the Degree
of
Doctor of Philosophy in Chemistry
at the
University of Waikato

by

Mark Humphrey Dines

University of Waikato
1998

Errata

The thesis is known to contain the following errors.

p. 3, section 1.2.2, line 1	"has the goal" should read "have the goal"
p. 19, Fig 1.9	"apon" should read "upon"
p. 26, section 1.3.3.2, line 16	"claisen" should read "Claisen"
p. 26, footnote	"claisen" should read "Claisen" and "positionaed" should read "positioned"; it should also be noted that a Claisen rearrangement does not necessarily involve an aromatic substrate
p. 28, line 10	"oxy-cope" should read "oxy-Cope"
p. 31, line 2	"peforms" should read "performs"
p. 34, line 4	"Baldwins rules" should read "Baldwin's rules"
p. 40, Fig 1.26	"Amonium cation" should read "Ammonium cation"
p. 41, line 7	"tetrahedral state" should read "tetrahedral transition state"
p. 41, line 14	"terahedral" should read "tetrahedral"
p. 45, line 7	"possess" should read "possesses"
p. 55, line 15	"synergestic" should read "synergistic"
p. 65, line 22	"reasonably" should read "reasonable"
p. 69, line 17	"of" should read "or"
p. 70, line 7	"preparatory" should read "preparative"
p. 84, section 2.2.2.5, line 17	"benzaldehye" should read "benzaldehyde"
p. 85, footnote	"alchol" should read "alcohol"
p. 104, lines 1 and 2	"Chemical shifts" should read "^{1}H NMR chemical shifts"
p. 112, compound **4**	"separated using preparatory silica plates (PLC)" should read "separated using preparatory silica plates (PLC) (CH_3OH–CH_2Cl_2, 1:24)"
p. 139, compound **33**	"was separated using flash chromatography" should read "was separated using flash chromatography (CH_3OH–Ethyl acetate, 5:95)
p. 141, compound **35**	"Riedel de Hann" should read "Riedel-de-Haën"
p. 166, line 5	"obtainded" should read "obtained"
p. 170, line 1	"aliqoted" should read "aliquoted"
p. 190, line 6	"lacrymation" should read "lachrymation"

ABSTRACT

Animals grazing endophyte infected pasture are exposed to the toxic effects of ergopeptine compounds which are produced by the grass–endophyte interaction. Grasses containing endophytic fungi have a competitive advantage and comprise over 60% of pastureland. Catalytic antibody vaccines would permit the use of endophyte-infected grasses without the risk of animal toxicoses. The production of catalytic antibodies capable of hydrolysing ergopeptine toxins was investigated. The literature pertaining to catalytic antibodies is reviewed with particular focus on hydrolytic reactions. Model systems were used to investigate the potential of this technique.

Model phosphorus–ester and –amide compounds were synthesised and characterised. Problems were experienced forming the $RPO(OCH_2CH_3)X$ where X is $NH(C_6H_4NO_2)$, and R is a protected benzyl system, successful generation of model compounds where X is $NHCH_2(C_6H_5)$ and $O(C_6H_4NO_2)$ was achieved. The compound $HOOCCH_2CH_2CONH(C_6H_4)CH_2PO(OH)O(C_6H_4NO_2)$ was synthesised as a transition–state emulator for the generation of polyclonal antibodies capable of hydrolysing $(C_6H_5)CH_2COO(C_6H_4NO_2)$ and $(C_6H_5)CH_2CONH(C_6H_4NO_2)$. The transition–state emulator was conjugated to Bovine Serum Albumin, Thyroglobulin and Keyhole Limpet Haemocyanin. Sheep, mice and a rabbit were immunised with the resulting conjugate material.

The immune rabbit serum was found to rapidly hydrolyse ester ($(C_6H_5)CH_2COO(C_6H_4NO_2)$) relative to the non–immune serum, however, purification of the immune rabbit antibodies indicated that the hydrolysis of ester ($(C_6H_5)CH_2COO(C_6H_4NO_2)$) was not due to antibody catalysis. The non–purified sera from the immune sheep and mice was found to hydrolyse ester ($(C_6H_5)CH_2COO(C_6H_4NO_2)$) at a similar rate to the non–immune sera and no immune sera was found to hydrolyse amide ($(C_6H_5)CH_2CONH(C_6H_4NO_2)$). Investigation of sera from

immunised animals by ELISA indicated production of polyclonal antibodies capable of binding the $HOOCCH_2CH_2CONH(C_6H_4)CH_2PO(OH)O(C_6H_4NO_2)$ material conjugated to protein. This protein was different to that used as immunogen. However, the non–conjugated $HOOCCH_2CH_2CONH(C_6H_4)CH_2PO(OH)O(C_6H_4NO_2)$ material did not competitively inhibit polyclonal antibody binding to the protein conjugates, suggesting that the polyclonal antibodies generated required the presence of a conjugated protein environment for binding.

An investigation of the ergot alkaloids produced by one grass–endophyte association (*Acnatherum inebrians*) known to contain high levels of ergot alkaloid was conducted. Extraction methodology and reverse phase HPLC separation systems were developed for these compounds. Use of these methods enabled the purification of *iso*–lysergic acid amide and ergonovinine from *Acnatherum inebrians*. These compounds were characterised using NMR.

This thesis details the generation of a model transition–state compound and subsequent immunisation of this compound into animals. Antibodies from the immune animals were not found to catalyse the hydrolysis of amide or ester bonds. This work and the work of others suggests that a better understanding of the emulation of the amide transition–state is required before detoxification of ergopeptines by amide hydrolysising antibodies will be achieved.

ACKNOWLEDGMENTS

Special thanks must go to Neale Towers and the staff at the Toxinology and Food Safety Research Group AgResearch for not only making this work possible, but also highly enjoyable. Thanks to: Ian, Jude and Kath for all the time and help with the immunochemistry; Chris, Rich and Allan for help with the chemistry; and a special thanks to Linda and Sarah for the proof reading.

Thanks to the University of Waikato for the support and scholarship funding required for undertaking this project. My supervisors Chris, Ian and Rick are thanked for the continued support and patience, while I thank Bill for taking up some 'supervisory reigns' and pointing out that an *" 'assignation' is an illicit love affair (according to the dictionary)"*, and simply not politically correct for describing NMR assignments. Thanks to Ralph and Alastair for all the help with the NMR. Alastair must also be mentioned for his 'surrogate' supervisory role. Thanks to Jannine and Wendy for their help with the mass spectrometry.

Thanks to my family and all my friends for helping me see this thing through. A special thanks to Dave and Mum for the quiet support which I knew, although unspoken, was always there. To my 'labbies' - Stef, Karen (and lately Blair) - thanks for enjoying the 'fun,' that is chemistry, with me. Thanks must also go to Sha for all the help (particularly with the references) and support. Now maybe we can get on and do some of those things we've been dreaming of.

TABLE OF CONTENTS

TABLE OF FIGURES

LIST OF TABLES

Chapter 4

LIST OF ABBREVIATIONS

Å	angstrom
ab	antibody
Amino acids	standard three letter code is used
AnalAR	analytical reagent grade
APC	antigen presenting cell
Ar	aromatic system
B cell	B lymphocyte cell
bp	boiling point
BSA	bovine serum albumin
BuBr	butyl bromide
cal	calories
calc	calculated
CD_3OD	deuterated methanol
CDR	antibody complimentary determining region
C_H	antibody heavy chain constant region
C_HX	antibody heavy chain constant region domain x
C_L	antibody light chain constant region
COSY	correlated spectroscopy, shows ^1H-^1H coupling within a spin system
δ	chemical shift in parts per million
d	doublet
d_6–DMSO	deuterated dimethyl sulfoxide
Da	daltons
dd	doublet of doublets
DEP	diethyl phosphite
DEPT	distortionless enhancement by polarisation transfer

ΔG°_{ES}	change in Gibbs free energy upon enzyme and substrate binding
ΔG°_{TS}	difference in Gibbs free energy between enzyme and uncatalysed reaction
$\Delta G^{\ddagger}_{cat}$	change in Gibbs free energy for the enzyme catalysed reaction
$\Delta G^{\ddagger}_{uncat}$	change in Gibbs free energy for the uncatalysed reaction
DHG	drunken horse grass (assume endophyte infected)
$\Delta H^{\ddagger}$	enthalpy of activation
DMSO	dimethyl sulfoxide
$\Delta S^{\ddagger}$	entropy of activation
E	enzyme
ELISA	enzyme linked immunosorbant assay
ESI–MS	electrospray ionisation–mass spectrometry
Et_2O	diethyl ether
Et_3N	triethyl amine
EtOH	ethanol
Fab	the antibody binding region consisting of both heavy and light chains
Fc	antibody crystallising fragment
FCA	Freunds complete adjuvant
Fd	antigen binding portion of the heavy chain
FIA	Freunds incomplete adjuvant
GC–MS	gas chromatography–mass spectrometry
GoF	goodness of fit
H	antibody heavy chain
HAT	hypoxanthine aminopterin and thymine medium
HGPRT	hypoxanthine-guanosine phophoribosyl transferase enzyme
HMBC	heteronuclear multiple bond correlation
HSQC	heteronuclear single quantum correlation

Hz	hertz
I_{20}	antibody concentration required for 20% of the maximal ELISA absorbance
I_{50}	antibody concentration required for half the maximal ELISA absorbance
I_{80}	antibody concentration required for 80%of the maximal ELISA absorbance
IEF	isoelectric focussing
IEP	isoelectric point
IgX	immunoglobulin X
in vitro	in artificial conditions (out of animal)
in vivo	within an organism
IM	intramuscular
IP	intraperitoneal
IV	intravenous
J	coupling constant
κ	antibody light chain class
K	binding constant
K	degrees kelvin
k_{cat}	rate constant in the presence of enzyme (or catalytic antibody)
KDa	kilodalton
κ_e	transmission coefficient for the catalysed reaction
K_I	the dissociation constant for enzyme– (or catalytic antibody–) inhibitor complex
KLH	keyhole limpet haemocyanin
K_M	the Michaelis constant which is the dissociation constant for enzyme– (or catalytic antibody–) substrate complex
k_n	rate constant for the uncatalysed reaction
κ_n	transmission coefficient for the uncatalysed reaction

$KOBu^t$	potassium tert–butoxide
K_S	the dissociation constant for enzyme– (or catalytic antibody–) substrate complex
K_T	transition–state dissociation constant
K_{TS}	the dissociation constant for enzyme (or catalytic antibody) transition–state complex
k_{uncat}	rate constant in the absence of enzyme (or catalytic antibody)
λ	antibody light chain class
L	antibody light chain
l	litre
$LiAlH_4$	lithium aluminium hydride
M	moles per litre
m	multiplet
m/z	mass to charge ratio
MHC II	major histocompatibillity complex II protein
MHz	megahertz
MilliQ	the Milli Q system produces ultra pure water of reagent grade (better than 10 mega ohm resistivity).
min	minutes
mol	mole
mp	melting point
MWCO	molecular weight cutoff
$NaOBu^t$	sodium tert–butoxide
NIS	non–immune sera
NOE	nuclear Overhauser effect
NMR	nuclear magnetic resononance
OVA	ovalbumin
P	product
π	pi bond

p	para substituted aromatic
PBS	phosphate buffered saline
PBS-T	phosphate buffered saline and tween–20
Pd/C	palladium upon carbon catalyst
Ph_3P	triphenyl phosphine
PLC	preparative thin layer chromatography
R_f	the Retardance factor which is distance travelled by compound/ distance travelled by solvent front
RP	reverse phase C_{18}
RP HPLC	reverse phase high performance liquid chromatography
R_T	retention time
RT	room temperature
S	substrate
s	second
s	singlet
sb	singlet broad
SC	subcutaneous
scFv	single chain antigen–binding fragment
SDS PAGE	sodium dodecyl sulfate polyacrylamide gel electrophoresis
LSIM	liquid secondary ion mass spectrometry
t	triplet
T cells	T lymphocyte cells
TEP	triethyl phosphite
TFAA	trifuoroacetic anhydride
THF	tetrahydrofuran
Thiomersal	ethyl (2-mercaptobezoato-S) mercury sodium salt, an antifungal agent
THY	thyroglobulin
TLC	thin layer chromatography

TMB	(3, 3', 5, 5'–tetramethylbenzidine)
UF	ultrafiltration
v_e	frequency of normal oscillation of transition–state complex for the catalysed reaction
V_H	antibody heavy chain variable region
VIP	vaso intestinal peptide
V_L	antibody light chain variable region
v_n	frequency of normal oscillation of transition–state complex for the uncatalysed reaction
ZEN	zearalenone

'we may be subject to hallucinogenic ergotism: aural-visual hallucination, dangerous and unlikely behaviour'

Dana Scully
X-Files

CHAPTER ONE

THE CONCEPT OF A TRANSITION–STATE VACCINE

1.1 INTRODUCTION

This chapter introduces the reasoning behind the concept of a catalytic antibody vaccine capable of ergopeptine hydrolysis. The chapter starts with a brief summary of the immune system paying particular attention to the antibody molecule. The concept of antibody catalysis is presented and the literature reviewed. The historical and current relationship between mankind and the grass–endophyte is discussed, with particular focus on the ergot alkaloid compounds. The ergopeptine compounds (a subgroup of the ergot alkaloids) adverse effect on livestock is discussed, as is the possibility of alleviating these effects by generation of a catalytic antibody vaccine capable of ergopeptine hydrolysis.

1.2 THE IMMUNE SYSTEM

1.2.1 HISTORY

Thucydides noted some 2500 years ago that victims of a plague who recovered could tend the sick of the same plague without themselves catching the disease again. That is to say those who recovered were immune. Many years later, in 1798, Jenner recorded how inoculation with cowpox (vaccina) led to immunity to cowpox and thus the term vaccination. Behring and Kitasato in 1890 noted that immunity (Latin *immunitas*, freedom from) to tetanus toxin was due to the appearance of a 'factor' in the serum that neutralised the toxin. This anti-toxin activity could be transferred to normal animals when serum from immune animals was injected. The body could thus respond to infectious or injurious agents by producing serum components which combined in some way and neutralised the

effects of the agents. The term antibody as used to describe the serum components while the provoking agents were called antigens (Steward, 1984).

In the 1930's, Landsteiner developed the ability to couple simple aryl systems to proteins and made use of this ability to investigate the specificity of the immune system (in Lerner *et al.*, 1990). Ehrlich was responsible for the concept of the receptor which he defined as *'the combining group of the protoplasmic molecules to which a foreign group or molecule, when introduced into the cell, attaches itself'* (in Lerner *et al.*, 1990) Ehrlich also proposed the 'side chain theory' which proposed that white blood cell surfaces bore receptors with side chains to which foreign substances became chemically linked. This caused the cell to produce the bound receptor in great excess. The surplus receptors (antibodies) were shed into the blood. Ehrlich simply assumed (correctly) that the cells naturally made side chains capable of binding all foreign substances (Ada *et al.*, 1987). With the passing of years much more has been learned about antibodies.

1.2.2 MODERN VIEW OF THE VERTEBRATE IMMUNE SYSTEM

The immune systems of vertebrates has the goal of distinguishing between self and non–self and removing these foreign particles. The system constantly scans huge numbers of molecules, identifies the foreign agents and initiates their destruction. Hallmarks of the immune system are its specificity, adaptability and memory. To achieve these objectives, the immune system uses two different systems, the cellular and humoral systems. The cellular immune response is a defence system designed to destroy microorganisms that exist inside host cells (eg viruses). This response produces T lymphocyte cells that detect foreign motifs on cell surfaces and destroy the infected cell (Roitt, 1988). In addition the cellular immune response stimulates the humoral response (Stryer, 1988).

The humoral immune system is the recognition system which consists of a large array of B lymphocytes (B cells) each bearing different antibodies that have their own individual recognition sites (Roitt, 1988). Antigens (foreign macromolecules capable of eliciting an

immune response) will only bind to receptors with which they make a 'good fit'. Lymphocytes with a bound antigen then become antibody–forming plasma cells and produce soluble proteins called antibodies (Roitt, 1988).

Each antibody (or immunoglobulin) has specific affinity for the foreign agent that stimulated its synthesis. An antibody's specific affinity is not for an antigen but rather for a specific site on the antigen called the antigenic determinant (or epitope). Small foreign molecules generally do not stimulate antibody formation. However, if conjugated to a macromolecule they can elicit a specific antibody. In this case the small molecule is termed a hapten. Antibodies thus generated will often bind the unattached hapten as well as the conjugate molecule (Stryer, 1988).

1.2.2.1 THE DILEMMA OF ANTIBODY DIVERSITY

In 1940, Pauling proposed the instructive theory which stated that the antigen was template–like, and directed the folding of the protein chain of the antibody (Pauling, 1940). Thus, an antibody of a given amino acid sequence would possess the potential for forming combining sites of differing specificities. The particular site generated would depend on the antigen present at the time of folding. In contrast, the clonal selection theory (or selective theory) was developed by Macfarlane Burnett *et al.* in the late 1940's and early 50's. This theory postulated that the combining site of an antibody is completely determined prior to encountering an antigen (Ada *et al.*, 1987). Evidence grew to discount the instructive theory and support the selective theory. For example, it was found that the unfolding of an antibody followed by refolding without antigen still resulted in an antibody which bound the antigen. In addition, antibody–producing cells synthesised large amounts of specific antibody in the absence of corresponding antigen (Stryer, 1988).

1.2.2.2 THE CLONAL SELECTION THEORY

The clonal selection theory is now widely accepted and provides a unifying view of the immune response (Ada *et al.*, 1987). The premises of the theory are outlined below:

- each antibody producing cell constructs antibody of a single kind;
- the amino acid sequence of an antibody is dependent on its DNA. It is the amino acid sequence that determines specificity;
- maturing antibody cells produce small amounts of specific antibody which are displayed on the cell surface. These immature cells are killed early in development if the displayed antibody corresponds to an antigen of 'self'. Thus animals do not usually produce antibodies to their own macromolecules. This is termed self tolerance. In contrast, mature cells are stimulated by encountering antigen. This triggers high levels of clonal antibody production and cell division. The antibodies produced have identical genetic makeup and therefore produce antibodies with the same specificity;
- a subgroup of the clones produced (the 'memory' cells) persist even after disappearance of the antigen, resulting in 'immunological memory' which provides a rapid response to reinfection.

1.2.2.3 THE BASICS OF ANTIBODY STRUCTURE

Initial investigation of antibody structure used 7S rabbit antibodies and the proteolytic enzyme papain. Following separation of the resulting three fragments, it was found that one fragment crystallised (Fc). The other two fragments were identical and unlike Fc were capable of combining with the antigen; these were termed fragment antibody binding (Fab) (Porter, 1959). Nisonoff, again using 7S rabbit antibodies, showed that treatment with pepsin elicited a bivalent antibody fragment which, when reduced, yielded two monovalent fragments (Nisonoff, 1960). Porter showed that reduction of an antibody and dissociation of non-covalent bonds in acidic gel conditions yielded constituent chains with molecular weights of about 20,000 and 50,000 Da (Fleischman *et al.*, 1963) These observations along with other detailed studies (Pain, 1963), (Crumpton *et al.*, 1963) were the basis for Porter

to propose a four polypeptide chain structure for immunoglobulin G (IgG) (Fleischman *et al.*, 1963) (Fig. 1.1). The work of Porter and Edelman resulted in their sharing of the Nobel prize for medicine in 1972 (Porter, 1973; Edelman, 1973).

The Fab region can swing out to an angle of 100° about the hinge region. It is this region that accounts for the enzyme sensitivity with the flexibility due to a large number of proline residues and accounts for the ability of antibodies to potentially bind two sites on a single antigen or link two antigenic particles (Steward, 1984).

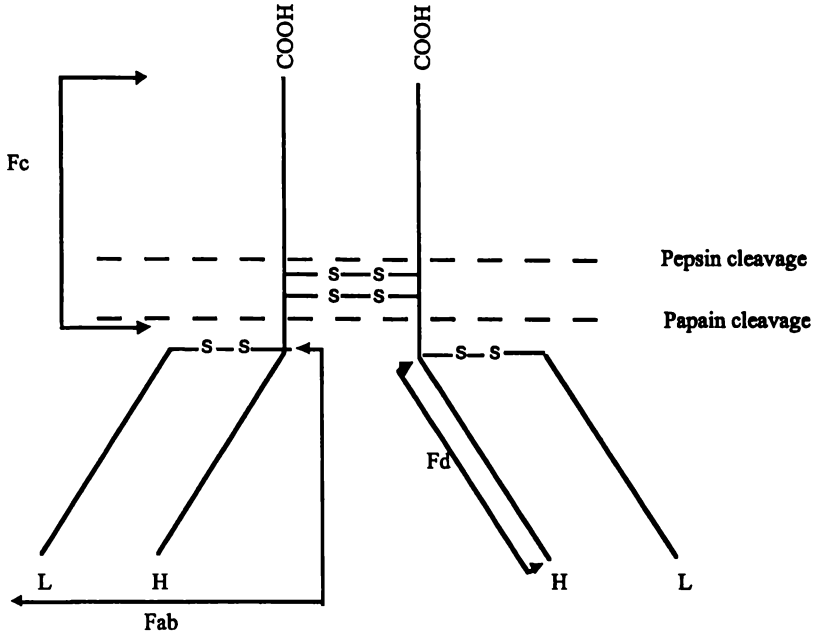

Figure 1. 1. The four chain structure for rabbit IgG as proposed by Porter, where H and L are the heavy and light chains respectively and Fd is the antigen binding portion of the heavy chain. Fab is the antibody binding region made up of both heavy and light chains and Fc is the fragment that crystallises following hydrolysis by papain (Porter, 1973).

The Different Classes of Immunoglobulin.

This four chain antibody 'Y' structure is found in all vertebrates from fish to mammals, and is the basis for all five of the immunoglobulin classes. The light chains are similar within each class, while the heavy chains are specific, and thus the distinguishing feature (Table 1.1). The five classes are IgG, IgM, IgA, IgD and IgE, and heavy chains associated with

each class are called gamma (γ), mu (μ), alpha (α), delta (δ), and epsilon (ε) respectively. Differences within the heavy chain polypeptide sequence (found in the Fc fragment) enable different types of reaction to occur at different stages of the immune response and maturation. Each immunoglobulin class has a specific role to play. The two classes of light chain (kappa (κ) and lambda (λ)) are found in all five classes of heavy chain (Kimball 1986; Harlow *et al.*, 1988; Stryer, 1988).

Table 1. 1 Properties of immunoglobulin classes (Stryer, 1988; Harlow *et al.*, 1988).

Class	Serum concentration (mg ml^{-1})	Mass (kD)	Light chains	Heavy chains	Chain structure	Structure
IgG	12	150	κ or λ	γ	$\kappa_2\gamma_2$ or $\lambda_2\gamma_2$	
IgA	3	180-500	κ or λ	α	$(\kappa_2\alpha_2)_n$ or $(\lambda_2\alpha_2)_n$	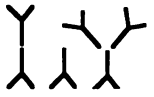
IgM	1	950	κ or λ	μ	$(\kappa_2\mu_2)_5$ or $(\lambda_2\mu_2)_5$	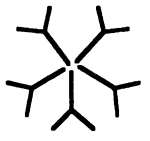
IgD	0.1	175	κ or λ	δ	$\kappa_2\delta_2$ or $\lambda_2\delta_2$	
IgE	0.001	200	κ or λ	ε	$\kappa_2\varepsilon_2$ or $\lambda_2\varepsilon_2$	

Note: n = 1, 2, or 3. IgM and oligomers of IgA also contain J chains that join immunoglobulin molecules. IgA in secretion has an additional secretory portion.

All immunoglobulins are glycoproteins with the different classes possessing a different percentage of carbohydrate. The carbohydrate is thought to facilitate secretion from the antibody–synthesising plasma cell, enhance solubility and protect from degradation (Stryer, 1988).

Domains

X-ray crystallographic studies have provided support for the domain hypothesis (Fig 1.2). The three–dimensional structure of the Fab fragment of a human immunoglobulin has been solved at 2.8 Å by Poljak *et al.* (1975). The fragment is a tetrahedral array of four globular subunits (domains): the variable light chain (V_L), variable heavy chain (V_H), constant light chain (C_L) and constant heavy chain domain 1 (C_H1). These domains are highly similar in three–dimensional structure (Poljak *et al.*, 1975).

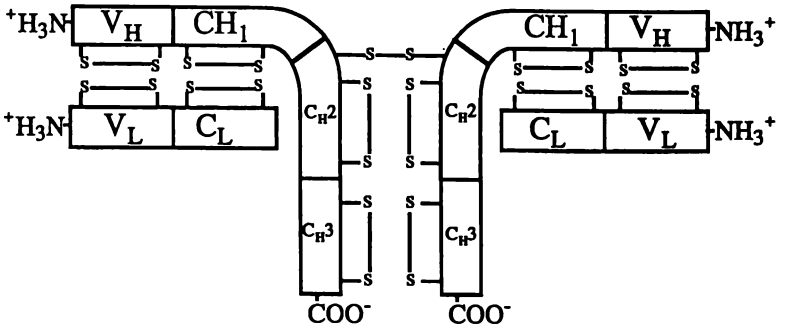

Figure 1. 2 The domain structure of an antibody (Edelman, 1973).

The Variable Domains

Variability of the N-terminal regions, in both light (V_L) and heavy (V_H) chains, is not of even distribution. Some amino acid positions remain conserved but others show high degrees of variability and have been termed hypervariable or complementary determining regions (CDR) (Steward, 1984). These hypervariable regions are involved with the antibody's ability to bind antigens.

The heavy chain was found to contain four regions of particularly high amino acid variability while the light chain contained three such regions. Kabat proposed that it was these hypervariable segments that formed the antigen binding site and therefore that antibody specificity was determined by the amino acids of the antibody (Wu *et al.*, 1970).

The Constant Domains

The constant and variable regions are sharply demarcated in both heavy and light chains. The constant regions are highly important as it is these regions that mediate common effector functions, these regions are involved in the binding of complement which is essential for the cascade reactions of the immune system. This binding enables functions like antibody crossing of the placental membrane and destruction or lysis of foreign microorganisms.

The Antigen Binding Site

The Fab fragment of an antibody contains the antigen binding site (Fig. 1.3). In IgG these fragments are associated such that C_L associates with C_H1 while V_L associates with V_H in a tight and extensive manner. In contrast, the segments joining V_L to C_L and V_H to C_H have little contact. As a result the Fab fragment consists of two globular regions, one containing the two constant domains, the other comprising the two variable domains (Branden *et al.*, 1991). The six CDR loops are quite different (Fig. 1.4), in both shape and size, and they can form flat extended surfaces for protein binding or deep binding clefts for smaller hapten molecules (Novotny, 1983).

The hapten phosphorylcholine has been used to investigate the immune response. The antibody binding cleft of the phosphorylcholine is about 15Å wide at the mouth and 12Å deep (Fig. 1.5). The cleft is lined by residues from all CDR loops with the exception of CDR2 of the light chain. Side chain amino acid residues bind phosphorylcholine in a manner reminiscent of substrate or inhibitor binding by an enzyme (Capra *et al.*, 1977).

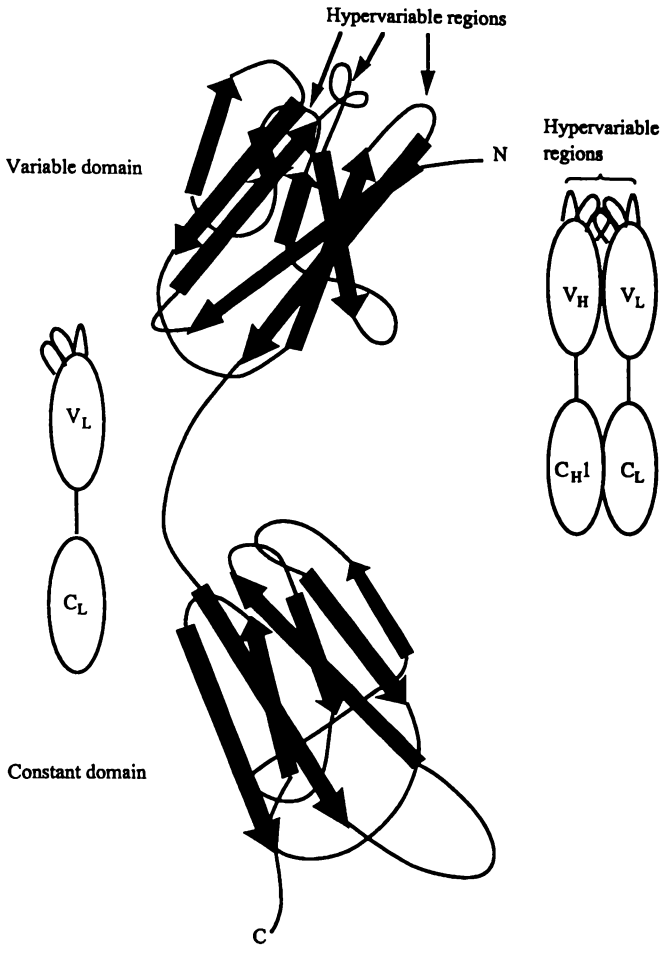

Figure 1. 3 The heavy and light chains of immunoglobulins exist as globular units, which combine to form the antigen binding site. The antigen binding site is formed from the overlap of variable domain light and heavy chain hypervariable regions. The domains interact in a pairwise manner (V_H and V_L, C_H1 and C_L) generating the antigen–binding site at the end of the barrel (Branden *et al.*, 1991).

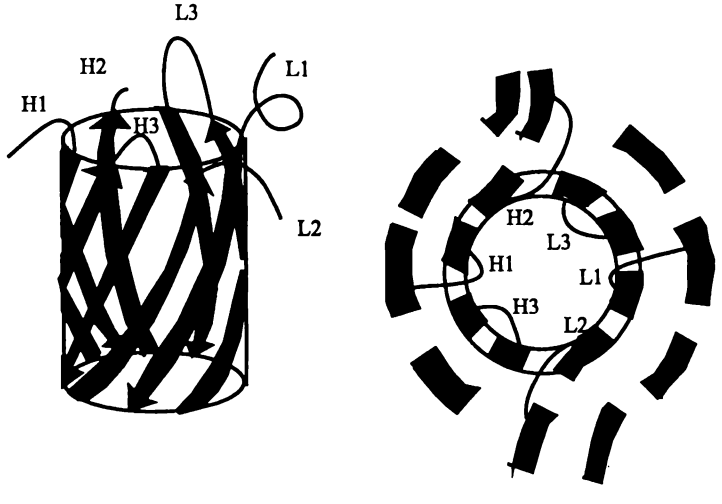

Figure 1. 4 The antibody–combining region consists of a barrel made up of four β-strands from the two variable domains. The CDR of the light chain (L1-L3) and the heavy chain (H1-H3) are situated at the end of the barrel (Novotny, 1983).

For enzyme catalysis, substrates in the reaction transition–state are thought to bind very tightly with appropriate amino acid residues positioned at the active site. The amino acids are positioned in such a way as to maximise contact forces such as hydrogen bonding, nonpolar (or hydrophobic forces), ionic (or coulombic) forces, van der Waals forces, and steric repulsive forces (Stryer, 1988). In fact it was this line of reasoning that suggested that it should be possible to create antibodies with enzyme–like activity by using transition–state analogues as haptens. Binding constants for most haptens range from K = 10^{-4} to 10^{-10} M while the standard free energies of binding range from -6 to -15 kcal mol^{-1} (Stryer, 1988). These binding parameters are of similar magnitude to enzyme–substrate interactions. This free energy is the result of a large number of comparatively weak non–covalent interactions, which as a whole result in a strong specific binding for complementary antibody and antigen. The weak non–covalent interactions which result from the goodness of fit between antigen-antibody electron clouds are important for specificity (Stryer, 1988).

The binding of lysozyme by immunoglobulin CDR loops (Fig. 1.6) is unlike that of the hapten-binding cleft seen for phosphorylcholine (Fig. 1.5). The antibody binding interactions of lysozyme occur over a large area with dimensions of ca 20 × 30 Å. The binding surface has small depressions and protuberances which are complimentary between antigen and antibody. All six of the CDRs contribute, with 17 amino acid residues of the antibody combining closely with 16 amino acid residues of the lysozyme molecule. Exchange of some of these residues would cause steric interference of the bonding or packing contacts and would not be tolerated. As an example, the Gln 121 of lysozyme protrudes from the protein surface and fits snugly into a minor indentation between the CDR3 loops of V_L and V_H (Fig 1.6) (Branden *et al.*, 1991).

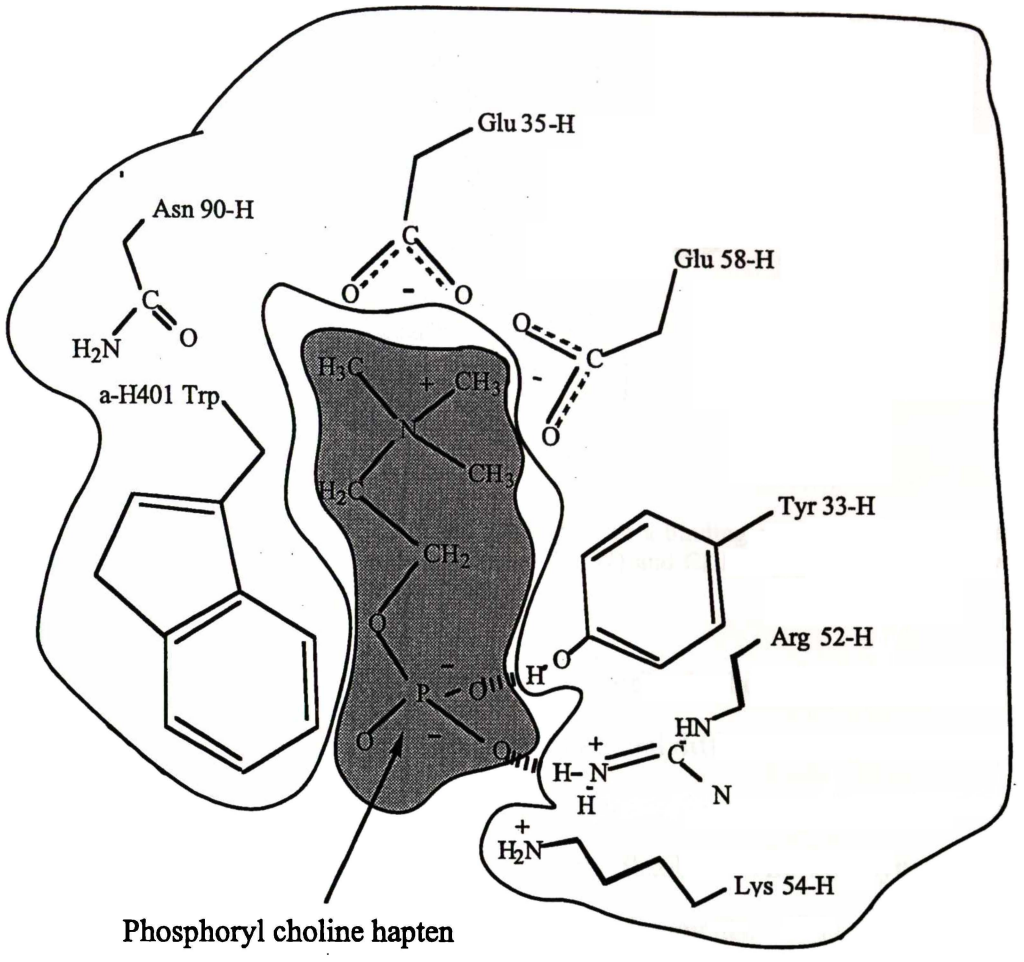

Figure 1. 5 Fab binding of phosphorylcholine (shaded) by protein side chains. The binding cavity consists of a cleft formed between the variable domain of both light and heavy chains (Capra *et al.*, 1977).

While the antibody binding of lysozyme is good, it could be improved by appropriate changes in the CDR loops. It is thought that this sort of adjustment could possibly occur through somatic mutations and would account for the observation that a second immune challenge often gives rise to higher affinity antibodies (Amit *et al.*, 1986).

Of the 17 residues that make contact with lysozyme, two are in the region bordering both the framework and the CDR suggesting that there may not be an absolute distinction between the two. CDR3 of the heavy chain makes up the highest proportion of the central binding region and is responsible for the specific recognition of antigen. Importantly it is the CDR3 of the heavy chain that is the principal focus of somatic mechanisms which are responsible for generating antibody diversity (Branden *et al.*, 1991; Amit *et al.*, 1986).

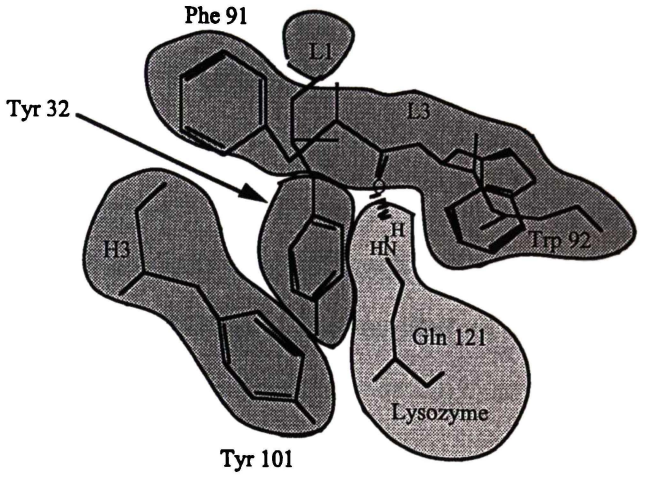

Figure 1. 6 Interaction of lysozyme Gln 121 (light shading) with a binding depression between formed by the CDR3 loops of both heavy (Tyr 101) and light chain (Trp 92) and CDR1 of the light chain (Tyr 32) of an immunoglobulin (dark shading) (Amit *et al.*, 1986).

The three–dimensional structure of lysozyme in the antibody–bound complex is the same as that in crystals of the free lysozyme. No conformational differences are seen, even in the regions that bind to the antigen. While the binding region of lysozyme (termed the antigenic determinant) is solvent exposed, it is not particularly flexible. The lysozyme complexed Fab fragment is very similar in structure to free Fab fragments. This suggests no gross conformation changes occur on antigen binding (Amit *et al.*, 1986), however this is only partly true for another antigen-antibody complex. Antibody–binding of the influenza virus protein (neuraminidase) causes changes in the interaction area between V_H and V_L such that the CDR loops are shifted approximately 3Å relative to other Fab structures. Whether this is due to antibody variability or to changes induced by antigen binding is unknown. In addition, the bound neuraminidase is somewhat distorted in structure and is no longer capable of catalysis (Colman *et al.*, 1987).

As yet, large conformational changes due to antigen–antibody binding have not been found, however, small local structure changes may occur to increase the complementary binding of antibody–antigen interacting surfaces. Generally it would seem that the classical 'lock and key' hypothesis is a reasonable description of antibody–antigen interaction.

1.2.2.4 GENETICS OF ANTIBODY DIVERSITY — AN EXERCISE IN BIOLOGICAL COMBINATORIAL CHEMISTRY

The Immune Repertoire

Animals generate large amounts of specific antibody against almost any foreign determinant within a few weeks of exposure. The number of different antibodies in the primary immunological repertoire has been estimated at between 1.0×10^8 and 1.0×10^{10} (French *et al.*, 1989).

Mice have about 200 genes for the variable region of the κ light chain (Vκ) and approximately the same number for variable region of the heavy chain genes (V_H). The combination of light and heavy chain variable regions gives 1×10^5 (200 x 500) combinations which is far lower than the estimated range available for the primary immune repertoire (Roitt, 1988). How, therefore, does the immune response generate the required level of diversity ?

Generation of Antibody Variable and Constant Regions

Antibody structure is determined by primary amino acid sequence, which is in turn genetically encoded. The large structural variation observed in antibodies is the result of a number of DNA recombination events. Neither the variable nor constant region genes are closely associated in embryonic (germline) DNA (Hozumi *et al.*, 1976). Both heavy and light chain variability are generated by splicing a number of genes in a non–exact manner. The variable region is then spliced next to a constant region (Tonegawa, 1983). At this stage lymphocytes undergo allelic exclusion holding all other variable genes in 'embryonic stasis'. The result is that each lymphocyte can only express one heavy and one light chain (Roitt, 1988). The particular variable and constant regions are then transcribed and translated to construct an antibody with a particular structure.

The process of antibody maturation involves further recombination events in the germ-line DNA. These occur in the heavy chain, constant and variable regions and do not enhance binding. The whole variable region of one class of immunoglobulins (and thus the antigen binding site) is spliced next to the constant region of a heavy chain of another class. This enables the immune response to shift the antigen binding site through the various classes of immunoglobulin and 'fine tune' the administration of binding site for the required challenge (Roitt, 1988).

Once an antigen triggers an immune response it stimulates a somatic mutational mechanism that generates antibodies of higher affinity, enabling a more effective immune response (French *et al.*, 1989). Somatic diversification results from single nucleotide substitutions in the variable regions of the immunoglobulin and can occur in both framework and hypervariable regions (Roitt, 1988).

1.2.2.5 BIOCHEMICAL APPLICATIONS OF THE IMMUNE SYSTEM

Obtaining an Immune Response

To make use of the immune system it is necessary to understand a number of its basic properties. Following engulfment by an antigen–presenting cell (APC), the antigen is partially degraded and displayed on the cell surface of the APC in the cleft of a major histocompatibility complex II protein (MHC II). Some antigen fragments do not bind to the MHC II cleft and therefore no immune response will occur. This problem can be avoided by immunising animals with different alleles at the MHC II loci (ie use a different animal species) or by chemically modifying antigens such that they will bind. The third step involves binding of helper T cells to the MHC II which is presenting the antigen fragments. Each T cell produces a particular binding site formed by a two–chain polypeptide behaving similarly to an antibody. Attempts to immunise against self, or similar to self components are unlikely to succeed, as self–recognising helper T cells are deleted. One solution to this problem is to use another animal species. The binding of a T

cell to an APC sets up a cascade of events resulting in T cell proliferation and differentiation which ceases 14 days after challenge (Harlow *et al.*, 1988).

Concurrently to helper T cells proliferating, similar events lead to production of antigen specific B cells. Antigens are processed by B cells in a manner similar to that of the APC's, the antigen is degraded and presented to the cell surface bound to a MHC II protein. Binding of B cells and T cells is required for antibody production and cell proliferation (the T cells, stimulated by the APC system, will bind to appropriate B cells). For B and T cell binding to occur, an antigen must bind to a B cell surface antibody as it is only those B cells binding antigen that are replicated (the surface bound antigen binding site will be the same as that in the secreted antibody). The processed antigen fragments must bind to the MHC II proteins of the B cells because only this complex is recognised by the T cells (Harlow *et al.*, 1988).

For similar reasons as found in the APC system some compounds fail to elicit an immune response in the T cell system. Small molecules do not elicit an immune response because they are too small to contain determinants necessary to simultaneously bind the MHC II protein and the T cell, even though they will bind to B cells (Harlow *et al.*, 1988).

Binding of T and B cells causes the B cells to undergo exponential division and it is at this stage that some B cells go on to form memory and plasma cells. Plasma cells are short lived cells (3-4 days) which produce large amounts of a specific antibody. In contrast the memory cells retain their cell surface antibody and can circulate for years. It is these cells that give the primed response to subsequent antigen exposure. Other B cells are further differentiated firstly by somatic mutation and class shifting (Harlow *et al.*, 1988).

Once the antibody (mostly IgM) binds antigen, and with no further challenge, the plasma cells die leaving the T cells and the memory cells in circulation (Harlow *et al.*, 1988). It is these memory cells that are responsible for the fast, potent and persistent response that

occurs upon subsequent challenge. In summary a good immunogen should have three chemical features:

- it must possess an epitope that can be recognised by the cell surface of B cells,
- it must have a size (or have an effective molecular weight when conjugated to a carrier) of 3000 Da or larger and,
- it should be degradable

The immune response of a vertebrate to the injection of a large foreign macromolecule is well understood (Fig. 1.7). First, the humoral immune system raises an IgM after a few days. There is a decrease in the amount of IgM concurrent with an increase in IgG after about ten days. Three weeks following re–injection of immunogen, the amount of IgG levels off and it is usual to give the animal a booster shot, which causes a further increase in IgG (Stryer, 1988). This secondary immune response is far more rapid because the circulating memory cells 'remember' the antigen and react accordingly (the basis of immunisation) (Roitt, 1988). The separated polyclonal antisera (ie serum containing antibodies) contains a number of proteins, including IgG, a high proportion of which is antigen–specific (Stryer, 1988; Roitt, 1988).

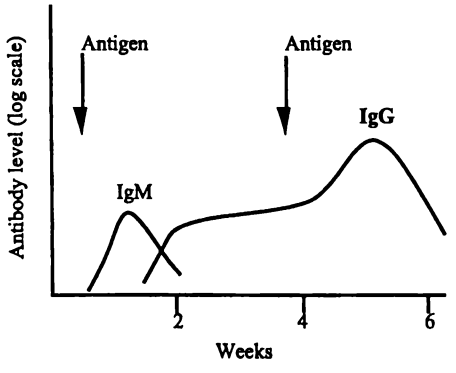

Figure 1. 7 Antibody response to antigen challenge (Stryer, 1988).

Monoclonal Antibodies.

While antibodies produced by a single cell are homogenous, antibodies isolated from sera, including those which have a common specificity, are normally heterogenous as they are the

product of many different antibody–producing cells (polyclonal). For the study and use of antibodies it is highly desirable to have a large number of plasma cells producing a single antibody (Harlow *et al.*, 1988).

In 1975 Milstein and Kohler fused an antibody–producing cell of desired specificity with an immortal cancerous myeloma cell (Milstein, 1980), thereby generating a hybrid cell (or hybridoma) capable of indefinite antibody production. The resulting single cell clones could be isolated and grown in culture to produce a bulk supply of mono–specific antibody.

In this technique, a mouse is immunised against a desired antigen and its spleen removed. The spleen is then disrupted and B cells are isolated. The B cells are fused *in vitro* with myeloma cells using a procedure that involves polyethylene glycol to permit nuclear transfer between cells. The fused cells are selected for, using hypoxanthine, aminopterin, and thymine (HAT) medium. The aminopterin of this media serves to block *de novo* synthesis of nucleotides. Hybrids thrive possessing both the hypoxanthine-guanosine phophoribosyl transferase (HGPRT) enzyme which catalyses the formation of inosinate (a AMP and GMP precursor) in the salvage pathway as well as the neoplastic vitality of the myeloma cancer line. Conversely the hypoxanthine cannot be used by the unfused mutant myeloma as they lack the HGPRT enzyme, while the unfused spleen cells die in culture as they cannot grow *in vitro*. The hybridoma antibodies are then screened and the desired hybrid selected (Stryer, 1988).

The produced hybridoma line can be kept indefinitely and will produce large amounts of homogenous antibody specific to the antigen desired — similar systems are available for chickens and sheep. The cells can be grown in culture media or injected into mice for bulk antibody production as ascites. Cells can also be preserved for later use by storage in liquid nitrogen. This technique has enabled many different biochemical applications requiring the high degree of molecular recognition of antibody eg clinical assay using ELISA and the generation of monoclonal catalytic antibodies.

1.3 CATALYTIC ANTIBODIES

1.3.1 THE CONCEPT OF TRANSITION-STATE

Investigation of the processes involved in enzyme catalysis has indirectly led to the development of the catalytic antibody. For some time it has been understood that the high reactivity of enzymes (E) is associated not so much with their ability to bind substrate (S) but with their ability to bind with high affinity, a strained form of the substrate ($ES^{\ddagger}$) which subsequently forms the products (P) of a given reaction (Fig. 1.8).

$$E + S \rightleftharpoons [\,ES\,]^{\ddagger} \rightleftharpoons E + P$$

Figure 1. 8 Enzyme (E) binding of substrate (S) forming an activated state (‡) which subsequently breaks down forming product (P).

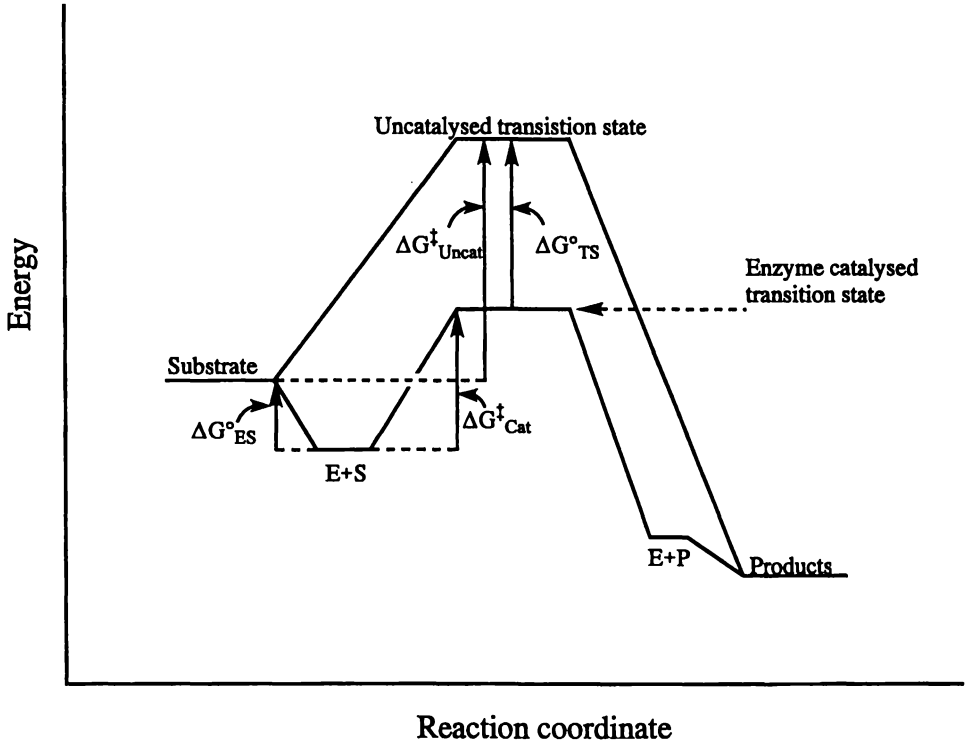

Figure 1. 9 Progression of an enzyme (E)–catalysed, and uncatalysed reaction with substrate (S) forming product (P). $\Delta G°_{ES}$ is the change in energy apon E and S binding, $\Delta G^{\ddagger}_{Cat}$ is the activation energy for the E catalysed reaction, $\Delta G^{\ddagger}_{Uncat}$ is the activation energy for the uncatalysed reaction, and $\Delta G°_{TS}$ is the difference in energy between enzyme–catalysed and uncatalysed reaction (Thomas, 1996; Lerner *et al.*, 1990).

Pauling suggested that an enzyme was essentially a flexible molecular template designed by evolution to precisely complement reactants in an activated transition–state geometry as opposed to ground–state configuration. The binding of the substrate by an enzyme is thought to provide an alternative pathway for the reaction to proceed, lowering the activation energy required for the given chemical transformation (Fig. 1.9). Highly efficient enzyme inhibition could be achieved with compounds resembling this strained substrate structure (Pauling, 1946). This idea was later revived by Jencks when he identified many examples in the literature of what he termed 'transition-state analogue' inhibitors (Jencks, 1969). Wolfenden expressed Jencks concept thermodynamically (Equ. 1.1) (Wolfenden, 1969).

$$\frac{K_m}{K_{TS}} = \frac{k_{cat}}{k_{uncat}}$$

Equation 1.1 The thermodynamic expression relating differential binding to rate enhancement derived from concepts of Wolfenden. This relationship holds true when both catalysed and uncatalysed reactions use a similar mechanism and where the Michaelis-Menten relationship is obeyed. K_m (the Michaelis constant) is the dissociation constant for enzyme (or antibody) substrate complex, K_{TS} is the dissociation constant for an enzyme or antibody transition–state complex, k_{cat} is the rate constant for reaction in the presence of enzyme or antibody catalyst, and k_{uncat} is the rate constant for reaction in absence of enzyme or antibody catalyst.

Wolfenden's theory states that it is differential binding of the transition–state emulator, not the substrate, that translates to an increased rate of catalysis, provided the Michaelis–Menten relationship is obeyed, and, the enzyme and the uncatalysed reactions use similar mechanisms (Kraut, 1988). The limiting factor in an enzyme–catalysed reaction is therefore the ability of an enzyme to bind the substrate transition–state tighter than the substrate ground–state. There is, however, a physical limit to rate enhancement due to the rate of encounter between catalyst and substrate in a solution of the order of 10^8–10^9 $M^{-1}s^{-1}$ (Stryer, 1988). In reality this translates to rate enhancement for enzymes of between 5×10^5 and 1×10^{17}, with 1×10^{11} being common (Radzicka *et al.*, 1995). This observation has led to the development of many enzymatic inhibitors (Wolfenden *et al.*, 1987) and is supported by significant structural and kinetic data (Kraut, 1988). Transition–state

analogues never bind as strongly as might be expected from enzyme rate accelerations. There also remains the question of how a stable molecule can be construed to truly emulate a transition–state complex. This is a very important consideration as it is this factor that limits production of catalytic antibodies.

$$\frac{k_{cat}}{K_S} = k_n \left(\frac{\kappa_e v_e}{\kappa_n v_n}\right)\left(\frac{1}{K_T}\right)$$

Equation 1.2 The relationship between transition–state complex in equilibrium with reactants. K_{cat} is the rate of catalysis, K_S is the substrate dissociation constant, k_n is the rate constant for the uncatalysed reaction, κ_e and κ_n are the transmission coefficients (correction factors for things such as: tunnelling, barrier recrossing, and solvent frictional effects) for the catalysed and uncatalysed reactions respectively, v_e and v_n are the frequency of 'normal mode' oscillation of the transition–state complex along the reaction coordinate (or more rigorously the average frequency of barrier crossing), K_T is the transition–state dissociation constant (Kraut, 1988, and authors therein).

Modern views of catalysis (which encompass such factors as proton tunnelling) enable derivation of essentially the same relationship with transition–state binding translating to an increase in the rate of reaction (Equ. 1.2). The theory has two assumptions: that there is a dynamic bottleneck (the reaction rate is controlled by decomposition of a transition–state complex), and that the transition–state complex is in equilibrium with the reactants (Kraut, 1988, and authors therein).

1.3.2 THE INFANCY OF THE CATALYTIC ANTIBODY

Armed with a theoretical basis for enzymatic catalysis, biochemists endeavoured to create catalytic antibodies. Like enzymes, antibodies possess the ability to recognise complimentary structure at an atomic level and form strongly binding complexes. The major difference between antibodies and enzymes is that while antibodies bind molecules in their ground–state, enzymes bind molecules most efficiently in higher energy transition–states (Dugas, 1989). It was anticipated that if a transition-state analogue for a given reaction was prepared and given as an antigen, then the antibody would selectively bind this

species in preference to the ground–state of the substrate(s) and hence, accelerate the reaction (Thomas, 1996). While this is generally found to be true, in some cases it is not quite so simple.

Recent studies in an Oxy-Cope rearrangement have suggested that tight transition–state binding and catalytic function are actually inversely correlated. In this case there seemed to be three factors that influence the catalytic mechanism: cyclic transition–state geometry, overlap of the π systems of the diene and aryl substituents, and electron density of a hydroxyl group. Increases in the binding energy of the antibody to the transition–state emulator during affinity maturation seemed to only favour one of these factors at the expense of the others and results in a decrease in rate of catalysis. Thus in this case the co–evolution of binding and catalytic function required a careful balance of a number of electronic effects (Ulrich *et al.*, 1998).

Initial attempts to produce catalytic antibodies used polyclonal sera. For example, Slobin generated polyclonal antibodies using a 4-nitrocarbobenzoxy conjugate. The antibodies generated were found to protect 4-nitrophenylacetate and 4-nitrophenyl-ε-amino carbonate from hydrolysis, provided the substrate concentration was less than the concentration of the antibody (Slobin, 1966). This protection was consistent with antibody binding of ground–state hapten. Raso *et al.* managed to generate polyclonal antibodies to a phosphopyridoxyltyrosine but no rate enhancement was detected (Raso *et al.*, 1975).

The advent of monoclonal antibodies enabled Kohen *et. al* to create monoclonal antibodies which were reactive against ester derivatives (Kohen *et al.*, 1980). While these antibodies were capable of hydrolysis of the ester hapten, the reaction was found to be stoichiometric rather than catalytic, possibly due to a tyrosine of the antibody becoming permanently acylated during reaction (Kohen *et al.*, 1980). The first truly successful catalytic antibodies were developed in 1986 by groups led by Schultz (Pollack *et al.*, 1986) and Lerner

(Tramontano *et al.*, 1986). This work of Schultz and Lerner initiated the extensive investigation of antibody catalysis.

1.3.3 THE CATALYTIC ANTIBODY

1.3.3.1 CATALYTIC ANTIBODY GENERATION AND SELECTION

Catalytic Polyclonal Antibodies

Early attempts to screen catalytic polyclonal antibodies versus haptens, which were already successful in generating catalytic monoclonal antibodies, gave non–reproducible results (Schultz *et al.*, 1988). More recently Gallacher *et al.* (1992) have isolated polyclonal sheep antibodies raised against a phosphonate hapten that were capable of the hydrolysis of both carbonate and amide substrates. Others have reported the generation of polyclonal antibodies possessing catalytic aldimine formation (Tubul *et al.*, 1994). The practical applications of polyclonal antibody vaccines in the degradation of toxins is also being investigated (Green *et al.*, 1991).

There are considerable advantages to using polyclonal antibodies. These include low production cost and ease of preparation compared to the production of monoclonals. With polyclonal antibodies the entire immune response is employed and as such may produce very high levels of catalytically active antibodies (Iverson, 1995). Gallacher *et al.* (1993) have reported good success rates for the generation of catalytic antibodies in polyclonal sera and there is growing evidence that the polyclonal sera produced is fairly homogenous (Shreder *et al.*, 1995).

Heterogenous Immunisation

A successful alternative to the classical immunisation regime was used by Suga *et al.* (1994b) and involves sequential immunisation of an animal with two different but structurally related haptens. Ideally the host immune system responds by mutating antibodies generated to the first hapten producing an antibody with high affinity for both haptens. For the case studied in this reference, the conventional procedure would have been

to generate a hapten with both acidic and basic groups, a synthetically challenging procedure. However, the heterogeneous immunisation regime simply made use of two readily available materials (Haptens 1, 2 of Fig. 1.10). The catalytic antibodies generated via the heterogenous method possess rate enhancements of up to 1.5×10^5 over those generated solely against hapten 2 (Suga *et al.*, 1994b).

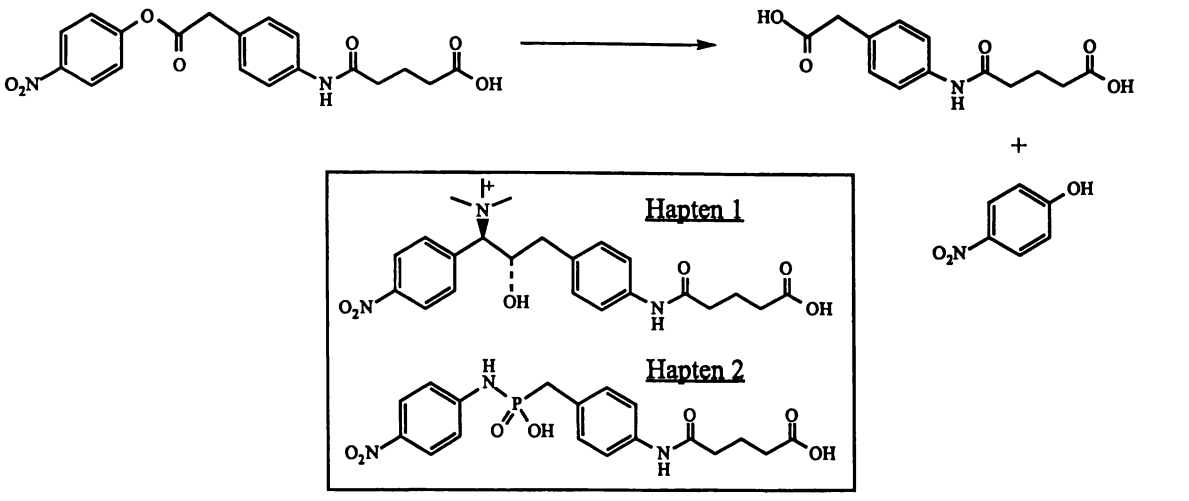

Figure 1. 10 Heterologous immunisation using two different haptens to induce a more effective antibody catalyst (Suga *et al.*, 1994b).

A variation on this theme, termed 'reactive immunisation', has been developed by Wirsching *et al.* (1995). Their hapten (3) has a half life of several days *in vivo* (Fig. 1.11). It was hoped that the hapten would elicit antibodies possessing reactive cysteine, tyrosine, histidine and serine moieties capable of forming phosphonyl-antibody intermediates. Concurrently the di–aryl ester was hydrolysing (*in vivo*) resulting in the negatively charged monoaryl ester (Hapten 4, Fig 1.11). Ideally this would cause further change of the

antibody–binding sites generated giving residues which could stabilise the oxyanion formed during the ester hydrolysis.

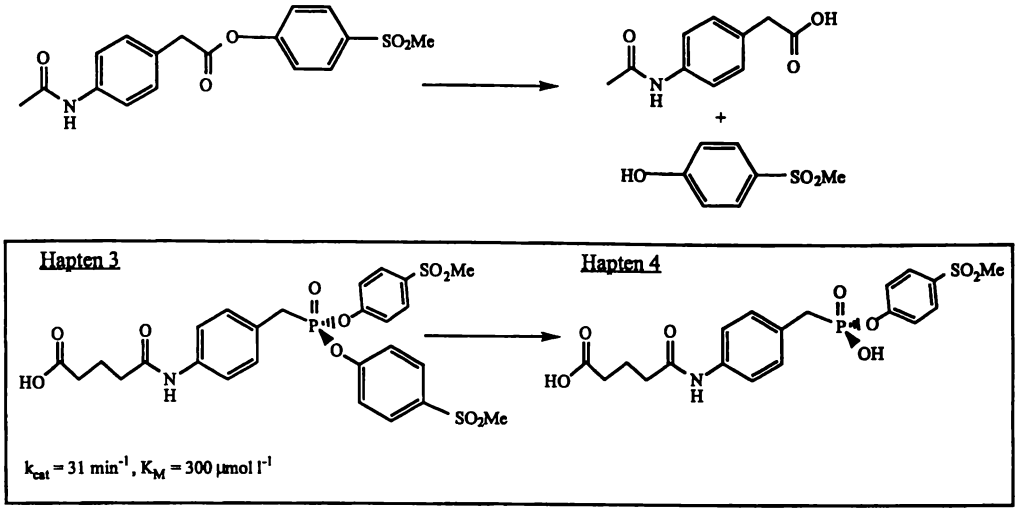

Figure 1. 11 Reactive immunisation where the immune system is exposed to two different haptens as the immunogen hydrolyses *in vivo* with time (Wirsching *et al.*, 1995).

Most of the monoclonal antibodies produced and selected for analysis had higher affinity for the monoaryl ester, and several showed burst kinetics suggesting an acyl antibody intermediate. The k_{cat}/K_m of the best antibody (SPO49H4) was 1 x 10^5 mol^{-1} l^{-1} min^{-1} which is among the most efficient of the hydrolytic antibodies generated to date.

Another catalytic antibody developed by reactive immunisation employed a diketone as a hapten and appeared to have produced antibodies with wider substrate-selectivity than presently characterised enzymes (Wagner *et al.*, 1995). The lysine residues at the binding site are thought to form schiff base associations with the carbonyls of the substrate mimicking the enamine mechanism used by class 1 aldolases.

Gene Expression Libraries and Phage Display of Immunoglobulins

Recent developments in phage display libraries have enabled the time frame for generation of catalytic antibodies to be reduced to less than two weeks. Gene libraries derived from mouse spleen cells are produced using reverse transcriptase and are screened using antigen-binding phage surface proteins (Thomas, 1996). This, coupled with the ability to select for

new catalytic activity from existing antibodies or for improvements on existing catalytic antibodies, is an exciting new development (Fujii *et al.*, 1998).

1.3.3.2 ANTIBODIES AS ENTROPIC TRAPS

In many types of peri– or bi–cyclic reactions, the entropy of activation ($\Delta S^{\ddagger}$) can contribute significantly to the overall change in free energy of activation needed for a reaction to occur. Catalysis of these entropically unfavourable reactions by enzymes is thought to occur by reducing the rotational and translational freedom of the reactants through the formation of a ternary complex in which the substrates are held in a reactive conformation. For bimolecular reactions, enzymes also hold the substrates in sufficiently close proximity for a reaction to occur (Thomas, 1996).

Chorismate Mutase Catalytic Antibodies

Antibodies capable of catalysing the conversion of chorismate to prephenate have been produced. This reaction is catalysed in nature by enzymes in *Escherichia coli* and *Bacillus subtilus* bacteria. A potent enzyme transition–state inhibitor was developed as a hapten by two groups (Fig. 1.12). Hilvert *et al* generated a catalytic antibody (IF7) capable of rate enhancement of 250–fold over the non–catalysed reaction (Hilvert *et al.*, 1988). Jackson *et al.* raised a more efficient catalytic antibody (11F1-2E11) with a rate enhancement of 10^4 (Jackson *et al.*, 1988). This rate enhancement is excellent, as the rate for the enzyme isolated from *B. subtilus* is only 10^6 over the non-catalysed reaction. Stereoselectivity was good for both antibodies as only the claisen[1] type rearrangement of the (-)isomer of chorismic acid occurred.

Studies of chorismate binding (Campbell *et al.*, 1993; Haynes *et al.*, 1994) suggested that the substrate is held in the binding site in a reactive diaxial conformation. When the active site of IF7 is compared to the enzymatic equivalents from *B. subtilus* (Chook *et al.*, 1993) and

[1] Traditionally the claisen rearrangement involves an aromatic intramolecular reaction that rearranges the bond between the terminal carbon of an allyl ether which forms a new C-C bond with an aromatic C and an ortho positionaed hydroxyl, the antibody catalysed reaction is, however, somewhat different.

E. coli (Lee *et al.*, 1995), inhibitor-protein interactions appear, at least qualitatively, to be similar (Fig 1.13) (Thomas, 1996). The most notable difference is that there are far more interactions in the binding site of enzyme than that of (IF7). This would suggest a more open binding pocket in (IF7) and this is supported by the ten–fold difference in inhibitor binding (K_i: *E. coli* = 0.08 μmol l^{-1} (Bartlett *et al.*, 1985), IF7 = 0.60 μmol l^{-1} (Hilvert *et al.*, 1988).

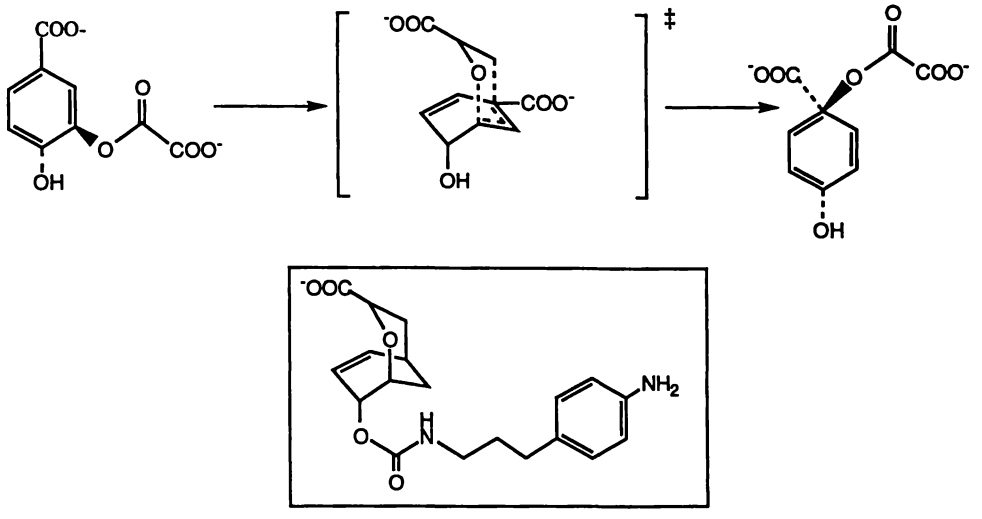

Figure 1. 12 Conversion of chorismate to prephenate catalysed by antibodies (11F1-2E11) and (IF7) (Jackson *et al.*, 1988), (Hilvert *et al.*, 1988).

More recently, detailed comparison of the chorismate mutase catalytic antibodies and enzyme active sites has suggested that while the antibody has the C10 and C11 carboxylate contacts, it lacks the positively–charged environment in the vicinity of the ether oxygen of the hapten. For the enzyme binding site, the positively charged environment stabilises the negative charge on the ether oxygen of the substrate, whilst in the transition–state, and aids the cleavage of the C5-O7 bond (Wade *et al.*, 1997). It is likely that re–design of the hapten, or site specific mutagenesis of the antibody, to include positively charged groups positioned to stabilise this part of the reaction would result in more efficient catalysis (Thomas, 1996).

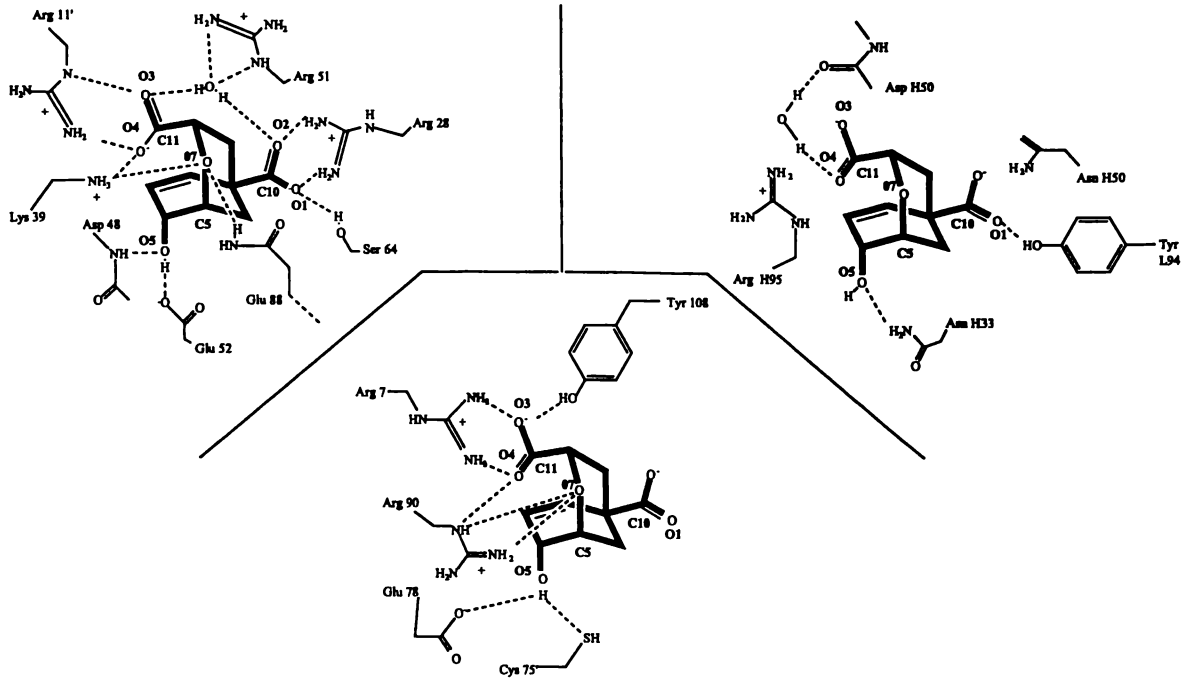

Figure 1. 13 Diagram depicting the similarity of chorismate mutase active sites of: *E. coli* (top left), *B. subtilis* (bottom), and antibody IF7 (top right) (Thomas, 1996).

Interestingly (11F1-2E11) and (IF7) appear to operate by different mechanisms. Antibody (11F1-2E11) was found to have a similar enthalpy of activation as the uncatalysed reaction (ie 20.7 kcal mol^{-1}), however, the change in entropy was significantly lower in the case of the antibody catalysed (-1.2 cal K^{-1} mol^{-1} compared to the non–catalysed case -12.9 cal K^{-1} mol^{-1}) (Jackson *et al.*, 1988). The energy difference suggests that the catalytic antibody works by 'freezing' the substrate into a 'Claisen–suitable' formation (Thomas, 1996). In contrast (IF7) operates by lowering the activation enthalpy to $\Delta H^{\ddagger}$ = 15 kcal mol^{-1} while the activation entropy is less favourable than for the uncatalysed reaction ($\Delta S^{\ddagger}$ = -22 cal K^{-1} mol^{-1}) (Hilvert *et al.*, 1988).

Oxy-Cope Catalytic Antibodies

A catalytic antibody–catalysing an oxy-cope ([3,3]-sigmatropic rearrangement) has been produced by Braisted *et al.* (1994) using a cyclohexane mimic of the ordered chair-like transition–state.

Diels-Alder Catalytic Antibodies

While a number of antibody catalysed Diels-Alder [4π + 2π] cycloaddition reactions have been reported, an enzyme equivalent is yet to be reported (Thomas, 1996). One of the problems associated with Diels–Alder reactions is the similarity of transition–state and product structures. Hilvert introduced a sulphonyl group to the substrate to avoid the potential problem of substrate inhibition. The sulphonyl group of the substrate self extracts following product formation giving a planar product dissimilar to the transition–state analogue used (Fig. 1.14) (Hilvert *et al.*, 1989).

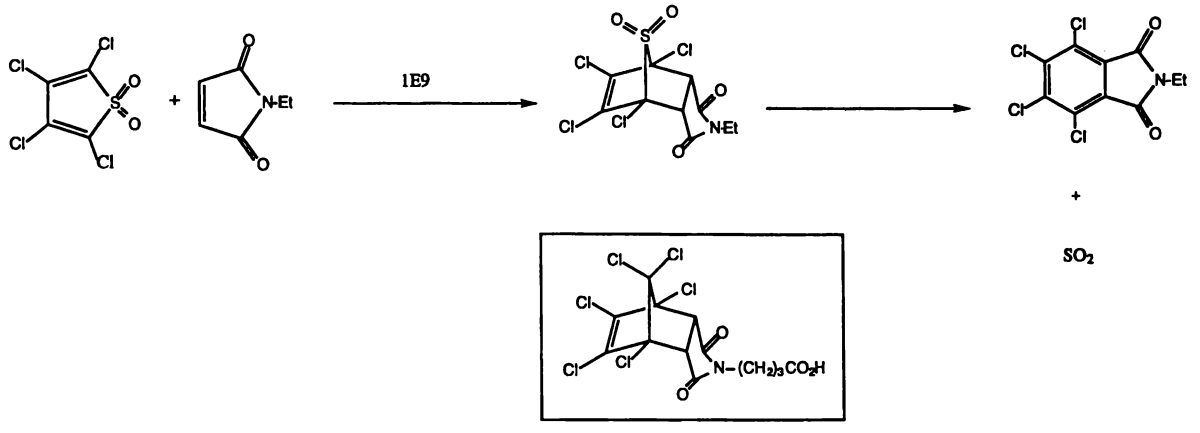

Figure 1. 14 Diels–Alder reaction between tetrachlorothiophene dioxide and N-ethylmaleimide giving the unstable adduct which extrudes the sulphonyl group to give a planar product dissimilar to the transition–state (Hilvert *et al.*, 1989).

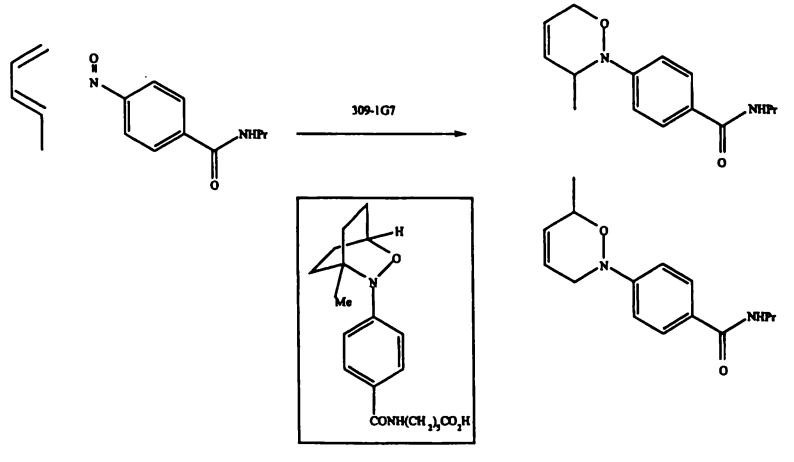

Figure 1. 15 An example of antibody catalysed hetero Diels–Alder reaction (Meekel *et al.*, 1995).

Other Diels-Alder catalytic antibodies have been produced (Braisted *et al.*, 1990; Suckling *et al.*, 1993), including one which catalyses a hetero Diels-Alder reaction (Fig. 1.15) (Meekel *et al.*, 1995).

Gouverneur *et al.* (1993) have reported the production of catalytic antibodies which selectively form the kinetically less favoured *exo* Diels-Alder adduct of 4-carboxyphenyl *trans*-1-buta-1,3, diene-1-1carbamate and N,N-dimethylacrylamide by using a bicyclo[2.2.2]octene hapten (Fig. 1.16).

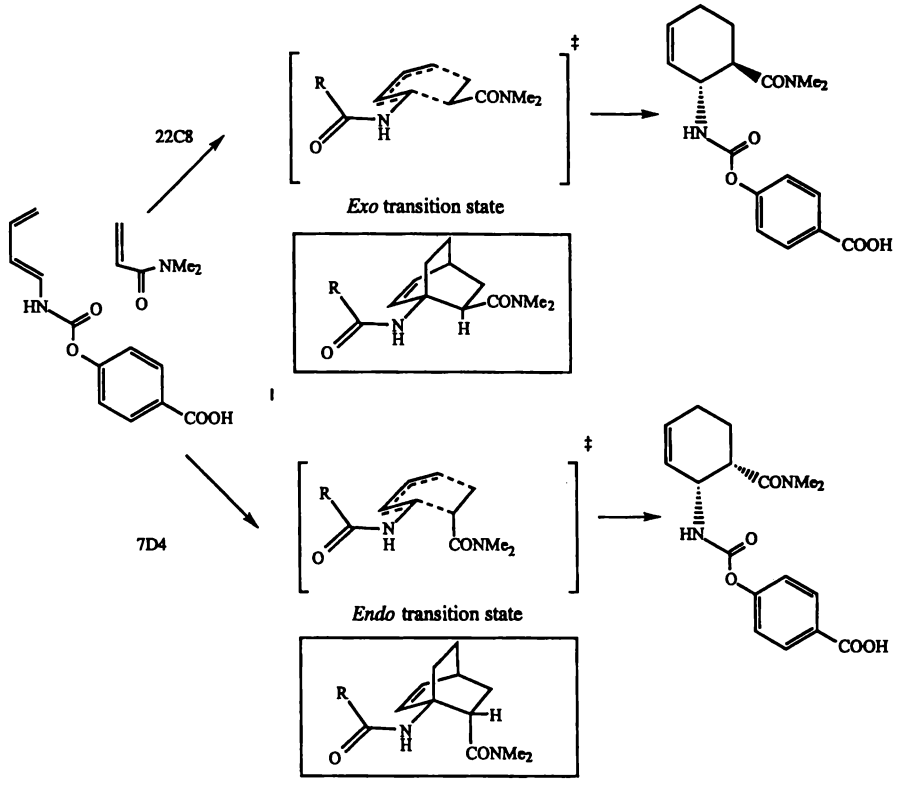

Figure 1. 16 Two different catalytic antibodies that catalyse the *exo* and *endo* products of a Diels–Alder reaction (Gouverneur *et al.*, 1993).

Yli-Kauhaluoma *et al.* (1995) extended this work, employing a conformationally flexible ferrocene derivation to mimic the same reaction. This approach was successful with a transition–state structure generating antibodies which produce ortho-*endo* and ortho-*exo* Diels–Alder reaction products (Fig. 1.17). The resultant catalytic antibodies showed kinetic parameters similar to those of Gouverneur *et al.* (1993).

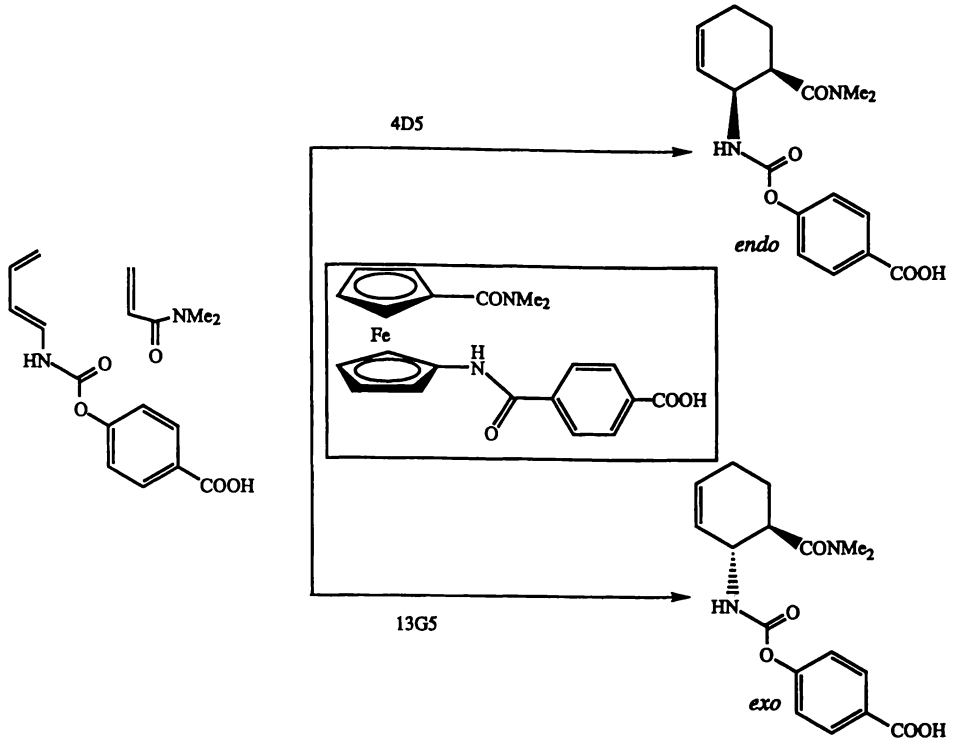

Figure 1. 17 Generation of Diels-Alder catalytic antibodies using a ferrocene based transition–state analogue (Yli-Kauhaluoma *et al.*, 1995).

Antibody catalysis of Pyrimidine Dimers– Retro [2π + 2π] cycloaddition

Antibody (15F1-B1) catalysed the retrocycloaddition of the thymine dimer with a turnover of the same order as DNA photolyase (an enzyme which peforms a similar function (Jacobsen *et al.*, 1995)).

Studies performed using a uracil dimer active catalytic antibody (UD4C3-5) suggest that both bond–making and –breaking reactions can be partially rate determining in the catalytic process. Fluorescence quenching experiments suggest the involvement of a photoexcited tryptophan residue at the active site which transfers an electron to the dimer, resulting in either a stepwise cleavage in which the breaking of the first bond is reversible, or, a concerted cleavage of the cyclobutane ring once a radical anion has been formed (Fig. 1.18) (Jacobsen *et al.*, 1995).

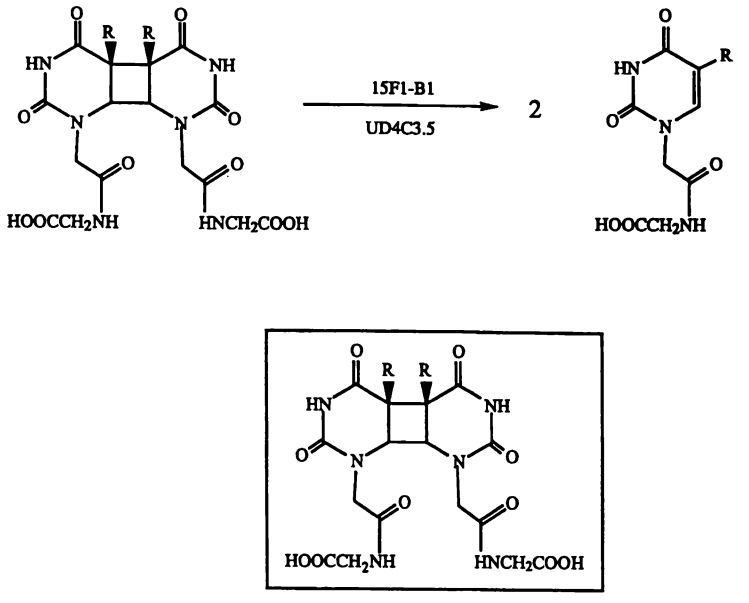

Figure 1. 18 Antibody (15f1-B1, R = OMe) and (UD4C3.5, R = H) catalysis of thymine dimers (Jacobsen *et al.*, 1995).

1.3.3.3 CATALYSIS BY DESOLVATION

One of the factors involved in enzyme catalysis is the exclusion of solvent by binding the substrate in a less polar environment (Dugas, 1989). Work with 6-nitro-3-carboxybenzisoxazole (and similar compounds) has demonstrated that decarboxylation occurs at different rates dependent, in the main, upon solvent polarity (Kemp *et al.*, 1975). Certain types of reaction can be accelerated by the removal of a polar solvent, a property exploited by a number of groups in the production of catalytic antibodies.

Lewis *et al.* (1993) generated catalytic antibodies capable of decarboxylation of 6-nitro-3-carboxybenzisoxazole to 2-cyano-5-nitrophenol. Of the hybridomas produced against hapten 1 (Fig. 1.19), 2% were found to be catalytic, the best of these giving a rate enhancement of 2.3×10^4. This is slower than the decarboxylation of benzisooxazole in neat hexamethylphosphoramide (10^8 relative to water), but comparable with that of mixed media systems involving micelles, macrocycles or polymers (Smid *et al.*, 1979). Alternate haptens (2 and 3, Fig. 1.19) designed to be the best mimics for decarboxylation did not

produce antibodies capable of catalysis (Lewis *et al.*, 1991). It is postulated that the 1, 5–naphthalene disulfonate hapten 1 elicits a positively–charged residue in the binding pocket. This residue attracts the carboxylate of the substrate providing sufficient binding energy to overcome the loss of solvation energy required for the movement of carboxylate from the aqueous environment into the non-polar binding site. As the neutral haptens (2, 3) did not generate catalytic antibodies it is thought that the antibodies generated to these haptens could not compensate energetically for the desolvation of the carboxylate through binding (Lewis *et al.*, 1991).

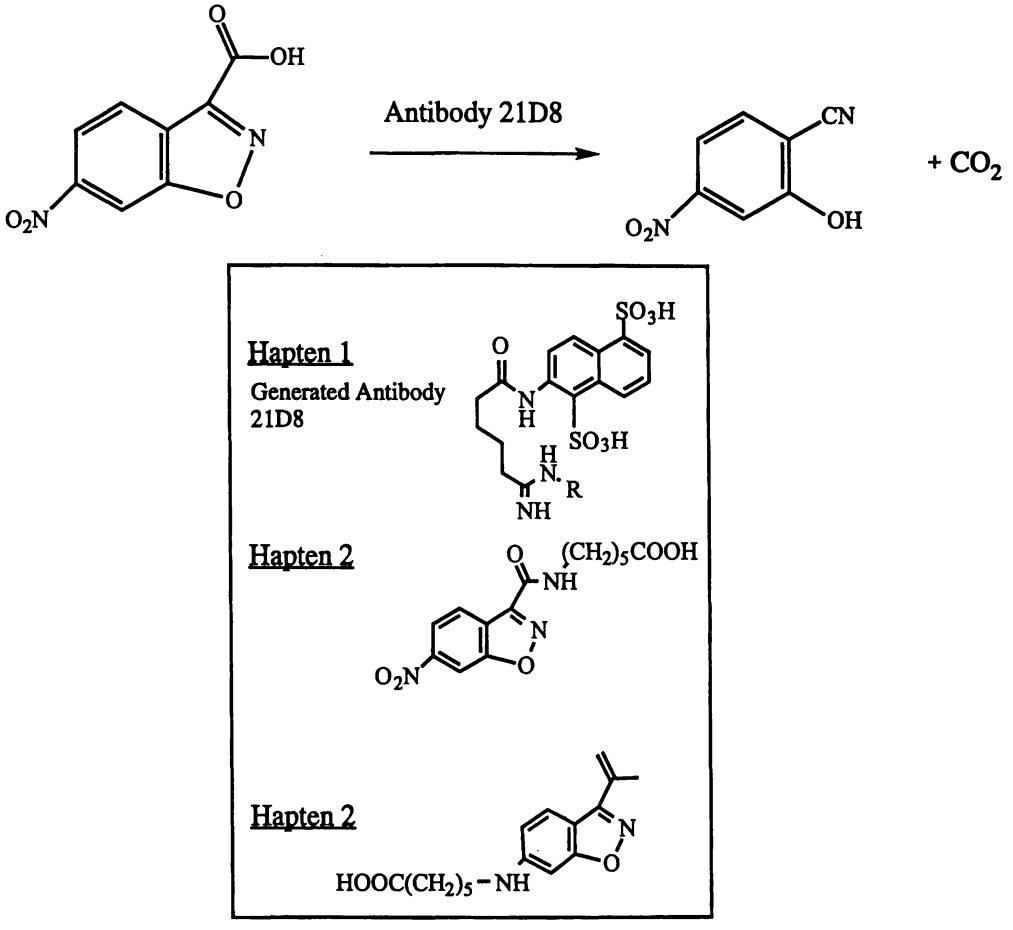

Figure 1. 19 Haptens trialed in attempted generation of a catalytic antibody which uses desolvation as a means of catalysis (Lewis *et al.*, 1991, 1993).

1.3.3.4 REROUTING OF A CHEMICAL REACTION

Theoretically, the only limit to antibody catalysis is the ability to generate a suitable transition–state emulator, meaning that reactions not known to be catalysed by 'nature' can

be achieved. Janda *et al.* (1993) generated catalytic antibodies against a piperidinium–N–oxide which catalyse a reaction favouring the ring closure of an epoxy alcohol to form a tetrahydropyran as opposed to the preferred tetrahydrofuran product predicted by Baldwins rules for cyclisation reaction (Baldwin, 1982).

Another antibody–rerouted cyclisation reaction is reported by Kitazume. Antibodies were responsible for catalysing either *exo*– or *endo*–lactonisation of α-trifluoromethyl γ, δ–unsaturated acids forming the corresponding γ– or δ–lactones (Fig. 1.20) (Kitazume *et al.*, 1995).

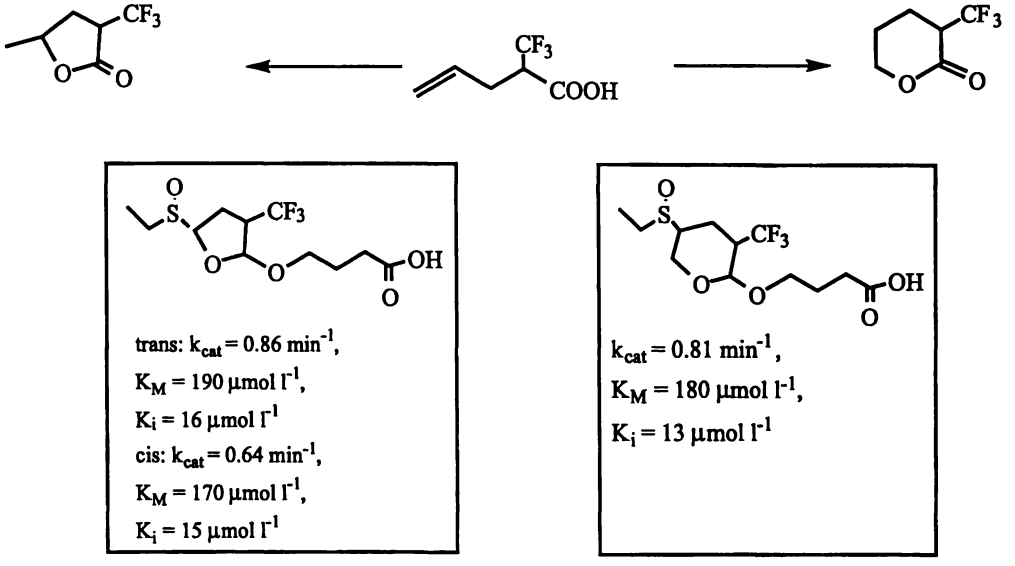

Figure 1. 20 Antibody catalysis of *exo* or *endo* lactonisation of α-trifluoromethyl γ, δ-unsaturated acids forming the corresponding γ- or δ- lactones (Kitazume *et al.*, 1995).

1.3.3.5 MULTISTEP REACTIONS

Liotta *et al* (1995) have described an antibody (RG2.2E4) which catalyses the conversion of asparaginylglycine N–phenethylamide to an intermediate succinimide which is subsequently hydrolysed to form aspartate and isoaspartate products (Fig. 1.21).

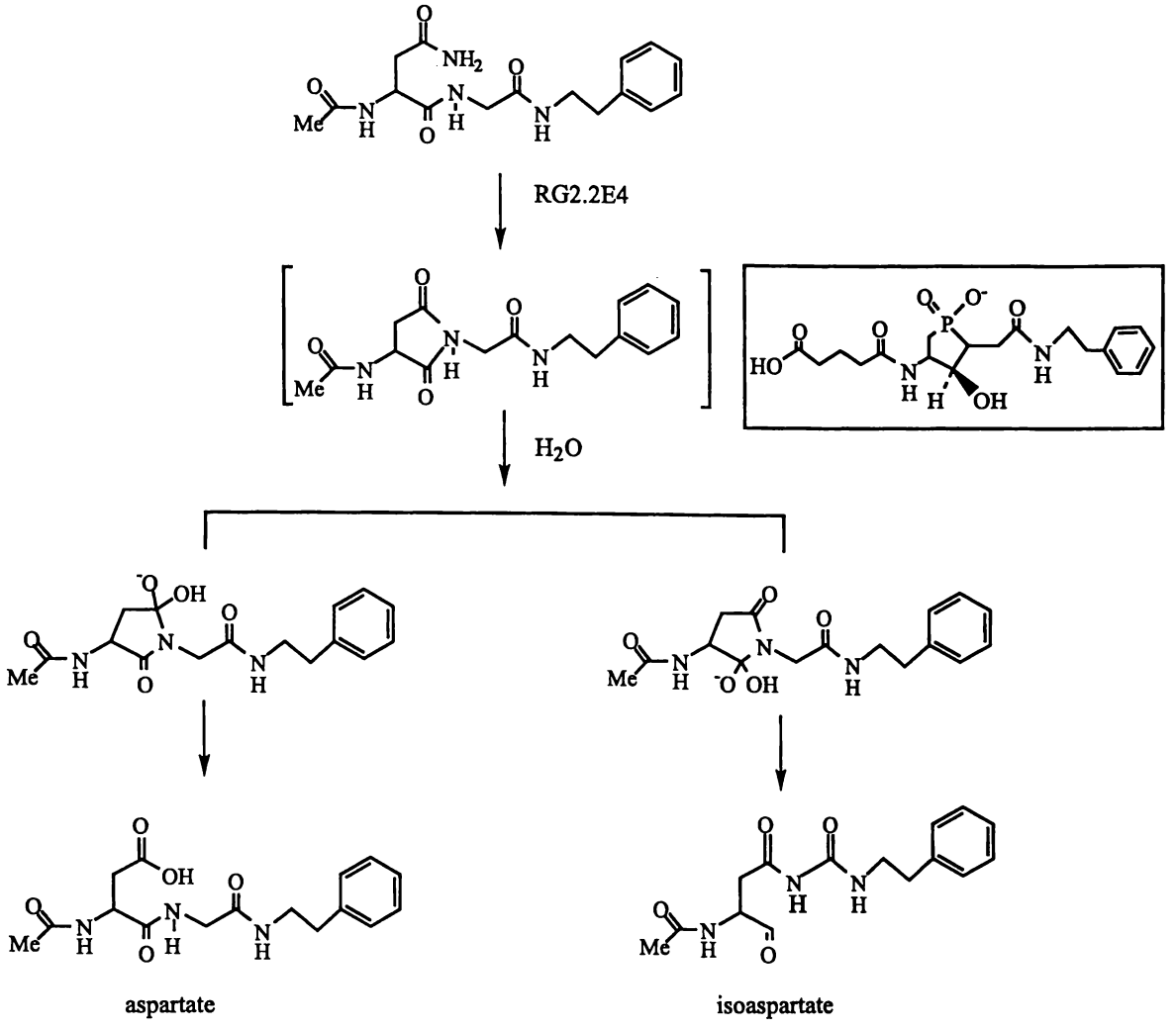

Figure 1. 21 Antibody–catalysed conversion of asparaginylglycine N-phenethylamide via a succinimide. Subsequent hydrolysis of the succinimide produces both aspartate and the isoaspartate compound (Liotta *et al.*, 1995).

One example of an antibody capable of multistep reaction is (78H6) produced by Reymond *et al.* (1995) which catalyses an aldol addition followed by an elimination reaction. Another antibody (24B11) catalyses lactonisation followed by an amidation reaction (Benkovic *et al.*, 1988).

1.3.3.6 COFACTOR ASSISTED ANTIBODY CATALYSIS

Following nature's lead, researchers have attempted to generate catalytic antibodies utilising cofactors by endeavouring to add chemical function to the antibody binding site. The

cofactor studies can be divided into two arbitrary groups: those using 'natural' cofactors (eg metals, porphyrins, pyridoxal phosphate), and those using simple inorganic reagents.

Natural Cofactors

In many cases the antibody acts as a template which controls substrate selectivity and regio- and stereo-specificity while the cofactor or coenzyme provides the catalytic functionality.

A pyridinium–based decarboxylase (Ashley *et al.*, 1993) and a number of metal–dependant hydrolytic antibodies have also been reported (Iverson *et al.*, 1989; Wade *et al.*, 1993). As yet attempts to engineer antibodies with binding sites including coordinated metals have not been particularly successful (Crowder *et al.*, 1995).

Redox Reactions

Catalytic antibody systems involving flavin or porphyrin cofactors have been reported (Janjic *et al.*, 1989). The antibody provides substrate specificity and a less polar environment.

Semi–synthetic Catalytic Antibodies

Pollack *et al.* (1989) generated a semi–synthetic catalytic antibody containing a covalently linked cofactor close to the antigen binding site (Figure 1.22). Using a cleavable affinity label, a free thiol was introduced at the periphery of the binding site. It was postulated that this could then act as a nucleophile or be further derivatised so that other reactive groups could be introduced into the antigen binding site. The introduction of free thiol increased the catalytic nature of the IgA antibody (MOPC315) for phosphocholine ester hydrolysis by 6×10^4.

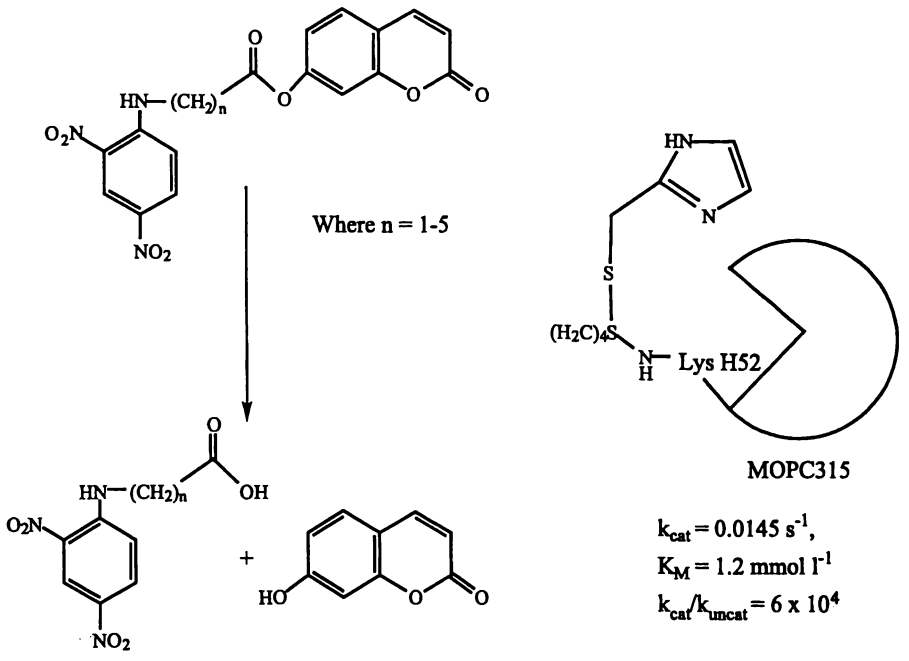

Figure 1. 22 Semi–synthetic catalytic antibody catalysing ester hydrolysis of phosphocholine (Pollack *et al.*, 1989)

A similar, more recent study involved the generation of a glutathione peroxidase. Selenium was introduced into the binding site of an antibody generated against a dinitrophenyl glutathione hapten (Fig. 1.23). The selenium introduction was achieved by modifying an antibody (4A4), firstly with toluene-p-sulfonyl fluoride, and subsequently hydrogen selenide (Luo *et al.*, 1995). The non-mutated IgG (4A4) had no detectable activity while (seleno-4A4) had very high activity approaching that of an equivalent naturally occurring enzyme (Luo *et al.*, 1995).

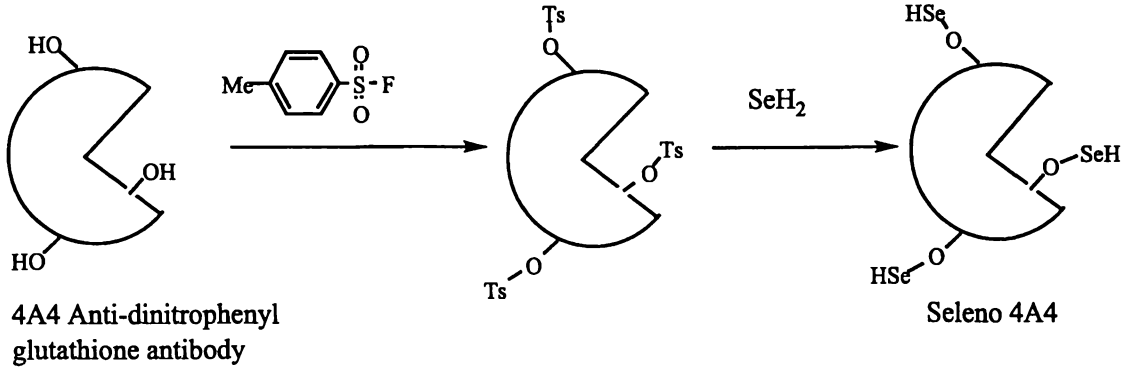

Figure 1. 23 Seleno semi-synthetic antibody with increased glutathione peroxidase activity (Luo *et al.*, 1995).

Inorganic Cofactors

At present one of the largest drawbacks to the preparative biotransformation of organic compounds is the need for expensive redox cofactors such as NAD(P) (Wong *et al.*, 1994). While good methods for recycling these biological cofactors exist, it is still of economical benefit to make use of inorganic redox reagents using the specificity of an antibody template (Thomas, 1996). One example of a catalytic antibody using such a reagent is (37B.39.3) which activates a specific ketone in such a way that reduction with sodium cyanoborohydride is possible. Catalytic antibody (37B.39.3) catalyses stereo–specific reduction of one pair of chemically similar ketones with the resulting alcohol being generated in 96% enantiomeric excess (Fig. 1.24) (Hsieh *et al.*, 1993). In addition the antibody was capable of more than 25 turnovers without undergoing deactivation, suggesting that the sodium cyanoborohyride does not significantly modify the antibody.

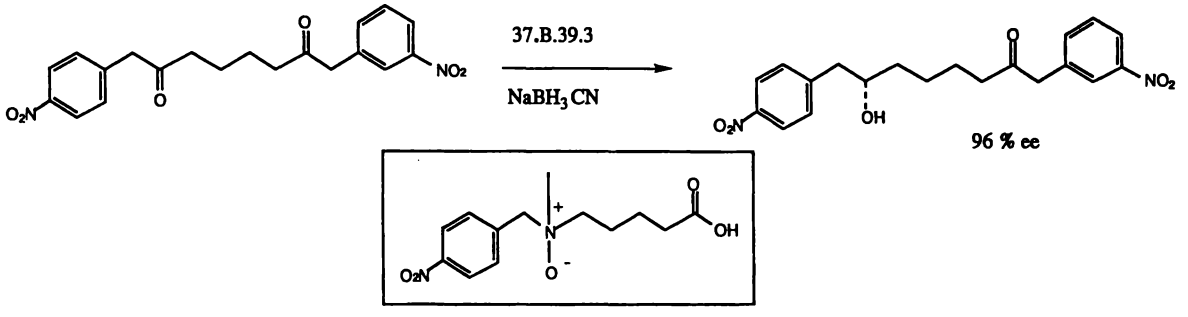

Figure 1. 24 Catalytic antibody reduction of a specific ketone using $NaBH_3CN$ (Hsieh *et al.*, 1993).

Another catalytic antibody making use of an inorganic cofactor was raised against an ammonium phosphonate hapten and catalysed the oxidation of a sulfide to a sulfoxide using a sodium periodate cofactor (Fig. 1.25) (Hsieh *et al.*, 1994). Extended exposure to this oxidant did not adversely affect the antibody. The catalytic efficiency and the turnover rate were similar to that of the P-450 enzymes.

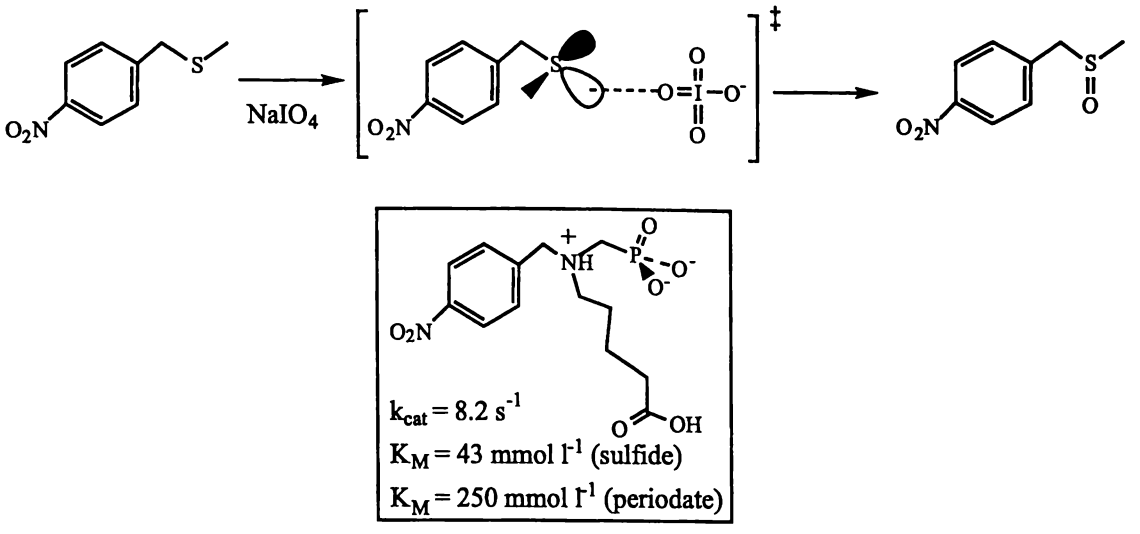

Figure 1. 25 Catalytic antibody oxidation of a sulfide to a sulfoxide (Hsieh *et al.*, 1994).

1.3.3.7 NON–HYDROLYTIC GENERAL ACID–BASE CATALYSIS

The literature contains references to a number of catalytic antibodies that catalyse elimination reactions. These catalytic antibodies are prepared employing a hapten that induces a basic functionality at the antigen binding site (Cravatt *et al.*, 1994; Shokat *et al.*, 1994; Tanaka *et al.*, 1996). An example of a catalytic antibody with these properties is (ID4) which catalyses a disfavoured *syn* elimination reaction via an eclipsed transition–state resulting in the *cis* (Z) olefine product (Cravatt *et al.*, 1994). The estimated difference in energy between a syn elimination (via the eclipsed transition–state) and an anti–elimination (via a staggered transition–state) is approximately 5 kcal mol^{-1} and is thus accessible through antibody binding. By using a hapten containing an amine in the position occupied by the proton to be removed, a general base is induced close to this position in the antibody binding pocket.

An example of a catalytic antibody was generated versus a benzimidazole hapten demonstrating an E2 elimination mechanism on 5-nitrobenzisoxazole to give 2-cyano-4-nitrophenol (Tanaka *et al.*, 1996). Chemical modification and pH dependence studies of the catalytic antibody suggest a carboxylate group with an elevated pKa at the active site is responsible for the rate–determining deprotonation. The antibody generated catalysed a

proton transfer of greater than 10^8 above background. The proton transfer was achieved via a combination of desolvation and general acid-base catalysis (Tanaka *et al.*, 1996).

1.3.3.8 HYDROLYTIC ANTIBODIES

Many early studies were directed towards production of hydrolytic antibodies with the target being the C-O or C-N bonds of esters, carbonates or activated amides. Previous work on esterase or protease inhibitors had laid a good knowledge foundation of the mechanism for hydrolytic enzymes. Methods of screening this type of catalysis were established and with substrate and resulting product being sufficiently different product inhibition was minimised.

Hydrolytic catalytic antibodies have been generated versus a variety of transition–state analogue structures (Fig. 1.26). There seems to be no one favoured method of transition–state stabilisation. Where mechanistic details have been established, catalytic antibodies employ a host of methods for transition–state stabilisation to perform any given reaction.

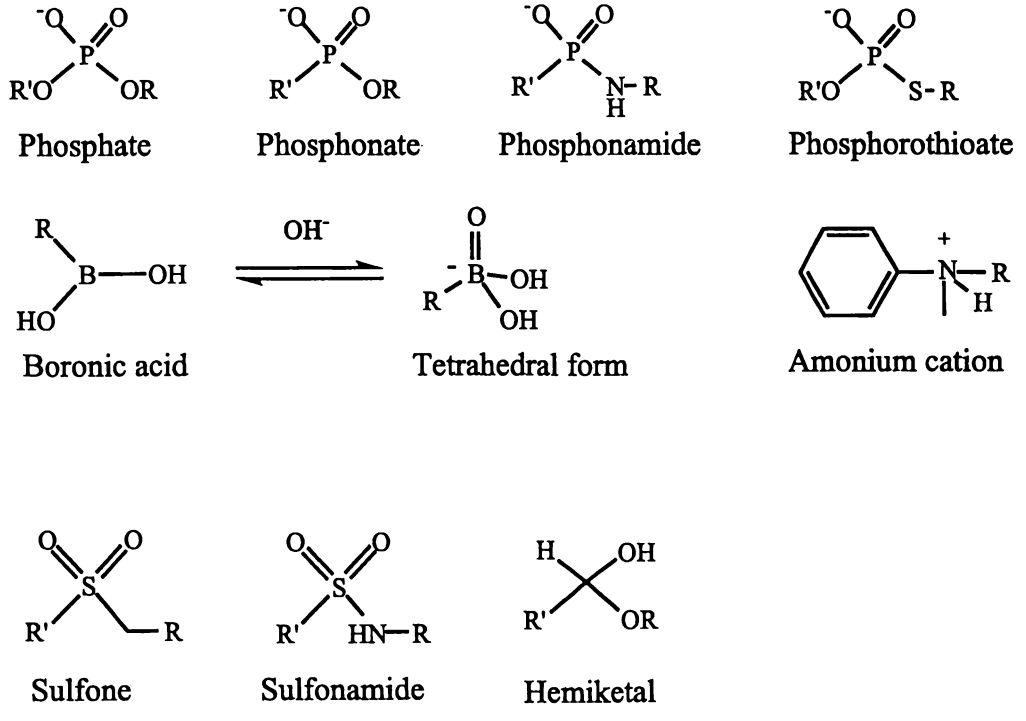

Figure 1. 26 Haptens used to date for generation of hydrolytic antibodies.

General Acid-Base Hydrolysis Mechanisms

Hydrolysis of esters and amides involves attack by a hydroxide ion or water molecule at the carbonyl carbon for formation of a transient high energy tetrahedral intermediate. The intermediate subsequently evolves the free carboxylic acid and either the alcohol or amine as is appropriate. The hydrolysis reaction of esters and amides passes through two transition–states and the pKa of the leaving group determines which of these transition–states is the rate limiting. With leaving groups capable of stabilising negative charge such as 4-nitrophenol and 4-nitroaniline, it is the generation of the tetrahedral state, with the associated addition of solvent, that is rate–determining. Conversely for hydrolysis of most esters and amides it is usually the protonation of the leaving group that is rate–determining (Thomas, 1996). As most haptens are designed to hydrolyse 4-nitroanilide or 4-nitrophenol ester compounds, most transition–state analogues employed for catalytic antibody production are tetrahedral sulfur or tetrahedral phosphorus compounds: sulfonamides, phosphonates, phosphates or phosphonamides (Fig. 1.26). These transition–state analogues mimic the rate–limiting terahedral intermediates well. Modelling using *ab initio* calculations for nucleophilic ester attack of methyl acetate (under alkaline conditions) gave a reasonable transition–state geometry. The Cramer-Truhlar solvation model was imposed on the methyl acetate transition–state and suggested that the phosphorus–oxygen bond distances of these mimics are 0.2-0.3 Å longer than those derived for the tetrahedral intermediate state that they mimic (Teraishi *et al.*, 1992). In addition the transition–state nucleophile (eg. OH^-) and carbonyl carbon interaction is 0.6 Å longer than the emulating phosphorus-oxygen bond.

Sulfur analogues appear to be far less successful than their phosphorus counterparts in generation of catalytic antibodies. It is thought that this is due to the size and increased acidity of phosphonates and phosphoamides which induces a positively–charged (basic) residue that interacts with the hapten. It is this positively–charged residue that is thought to act as a proton donor contributing electrostatically to stabilise the oxyanion formed in the key transition–state, or in protonation of the leaving group (Thomas, 1996).

Recent work investigating the effect of charge on the catalytic antibody mechanism has suggested that charge is a very important factor in the catalytic event. One study involved generation of an esterolytic antibody, not making use of a tetrahedral intermediate but employing a cyclopropene (Grynszpan *et al.*, 1998).

There are a number of problems associated with amide hydrolysis by catalytic antibodies. While there is no thermodynamic problem for hydrolysis of amides at pH 7, there exists a major kinetic barrier. Furthermore, it is thought that amide hydrolysis involves more than a single tetrahedral transition–state intermediate, thus an effective amide catalyst must cope not only with the formation of the tetrahedral intermediate but also its breakdown. It has been found that bond hydrolysis is possible where the two transition–states have the same nett charge, or where protonation of a leaving group is not critical (such as with esters, carbamates, and the activated 4-nitroanilides (Blackburn *et al.*, 1993)). As yet there are no examples of hapten–generated catalytic antibodies capable of hydrolysing an unactivated amide bond. There are, however, naturally occurring catalytic antibodies capable of unactivated amide hydrolysis.

Some human patients with thyroditis display the ability to hydrolyse thyroglobulin highly efficiently via catalytic antibodies (Li *et al.*, 1995). It has also been noted that some asthmatic patients possess antibodies that bind vaso intestinal peptide (VIP). A proportion of the antibody population is also capable of hydrolysing this peptide, leading to the suggestion that there exists a 'natural role' for catalytic antibodies (Paul *et al.*, 1989). While the mechanism of anti-VIP antibodies remains unclear it raises support for the idea that amidolytic catalytic antibodies should be possible through appropriate manipulation of the immune system (Shchurov, 1997).

Work toward generation of antibodies capable of unactivated amide hydrolysis and antibody hydrolysis of a primary amide with a modest rate acceleration continue (Martin *et al.*, 1994). New compounds using boronic acid (Fig. 1.26) as a transition–state emulator have been shown to be suitable for generation of antibodies which hydrolyse a primary amide bond (Gao *et al.*, 1998).

Transition–State Stabilisation by H-Bonding to the Oxy-Anion

The preferential binding by antibodies of the tetrahedral transition–state emulated by a tetrahedral phosphorus compound can provide catalysis (Fig. 1.27). This binding has been shown for catalytic antibodies (6D9), (4B5), (8D1) and (9C10) (Fujii *et al.*, 1995). Chemical modification and pH rate data suggest that the (6D9) mechanism involves attack of hydroxide at the ester carbonyl. It is thought that the side chain of His^{H27d} forms a hydrogen bond with the oxy–anion of the hydrated ester of the transition–state. This has been confirmed for (6D9) (Miyashita *et al.*, 1997). A similar role has been suggested for the histidine moiety in thermolysin (Monzingo *et al.*, 1984).

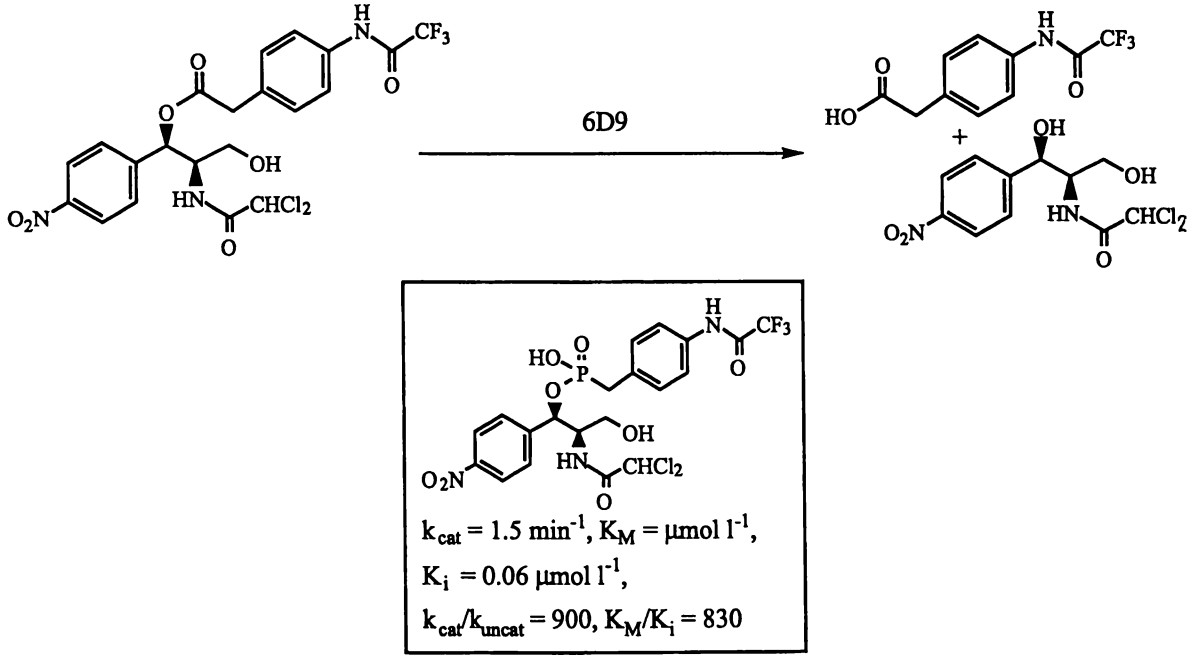

Figure 1. 27 Ester hydrolysis by the (6D9) catalytic antibody. The hapten was also used in the generation of (4B5), (8D1), and (9C10) (Fujii *et al.*, 1995).

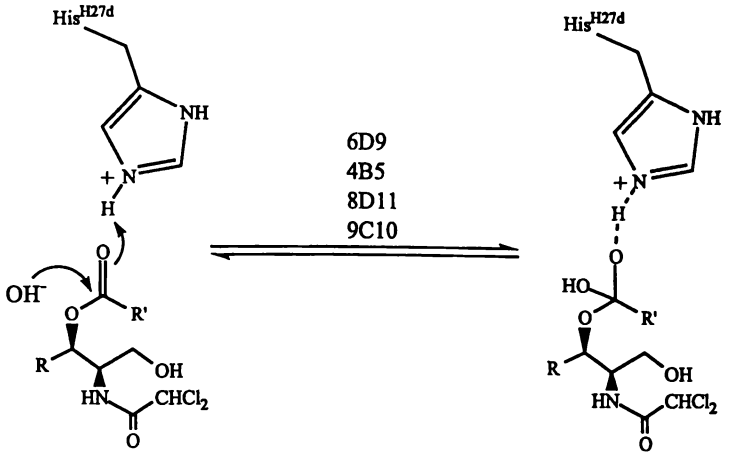

Figure 1. 28 Tetrahedral transition–state complex thought to be adopted by various catalytic antibodies.

The observation that β–lactamases are inhibited by phosphonates and boronates, via the formation of covalent tetrahedral adducts (Curley *et al.*, 1997), led to the development of amide–hydrolysing catalytic antibodies making use of boronic acid (Gao *et al.*, 1998). While the mechanism is yet to be elucidated, it appears that the catalytic antibody generated may act by stabilising of an oxyanion intermediate. In an attempt to overcome the problems of amide hydrolysis, boronic acids have been investigated. At blood pH, ca 7.4, α-amino boronic acids (with a pKa around 8.0) exist as a population of trigonal boronic acids and tetrahedral hydrates, the latter of which form an excellent transition–state emulator for amide and ester hydrolysis. The catalytic antibodies were extracted from an active immunisation, 'panned' (selected for) and amplified, making use of phage technology[2]. One of the benefits of using the boronic system is that by adjusting the pH of a panning cycle, a new range of antibodies can be selected for (Gao *et al.*, 1998).

[2] Phage technology is the process by which antibody cDNA is spliced into a phage which then displays the antibody on the phage surface. The antibody displayed phage particle can then be screened and amplified making use of pH sensitive binding.

Nucleophillic Catalysis

The process of nucleophilic catalysis in enzymes has been well characterised. There now exists significant evidence that nucleophilic attack, by a binding site residue, at the carbonyl carbon of substrate, is involved in a number of catalytic antibody mechanisms (Stryer, 1988).

The catalytic antibody (17E8) catalyses the hydrolysis of an *S*-amino acid (Fig. 1.29). Zhou *et al.* (Zhou *et al.*, 1994) have solved the crystal structure of this antibody bound to its transition–state analogue at 2.5 Å resolution (Fig. 1.30). The antibody possess two binding pockets, one for the butyl side chain and another for the phenyl ring; the succinimide tether extends out of the binding site.

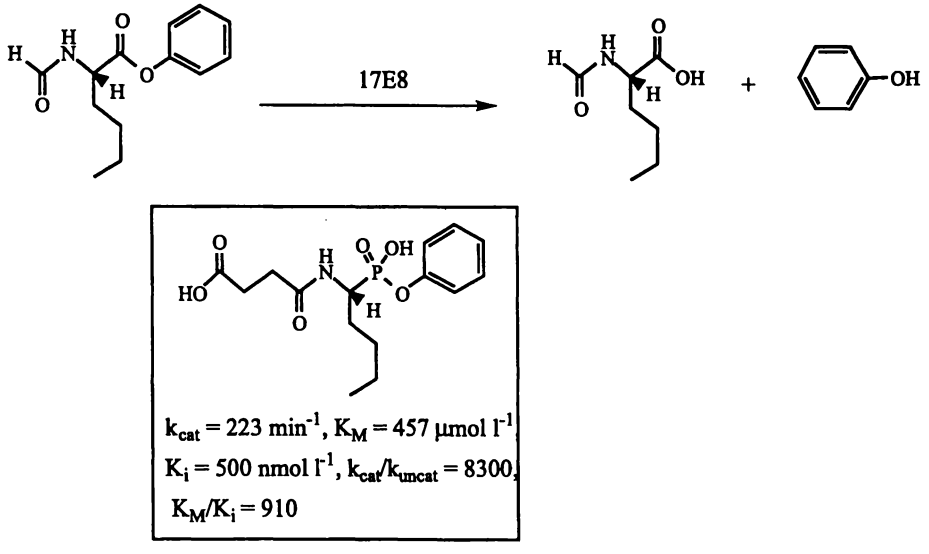

Figure 1. 29 Catalytic antibody hydrolysis of an *S*-amino acid (Zhou *et al.*, 1994).

A salt bridge between Lys^{H97} and the *pro-S* diastereotropic oxygen of the phosphonate suggests the protonated ε-amino group electrostatically stabilises the oxyanion esterolytic transition–state. Mechanistic studies of (17E8) have been conducted and suggest that a catalytic dyad is formed by His^{H35} and Ser^{H99} similar to the catalytic triad of serine proteases. The proton donor role is thought to be filled by the Tyr^{101} which acts as a pH–sensitive 'switch' with a low pH switching 'off' the nucleophilic serine (Fig. 1.31).

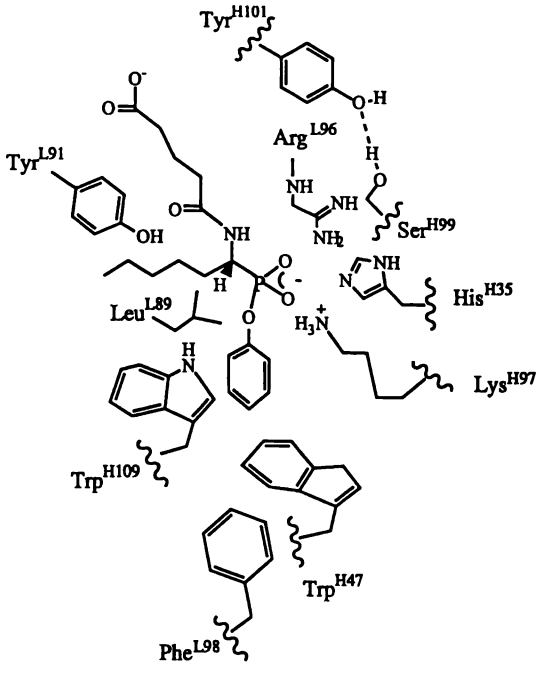

Figure 1. 30 The binding site of the catalytic antibody (17E8) (Zhou *et al.*, 1994).

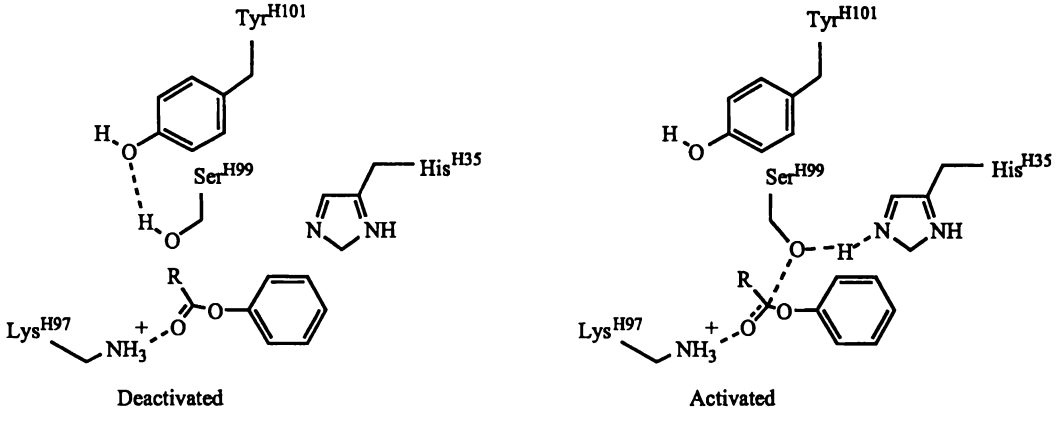

Figure 1. 31 The hypothesised 'pH switch' in the (17E8) catalytic antibody (Guo *et al.*, 1994).

The catalytic antibody (NPN43C9) generated versus a phosphonamide hapten was found to catalyse both ester and amide hydrolysis (Fig. 1.32) (Janda *et al.*, 1988a). Cloning of the antibody has enabled its extensive study (Benkovic *et al.*, 1990; Gibbs *et al.*, 1992; Stewart *et al.*, 1994).

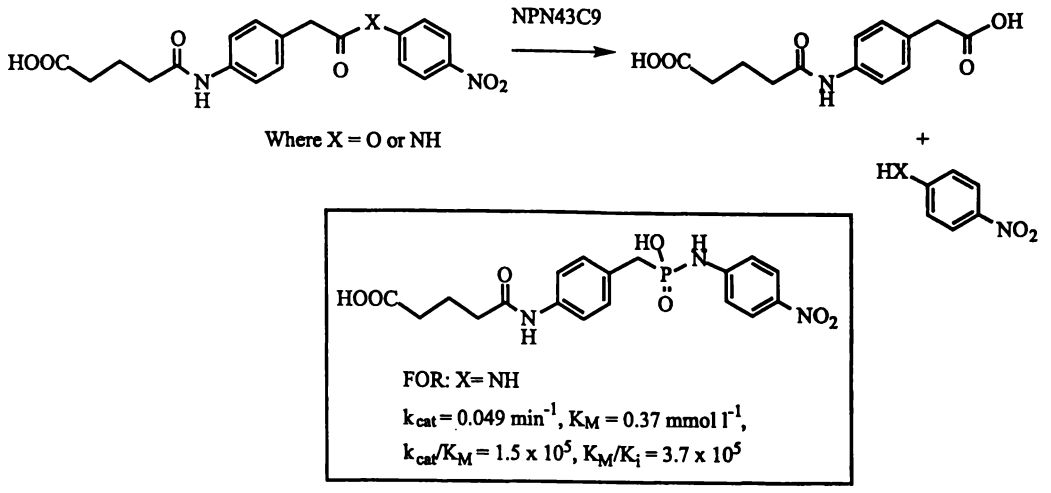

Figure 1. 32 The catalytic action of antibody (NPN43C9) (Benkovic *et al.*, 1990).

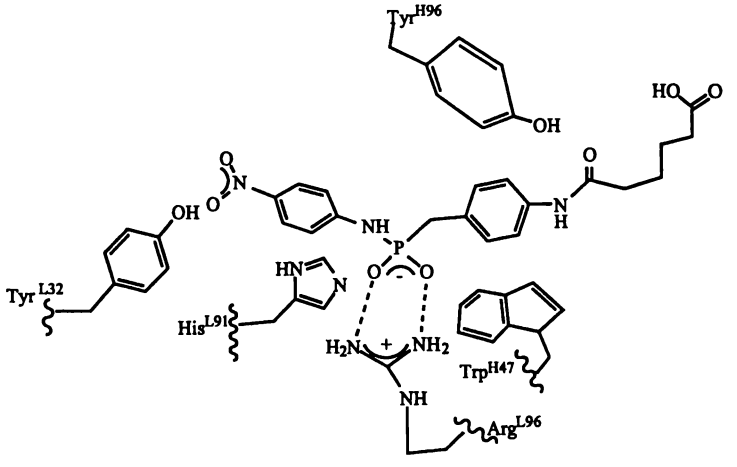

Figure 1. 33 The computer–predicted binding site of catalytic antibody (NPN43C9) (Roberts *et al.*, 1994).

The binding site of the expressed single chain antigen–binding fragment (scF_v) has been computer modelled using the McPC603 V_L and D1.3 V_H crystal structures as templates for the appropriate regions (Fig. 1.33) (Roberts *et al.*, 1994). This modelling suggests that the nucleophile responsible for the generation of the acyl intermediate is the imidazole of His^{L91} and this has been confirmed by detection of the acyl-imidazole intermediate via ESI–MS (Krebs *et al.*, 1995).

General Acid Base Catalysis

Suga *et al.* used haptens with highly polar groups to generate complimentary charges in the antibody binding pocket in the hope that they would generate a 'bait and switch' type mechanism, similar to that of an aspartate protease. Three different haptens (Fig. 1.34) were constructed with the intent of generating a group that would act as a general base, and thus aid proton transfer from H_2O to the alcohol or amine product. A suitable basic or neutral group that would stabilise the generation of a transition–state oxy–anion was also sought (Suga *et al.*, 1994a). All of the three haptens generated esterolytic antibodies with similar specificity constants and rates (Fig. 1.34).

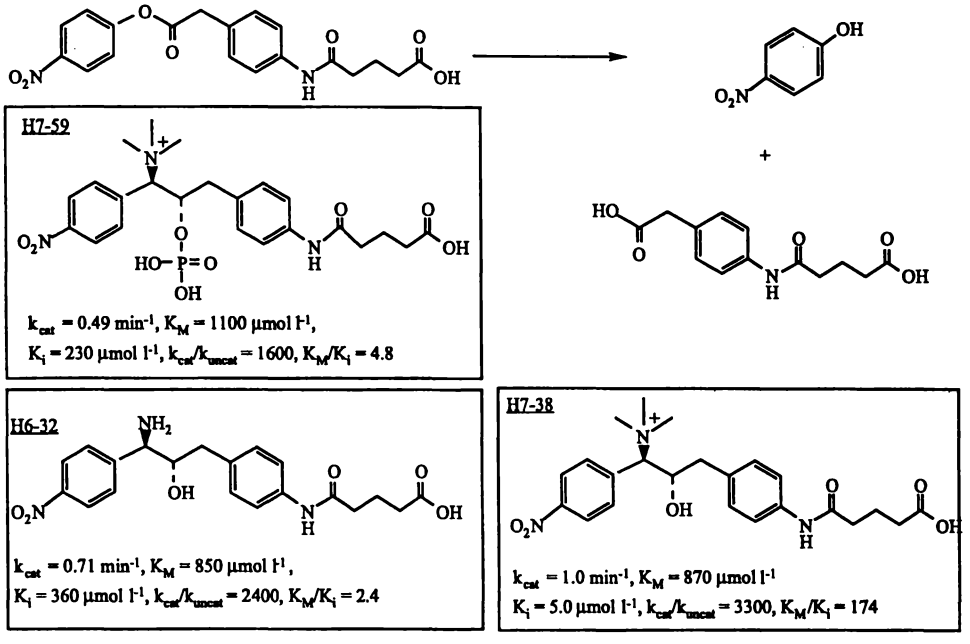

Figure 1. 34 General acid base antibody catalysis of three different haptens generated for the same reaction (Suga *et al.*, 1994b).

Glycoside Hydrolysis

Reymond *et al.* (1991) have successfully used a piperidinium ion hapten to mimic the cationic transition–state proposed for the acid–catalysed cleavage of an acetal. Another group (Suga *et al.*, 1994) used a hapten containing a cyclohexane ring locked into a half chair conformation by the introduction of an azetidinium moiety. In addition, the azetidinium group mimics the protonated *exo*–oxygen of the transition–state and it was anticipated that this might induce an antibody residue(s) capable of carbocation stabilisation. The resulting antibody gave catalysis five–fold greater than that obtained by Reymond. Yu *et al.* (1994)

took a slightly different approach, trying haptens based on three well–known glycosidase transition–state inhibitors. One hapten containing a cyclic amine produced an efficient catalyst with a large rate enhancement.

Ester and Amide Bond Formation in Aqueous Solution

A number of catalytic antibodies which catalyse ester and amide bond formation in aqueous solution have been reported. The haptens that have been used to generate these catalytic antibodies contain neutral phosphonate diester groups or phosphonamide transition–state emulators. Some of the ester–active catalytic antibodies are: (24B11), which catalyses both lactonisation and amide formation (Benkovic *et al.*, 1988) and (17G8) which is capable of benzylamide formation (Janda *et al.*, 1988). The peptide–forming antibodies (16G3) (Hirschmann *et al.*, 1994) and (9B5.1) (Jacobsen *et al.*, 1994) have also been described.

Phosphate Hydrolysis

The literature contains references to a number of catalytic antibodies capable of phosphate ester hydrolysis. The antibody catalysis includes: specific dephosphorylation or phosphorylation and degradation of insecticides and biological warfare agents such as Sarin, Soman, and Tabun.

Catalytic antibodies that hydrolyse phosphate mono- and tri-esters have been documented. These employ a penta–coordinated vanadate or a penta–coordinate phosphorus structure. Unfortunately, these structures are toxic and show conformational or chemical instability under standard immunisation regimes (Hillerns *et al.*, 1991). . The use of α-hydroxy phosphonate haptens (Fig. 1.35) (Scanlan *et al.*, 1991) or haptens containing cyclic amine oxide, which hydrolyses phosphate tri-esters, have been reported (Rosenblum *et al.*, 1995). A catalytic antibody generated against a penta–coordinated phosphorus species may hydrolyse Soman (Brimfield *et al.*, 1993). However, none of these antibodies has given large rate increases for the respective phosphate ester hydrolysis reaction. Further work

using penta–coordinated esters with a VO^{3+} core should possess appropriate qualities for phosphorus ester hydrolysis (Hillerns *et al.*, 1991).

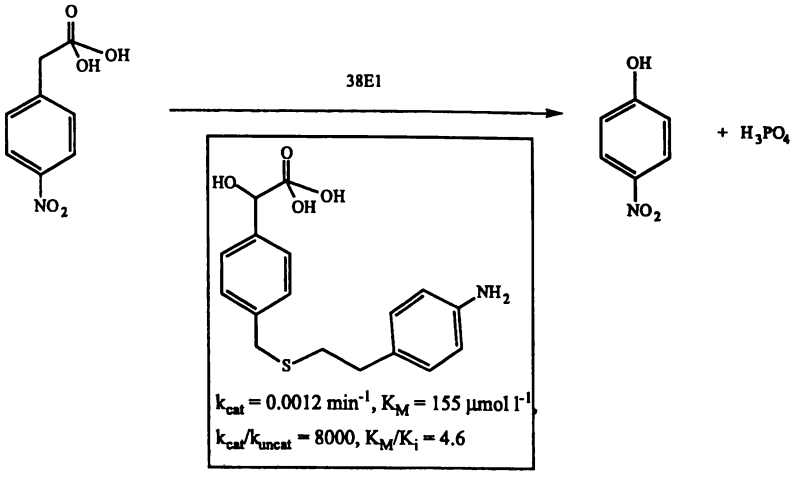

Figure 1. 35 Phosphorus ester–hydrolysing antibody (Scanlan *et al.*, 1991).

1.3.3.9 FURTHER INTERESTING CONCEPTS

It has been found that proteins have the ability to 'memorise' their conformation from an aqueous to an anhydrous environment. This molecular imprinting of a protein freeze dried with a transition–state inhibitor enabled a modest rate for a β-elimination reaction over the non-imprinted counterparts (Slade *et al.*, 1998). The use of anti-idiotypic antibodies[3] is another idea which is being investigated. These antibodies enable conversion of the enzyme–active site to a new proteinaceous 'image' on the antibody which should theoretically be capable of catalysis (Shchurov, 1997).

[3] An anti-idiotype antibody is an antibody that binds to another antibody and in particular to the binding site and as such contains an 'inverse image' of the binding site. The anti-idiotype antibody generated to an antigen–binding antibody is therefore like a 'protein image' of an antigen, if this is in turn bound by an antibody this should emulate the binding of the original enzyme binding site.

1.4 ENDOPHYTIC INFECTION OF GRASS

1.4.1 HISTORY OF ENDOPHYTE–INFECTED GRASS

The first documented case of grass infection by an endophytic fungus[4] and associated toxic properties was noted in the Bible. This first reference, estimated to have been written *c.* 50 AD, noted that fungus–infected seed of darnel (*Lolium temulentum* L.) was a toxic weed causing problems in both humans and livestock (Matthew 13:24–40). There is strong evidence to suggest that darnel toxicosis existed in pre–recorded time. Darnel seed from 4000 -year old Egyptian archaeological material has been shown to contain an endophytic fungus (Bacon 1995, and authors therein).

In the Middle Ages, ingestion of ergot[5] from endophyte–infected edible rye (*Secale cereale*) caused severe health problems that ravaged Europe in epidemic proportion (Beardall *et al.*, 1994). Symptoms resulting from ingestion of contaminated rye have been traditionally divided into two forms[6]. One form, gangrenous ergotism, was described as *'a great plague of swollen blisters which consumed the people by a loathsome rot so that their limbs were loosened and fell off before death'* (Tfelt-Nansen *et al.*, 1995 and authors therein). The other form, convulsive ergotism, was described as *'a fire which twisted the people'* (or St Anthony's fire) (Tfelt-Nansen *et al.*, 1995 and authors therein). Gangrenous ergotism was seen mainly in France while the convulsive form was seen in Germany; both forms occurred in Russia. It is thought that the geographic distribution of the two forms was diet–related (Tfelt-Nansen *et al.*, 1995).

Up until the nineteenth century large ergot–induced epidemics occurred throughout Europe. Those afflicted often sought the aid of the patron saints, most notably St Anthony, presumably due to the miraculous cures evidenced in those who made their pilgrimage to his

[4] An endophytic fugus is one that lives within a host grass
[5] The term ergot describes the darkened brown horn shaped pegs (sclorotia) found in the ears of rye in place of the rye grains. These are the compact interwoven hyphae (filaments of filamentous fungi of *Claviceps pupurea*
[6] Both forms are thought to be different physiological aspects of the same disease.

shrine in France. The full recovery following pilgrimage was thought to be due to the local diet being free from ergot (Mann, 1992). The connection between eating bread containing ergot and subsequent symptoms was realised in the seventeenth century. Evidence was largely ignored and offers to exchange good for diseased rye were often rejected by peasants who preferred to use their own grain. As a result, epidemics became more severe and frequent (Tfelt-Nansen *et al.*, 1995).

It was not until improved agricultural practises and increased usage of alternative crops, such as potatoes and wheat, became commonplace that the incidence of ergotism began to decline. This decline did not occur until the beginning of the nineteenth century (Tfelt-Nansen *et al.*, 1995). It is thought that the famous 'bewitchings' in the American town of Salem in 1691 may have been due to a mild outbreak of ergotism (Mann, 1992).

1.4.2 THE MODERN VIEW

Tall fescue, (*Festuca elatior arundinacea)* or 'Kentucky 31', the major grass species in the United States, was noted to have adverse effects on cattle in the colder New Zealand climates. The disease termed 'fescue foot' was noted to resemble ergotism (Cunningham, 1948). As early as 1956 Maag *et al.* (1956) noted the presence of ergot alkaloids in grass associated with cattle lameness but did not find ergot sclorotia.

Fescue toxicosis, including 'fescue foot' and 'summer fescue toxicosis' is associated with poor cattle performance despite the high quality of forage (Bacon, 1995, and authors therein). As early as 1941, Neill (1941) noted the presence of endophyte in both tall fescue and lolium grasses, however, animals grown on feed containing endophyte–infected seed showed no adverse effect. Of particular note is Neill's comment that *'endophytic hyphae present in Festuca arundinacea closely resemble that of Epichloe typhina'*. Cognisance of this point could have sped up research in this area by decades.

However, it was not until 1977 that Bacon *et al.* (1977) noted that *Epichloe typhina* was present in tall fescue and might be involved in the toxicity syndrome. This was

substantiated by Hoveland *et al.* (1980) who showed that toxicity was indeed associated with presence of endophyte. Initially, the tall fescue endophyte was classified as a non–sporulating (or symptomless) *Epichloe typhina.* This was later challenged and the fungus was renamed *Aremonium coenophilum* (Morgan-Jones *et al.*, 1982). Following discovery of a tall fescue endophyte, a similar endophyte was located in perennial ryegrass (Fletcher *et al.*, 1981) and was subsequently named *Acremonium lolli* (Latch *et al.*, 1984). The toxin lolitrem B, which was later found to cause ryegrass staggers was discovered in endophyte infected perennial ryegrass in 1984 (Gallagher *et al.*, 1984). Lolitrem B was also found in tall fescue (Christensen *et al.*, 1993; Siegel *et al.*, 1990). It was not until 1985 that the ergot alkaloid toxins were reported *in planta* for tall fescue (Yates *et al.*, 1985) and in endophyte–infected ryegrass (Rowan, 1987). The link between grass–endophyte and the production of the toxic ergot alkaloids had been made and became an area of intense research.

The name of the *Acremonium* species endophyte was again changed, on the results of genetic studies (Glenn *et al.*, 1996), to *Neotyphodium.* Symbiotic interactions of grasses with a fungal endophyte, either *Epichloe* species or their asexual relatives *Neotyphodium,* generally provide the host with major fitness enhancements (Scott *et al.*, 1993; Bush *et al.*, 1997, and references therein). The endophyte is thought to help protect the plant from both biotic and abiotic stress. Documented enhancements to host fitness include greater resistance to mammalian and insect herbivores, pathogens and nematodes, and drought. The mechanisms for these benefits are not well understood, however, it is thought that the anti–herbivore fitness enhancement is due to endophytic production of four groups of alkaloids: lolines, peramine, lolitrems and the ergot alkaloids (Bush *et al.*, 1997).

The life cycles of the grass–endophyte symbiota are intimate. Each has one of three possible life histories:

- pure vertical transmission of endophyte[7],
- pure horizontal transmission of endophyte[8],
- or a mixture of vertical and horizontal transmission

The asexual *Neotyphodium* species is only able to function using pure vertical transmission involving highly efficient clonal growth in flowering meristems, seeds, ovules and finally progeny seedlings of the infected 'mother' plant. However, in contrast the purely horizontal transmission strategy of some *Epichloe* species relies on production of contagious sexual spores. This strategy involves production of a fungal structure (stroma) which is produced surrounding the grass flagsheath. Once the stroma is produced the inflorescence of the affected tiller ceases development. The resulting suppression of seed production is called 'choke disease'. With most pathogenic *Epichloe* species, the host seed production is stopped and the host can no longer be a vehicle for dissemination of the endophyte. The endophyte must therefore spread in a sexual horizontal manner. Other *Epichloe* use a balance of both vertical and horizontal transmission. These fungi choke some flowering tillers but leave the majority unaffected and fertile. Thus they are also transmitted in almost all seed produced in infected 'mother' plants (Bush *et al.*, 1997).

1.4.2.1 THE ALKALOIDS FOUND IN *NEOTYPHODIUM*

The grass–endophyte symbiosis produces bioprotective alkaloids: pyrrolizidines, pyrrolopyrazines, indole-diterpines and the ergot alkaloids. The pyrrolopyrizidines, or 'lolines', are potent insecticides (Rowan *et al.*, 1994), as is the *Neotyphodium* pyrrolopyrazine peramine which seems to have no effect on mammalian herbivores. The indole-diterpine alkaloids include the tremogenic neurotoxins, known as the lolitrems, which are implicated in the sheep disease 'ryegrass staggers' (Latch *et al.*, 1984).

[7] Vertical transmission describes clonal reproduction and involves fungus invading the seed of the host species and being disseminated with seed dispersal.
[8] Horizontal transmission describes obligately sexual reproduction with dissemination via a fly species vector.

Ergot Alkaloids

It was the ergot alkaloids that were to be the focus of the work conducted in this study so they will be discussed in some detail (Fig 1.36). The major reason for interest in the ergot alkaloids lies in the supposition that ergopeptine alkaloids are a major factor in fescue toxicosis. While this is yet to be unequivocally established due to scarcity of compound, the symptoms displayed by grazing animals are similar to those found for animals grazing on grass containing other ergot alkaloids (Griffith *et al.*, 1978). These symptoms include: reduced weight gain, elevated body temperature, restricted blood flow (vasoconstriction), reduced reproductive efficiency, and reduced milk production (Strickland *et al.*, 1993; Ball *et al.*, 1993; Maag *et al.*, 1956; Oliver, 1997). The ergopeptine compound ergovaline[9] is the major ergot alkaloid in endophyte–infected tall fescue and perennial ryegrass (Fig. 1.36). These *Neotyphodium*–infected grasses typically contain 0.5-3.0 $\mu g\ g^{-1}$ of ergovaline, although much higher concentrations have been detected (Lane *et al.*, 1997). Recent investigations using ergovaline at *in planta* concentrations did not entirely reproduce the effects of animals grazing on infected plant material (Gadberry *et al.*, 1997). There exists the possibility that some or all the ergot alkaloids may act in a synergestic way resulting in a physiological response dissimilar to the individual parts. The modes of action of the ergot alkaloids suggest an endocrine effect supporting a dopaminergic mechanism for toxicity. In addition the ergot alkaloids provide host protection from insect predation (Ball *et al.*, 1997; Prestidge *et al.*, 1993; Yates *et al.*, 1989).

1.4.2.2 REASONS FOR INTEREST IN THE ERGOT ALKALOIDS

Tall fescue is the major forage grass (over more than 14 million ha) grown in the United States which has an estimated loss of income due to fescue toxicosis of ca $600 million US (Joost, 1995). Perennial ryegrass, New Zealand's (NZ) most important pasture species, contains a similar *Neotyphodium* endophyte producing the same type of ergopeptine compounds. Both the US and NZ would benefit hugely if a means of combating grass–endophyte toxicosis were available. One approach would be to genetically engineer an

[9]Ergot alkaloids occurring as lysergic acid amides occur as an epimeric pair due to isomerisation at the C-8 position

endophyte which does not produce ergot alkaloids, however this is not a desirable option as it would appear that many of the anti-insect qualities are related to ergopeptine presence (Ball *et al.*, 1997). Another possible solution would be to create an antibody vaccine which could render ergopeptine compounds non–toxic to grazing livestock.

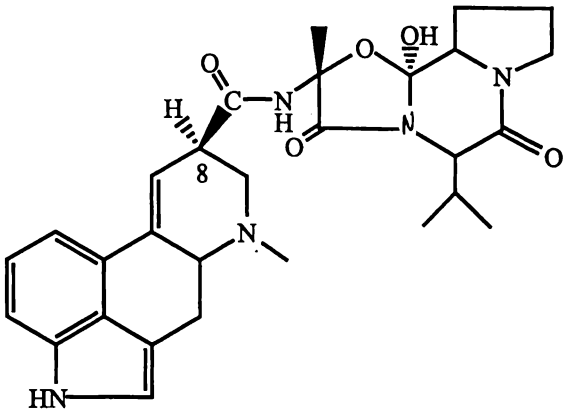

Figure 1. 36 The ergot alkaloid ergovaline..

1.5 ANTIBODY VACCINES

It was the assumption that the toxicity of perennial ryegrass and tall fescue is due largely to the presence of endophyte–produced ergot alkaloids, primarily the ergopeptines, that led to the proposal of the project. The aim of the project was to produce a hapten capable of eliciting catalytic antibodies capable of ergopeptine hydrolysis. This hapten could then be used to vaccinate grazing livestock and protect against ergopeptine compounds.

The use of antibody vaccines is not new, Chanh *et al.* (1990, 1991) have successfully generated an anti-idiotype vaccine that protected against trichothocene mycotoxins. Work by Ralph *et. al* (1990) suggests success in the generation of an anti–lupinosis vaccine. Antibodies that bind the lysergic moiety of ergovaline have been shown to affect serum prolactin levels[10]. When steers grazing on endophyte–infected tall fescue were immunised with mouse monoclonal antibodies able to bind ergovaline, an increase in prolactin levels

[10] Prolactin concentrations are frequently decreased in stock grazing on *Neotyphodium* infected grass and is thought to be linked to a decrease in animal welfare.

was noted suggesting that the antibody binds up ergovaline in the bloodstream preventing at least this aspect of grass toxicosis (Hill *et al.*, 1994).

However, in many cases antibody vaccination does not appear to work. Toxicity of zearalenone (a fusarian toxin) in gilts is actually increased when zeralenone–binding antibody is injected (MacDougald, 1990). In ewes, zearalenone causes reduced rates of estrus, ovulation and lambing. When ewes are vaccinated against zearalenone a further drop in reproductive performance is noted (Smith, 1992). One possible interpretation for these results may be that the antibodies decreased the rate of zearalenone metabolism. A similar attempted antibody protection trial against the mycotoxin sporidesmin also failed to protect animals from challenge (Fairclough *et al.*, 1984).

As an example of some of the practical problems associated with an antibody vaccine toward a low molecular weight toxin, consider the following:

- each day the animal consumes 1 mg of toxin with a molecular weight of 500
- an antibody has two binding sites (molecular weight 75,000 per active site),
- so 150 mg of antibody would be needed each day to bind the 1 mg of toxin

This is a best case scenario, since if antibodies are saturated, the toxin is still available to mediate a biological response. In some cases the antibody is found to give a more toxic effect possibly through concentration of toxin in places like the liver. In any case, antibody binding of the toxin increases toxin half–life by an order of magnitude (Fairclough *et al.*, 1984). A large improvement on the traditional antibody vaccine would be for the antibody to posses the ability to hydrolyse the toxin and render it non–toxic.

1.5.1 A CATALYTIC ANTIBODY VACCINE

The concept of a catalytic antibody vaccine is not new but a successful example is yet to be developed (Green *et al.*, 1991) The ergopeptine compounds contain an amide link between the lysergic acid portion and the cyclic tripeptide moiety (cyclol), which is a possible site for catalytic antibody cleavage (Fig. 1.39). If a suitable transition–state emulator for

hydrolysis of this bond could be produced, then grazing livestock could be to immunised with this material. This should enable the vaccinated livestock to produce an *in vivo* catalytic antibody capable of hydrolysing the ergopeptine compounds and thus rendering them non–toxic. The hydrolysed ergopeptine would produce lysergic acid and a cyclic tripeptide. Lysergic acid is found to be pharmacologically inactive (Bossier, 1978). The cyclic tripeptide is very base sensitive and degrades rapidly in aqueous systems (Smith, F. 1998, pers. comm.) so is not expected to mediate a biological response before metabolism.

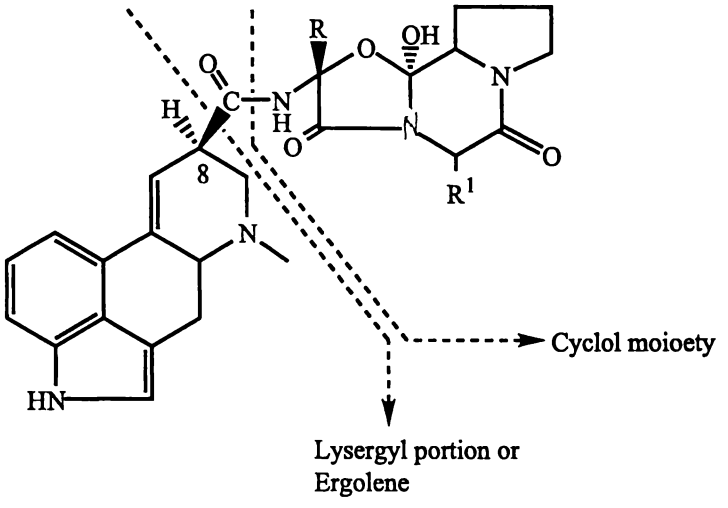

Figure 1. 37 The general structure of an ergopeptine compound.

The financial loss to agriculture due to the ergopeptine compounds is thought to be enormous. If this loss could be decreased or removed, the economic rewards, particularly for an agricultural–based economy like that of New Zealand, would be significant. The aim of the project was to create a hapten which causes the production of antibodies capable of hydrolysing ergopeptine compounds. Immunisation with this hapten should therefore enable protection of stock from ergopeptine material.

Every bond you break,
every step you take,
I'll be watching you.

The Police

CHAPTER 2

TOWARD GENERATION OF A TRANSITION–STATE EMULATOR

2.1 INTRODUCTION

To generate a successful hydrolytic catalytic antibody vaccine against ergopeptine compounds it is first necessary to generate a suitable transition–state emulator. In this case a successful transition–state emulator should chemically resemble the transition–state of the amidolytic reaction. In the ergopeptine compounds the cyclic tripeptide moiety is linked, via an amide bond, to the lysergic acid portion of the molecule (**A**, Fig. 2.1). As discussed in Chapter One, catalytic antibody cleavage of an amide bond is an attractive option for a number of reasons:

- amidolytic hydrolysis of nitroanilide derivatives is amongst the more successfully generated and characterised set of catalytic antibody reactions,
- the dissimilarity of the reactants to the products and high charge density of the transition–state make a favourable immune response likely,
- if a suitable amidolytic catalytic antibody can be generated against ergopeptine compounds the two products of the reaction are believed to be non-toxic *in vivo* (Bossier 1978; Smith, F. 1998, pers. comm.).

The amide–hydrolysing catalytic antibodies cited in the literature generally possess a tetrahedral phosphorus, instead of the carbonyl carbon of the amide linkage which is to be cleaved. This might suggest that a compound like **B** (Fig. 2.1) could be used to generate an ergopeptine–hydrolysing antibody. However, when the mechanism of amide hydrolysis (as described in Chapter One) is considered, it seems unlikely that **B** would be a successful

transition–state emulator, as the previously generated amide–hydrolysing antibodies were designed to cleave the amide of a nitroanilide moiety. The cleavage of a nitroanilide amide differs from the cyclol cleavage of an ergopeptine compound because, unlike for an ergopeptine, the rate limiting step for hydrolysis is not the ability to protonate the nitrogen of the leaving group, but the ability to form a tetrahedral transition–state involving attack of water at the carbonyl of the amide (Thomas, 1996; Blackburn *et al.*, 1993). As yet, there are no synthetic examples of non–aromatic secondary amide hydrolysing antibodies. This situation would need to be rectified if antibody ergopeptine hydrolysis were to be realised.

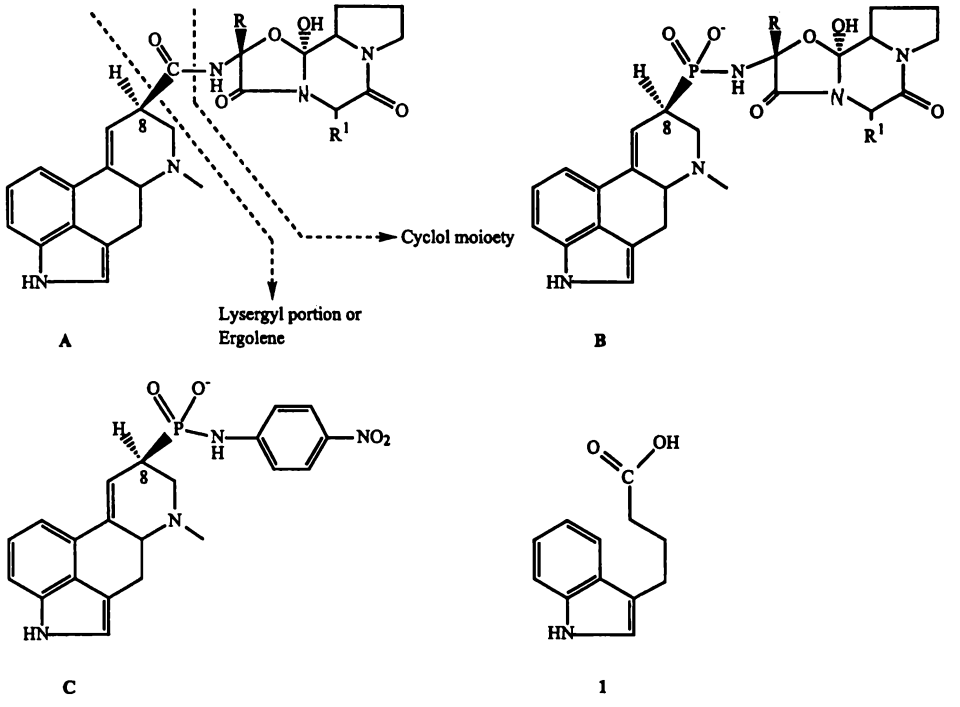

Figure 2. 1 Possible transition–state structures for hydrolysis of ergopeptine or similar model compounds.

To give a general understanding of the chemistry and problems likely to be encountered in generating a catalytic antibody capable of hydrolysing ergopeptine compounds it was decided that initially a catalytic antibody would be generated that was capable of hydrolysing a lysergyl–nitroanilide model compound **C** (Fig. 2.1). An ideal lysergyl–nitroanilide model compound would have an intact lysergyl portion, to induce antibody recognition and specificity for the ergopeptine group, while the nitroaniline moiety would

provide a useful spectrophotometric 'label' (Gallacher *et al.*, 1992). The nitroaniline moiety is expected to elicit a good immune response (Roitt, 1988) and provide a good leaving group for amidolysis (Thomas, 1996; Blackburn *et al.*, 1993). A tetrahedral phosphorus group, in place of the carbonyl of the amide linkage, should enable generation of an antibody capable of hydrolysing the nitroanilide moiety (Janda *et al.*, 1988a). Conjugation of the lysergyl–nitroanilide hapten could take place through the nitrogen in the lysergic portion using a N, N'-dicyclohexylcarbodiimide reaction (Ranadive *et al.*, 1976).

The lysergyl–nitrophosphonanilide compound **C** (Fig. 2.1) could be synthetically achieved by:

(i) halogenation of lysergol,

(ii) subsequent elimination of the halogen with replacement by a phosphorus diester,

(iii) generation of the monohalogenated phosphorus monoester

(iv) reaction of (iii) with 4-nitroaniline and,

(v) generation of the desired phosphorus acid compound with trimethylsilylbromide

This is a gross simplification of the synthetic steps (Fig. 2.2) that would be required for a successful generation of compound **C** as many of the reagents and reaction conditions may lead to cross–reaction with the lysergyl moiety, thus significant protection and deprotection would be required to avoid these problems.

Due to the significant synthetic difficulties associated with using a lysergyl moiety, (not to mention the problems of expense and availability) it was decided to further simplify the situation by using compound **1** (Fig. 2.1). Compound **1** possesses the indole present in the lysergyl moiety and is the portion most likely to cross–react. It should therefore give an indication of the circumstances under which protection reactions protection of the lysergyl moiety would be necessary. The indole system contains an easily detectable

fluorescent moiety (Wehry, 1976), is far less expensive than lysergol, and would enable gram–scale reactions.

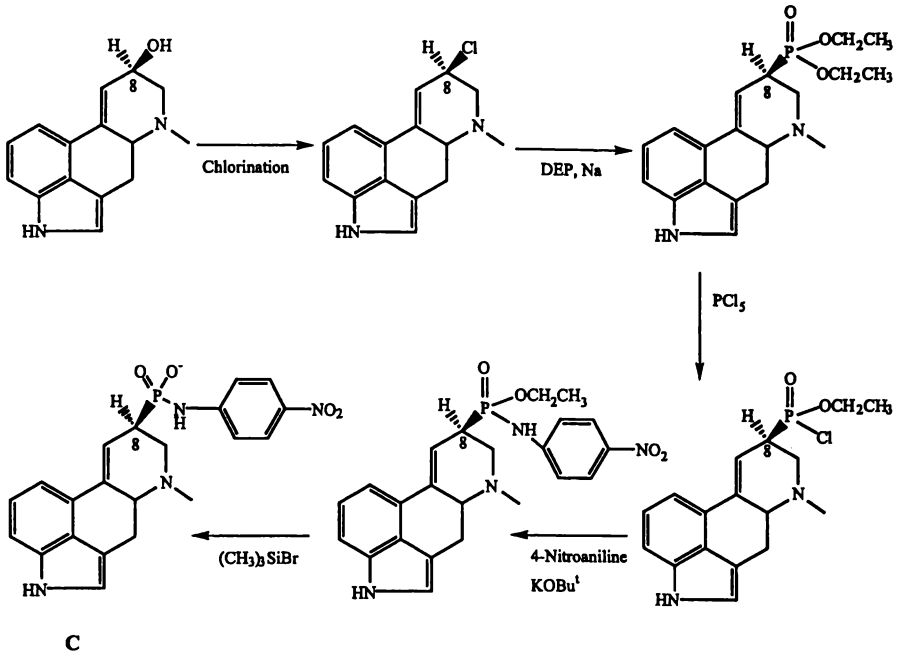

Figure 2. 2 Proposed general synthetic pathway for production of a lysergyl 4-nitrophosphonanilide (C).

2.2 DISCUSSION

2.2.1 INDOLE SYSTEM

Using compound **1** as a model of the ergolene moiety of an ergopeptine, the generation of a tetrahedral phosphonamide indole compound was attempted (Fig. 2.3). The acid-**1** is conveniently converted to ester-**2** in good yield using acidic methanol. NMR spectra show a shift of the carbonyl signal from δ ^{13}C 180.1 to 174.5, and appearance of new methoxy signals at δ ^{13}C 51.6 and δ ^{1}H 3.71. These signals are consistent with formation of a methyl ester (Breitmaier *et al.*, 1987). Further characterisation of **2** using GC–MS gave a molecular ion consistent with the desired product. Previous formation of both methyl-**2** and ethyl esters has been described by Jackson et al. (1930) but in that case was achieved in the process of synthesising the indole compound using a Fischer ring closure. The

melting point obtained for compound **2** was consistent with that noted by Jackson *et al.* (1930).

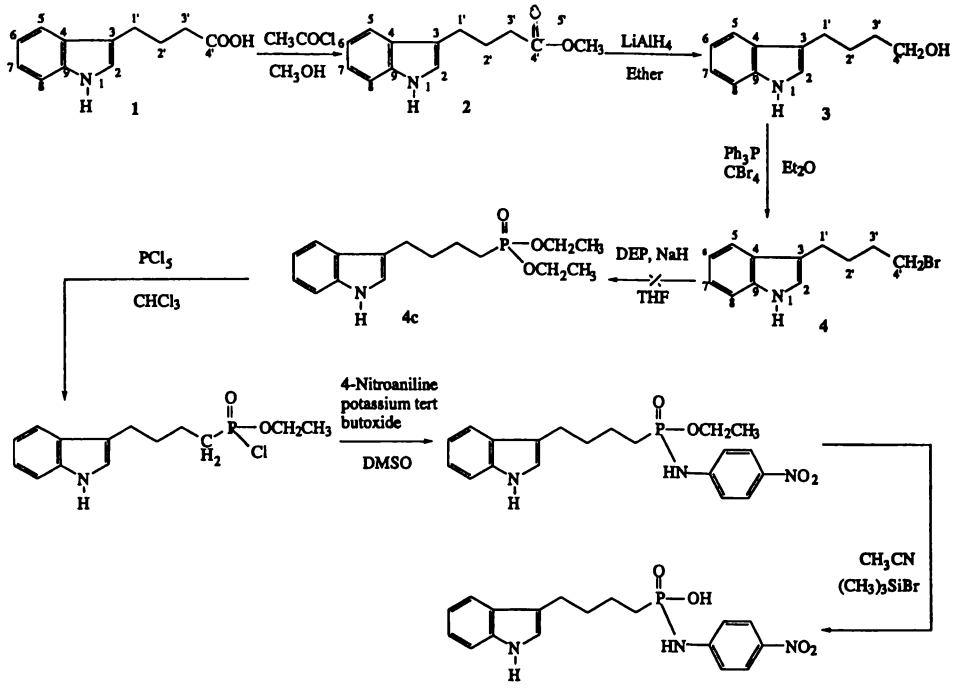

Figure 2. 3 Proposed synthetic pathway for the indole model system.

Attempts at direct reduction of acid-**1** with lithium aluminium hydride gave alcohol-**3** in low yield. For this reason acid-**1** was converted to ester-**2**, and **2** was converted to alcohol-**3** in reasonable yield. NMR spectra show loss of the signals associated with a methyl ester and new signals, at δ ^{13}C 62.9 and δ ^{1}H at 1.94, consistent with formation of the desired alcohol-**3**. Formation of **3** has been previously described by Jackson *et al.* (1930) but in that case the synthesis was conducted on a larger scale and it made use of metallic sodium. The melting point could not be compared with that described by Jackson *et al.* (1930) as attempts at crystallisation of (**3**) failed.

Attempts at chlorination of alcohol-**3** using thionyl chloride were abandoned when it become apparent that the thionyl chloride was attacking the indole and possibly dehydrating the butyl side chain. Some of the desired chlorinated product was thought to be produced (^{1}H, ^{13}C NMR and GC–MS) but it proved difficult to separate from the large

number of by–products generated. A mild ylide bromination performed in a similar manner to that described by Hooz *et al.* (1968) was investigated. This reaction gave the desired bromide-**4**, and should be applicable for bromination of the lysergol moiety. Formation of the bromide-**4** showed the expected shift of the signals in the NMR spectra, δ ^{13}C from 62.9 to 31.7 and δ ^{1}H from 3.67 to 3.45. Negative ion mode ESI–MS of compound **4** gave a triplet isotope pattern centred about 332.4 m/z which is consistent with compound **4** and an associated bromide ion. Compound **4** has been synthesised previously by Suvorov *et al.* (1973) using Br_2 and HgO and more recently by the same author using bromination of the corresponding alcohol using PBr_3 (Suvorov *et al.*, 1975).

The attempt to generate diethyl 4-(4-indolyl)butylphosphonate was not successful using the sodium diethylphosphite (DEP) reaction. Many variations on the reaction conditions described in the experimental section were conducted: various mole ratios of reactants, more scrupulous solvent drying, but the reaction refused to proceed. It was decided to test if the reaction conditions employed were suitable for formation of an alkyl phosphonate or whether the indole moiety was complicating the reaction in some unforseen manner. Using the same reaction conditions as described in the experimental section but substituting butyl bromide for compound **4** the reaction was repeated. The reaction was found to proceed but the yield of compound **4a** was low which may have been due to low solubility problems of the diethyl phosphite sodium salt (Kosolapoff, 1945). NMR spectra showed large changes in both the ^{1}H and ^{13}C spectra due largely to the coupling of the ^{31}P with the ^{13}C and ^{1}H environments of the butyl moiety. The chemical shift data of both ^{1}H, and ^{13}C NMR for compound **4a** are in reasonably agreement with that described by Ludger (1977). Most ^{13}C chemical shifts were within δ ± 2, despite the NMR experiments being conducted in different solvents. The large coupling of the signal at δ ^{13}C 30.0, ^{1}J (^{13}C-^{31}P) 140.4 Hz, associated with the methylene group next to the phosphorus, is diagnostic for the formation of a CH_2P bond and compares well with 140.7 Hz described by Ludger (1977) for this compound. The longer range couplings $^{2\text{-}4}J$ (^{13}C–^{31}P) are again similar to those described by Ludger (1977), thus confirming formation of compound **4a**.

The inability to form the 4-(4-indolyl)butylphosphonate compound using the same conditions that were successful for generation of compound **4a** suggested that the indole moiety was influencing the reaction. Attempts to protect the indole nitrogen via formylation or acetylation were unsuccessful. It was decided that investigation of an even simpler aromatic system would be beneficial to better understand the problem of phosphonate formation.

2.2.2 THE AROMATIC SYSTEMS

2.2.2.1 4-AMINO BENZOIC ACID SYSTEM

As a very simple model of the indole system a bifunctional benzene system was desired. One functional group of the ring was used for addition of the phosphorus moiety while the other was suitable for later conjugation to a protein. It was thought that 4-amino benzylalcohol would be a suitable system. As this compound was not readily available it was decided to try to synthesise it from 4-amino benzoic acid.

Problems were experienced with the reduction of both the acid-**5** and methyl ester-**7** using lithium aluminium hydride. When both of these compounds were reacted with lithium aluminium hydride, toluide-**6** was formed, instead of the desired alcohol compound. The toluide-**6** was identified from the highly diagnostic methyl signals in the NMR spectra, δ ^{13}C 20.5 and δ ^{1}H 2.27 respectively. Hydrogenolysis has been noted previously in the 4-aminobenzoic acid system (Miles, 1983), as well as in other similar systems (Conover *et al.*, 1950). Compound **7** has been previously synthesised by Hosangadi *et al.* (1996) who used thionyl chloride to generate the acid chloride which was subsequently reacted with methanol in good yield. The ^{13}C NMR data for **7** are in good agreement ($\delta \pm 3$) with those previously described by Gould *et al.* (1979). The ^{1}H NMR data from the aromatic protons are very similar ($\delta \pm 0.1$) to those described by Shapiro *et al.* (1977).

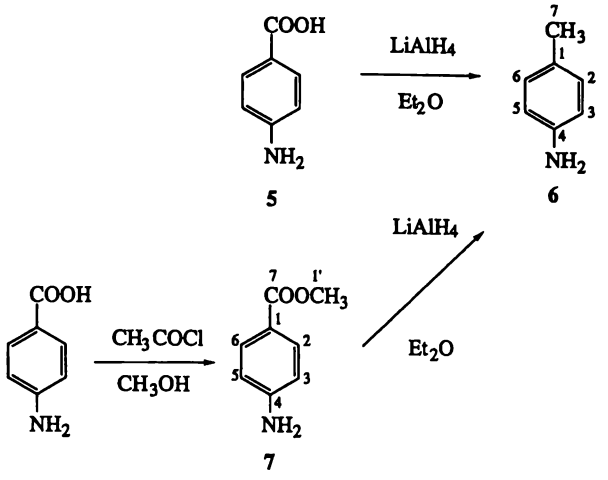

Figure 2. 4 Attempted formation of 4-aminobenzylalcohol which instead resulted in the production of compound **6**.

Another approach to generation of the 4-aminobenzyl phosphorus system would be to reduce the corresponding 4-nitrobenzyl phosphorus derivative. As problems were experienced with the addition of a phosphonate to the indole alkyl chain, it was decided to investigate whether the formation of the alkyl phosphonate could be conducted prior to investigating the reduction of the nitro group.

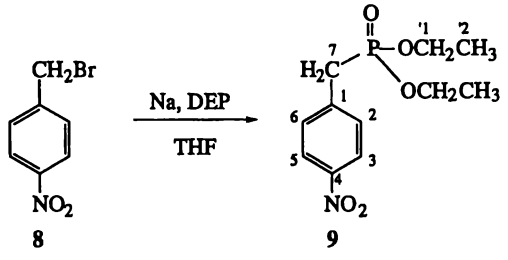

Figure 2. 5 Formation of compound **9** making use of sodium and diethylphosphite.

Compound **9** was generated in low yield giving a ^{31}P NMR signal at δ 24.9, and a ^{1}H spectrum with signals consistent with an aromatic and phosphorus ester environment. The characteristic coupling associated with CH_2–P bond formation was also evidenced. GC–MS of compound **9** detected the expected molecular ion. Compound **9** has been previously prepared in excellent yield by Kagan *et al.* (1958) using a benzyl halide and triethyl phosphite with subsequent conversion to the 4-nitro derivative by reaction with a nitric acid–sulphuric acid mixture. The same author managed to produce the desired 4-

aminobenzylphosphonate product by reducing the 4-nitrobenzylphosphonate compound using Pd/C with the H_2 at 50 psi. Attempts to form 4-aminobenzyl phosphonate from compound **9** were not successful using Pd/C with a bubbling hydrogen atmosphere as these conditions were probably not forcing enough. Formation of the desired 4-nitrobenzyl bromide compound has also been previously achieved using catalytic hydrogenation of 4-bromobenzonitrile at 120 atmosphere pressure (Mravec *et al.*, 1975). As this system was proving synthetically challenging it was decided to investigate another system.

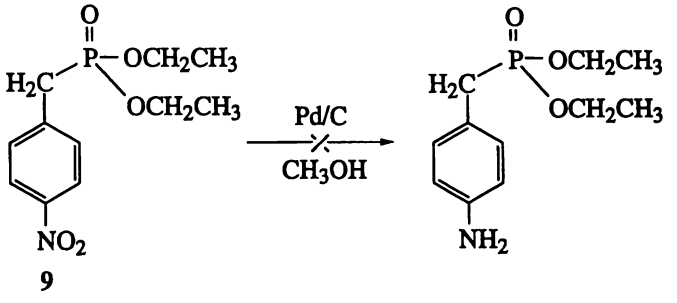

9

Figure 2. 6 Attempted generation of 4-nitrobenzylphosphonate.

2.2.2.2 THE BENZOYL PROTECTED SYSTEM

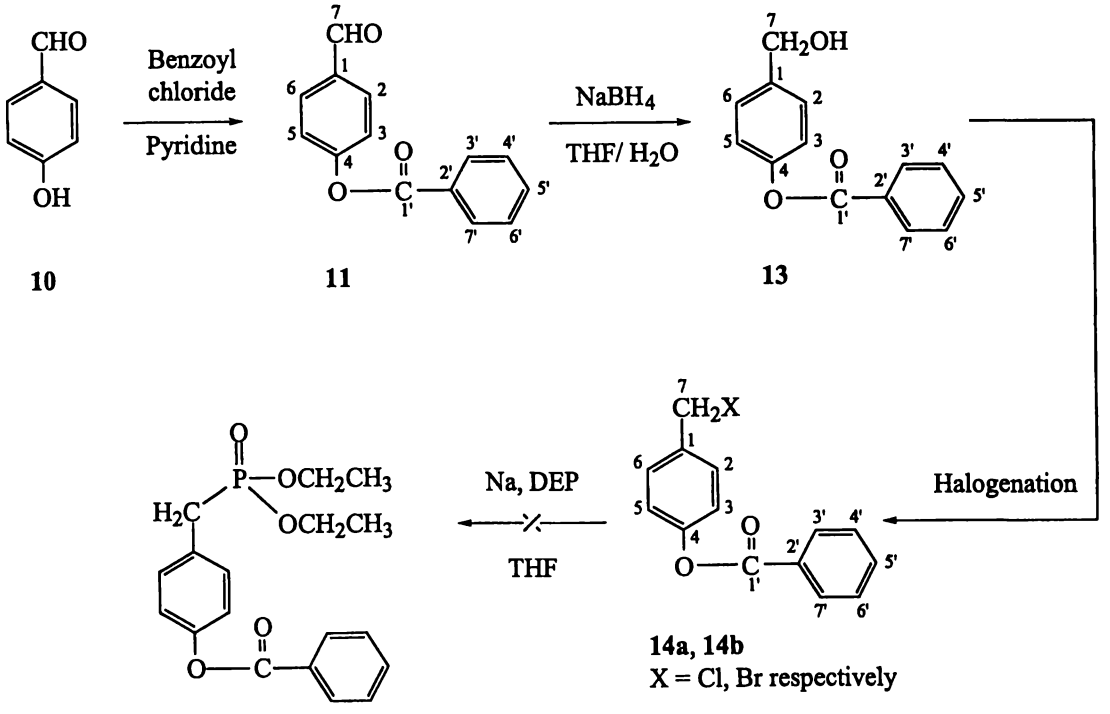

10 11 13

Figure 2. 7 Synthetic pathway used in the benzoyl protected system.

Benzaldehyde-**10** was reacted with benzoyl chloride giving the corresponding benzoyl ester-**11** in good yield (95%). The ^{13}C NMR spectrum shows the appearance of a signal at δ 164.4 and a shift of the signal δ 167.2 to 155.7 (4) consistent with the formation of an ester. ^{13}C NMR spectra showed an increase in aromatic environments from four to eight, along with the increase in aromatic signal integral evidenced in the ^{1}H spectrum. GC–MS gave detection of the expected molecular ion. The data for **12** are in good agreement with those previously described by Li *et al.* (1989) with a similar melting point and the same molecular ion detected via mass spectrometry.

Attempted reduction of benzoate-**11** in ethanol gave transesterification to the corresponding diethyl acetal-**12**. The ^{13}C NMR spectrum shows loss of the aldehyde signal δ 194.9 and appearance of signals associated with acetal formation (δ 151.0 (7), 61.2 (1") and 15.3 (2")). The 1" and 2" environment integrals are twice the intensity of other ^{13}C signals. The ^{1}H NMR spectrum shows: loss of the aldehyde signal δ 9.93, new signals associated with the acetal (1", 2") at twice the intensity of other proton signals and a new signal at δ 5.55 (7), consistent with formation of compound-**12**. The formation of compound **12** as the major product was confirmed using GC–MS and it was not further purified of characterised due to its irrelevance to the project.

Changing the solvent system of the reduction to THF–H_2O (1:1) produced the desired alcohol-**13**. The NMR spectra show loss of the aldehyde signal δ ^{13}C 190.9, ^{1}H 9.93 and appearance of a new signal at δ ^{13}C 64.4 as well as a broad signal at δ ^{1}H 3.28 consistent with reduction of the aldehyde-**11** to alcohol-**13**. GC–MS gave the expected molecular ion for alcohol-**13**.

Compound **13** was chlorinated using thionyl chloride to give compound **14a**. The NMR spectra show loss of signals associated with alcohol-**13** (δ ^{13}C 64.4, 3.28) and appearance of new signals (δ ^{13}C 45.7 and ^{1}H 4.61), consistent with formation of chloride-**14a**. The

GC–MS showed the expected molecular ion. Reaction of compound **14a** with DEP was conducted in the manner that had been successful for butyl bromide but again the desired product was not detected by NMR with only the starting materials being recovered. The lack of formation of the desired product was further investigated by making the more reactive bromide-**14b** in the hope that this would give the desired alkyl phosphonate.

The mild ylid bromination was used to generate the bromide-**14b** which was subsequently purified via preparatory plate chromatography (PLC) in modest yield (23%). The formation of the bromide-**14b** was evidenced with the loss of signals in NMR spectra associated with the alcohol (δ ^{13}C 64.4, ^{1}H 3.28) and appearance of signals consistent with alkyl bromination (δ ^{3}C δ 32.9, ^{1}H 4.52).

When compound **14b** was reacted with the DEP the desired alkyl phosphonate was not formed, suggesting that further examination of this step was required. To further simplify the system and facilitate investigation of phosphonate formation it was decided to use a system that could be considered essentially monofunctional. Later literature investigation found a method for formation of the desired alkyl phosphonate system (Tchani *et al.*, 1992) and the synthetic pathway used was as described herein, with the exception that triethyl phosphite (TEP) was used for generation of the alkyl phosphonate. Problems previously encountered with DEP were avoided in the subsequent synthetic pathway by using TEP for formation of the alkyl phosphonate.

2.2.2.3 ANISALCOHOL SYSTEM.

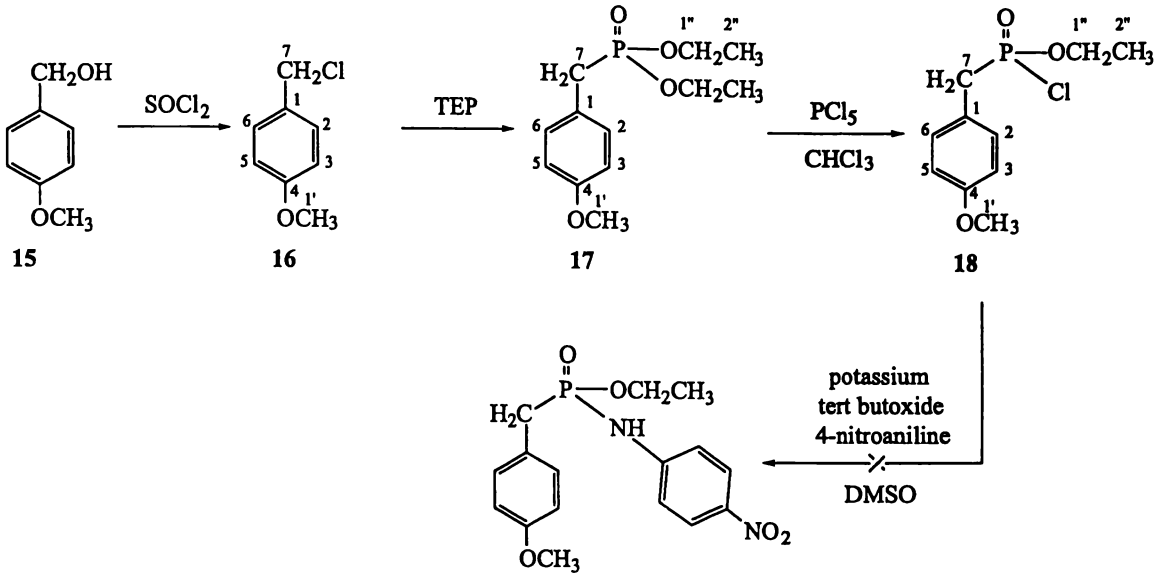

Figure 2. 8 Synthetic pathway used for the anisalcohol system.

Anisalcohol-**15** contains a methyl ether which is particularly stable and difficult to remove. This essentially meant that the anisalcohol system was monofunctional and was ideal for investigating the generation of the alkyl phosphonate.

The chlorination of alcohol-**15** proceeded well with pure compound **16** being obtained using fractional vacuum distillation. The NMR spectra showed changes in chemical shift consistent with change of the alcohol (δ ^{13}C 63.9, ^{1}H 4.47) to chloride (δ ^{13}C 46.1, ^{1}H 4.61). The ^{1}H NMR data for **16** are in excellent agreement ($\delta \pm 0.05$) with those previously described for this compound by Rivero *et al.* (1993). This synthesis has also been achieved in excellent yield using WCl_6 as a catalyst (Habib *et al.*, 1996).

Formation of phosphonate-**17** was initially trialed using sodium and DEP, however, monitoring of the reaction by ^{31}P NMR at various times by removal of a small aliquot of material from the reaction mixture indicated that the reaction had gone to approximately 40% completion. For this reason the DEP reaction mixture was refluxed for an additional 17 hours with triethyl phosphite (TEP). Again the reaction mixture was examined using ^{31}P NMR and found to have gone to compound **17** almost quantitatively. The residual

TEP was conveniently removed under reduced pressure distillation giving compound **17** in good yield (89%) and purity. Whether the TEP method would be suitable (with the harsh reflux conditions (158°C) for a lysergyl ring system is doubtful, but milder conditions of the lower yielding DEP method could be investigated for suitability with this system.

The ^{1}H, ^{13}C and ^{31}P NMR spectra of compound **17** following vacuum distillation (Fig. 2.9-2.11 respectively) showed the coupling characteristic of the alkyl phosphonate systems studied. There appears to be a minor phosphorus containing component which tends to appear superimposed or as a shoulder to compound **17** signals in the ^{1}H NMR spectrum. The ^{1}H NMR spectrum shows the characteristic pattern of signals found for a diethyl phosphorus ester compound, the extensively split multiplet at δ 3.98 (1"), the large coupled signal centred at δ 3.07 ^{1}J (^{31}P-^{1}H) 21.0 Hz (7) and the triplet methyl signal centred at δ 1.22 (2"). The formation of the phosphonate-**17** can be seen in the ^{13}C NMR spectrum along with a second minor component which also contains a ^{31}P environment indicated by the minor signals showing characteristic fine coupling. The ^{13}C NMR spectrum shows signals associated with compound **17** centred at δ 61.9 which compares favourably with that noted by Ludger (δ 61.1-62.6) in other benzyl phosphonates as does the coupling ^{2}J (^{31}P-^{13}C) 5.1 Hz (1', PO$\underline{C}H_2$) although Ludger notes a higher average value (^{2}J 6.3-6.7) (Ludger, 1977). The large coupled signal centred at δ ^{13}C 32.7 (7, $\underline{C}H_2P$) is in good agreement with the range described by Ludger for other benzylphosphonates (δ 30.3-33.8) as is the coupling constant ^{1}J (^{31}P-^{13}C) 139.0 Hz when compared to that found by Ludger (1977) (137.0-139.4 Hz). The signal at δ 16.3 (2') with coupling ^{3}J (^{31}P-^{13}C) 5.4 Hz is also in good agreement with the ranges described by Ludger for benzylphosphonates (δ 16.4-16.6, and 5.5-5.9 Hz). Comparison of the coupling constant obtained (^{1}J (^{1}H–^{31}P) 21.○Hz) with that described for the same compound was in good agreement ($^{1}J \pm 0.5$ Hz) (Fresneda *et al.*, 1981). Compound **17** has also been formed by Bellucci *et al.* (1987) by reaction of methyl iodide with the 4-hydroxybenzylphosphonate.

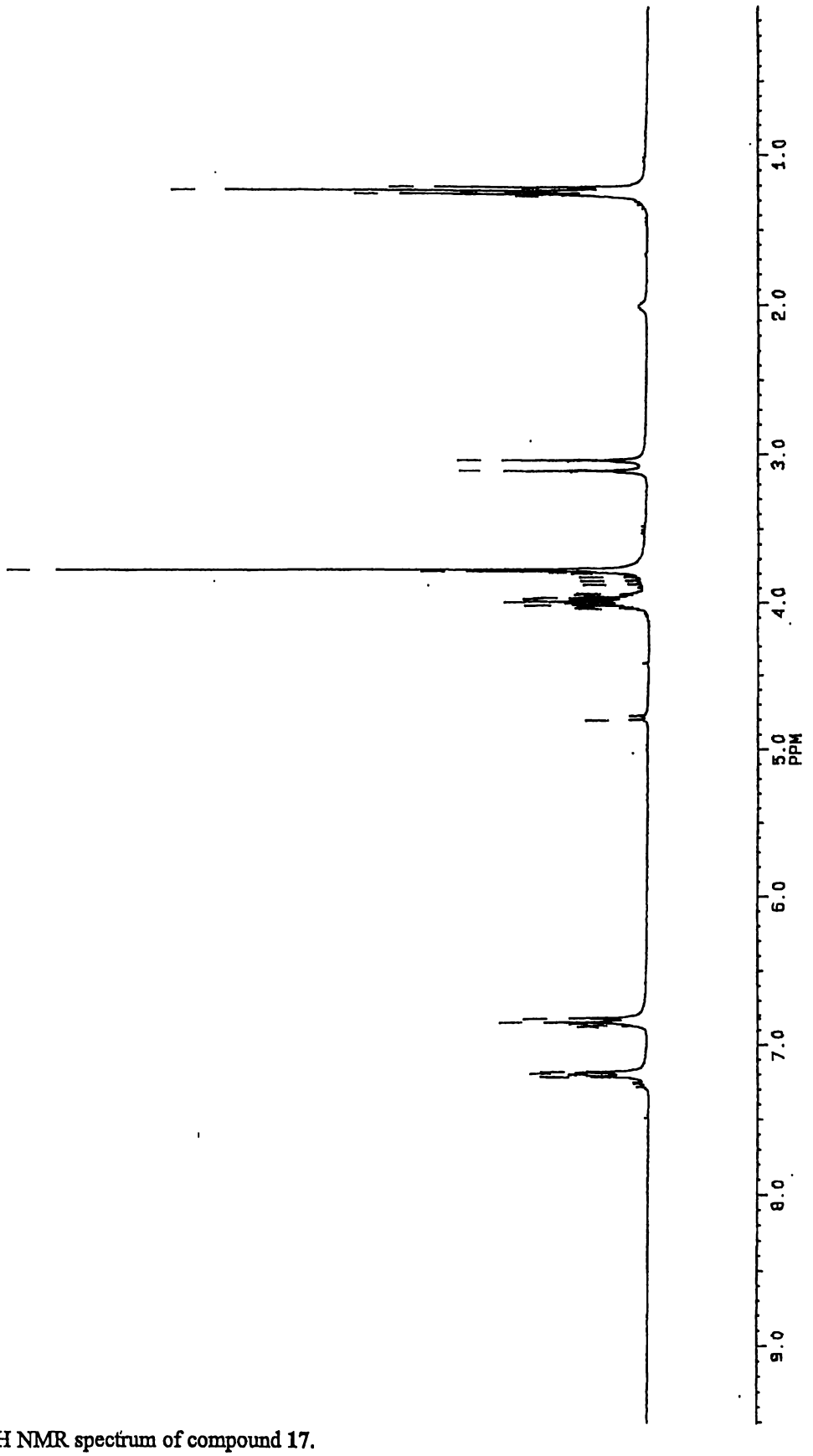

Figure 2. 9 ^{1}H NMR spectrum of compound **17**.

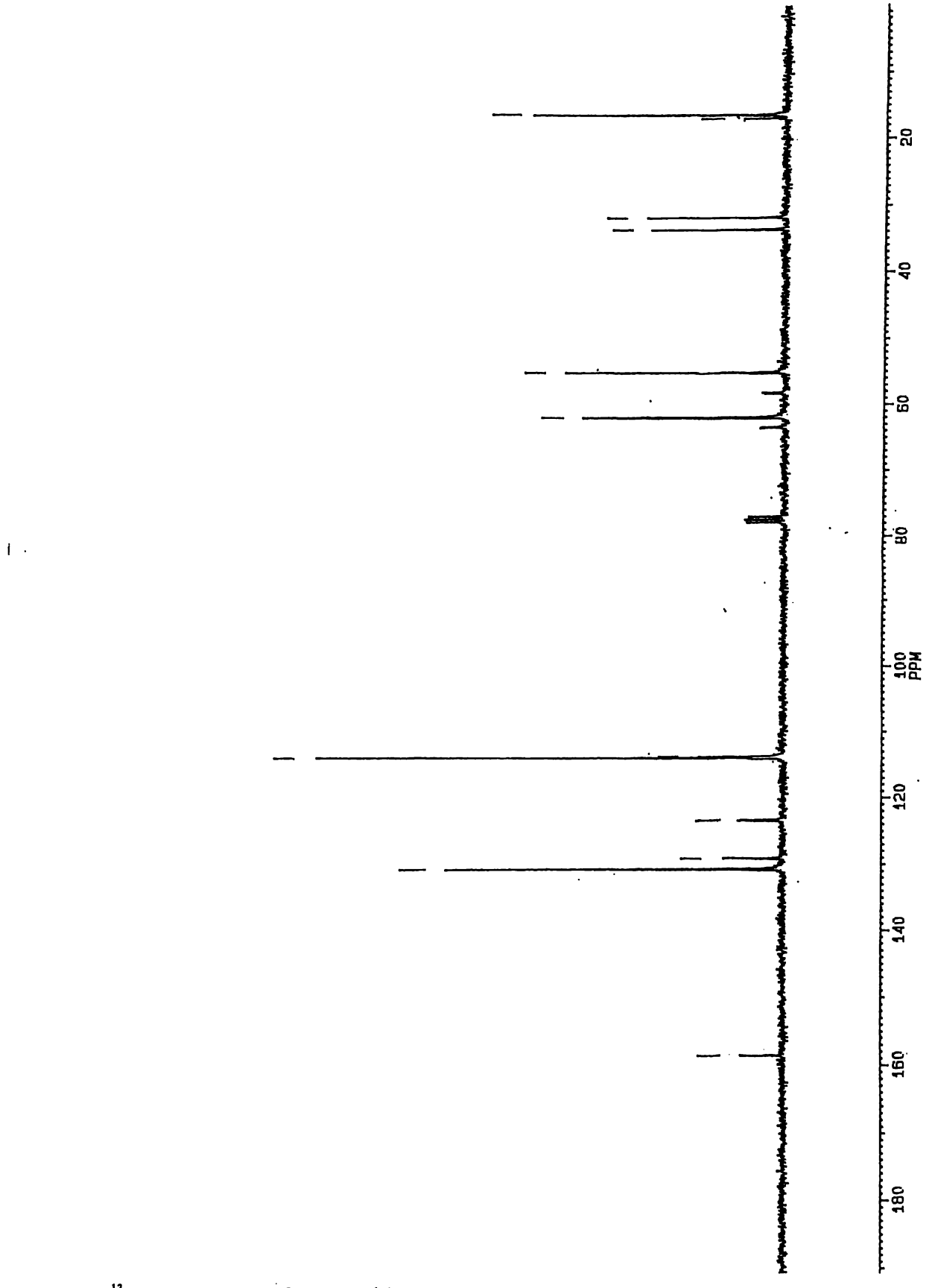

Figure 2. 10 ^{13}C NMR spectrum of compound **17.**

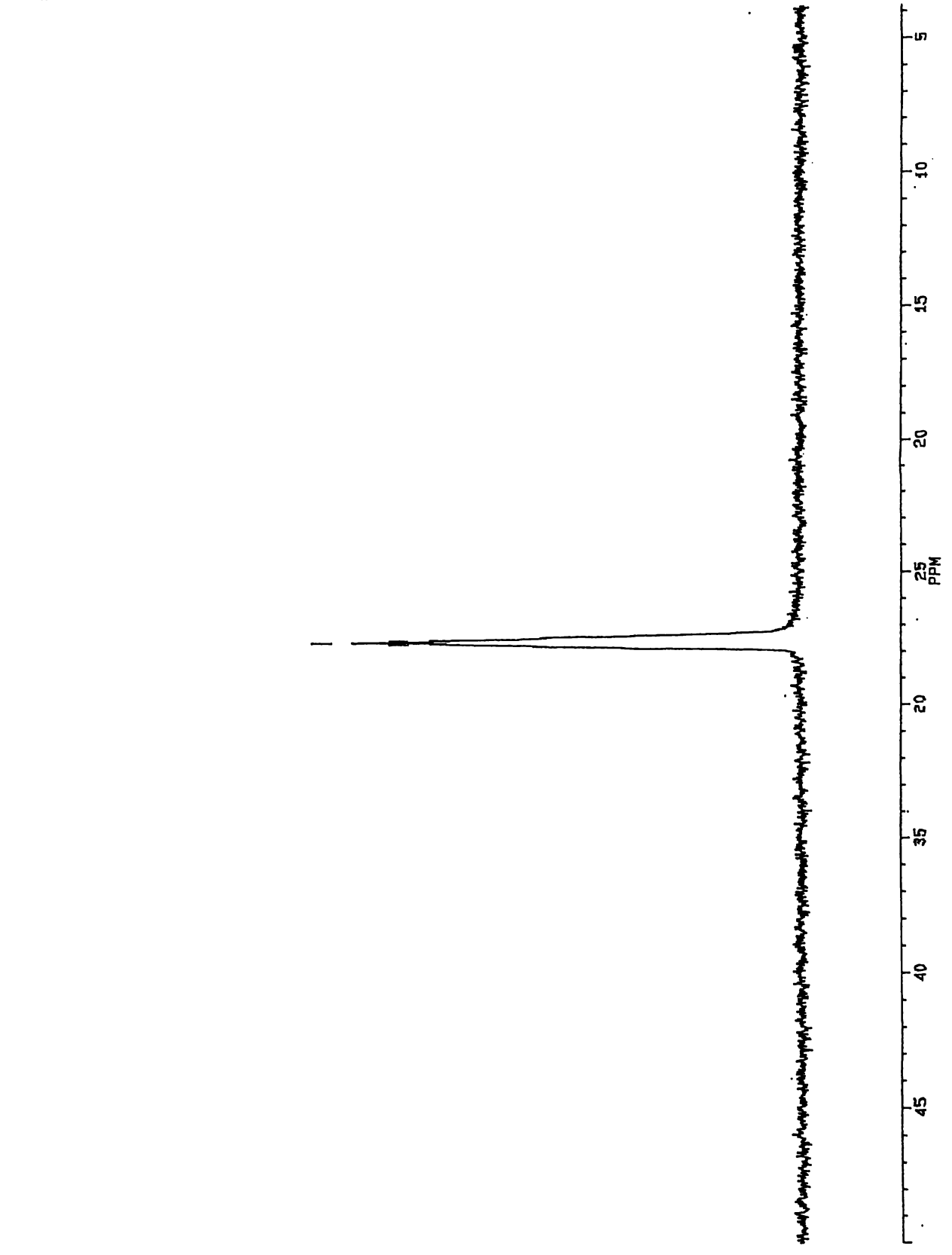

Figure 2. 11 Coupled ^{31}P NMR spectrum of compound **17.**

The ^{31}P NMR spectrum shows a multiplet centred at δ 27.6 with higher order splitting due to ^{31}P-^{1}H coupling. GC–MS gave the molecular ion and ESI–MS gave the $[M+H]^+$ and $[M+NH_4]^+$ species.

The NMR chemical shift and coupling data are highly diagnostic for the benzyl phosphonate systems that were subsequently investigated with both ^{1}H and ^{13}C NMR. The ^{13}C chemical shift values for the P-CH_2 environment were δ 32.1-40.2 with typical coupling constants ^{1}J (^{13}C–^{31}P) of 121.2-139.5 Hz (Table 2.1, 2.2). Long range phosphorus coupling was routinely detected ^{4}J (^{31}P-^{1}H) and was diagnostic in the assignment of aromatic systems particularly in the dibenzyl systems where the aromatic carbons are of similar chemical shift. The ^{1}H chemical shift values for the P-CH_2 environment were δ 3.02-3.45 with typical coupling constants ^{1}J (^{1}H–^{31}P) of 19.8-21.7 Hz (Table 2.3). The ^{1}H (Table 2.3) and ^{13}C NMR signals and coupling (Table 2.1 and 2.2) associated with the $POCH_2CH_3$ environment and ^{31}P NMR (Table 2.3) were also highly diagnostic for the systems investigated and agree well with those previously described by Ludger (1977).

As harsh synthetic conditions had already been used (for the formation of the C-P bond) it was again decided to use forcing conditions for the generation of phosphonyl chloride and improve yield so that study of the subsequent reactions could be conducted on a larger scale.

Using PCl_5, the chlorination of phosphonate-**17** proceeded almost quantitatively to give compound **18**. Evidence for the formation of the P-Cl bond is seen as a drop in intensity of signals associated with the ethyl group of the phosphorus ester in both the ^{1}H and ^{13}C NMR spectra. A drop in coupling constant of the ^{1}J ($^{13}CH_2$-^{31}P) from 139.0 to 121.1 Hz was also noted.

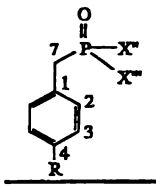

X'' is labelled as O-CH_2-CH_3 (1'' 2'')

Table 2. 1 ^{13}C NMR chemical shifts and coupling constants ^xJ (^{31}P-^{13}C) for benzylphosphonates

Compound	R	X', X''	δ 1	1, ^2J	δ 2	2, ^3J	δ 3	3, ^4J	δ 4	4, ^5J	δ 7	7, ^1J	δ 1''	1'', ^2J	δ 2''	2'', ^3J
17	OCH_3	OCH_2CH_3, OCH_2CH_3	123.4	9.1	130.7	6.3	113.9		158.5		32.7	139.0	61.9	5.1	16.3	5.4
18	OCH_3	OCH_2CH_3, Cl	121.1	10.8	131.2	7.5	114.2		159.2		40.2	121.1	63.8	8.6	15.9	6.9
22	$OCH_2C_6H_5$	OCH_2CH_3, OCH_2CH_3	123.6	9.3	130.6	6.5	114.8	1.6	157.6	2.9	32.1	139.0	61.9	6.9	16.2	5.9
23	$OCH_2C_6H_5$	OCH_2CH_3, Cl	121.5	10.8	131.3	7.5	115.2	3.5	158.5	4.3	40.3	121.2	63.8	8.6	16.0	7.1
27	OCH_2-($COOCH_2CH_3$)	OCH_2CH_3, OCH_2CH_3	124.7	9.3	130.8	6.5	114.8	2.1	156.9	3.6	32.7	139.2	62.0	6.7	16.4	5.7
28	OCH_2-($COOCH_2CH_3$)	OCH_2CH_3, Cl	122.4	10.5	131.3	7.5	115.1		157.5		39.7	121.5	63.8	8.6	15.9	6.9
29	NH_2	OCH_2CH_3, OCH_2CH_3	121.1	8.4	130.6	6.6	115.3	2.3	145.3		32.8	139.2	62.0	6.7	16.4	6.1
30	$NHCOCF_3$	OCH_2CH_3, OCH_2CH_3	128.1	8.9	130.2	6.5	121.3	2.1	135.5	3.8	32.9	139.5	62.4	7.1	16.2	5.7
31	$NHCOCF_3$	OCH_2CH_3, Cl	126.3	10.6	130.6	7.5	121.2	3.3	135.9	4.8	40.2	121.3	64.1	8.7	15.7	6.8

All compounds were $CDCl_3$ solutions and were referenced as described in the experimental section of this chapter.

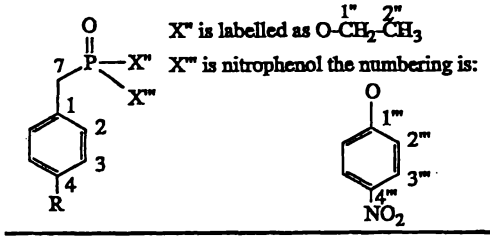

Table 2. 2 ^{13}C NMR chemical shifts and coupling constants ^{x}J (^{31}P-^{13}C) for benzylphosphonates

Compound	R	X",X"'	δ 1	1, ^{2}J	δ 2	2, ^{3}J	δ 3	3, ^{4}J	δ 4	4, ^{5}J	δ 7	7, ^{1}J	δ 1"	1", ^{2}J	δ 2"	2", ^{3}J
32	$NHCOCF_3$	OCH_2CH_3, $NHCH_2C_6H_5$	129.1	8.5	130.4	6.3	121.3		135.3		34.8	126.8	60.5	6.9	16.3	6.6
33	NH_2	OCH_2CH_3, $NHCH_2C_6H_5$	121.9		130.6	6.3	115.4		145.2		34.6	126.6	60.2	6.9	16.4	6.3
34	$NHCOCH_2$-CH_2-COOH	OCH_2CH_3, $NHCH_2C_6H_5$	121.2		130.3		120.2		137.1		33.7	125.6	60.7	7.0	16.2	6.6
35[d]	$NHCOCF_3$	OCH_2CH_3, $OC_6H_4NO_2$	127.2	9.7	130.4	6.9	121.3	2.3	135.6	3.8	33.1	139.4	63.9	7.5	16.1	5.6
36[e]	NH_2	OCH_2CH_3, $OC_6H_4NO_2$	118.7	9.8	130.7	6.7	115.3	2.4	146.2	3.0	32.9	139.4	63.5	7.3	16.3	5.9
37[c]	$NHCOCH_2$-CH_2-COOH	OCH_2CH_3, $OC_6H_4NO_2$	125.1	9.7	130.4	6.5	120.4		137.7	3.4	33.0	139.5	64.1	7.3	16.3	5.7
38[d, e]	$NHCOCH_2$-CH_2-COOH	OH, $OC_6H_4NO_2$	127.0	9.0	129.7	6.5	118.6		137.3		33.5	135.1				

All compounds were $CDCl_3$ solutions and were referenced as described in the experimental section of this chapter (except where noted otherwise)
d 1"' δ 155.3, 2"' δ 121.0 (^{3}J 4.5), 3"' δ 125.5, 4"' δ 144.6
e 1"' δ 155.9 (^{2}J 8.6), 2"' δ 121.0 (^{3}J 4.5), 3"' δ 125.5, 4"' δ 144.3
c 1"' δ 155.4 (^{2}J 8.9), 2"' δ 121.1 (^{3}J 4.4), 3"' δ 125.6, 4"' δ 144.6
d 1"' δ 156.0 (^{2}J 7.0), 2"' δ 120.7 (^{3}J 4.5), 3"' δ 125.2, 4"' δ 142.8
e Compound 38 was a d_6–DMSO solution

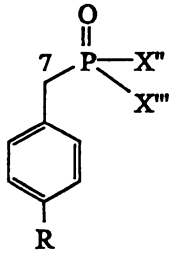

1" 2"
X" is labelled as O-CH_2-CH_3

Table 2. 3 ^{31}P and ^{1}H NMR chemical shift and coupling constants ^{x}J (^{31}P-^{1}H) for benzylphosphonates

Compound	X"	X'''[b]	R	^{31}P	1"	2"	2" ^{3}J	7	7 ^{1}J
17	OCH_2CH_3	OCH_2CH_3	OCH_3	27.6	3.98	1.22	6.9	3.07	21.0
18	OCH_2CH_3	Cl	OCH_3	40.3	4.16	1.20		3.41	18.0
22	OCH_2CH_3	OCH_2CH_3	$OCH_2C_6H_5$	27.5	4.00	1.23	6.9	3.08	21.1
23	OCH_2CH_3	Cl	$OCH_2C_6H_5$	40.1	4.21	1.32	7.1	3.45	19.9
27	OCH_2CH_3	OCH_2CH_3	$CCH_2COOCH_2CH_3$	27.2	3.91			2.99	21.3
28	OCH_2CH_3	Cl	$CCH_2COOCH_2CH_3$	40.1	4.01			3.44	19.8
29	OCH_2CH_3	OCH_2CH_3	NH_2	27.9	3.98	1.23	6.9	3.02	21.9
30	OCH_2CH_3	OCH_2CH_3	$NHCOCF_3$	26.8	3.96	1.20	7.0	3.06	21.6
31	OCH_2CH_3	Cl	$NHCOCF_3$	39.3	4.17	1.26	7.0	3.44	
32	OCH_2CH_3	$NHCH_2C_6H_5$	$NHCOCF_3$	30.0	4.00	1.25	7.2	3.11	
33	OCH_2CH_3	$NHCH_2C_6H_5$	NH_2	31.0	4.02	1.24	7.0	3.03	20.1
34	OCH_2CH_3	$NHCH_2C_6H_5$	NH_2	32.7		1.20	6.9	3.05	21.0
35	OCH_2CH_3	$OC_6H_5NO_2$	$COCF_3$	24.3	4.11	1.22	7.1	3.33	21.7
36	OCH_2CH_3	$OC_6H_5NO_2$	NH_2	25.6	4.11	1.24	7.1	3.24	20.9
37	OCH_2CH_3	$OC_6H_5NO_2$	$NHCOCH_2CH_2CH_3$	25.2	4.08	1.19	7.1	3.29	21.2
38[a]	OH	$OC_6H_5NO_2$	$NHCOCH_2CH_2CH_3$	21.2				3.33	20.4

All compounds are $CDCl_3$ solutions and are referenced as described in the experimental section of this chapter (except where noted otherwise).
[a] Compound 38 was a d_6-DMSO solution except for the ^{31}P NMR experiment was conducted using D_2O as the solvent.
[b] Where X''' = OCH_2CH_3 ^{1}H signals for 1" and 2" are twice the intensity of ^{1}H environment 7.

The ^{31}P NMR spectrum shows a large shift from δ 27.6 to 40.3 on formation of the P-Cl bond. Compound **18** does not seem to have been described previously in the literature but was not further characterised as the subsequent reaction step was not successful.

A milder method for chlorination of phosphorus esters called the Atherton–Todd reaction uses carbon tetrachloride and triethylamine to generate a phosphonyl chloride (Mucha *et al.*, 1994). Although this method was not trialed it is expected to be suitable for the chlorination of the phosphorus ester in the more cross–reactive lysergyl system.

The next synthetic challenge was the generation of the 4-nitrophosphonanilide. However, this was never achieved despite a multitude of attempts under a variety of conditions. Various mole ratios of reagents were trialed and the amount of base used was varied due to concerns over possible residual acidity of compound **18** due to unreacted PCl_5 material. The reaction was also trialed under air and nitrogen atmospheres with progressively more stringent drying of all solvents. The literature documents the formation of a phosphonamide of nitroaniline under very similar experimental conditions to those trialed (Janda *et al.*, 1988a). Although this report does not provide any experimental detail or product characterisation data to support their claim. As it was uncertain whether the lack of reaction was a problem peculiar to this particular system, it was decided to investigate another system.

2.2.2.4 BENZYL PROTECTED SYSTEM

The next system investigated was the benzyl ether equivalent of the previous system. The benzyl ether formation was found to proceed well and evidence for this is seen in the NMR spectra with loss of signals associated with the alcohol-**10** (δ ^{13}C 167.2 , ^{1}H δ 2.58) and appearance of shifts compatible with formation of ether-**19** (δ ^{13}C 163.8 (4) and δ ^{1}H 5.14 (1')). The appearance of the expected number of signals in ^{13}C NMR spectrum and increase of the aromatic integral in the ^{1}H NMR spectrum is consistent with the addition of the benzyl ring system. GC–MS shows the expected molecular ion. Preparation of

compound **19** has recently been described by van Nunen *et al.* (1997) with ^{1}H NMR, mass spectrometry and melting point were found to be in good agreement with **19**.

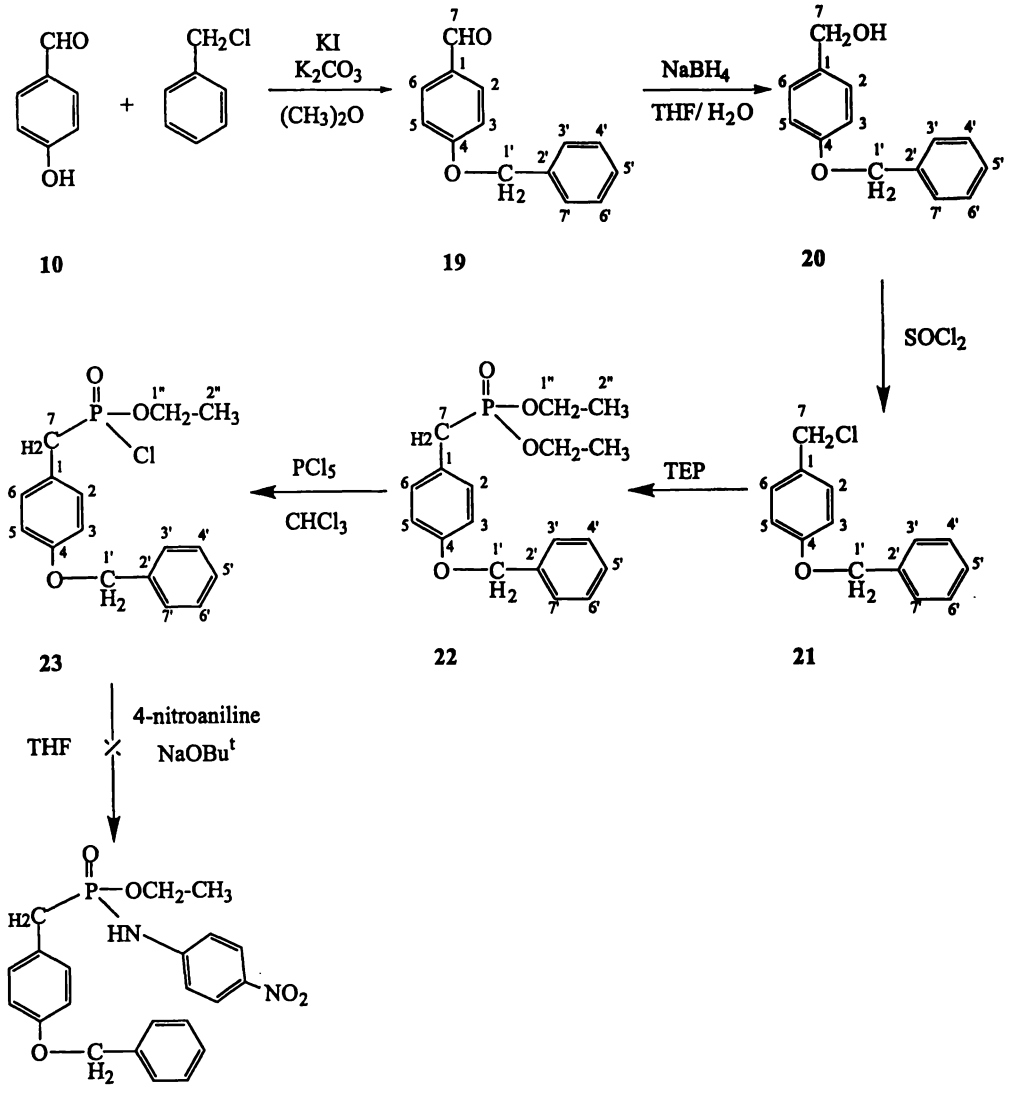

Figure 2. 12 Synthetic route taken in the attempted generation of a 4-nitrophosphonanilide.

The reduction of aldehyde-**19** to alcohol-**20** proceeded in good yield. The NMR spectra show the loss of the aldehyde signal (δ ^{13}C 194.9, δ ^{1}H 9.88), the appearance of new resonances δ ^{13}C 65.1 (7), δ ^{1}H 4.61 (7) and a broad signal at δ 1.69 which are consistent with alcohol-**20** formation. GC–MS shows the expected molecular ion. Comparison of data obtained for **20** with that described in the literature, synthesised, either directly from

condensation of 4-hydroxybenzyl alcohol with benzyl chloride, or as described herein, shows good agreement in melting point (Jorge *et al.*, 1981).

Chlorination proceeded well with appropriate change of signals in NMR spectra from those associated with alcohol-**20** (δ ^{13}C 65.1, δ ^{1}H 4.61 and 1.69), to those consistent with formation of a chloride-**21**, (δ ^{13}C δ 49.5 (7) and δ ^{1}H 4.65 (7)). GC–MS showed a molecular ion and isotope pattern consistent with formation of the chloride-**21**. Comparison of ^{1}H data obtained for **21** shows good agreement with that previously described (Pouchert *et al.*, 1974). The melting point obtained was also similar to that previously described (Jorge *et al.*, 1981).

Formation of the alkyl phosphorus diester by reaction of compound **21** with TEP gave phosphonate-**22** in good yield. The characteristic changes due to extensive coupling of the ^{31}P with both ^{1}H and ^{13}C nuclei on formation of the CH_2P bond was found on formation of compound **22**. The ^{13}C NMR spectrum has signals at δ 61.9 (1'), 16.2 (2') which show fine coupling and a signal centred at δ 32.1 (7) with a large coupling ^{1}J (^{31}P-$^{13}CH_2$) 139.0 Hz. The ^{1}H NMR spectrum has a multiplet at δ 4.00 (1'), a triplet at δ 1.23 (2') and a signal centred on δ 3.08 (7) with a coupling ^{2}J (^{31}P-^{1}H) 21.1 Hz. ^{31}P NMR spectrum of compound **22** shows a signal at δ 27.5 similar to that for compound **17** (δ 27.6). GC–MS provides further support for the formation of phosphonate-**22** with the expected molecular ion evidenced. The melting point could not be compared with that described by (Tchani *et al.*, 1992) as attempts at crystallisation of **22** failed.

Formation of compound **23** by reaction of **22** with PCl_5 was found to proceed almost quantitatively. The NMR spectra showed the expected drop in intensity of signals associated with the phosphorus ester, (δ ^{13}C 63.8 (1') and 16.0 (2'), δ ^{1}H 4.21 (1') and 1.32 (2')). The change in coupling ^{1}J ($^{13}CH_2$-^{31}P) from 139.0 to 121.2 Hz is very similar to that seen for transformation of compound **17** (139.0 Hz) to **18** (121.1 Hz). The characteristic

signal shift downfield from δ 27.5 to 40.1 was seen in the ^{31}P NMR spectrum. This downfield shift is characteristic of the formation of a P-Cl bond and has been noted by Mucha *et al.* (1994). Once characterisation of compound **23** had been conducted it was found unnecessary to workup the reaction. Formation of **23** was confirmed by ^{31}P NMR and **23** was used immediately in the subsequent step. Compound **23** does not appear to have been previously described.

Concern with the possible effect of residual acidity (from the PCl_5 treatment) was alleviated by reacting the chlorinated product with a large excess of base in the subsequent step. However, attempts at formation of 4-nitrophosphonanilide of **23** (not previously described) were unsuccessful, with the phosphonic acid mono ethyl ester and nitroaniline being the only material detected via NMR and ESI–MS. Many different reaction conditions were trialed including:

- use of reflux;
- different bases: sodium tert–butoxide ($NaOBu^t$): potassium tertiary butoxide ($KOBu^t$), and a mixture of triethylamine and $KOBu^t$;
- different solvent systems: DMSO; THF;
- air and nitrogen atmospheres.

In an increasingly more rigorous manner, freshly dried and distilled solvents were trialed but the reaction did not proceed, contrary to reports similar compounds reported in the literature (Janda *et al.*, 1988a). Refluxing compound **23** and 4-nitroaniline in THF for one week in a manner similar to Phillips *et al.* (1996) was again unsuccessful in generating of 4-benzyloxybenzylphosphonyl-4-nitroanilide. The recovered material was a mixture of the phosphorus acid mono ethyl ester and a small amount of a number of unidentified compounds. Methyl iodide was trialed in place of **23** under the reaction conditions described for attempted generation of 4-benzyloxybenzylphosphonyl-4-nitroanilide in the experimental section. However, the methyl-4-nitroanilide compound was not formed. Attempts to form the 6-aminophosphon–quinalide and 4-nitrophosphonanilide of **23**, using

the lithiated compound **23** with experimental conditions described by Janda *et al.* (1988) for a 8-aminoquinoline system, were also unsuccessful. Endeavouring to determine if the problems experienced with forming a phosphorus–nitrogen bond were a peculiarity of this system, it was decided to investigate an alkyl protecting group.

2.2.2.5 METHYL ETHANOATE PROTECTED SYSTEM

Benzaldehyde-**10** was protected using methyl bromoacetate to give compound **24** in 87% yield. The ^{13}C NMR spectrum showed the quaternary aromatic signal shift from δ 167.2 to δ 162.6 (4) and appearance of new signals at 168.5 (2'), 65.1 (1') and 52.4 (3'). The ^{1}H spectrum showed new signals at δ 4.67 (1'), 3.75 (3'), consistent with formation of compound **24**. GC–MS showed the expected molecular ion. This reaction has been described previously by Buckle *et al.* (1987) and made use of methyl bromoacetate under mildly basic conditions. The melting point obtained for **24** was in good agreement with that described for this compound by Buckle *et al.* (1987). The ^{1}H NMR data for **24** are in good agreement (δ ± 0.1) with that described previously for a compound containing the methyl ethanoate moiety (Morrison *et al.*, 1972).

The reactivity of the methyl acetate protecting group proved problematic for the reduction of aldehyde-**24**. Initially the reaction was conducted in THF–H_2O (9:1) (as described for production of compound **20**) but under these conditions the sodium borohydride was found to be too reactive and reduced the methyl ester of the protecting group to the corresponding alcohol as well as the desired aldehye-**24** to the benzyl alcohol product. This problem was partially solved by using ethanol as the solvent and cooling the reaction but while this reduced the benzaldehye-**10** it also transesterified the methyl ester to the corresponding ethyl ester. Evidence for the formation of ethyl ester-**25** is seen in the loss of signals in the NMR spectra associated with the aldehyde (δ ^{13}C 190.7, δ ^{1}H 9.82),

appearance of new signals consistent with formation of an alcohol (δ ^{13}C 64.5[1] and δ ^{1}H 4.51 (7), a broad signal at δ 2.86). Formation of the diethyl ester is evidenced with signals at ^{13}C δ 61.5 (3'), 14.2 (4'), and ^{1}H, a quartet at δ 4.21 (3') and triplet at δ 1.25 (4'). GC–MS showed the expected molecular ion of compound **25**. As the transesterification product would pose no problems in subsequent steps the synthetic pathway was continued with the ethyl ester-**25**. Compound **25** ^{1}H NMR data is in good agreement (δ ± 0.05) with that previously described by Mase *et al.* (1986).

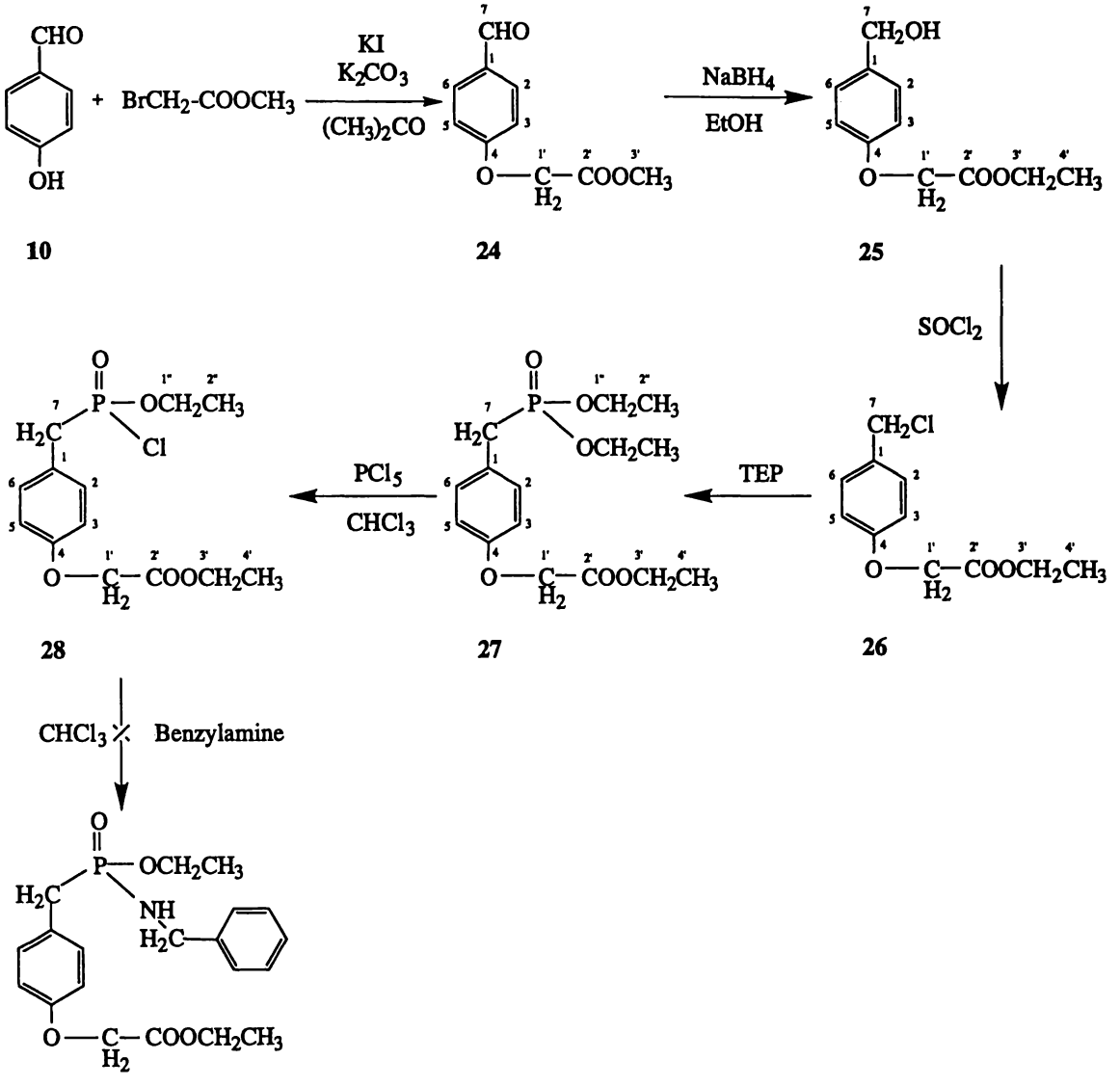

Figure 2. 13 Synthetic pathway used for the methyl/ ethyl ethanoate system.

[1] Despite the number of signals in this area of the ^{13}C spectrum the assignment of this shift is reasonably certain as it shifts in the subsequent reaction as would be expected for chlorination of an alchol.

Chlorination of compound **25** proceeded in almost quantitative yield giving compound **26**. NMR spectra showed signal changes consistent with loss of alcohol environment (δ ^{13}C 64.5 and δ ^{1}H 4.51 and the broad signal at δ 2.86), and appearance of new signals at δ ^{13}C 46.1 (7) and δ ^{1}H 4.54 (7) associated with the alcohol formation. Compound **26** has been described previously, and the ^{1}H NMR data for **26** are in good agreement (δ ± 0.06) with that obtained by Kawashima *et al.* (1995).

The phosphonate ester-**27** was produced in good yield (85%) using TEP. NMR spectra showed the loss of signals associated with the chloride-**26** (^{13}C 61.5) and new signals with coupling characteristic of diethyl phosphonate formation (^{13}C 62.0 (1"), and 16.4 (2")). A new signal centred at δ 32.7 (7) with coupling constant ($^{13}CH_2$–^{31}P) 139.2 Hz was also noted. The ^{1}H NMR spectrum shows loss of the signal at δ 4.54 and gains new signals at 3.91 (1"), 2.99 (7) and 1.19 (2"). ^{31}P NMR gave a multiplet at δ 27.2 and GC–MS showed the expected molecular ion. This compound does not appear to have been previously described so EI–MS was performed. The expected and experimentally found composition for **27** was in good agreement.

The chlorination of compound **27** proceeded well in almost quantitative yield, supported by the characteristic large shift in ^{31}P NMR δ 27.23 to δ 40.1. The expected drop in intensity in ^{13}C and ^{1}H NMR signals associated with the phosphorus ester was apparent along with the characteristic change in coupling ^{1}J ($^{13}CH_2$–^{31}P) 139.2 Hz.

When compound **28** was reacted to form the benzylphosphonanilide of **27**, the desired product was not obtained with only benzylamine and the phosphorus acid mono ethyl ester of **27** being recovered. Lack of success with benzylamine saw butylamine trialed with the same reaction conditions. This was also unsuccessful. It was decided that it would be of benefit to try and duplicate the work of Janda *et al.* (1988a) as this might provide insight into the difficulties encountered with the phosphonamide reaction.

2.2.2.6 SUCCESSFUL GENERATION OF A TETRAHEDRAL TRANSITION–STATE EMULATOR

Significant problems had been encountered with the generation of the 4-nitrophosphonanilide required for the generation of the tetrahedral phosphorus hapten that was desired for transition–state emulation. To solve these problems it was decided to use exactly the same system in which this type of compound had been generated (Janda *et al.*, 1988a).

The starting compound **29** (diethyl 4-aminobenzylphosphonate) is commercially available but protection of the amine is required as the chlorination of the phosphorus compound uses PCl_5. Protection of the amine using pyridine and trifluoroacetic anhydride was conducted as described by Janda *et al.* (1988a), and proceeded in good yield and purity. The trifluoroacetyl protecting group can be seen in the ^{13}C NMR spectrum with the appearance of two highly diagnostic quartets centred at δ 156.4 (1') ^2J (^{13}C–^{19}F) 37.6 Hz and δ 116.1 (2') ^1J (^{13}C–^{19}F) 288.4 Hz. The trifluoroacetylation of the amine group is also evidenced in the ^{19}F spectrum with the appearance of a signal at δ -76.41. The GC–MS of compound **30** gave the expected molecular ion. Janda *et al.* (1988a) and Tramontano *et al.* (1986a) describe N-trifluoroacetylation of compound **29** but no experimental data was given.

The chlorination of **30** proceeded almost quantitatively giving compound **31**. Evidence for formation of **31** can be seen via NMR in the drop in intensity of signals associated with the phosphorus ester in both the ^{13}C spectrum (δ 64.1 (1"), 40.2 with large coupling ^1J ($^{13}CH_2$–^{31}P) 121.3 Hz, 15.7 (2")), and ^1H spectrum (δ 4.17 (1"), 1.26 (2")). The ^{31}P NMR spectrum shows a large downfield shift from δ 26.6 to 39.3 as is expected, while the ^{19}F spectrum showed no appreciable change.

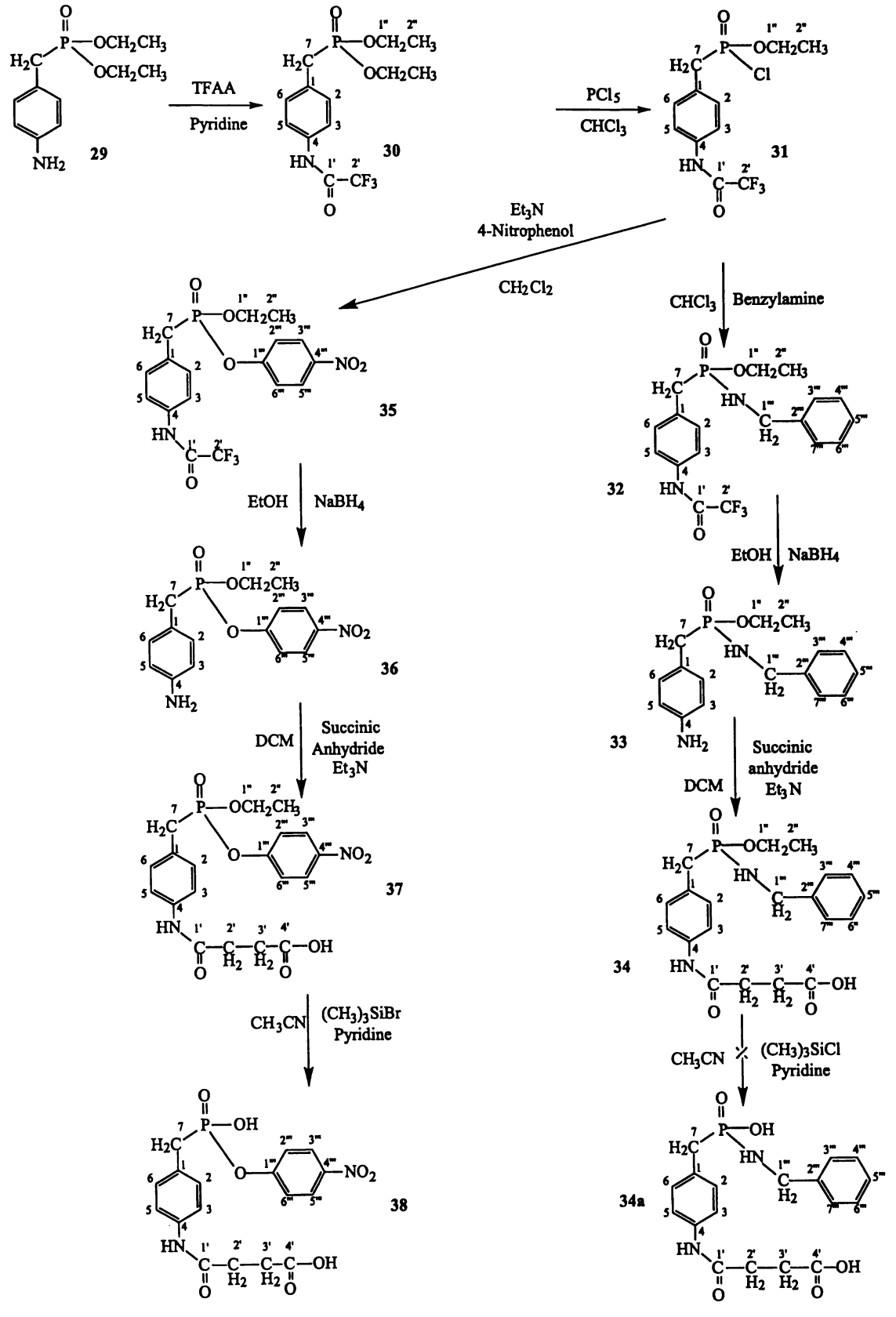

Figure 2. 14 Synthetic pathways used for generation of compounds **34** and **38**.

Attempts at generating the phosphonamide of compound **31** using the method as described by Janda *et al.* (1988a) were unsuccessful. With only the phosphorus mono acid ester of **31** and 4-nitroaniline being recovered. Attempts at communication with the authors in an attempt to resolve this issue were unsuccessful.

As the chlorinated compound **31** had not been purified, concerns were held about the residual acidity due to unreacted PCl_5 or HCl present. A number of trials were conducted with neutral pH extraction of compound **31** into ethyl acetate. When this material was reacted using the conditions described in the experimental section the 4-nitrophosphonanilide was still not generated.

It is not anticipated that acidity due to excess PCl_5 or HCl would cause problems for the formation of the phosphonamide as a very similar method was employed by Thorsett *et al.* (1982). In Thorsett's case, dibenzylphosphorus ester was chlorinated with PCl_5 and coupled to the amine of an amino acid in the presence of triethylamine (Thorsett *et al.*, 1982). Further, it has been reported that the methyl ester of the phosphonamides is an acid stable entity (McLeod *et al.*, 1991). It is therefore expected that the ethyl ester of the studied system would also be acid stable. The use of excess base in the attempted generation of the phosphonamide synthetic step would be expected to neutralise any residual material from the chlorination reaction. As further evidence that this was not the cause of the problem associated with the formation of the 4-nitrophosphonanilide, production of amide-**32** and ester-**36** compounds was found to be possible with no neutralisation step necessary prior to these reactions.

Once it was found that the corresponding phosphorus ester of 4-nitrophenol-**35** could be generated using triethylamine (preincubated with either **31**, or with the 4-nitroaniline), but neither of these methods was found to be successful for reaction with 4-nitroaniline. This lack of success is contrary to literature examples of improvement in reaction rate and yield for generation of phosphonamide and phosphorus esters when chlorinated phosphorus

compounds are incubated with triethylamine prior to addition of the amine or ester of interest (Hirschmann *et al.*, 1995; 1997).

The mechanism for formation of a P-N or P-O bond is thought to involve the S_N2 attack of the phosphorus by the alcohol or amine in question (Dostrovsky *et al.*, 1953; Hudson *et al.*, 1960). The presence of base in these reactions is thought to neutralise the HCl generated, although the use of triethylamine has been demonstrated to form a more reactive phosphonyltrialkylammonium salt (Hirschmann *et al.*, 1997). Previous work has suggested that steric factors may well affect the attack of the phosphorus, by bulky groups such as 4-nitrobenzyl often precluding formation of phosphonamides (Hirschmann *et al.*, 1997). The inclusion of the nitro group (with known electron withdrawing properties associated with the resonance effect) would be expected to decrease the electron density at the amine (noted to be a reasonably weak nucleophile (Keay 1963) of 4-nitroaniline and thus further hindering the reaction. This decrease in reaction rate has been noted by Komarov *et al.* (1995) with a nitro group on a heterocyclic compound decreasing attack at a chlorinated phosphorus. In a similar compound to the attempted 4-nitrophosphonanilide (the P=O is instead P=S), it has been noted that the formation of the 4-nitrothiophosphonanilide was slow compared to reaction with other primary and secondary amines (Phillips *et al.*, 1996). Previous work has suggested that the free energy gained during formation of the P-O bond is such that overcoming the kinetic barrier resulting from steric hindrance is more easily achieved than that for formation of the P-N bond (Hirschmann *et al.*, 1997).

It would seem that the phosphonamide generation with 4-nitroaniline is a disfavoured process with both steric and electronic effects suggesting that this reaction may not be expected to proceed. This is contrary to the report by Janda *et al.* (1988a), however, no comprehensive description of the synthetic methods or experimental data are contained in the report. As a lot of work has been conducted on the generated catalytic antibody (NPN43C9), it must be assumed that the 4-nitrophosphonanilide compound was

produced. With the lack of success in generating 4-nitrophosphonanilide compound it was decided to investigate whether another aromatic amine could be coupled to compound **31**.

Benzylamine was reacted in excess with **31** and found to give compound **32** with 80% yield. Compound **32** was characterised using one– (^{1}H, ^{13}C and P^{31}) and two–dimensional experiments (HSQC and HMBC). The ^{13}C NMR spectrum contains evidence for the formation of the (P–N) bond as the quaternary (2''') signal of the benzylamine aromatic environment appears as a finely split doublet, due to long–range ^{31}P coupling. Gain of signals consistent with addition of the benzylamine (Ar''') are seen in the ^{13}C NMR spectra and the expected increase of the aromatic integral in the ^{1}H spectrum is evidenced. A signal due to ^{31}P–^{1}H coupling to the proton on the benzylamine nitrogen was also present at δ 4.05. The ^{31}P NMR spectrum showed a shift from δ 39.3 to δ 30.0 consistent with that observed in a similar phosphonamide system (δ 29.9) (Harger *et al.*, 1990). HSQC and HMBC data also support the structure of compound **32**. Both GC–MS and ESI–MS give the expected ion species. As **32** does not appear to have been previously describe EI-MS was conducted giving the expected molecular ion.

Removal of the trifluoroacetyl group was achieved in good yield (71%) giving compound **33**. The removal of the trifluoroacetyl protecting group is seen with the loss of the two quartets due to ^{19}F–^{13}C coupling in the ^{13}C NMR spectrum (δ 155.4 J (^{19}F–^{13}C) 37.8 Hz and δ 116.1 ^{1}J (^{19}F–^{13}C) 288.5 Hz), and appearance of a broad NH_2 signal (^{1}H δ 3.64) suggests formation of **33**. ESI–MS gave the expected species and EI-MS was conducted and gave the expected molecular ion.

Compound **34** was formed in good yield (90%) by reacting succinic anhydride with compound **33**. The method used is derivative of that described in general terms in March (1992). Evidence for the attachment of the succinic moiety is seen in the ^{13}C NMR spectrum with the appearance of four new signals (δ 176.1 (4'), 171.1 (1'), 31.9 (2') and

29.7 (3')) In the ^{1}H NMR spectrum signals at δ 8.76 ($NHCH_2C_6H_5$) and a multiplet of appropriate intensity at δ 2.58 (2', 3') were apparent. ESI–MS gave an ion corresponding to both the deprotonated acid in negative ion mode and the ammoniated species in positive mode. EI-MS gave the expected molecular ion with loss of water due to succinimide formation.

Attempts to prepare the compound **34a** were unsuccessful as, in hindsight, the conditions used were probably too harsh when compared to the milder conditions used in formation of compound **38**. The benzylamine system was abandoned in favour of the 4-nitrophenol system.

Adoption of the 4-Nitrophenol system

The inability to produce **34a** was problematic but there is at least one documented case in the literature where a 4-nitro phosphonanilide was hydrolysed by antibodies generated to the corresponding ester transition–state compound (Gallacher *et al.*, 1992). With this precedent, it was decided to use a tetrahedral phosphorus ester linkage to 4-nitrophenol as a model for the transition–state of phosphonamide cleavage.

4-Nitrophenol pre-incubated with triethylamine was reacted with the chloride-**31** giving compound **35** which was purified readily using flash chromatography (yield 77%). Attempts to improve the yield by preincubation of **31** triethylamine were not successful. Characterisation of ester-**35** by NMR showed appearance of signals consistent with formation of a second aromatic environment in the ^{13}C NMR spectrum and the anticipated increase in aromatic integral was seen in the ^{1}H NMR spectrum. Proof of the formation of the P–O bond to the 4-nitrophenol was difficult to detect in the ^{13}C NMR spectrum as the fine coupling at δ 155.3 (1''') was not clear due to overlap of signal with the trifluoroacetyl group (1') signals. However, the subsequent synthetic step removed the trifluoroacetyl group and reveals the finely split doublet at the expected chemical shift. The ^{31}P NMR showed a signal at δ 24.3 (upfield compared to **32**). GC–MS gave the expected molecular

ion and ESI–MS gave the $[M+H^+]$ and $[M+NH_4^+]$ ion in the positive mode. EI-MS was conducted and gave the expected molecular species.

The formation of compound **35** has been previously described by Tramontano *et al.* (1986a) but no experimental data were noted. The crystal structure for compound **35** was also solved. Comparison of the crystal structure of compound **35** with compounds of the type $RCP(O)(OCR_1)(OCR_2)$[2] from the CSD database suggests that the atomic arrangement about the phosphorus is tetrahedral. The crystal data for compound **35** show standard bond lengths (Table 2.4) and standard angles (Table 2.5) when compared to those generated from a search of similar crystal structures using the CSD database.

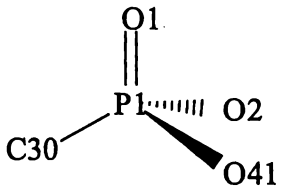

Figure 2. 15 Tetrahedral structure of compound **35**. O2 is linked to CH_2CH_3 and O41 is linked to 4-nitrophenyl and C30 is the CH_2 of the benzyl moiety.

Table 2. 4 Comparison of bond lengths of **35** with those reported in the literature

Description of bond	Bond length **35** (Å)	Bond length expected[2] (Å)
C(30)-P(1)	1.787(2)	1.81 ± 0.03
P(1)-O(1)	1.465(2)	1.46 ± 0.02
P(1)-O(2)	1.558(2)	1.57 ± 0.02
P(1)-O(41)	1.606(2)	1.57 ± 0.02

The bond length value in brackets is the uncertainty associated with the measurement.
The expected bond length error is ± one standard deviation.

[2]Calculated using CSD. Two hundred structures were selected with the structural unit decribed in Fig 2.15, however, compounds where O2 and O41 were linked to the the same moiety through a bifunctional entity; or if O1, O41 or O1 were bond to a metal center, were not used.

Table 2. 5 Comparison of bond angles of **35**) with those reported in the literature

Description of bond angle	Bond angle **35** (°)	Bond angle expected[2] (°)
C(30)-P(1)-O(1)	115.42(14)	115.8 ± 2.2
O(1)-P(1)-O(2)	116.66(12)	115.0 ± 1.9
O(1)-P(1)-O(41)	112.01(11)	115.2 ± 2.2
C(30)-P(1)-O(2)	102.99(13)	104.6 ± 2.9
C(30)-P(1)-O(41)	104.93(13)	104.2 ± 2.9
O(1)-P(1)-O(41)	112.01(11)	115.2 ± 2.2
O(2)-P(1)-O(41)	103.41(12)	102.4 ± 2.8

The bond angle values in brackets are the uncertainty associated with the measurement.
The expected bond angle error is ± one standard deviation.

Removal of the trifluoroacetyl protection group to give compound **36** was achieved in low yield (18%) when compared to the benzylamine version **33**. The NMR spectra showed the loss of the extensively–coupled signals associated with the trifluoroacetyl moiety (δ ^{13}C 155.4 (1'), 115.9 (2')) and appearance of a broad signal due to the amine ^{1}H δ 3.66, similar to that found for compound **33**. ESI–MS detected [M+H$^+$] and [M+NH$_4^+$] ion in the positive mode. EI-MS gave the expected molecular ion.

The addition of the succinic anhydride to compound **36** gave **37** in moderate yield (30%). Compound (**37**) was characterised using one– and two–dimensional NMR. Evidence for the successful addition of the succinic moiety was seen in the appearance of four new signals in the ^{13}C NMR spectrum (δ 176.4 (4'), 171.1 (1'), 31.6 (3') and 29.4 ppm (3')). The ^{1}H NMR spectrum had two new signals associated with the succinic moiety (δ 2.59 (3'), 2.54 (2')). ESI–MS of **37** gave the [M-H$^+$] in negative ion mode and the [M+NH$_4^+$] in the positive ion mode and EI–MS gave the expected molecular ion with loss of water, presumably due to succinimide formation.

The dealkylation of carboxylic esters using trimethylsilyl halides is well documented (Ho *et al.*, 1976; Jung *et al.*, 1976). Trimethylsilyl halides allow the dealkylation of nonaromatic phosphorus esters (Rabinowitz, 1963), with the bromide being particularly effective (McKenna *et al.*, 1977).

Removal of the phosphorus ethyl ester was achieved using trimethylsilyl bromide. The reaction was carried out in an NMR tube so that the formation of compound **38** could be easily monitored. However, as the reaction proceeds a precipitate formed (presumably pyridinium bromide) which caused considerable mixing problems. Preliminary studies had separated a small amount of **38** which was characterised by ^{31}P NMR. This ^{31}P NMR data indicated which of the forming signals observed while monitoring the reaction was associated with compound **38**. The ^{31}P NMR observations suggested that the desired compound forms quickly then proceeds to decompose to form several other non-characterised compounds. When solvents were dry the reaction was typically over in 10-20 minutes. This is in contrast to the longer time and harsher conditions used by Janda *et al.* (1988a) for their phosphonamide system. The time required for removal of the ethyl phosphorus ester of **37** is similar to that for removal of dialkyl phosphonates using trimethylsilyl chloride in the presence of NaI as reported by Morita *et al.* (1978). Compound **38** was produced in a somewhat variable yield and was characterised using one– and two–dimensional NMR techniques. Compound **38** gave a triplet in the coupled ^{31}P spectrum at δ 21.2 with coupling (^{1}J (^{31}P–^{1}H) 20.4 Hz) in the coupled spectra with the signal shifting from δ 25.2 in compound (**37**). The triplet is caused by coupling of the benzyl $C\underline{H}_2$ to the ^{31}P environment. As compound **38** had not been previously described in the literature LSIM-MS (negative mode) was conducted and the expected molecular ion with loss of water due to succinimde formation was obtained. Low resolution LSIM-MS (positive mode) was conducted and indicated an ion associated with $(M\text{-}H_2O\text{+}Na)^+$ species.

As this is the last compound of the synthetic pathway, a comprehensive two–dimensional NMR assignment was conducted, similar techniques were used in this thesis for other compounds to help resolve assignment ambiguities.

Two–dimensinal NMR— Example for compound 38

The COSY[3] experiment enables the relationship between ^{1}H's within a particular spin system to be investigated. The COSY spectrum diagonal shows the position of the various ^{1}H environments (Fig. 2.17). In the portion of the COSY spectrum shown the dotted lines indicate the correlations between four aromatic ^{1}H environments (δ 7.31 (2, 6) correlates to δ 7.58 (3, 5) and δ 7.43 (2''', 6''') correlates to δ 8.31 (3''', 5''')).

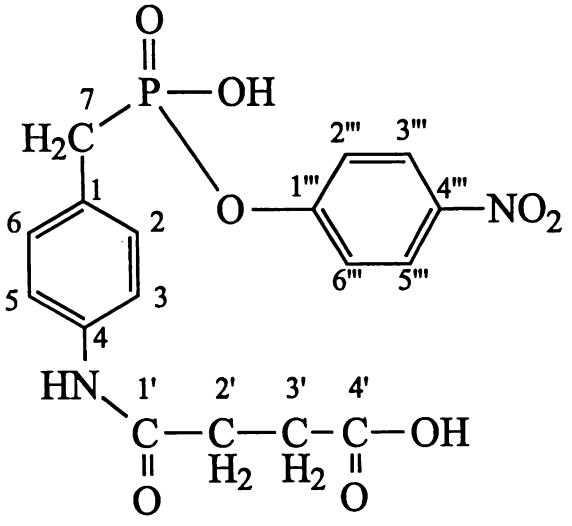

38

Figure 2. 16 Labelled structure of compound **38**

[3]The definition and practical considerations required for the two–dimensional NMR techniques is discussed in the experimental section of this chapter.

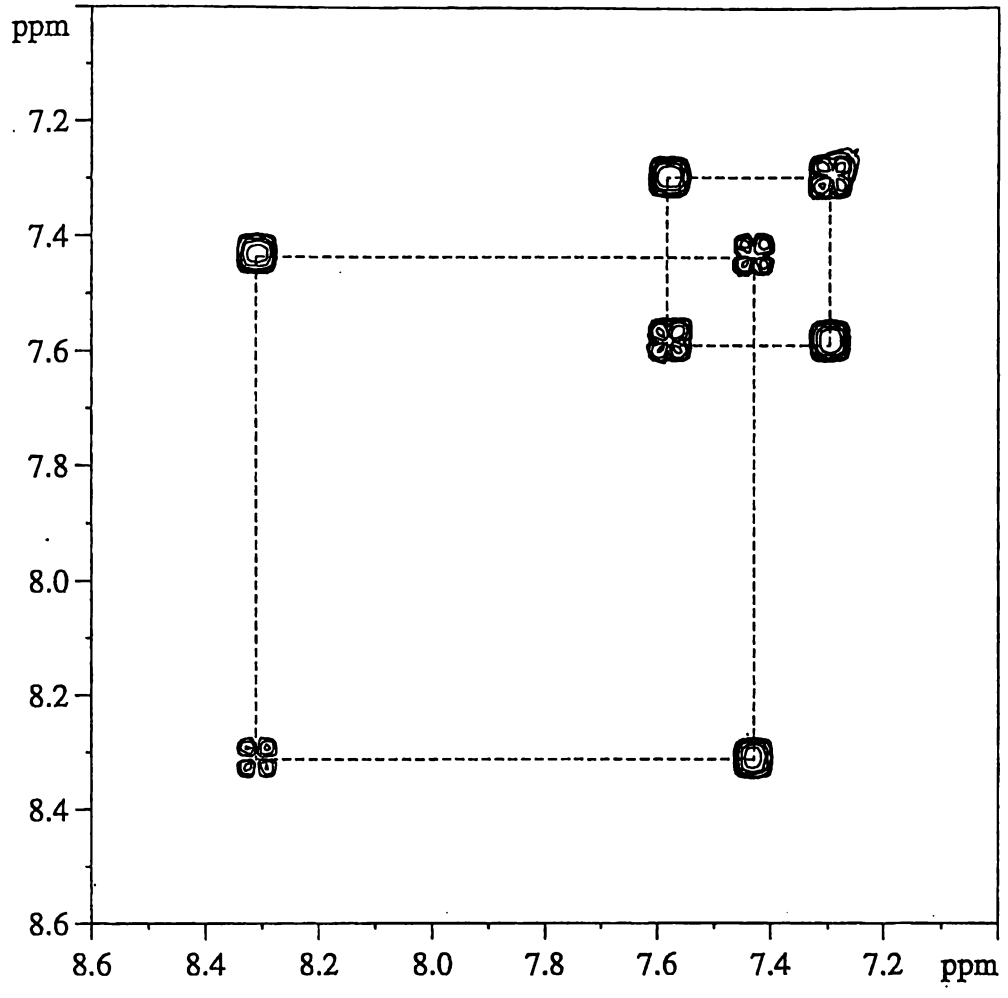

Figure 2. 17 Portion of a COSY spectrum showing correlation of ^{1}H environments δ 7.31 to δ 7.58 and δ 7.43 to δ 8.31.

The HSQC experiment enables assignment of ^{1}H(s) to a particular ^{13}C environment. The example portion of the HSQC spectrum (Fig. 2.18) shows; ^{1}H environment at δ 7.31 (2, 6) correlates to a ^{13}C environment at δ 129.7, a ^{1}H environment at δ 7.43 (2''', 6''') correlates to a ^{13}C environment at δ 120.7, a ^{1}H environment at 7.58 (3, 5) correlates to a ^{13}C at environment δ 118.6, and another ^{1}H environment at 8.31 (3''', 5''') correlates to a ^{13}C environment at δ 125.2 (Table 2.6).

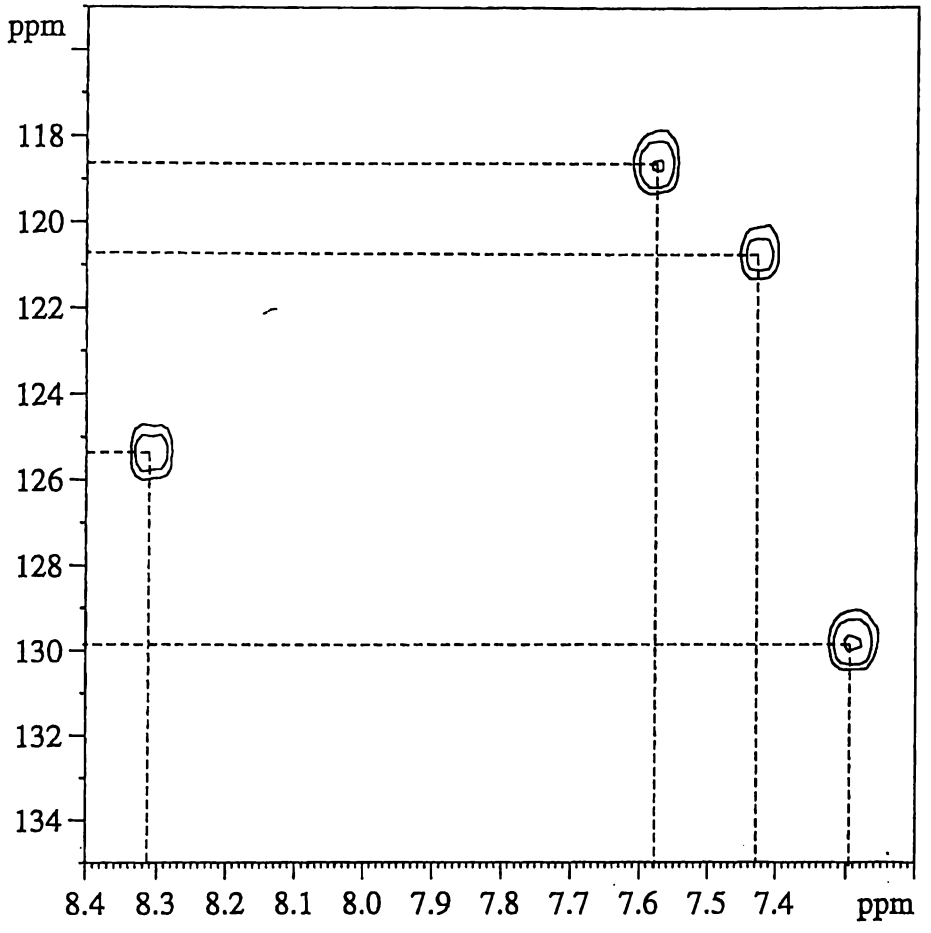

Figure 2. 18 Portion of a HSQC spectrum showing; ^{1}H δ 7.31 correlated to ^{13}C δ 129.7, ^{1}H δ 7.43 correlated to ^{13}C δ 120.7, ^{1}H δ 7.58 correlated to ^{13}C δ 118.6 and ^{1}H δ 8.31 correlated to ^{13}C δ 125.2.

The HMBC is a long range ^{1}H to ^{13}C correlation experiment and is conducted with values of J such that the ^{3}J and ^{4}J interactions are maximised. In some cases the ^{1}J correlations are seen due to incomplete cancellation of ^{1}J. The example portion of the HMBC shows (Fig. 2.19) the ^{1}H environment at δ 7.31 correlating to two ^{13}C environments (of the three it correlates to), one at δ 137.3 (4) which is a ^{3}J correlation, the other ^{3}J (not shown) correlation is at ^{13}C δ 33.5 (7). The other correlation seen by the ^{1}H environment at δ 7.31 is ^{13}C δ 129.7 which is due to a partially cancelled ^{1}J interaction. The HMBC enables 'stepping along' the carbon backbone of a molecule and positioning of the ^{1}H and ^{13}C

environments determined by the HSQC experiment. The HMBC experiment often shows two or three ^{13}C correlations for a particular ^{1}H environment and this information is similar to puzzle pieces which when correctly fitted together gives the two dimensional structure of the molecule.

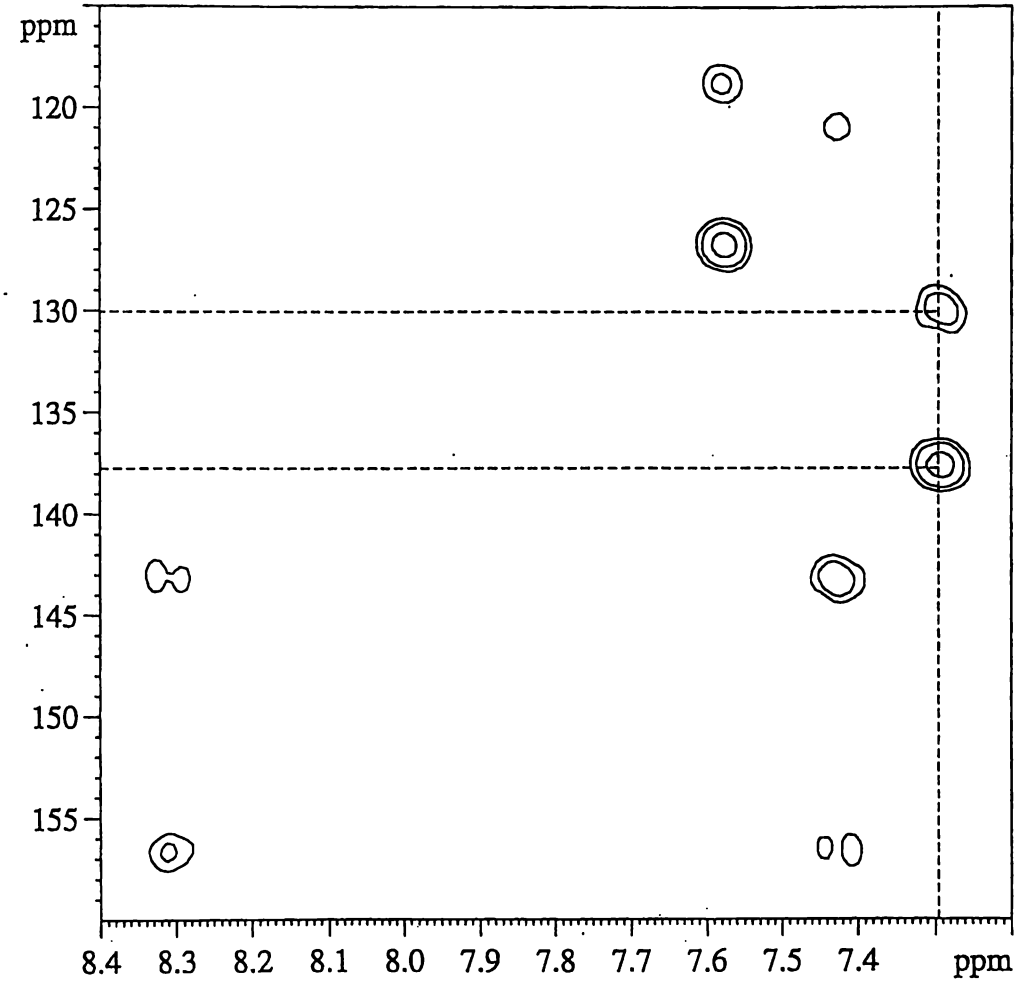

Figure 2. 19 Portion of a HMBC spectrum showing correlation of ^{13}C environments at δ 137.3 and δ 129.7 to ^{1}H at δ 7.31.

The ROESY NMR experiment shows through space (nuclear overhauser effect, NOE) ^{1}H to ^{1}H correlations, however, the value of *J* is set up in such a way as to maximise longer range correlations. The example portion of the ROESY spectrum shows that the ^{1}H environment at δ 7.43 correlating to the ^{1}H environment at δ 8.31 . The elegance of this experiment is that it can enable the connecting of spin systems past non–^{13}C or –^{1}H

environments. In compound **38** the ROESY experiment was useful as it enabled the linking of aromatic spin system environment (^{1}H δ 7.58 (3, 5)) to the environment at δ 10.02 ('NH). The δ 10.02 ('NH) environment in turn shows HMBC correlations to the succinic portion of the molecule. These correlations enabled the linking of the aromatic spin system[4] assignments to those of the succinic moiety.

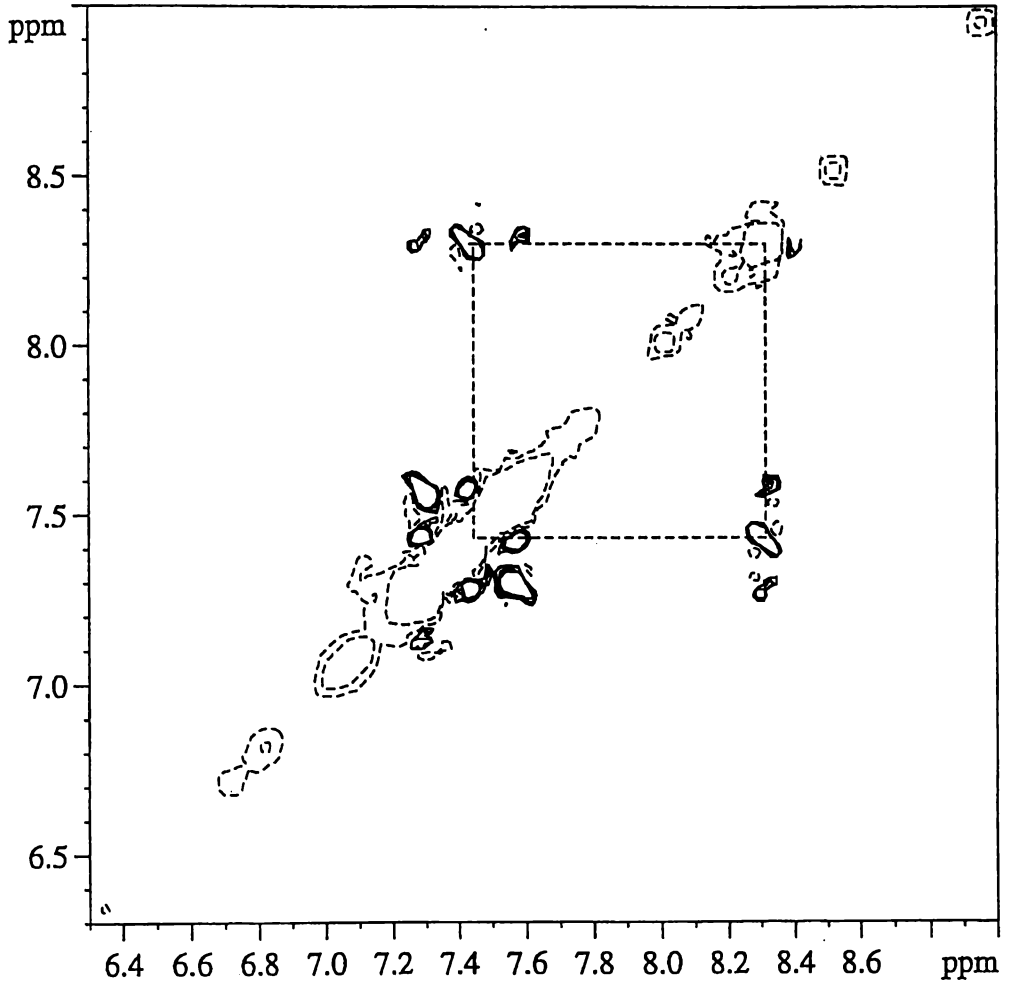

Figure 2. 20 Portion of a ROESY spectrum showing correlation of the environment at δ 7.43 to δ 8.31.

[4] A spin system is a set of interacting nuclei which exhibit mutual coupling (some couplings within the spin system may be zero).

Table 2. 6 Selected HSQC and HMBC correlations for compound **38**

^{1}H (δ)	^{13}C (δ)	Assignment	HMBC ^{1}H (δ) correlation to environment ^{13}C (δ)
7.31	129.7	2, 6	129.7 (itself), 137.3 (4), 33.5[a] (7)
7.43	120.7	2''', 6'''	120.7 (itself), 142.8 (4'''), 156.0 (1''')
7.58	118.6	3, 5	118.6[a] (3, 5), 127.0[a] (1)
8.31	125.2	3''', 5'''	125.2[a] (3''', 5'''), 142.8[a] (4'''), 156.0[a] (1''')

[a] Not shown in the portion of the example spectra.

The production of the compound **38** signified the formation of a tetrahedral phosphorus compound thought to suitable for generation of catalytic polyclonal antibody sera capable of ester and amide hydrolysis of 4-nitrophenol and 4-nitroanilide compounds respectively. Due to the time taken and extensive problems experienced in generating compound **38** it was decided to attempt the generation of polyclonal catalytic antibodies to this material. The conjugation and immunisation of compound **38** and resulting screening of immunoglobulins is the subject of the Chapter 3.

The generation of suitable substrates for screening of the polyclonal sera to be generated to **38** was necessary. To this end, two simple UV detectable substrates were synthesised.

2.2.2.7 SUBSTRATE GENERATION

Reaction of phenylacetyl chloride and 4-nitroaniline gave amide-**39** (Fig. 2.21). Evidence for the formation of **39** is seen in the NMR spectra with appearance of signals consistent with formation of an amide (δ ^{13}C 169.6 (8)), and a phenyl system (δ ^{13}C 143.7 (1'), 143.5 (4'), 125.1 (3', 5'), 119.2 (2', 6'), and δ ^{1}H 8.15, 7.39 and 3.78 (7). GC–MS gave the expected molecular ion. Formation of compound **39** has been reported, however, no melting point is noted (Lewis *et al*, 1991).

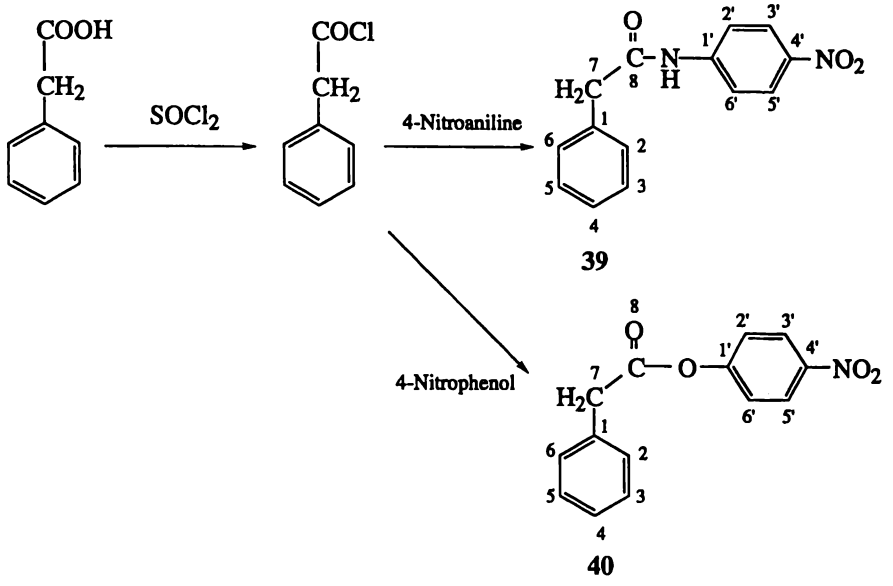

Figure 2. 21 Synthetic route for generation of compounds **39** and **40**.

In a very similar manner reaction of phenylacetyl chloride and 4-nitrophenol gave the resulting ester-**40** (Fig. 2.21). Evidence for the formation of **40** is seen in the NMR spectra with appearance of signals consistent with formation of an ester (^{13}C δ 169.1 (8)) and addition of a phenyl system (^{13}C δ 155.5 (1'), 145.4 (4'), 125.2 (3', 5'), 122.4 (2', 6'), and ^{1}H δ 8.25, 7.26 and δ 3.90 (7)). GC–MS of compound **40** gave the expected molecular ion. Comparison of the melting point of **40** with that described previously by Kirsch *et al.* (1968) gave good agreement.

2.3 EXPERIMENTAL

2.3.1 MATERIALS AND METHODS

2.3.1.1 REAGENTS AND SOLVENTS

All reagents were of LR grade (BDH) or higher unless otherwise noted. All solvents used were AnalR grade (BDH) unless noted otherwise: dichloromethane (CH_2Cl_2, drum grade), dimethyl sulfoxide (DMSO), triethylamine (Et_3N), acetonitrile (CH_3CN) and petroleum spirit bp 40-60°C (drum grade) were dried over calcium hydride and freshly distilled under nitrogen. Diethyl ether (Et_2O) and tetrahydrofuran (THF, lab grade) were dried by distillation from sodium benzophenone under nitrogen.

2.3.1.2 CHROMATOGRAPHY

Reactions were monitored by thin layer choromatography (TLC) on plates coated with fluorescent impregnated silica gel (Merck, art 9385). Preparative plate chromatography (PLC) was conducted using fluorescent impregnated silica layered (0.3 cm) on a glass plate (20 × 20 cm). Separation using flash chromatography was performed on silica gel (Merck, art 9385) with the same solvent mixture as used for TLC (Still *et al.*, 1978). Columns (ca 3 × 20 cm) were prepared by slurry packing with the eluent solvent. The size of the fraction collected was generally 5-10 ml with elution conducted at approximately 2 ml min^{-1}. Fractions were examined using TLC and appropriate fractions combined to give the purified compounds.

2.3.1.3 NMR

One–dimensional

Unless noted, all experiments were performed with a Bruker AC-300P NMR spectrometer fitted with a 5 mm dual $^{13}C/^{1}H$ probehead. One- and two-dimensional ^{1}H (300.13 MHz), ^{13}C (75.47 MHz), ^{19}F (282.41 MHz) and ^{31}P (121.51 MHz) NMR experiments were performed on $CDCl_3$ solutions unless noted otherwise. Two–dimensional experiments were conducted on a Bruker DRX-400 spectrometer ^{1}H (400.13 MHz), ^{13}C (100.62 MHz)

fitted with a 5 mm dual $^{13}C/^{1}H$ probehead or a 5 mm inverse $^{1}H/^{13}C$ probehead. Chemical shifts are reported relative to TMS.

^{1}H NMR.

Spectra were referenced with respect to the $CHCl_3$ (δ 7.26) and DMSO (δ 2.60) signal as appropriate. One dimensional ^{1}H NMR data are reported in the following format δ ^{1}H: x.xx (a, b Hz, c, d), where: x.xx is proton chemical shift (δ) in ppm, a is the splitting type eg triplet (t), b is the coupling constant (*J*) in Hz, c is the number of protons in the environment, and d is the assignment of the environment to the structure for the given compound. Coupling constants are ± 0.03 Hz due to the number of data points collected and are reported as observed with no averaging of values in the aromatic ring systems. Where uncertainty exists more than one assignment may be listed. Spectra were assigned using the characteristic chemical shifts for appropriate ^{1}H environments and making use of coupling where splitting of signals was observed. Where ^{31}P-^{1}H coupling was observed it is reported as seen in the spectrum. For example in the ^{1}H spectra the $C\underline{H}_2P$ environment (where both protons are equivalent) will be observed and reported as a doublet with the ^{31}P-^{1}H coupling noted as for ^{1}H–^{1}H coupling in brackets.

^{31}P NMR

Spectra were externally referenced using 85% H_3PO_4 set to δ = 0.

^{13}C NMR.

Spectra were referenced with respect to the centre peak of the multiplet of $CDCl_3$ (δ 77.06) and d_6–DMSO (δ 39.50). One dimensional ^{13}C NMR data reported were obtained from the ^{1}H decoupled experiment and are presented in the following format: δ ^{13}C: X.X (A, B Hz, C), where: X.X is carbon chemical shift (δ) in ppm, A is the splitting type (eg doublet (d)) if coupling is seen to another NMR active nuclei (such as ^{31}P), B is the coupling constant (*J*) in Hz, C is the assignment of the signal to the structure for the given

compound. Assignments of ^{13}C NMR signals in the simple aromatic systems were aided by calculating empirical increments for a substituted benzene as described by Breitmaier *et al.* (1987). In some cases data for substituent groups of interest were not available, and in such cases analogous substituents were used in these situations. Spectra were generally assigned using the characteristic chemical shifts for appropriate ^{13}C types in addition to the following considerations:

- aromatic quaternary (C) signals were of reduced intensity relative to aryl methine (CH) environment
- aliphatic carbons of the methylene (CH_2) and methyl type (CH_3) appeared in reported regions eg $PO\underline{C}H_2CH_3$ $\underline{C} \cong \delta$ 62 and $\mathbf{C} \cong \delta$ 16.

For spectra exhibiting ^{31}P-^{13}C coupling signal assignment was often straightforward and it was for this reason DEPT^{135} NMR experiments were only run for selected compounds. Where ^{31}P-^{13}C coupling was observed it is reported as seen in the spectrum. For example in the ^{13}C spectra the $\underline{C}H_2P$ environment will be seen and reported as a doublet with the ^{31}P-^{13}C coupling noted (B) in brackets. The same notation is used for ^{19}F-^{13}C coupling.

^{19}F NMR

Spectra were externally referenced versus $C_6H_5CF_3$ set to δ -63.9.

DEPT^{135}

Distortionless Enhancement by Polarisation Transfer (DEPT) experiment makes use of the ^{1}H environments attached to ^{13}C nuclei to enhance signal strength. The setting of the pulse length in the sequence determines the relative phase of signals from different environments (C, CH, CH_2, CH_3); a tip angle of 135° gives the CH_2 signals the opposite phase to CH and CH_3 environments and no signal for the non-protonated (C) environments (Braun *et al.*, 1996).

Two–dimensional NMR experiments

A worked example of two dimensional techniques used is shown for compound **38** in the discussion section of this chapter.

COSY

The correlated spectroscopy experiment (COSY) correlates ^{1}H-^{1}H coupling within a spin system. Correlation peak intensity is dependent on *J* and the time delays used (Braun *et al.*, 1996).

HSQC

The heteronuclear single quantum correlation (HSQC) experiment is designed to correlate ^{1}J (^{13}C-^{1}H) chemical shifts using a double INEPT polarisation transfer technique, in addition to gradient suppression of ^{12}C-^{1}H signals (Braun *et al.*, 1996). Delays were typically set such that ^{1}J couplings investigated were in the range 125-160 Hz (due to the presence of both aliphatic and aromatic environments an average value for ^{1}J of 145 Hz was used this translates to a delay (d_2) of 3.45 ms).

HMBC

While the HSQC is designed give correlations resulting from ^{1}J(C-H), the Heteronuclear Multiple Bond Correlation (HMBC) obtains correlations resulting from $^{2,3}J$ (C-H) (Braun *et al.*, 1996). The delay times in the experiment endeavour to cancel ^{1}J (C-H) while appropriate delays (d_2 of 3.45 ms, and a mixing time of 80 ms) enable $^{2,3}J$ (^{13}C-^{1}H) precession. The gradients used in HMBC suppress the ^{12}C-^{1}H signals and enable higher receiver gain to be used and thus improve the signal to noise.

NOESY

Nuclear Overhauser Enhancement Spectroscopy (NOESY) experiment is a two–dimensional equivalent of the NOE experiment. The NOESY gives through space correlation between nuclei in close spatial relationship (less than 2.5 Å, (Friebolin, 1993)) . This powerful technique enables 3D structural determination in certain circumstances.

When these NOE data are used as constraints in computer modelling they can help to determine conformation and spatial arrangement. However, chemical exchange (with for example a solvent) will also give correlations and careful phasing must be conducted to avoid residual COSY type correlations. The correlation time of the molecule (molecular tumbling) may mean that no NOE correlation is evidenced; in these situations the ROESY experiment should be used.

ROESY

Rotating Frame Overhauser Enhancement Spectroscopy (ROESY) experiment is a rotating frame equivalent of NOESY and is useful where the molecular correlation time of the molecule is such that no NOE is evidenced. With the ROESY experiment vector evolution takes place in a spin lock. A complication that can occur with ROESY is the presence of residual TOCSY (rotating frame version of COSY) interactions. These residual TOCSY correlations can generally be identified as negative peaks in phase sensitive spectra.

2.3.1.4 MASS SPECTROMETRY

Gas chromatography-mass spectrophotometry (GC–MS) was performed on a Hewlett Packard 5890A Gas Chromatograph with a 7673A autosampler, using a mass selective detector (MSD 5970) with a Hewlett Packard (HP) crosslinked methyl silicone gum column (HP 1: 25 m × 0.2 mm id, 0.3 μm film thickness). The oven temperature was ramped at 8°C min^{-1} from 50-280°C (10 minute hold). Samples (1 μl) in an appropriate volatile solvent (usually $CHCl_3$) were automatically loaded with the purge valve to waste after 0.3 minutes. The data obtained were manipulated on HP Chemstation software. The format used for presentation of mass spectrometry data is; e (f, g), where e is the ion mass detected, f is the ion assignment (if given), g is the percentage intensity of the ion relative to the base peak. Generally the molecular ion is noted plus the seven most abundant ions.

High resolution electron impact (EI) and liquid secondary ion mass spectrometry (LSIM) was performed by J. M. Allen (Hort+Research, Palmerston North, NZ) using a VG70-250S double focusing magnetic sector mass spectrometer.

A standard EI-MS source was fitted running at 8kV source potential and using a 70 eV and 200 μA electron beam. The source was tuned to 5000 resolving power and PFK calibrant was bled into the source as a secondary mass reference. Samples were dissolved in either CH_2Cl_2 (AnalR) or CH_3OH (AnalR), 1μl of this sample solution was pipetted to a standard solids probe sample cup and solvent removed under vacuum. Samples were desorbed from the sample cup from 40-400°C with a ramp of 10°C s^{-1}. Accurate mass measurements were then determined to four decimal places calibrated versus the PFK calibrant. Data processing was conducted using Opus software.

Negative ion LSIM–MS was conducted using a liquid secondary ion mass spectrometry source. The ion gun source consisted of a caesium ion primary beam 15 keV and 1 mA (as measured at the gun cathode), the secondary ion beam was accelerated from the source at 4 kV in negative ion mode. Samples were dissolved in water–CH_3OH (50:50) and 1 μl of this sample solution was spotted to the surface of a glycerol matrix (1μl) layered onto a stainless steel target. Negative ion spectra were obtained over a 10-1000 Da mass range with a scan rate of 5 s $decade^{-1}$. Spectra were background subtracted to remove matrix ions. Accurate mass measurements were determined to four decimal places and were conducted at 5000 resolving power and linear scanning over 350-500 Da with glycerol used as a secondary mass calibrant. Data processing was conducted using Opus software.

Electrospray mass spectrometry (ESI–MS) was performed in positive and negative ion mode on a VG Platform II (Fisons) equipped with MassLynx data analysis system. The cone voltage typically used was 20 V and concentration of sample injected were approximately 0.1 mg ml^{-1}. The solvent system used was CH_3CN–H_2O (1:1) unless noted otherwise. The positive ion mode often detected an ion which corresponds to addition of an ammonium cation $[NH_4]^+$ to the molecular ion of interest and is due to adventitious ammonium present in the mobile phase.

2.3.1.6 CRYSTALLISATION

Crystallisation was performed by the vapour diffusion method. The compound to be crystallised was dissolved in the minimum of a polar solvent placed in a container, which was then placed in a larger container filled with an excess of a less polar solvent with approximately the same boiling point and left for several days. If crystallisation was evidenced the crystals were carefully removed from the mother liquor.

2.3.1.7 MELTING POINT

Melting points (mp) were taken on a Reichert Nr341786 apparatus and were uncorrected.

2.3.2 RESULTS AND SYNTHESIS

2.3.2.1 THE INDOLE SYSTEM

3-Indolebutyric Acid (1)

3-Indolebutyric acid (1) was obtained (Aldrich). Its identity was confirmed by NMR spectroscopy and a full assignment of resonances was obtained to facilitate assignments of subsequent derivatives.

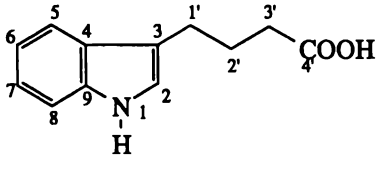

1

1 NMR: δ ^{1}H (400 MHz); 7.94 (sb, 1H, 1), 7.65 (m, 1H, 5), 7.38 (m, 1H, 8), 7.24 (m, 1H, 7), 7.15 (m, 1H, 6), 7.02 (m, 1H, 2), 2.88 (t, 10.4 Hz, 2H, 1'), 2.48 (t, 9.8 Hz, 2H, 3'), 2.08 (m, 2H, 2')

δ ^{13}C (400 MHz); 180.1 (4'), 136.8 (9), 127.8 (4), 122.4 (7), 121.9 (2), 119.7 (6), 119.3 (5), 115.9 (3), 111.5 (8), 33.9 (3'), 25.5 (2'), 24.8 (1')

ESI–MS: negative ion, cone voltage 20 V, *m/z* 202, $[M\text{-}H^{+}]^{-}$

Table 2.7 HSQC NMR correlation for compound **1**

^{1}H signal (δ)	Correlated ^{13}C signal (δ)	Assignment
2.08	25.5	2'
2.48	33.9	3'
2.88	24.8	1'
7.02	121.9	2
7.15	119.7	6
7.24	122.4	7
7.38	111.5	8
7.65	119.3	5

Table 2.8 HMBC NMR correlations for compound **1**

^{1}H signal (δ)	Correlated ^{13}C signals (δ)
2.08	24.8, 115.9, 33.9, 180.1
2.48	24.8, 25.5, 180.1
2.88	25.5, 33.9, 115.9, 121.9, 127.8
7.02	115.9, 127.8, 136.8
7.15	111.5, 127.8
7.24	119.3, 136.8
7.38	119.3, 127.8
7.65	115.9, 122.4 ,127.8, 136.8

Production of Methyl 4-(3-Indolyl)butyrate (**2**)

Although compound **1** was reduced with lithium aluminium hydride ($LiAlH_4$) to the alcohol-(**2**) (20%) a better yield of the alcohol is obtained (40%) if the methyl ester is first formed and subsequently reduced. Esterification was accomplished with HCl in dry methanol (generated by reaction of acetyl chloride with methanol).

Compound **1** (0.50 g, 2.5×10^{-3} mol) was dissolved in methanol (CH_3OH) (100 ml, 2.5 mol), and acetyl chloride (5.89 ml, 8.0×10^{-2} mol) was added dropwise with vigorous stirring from a glass Luerlock syringe. The mixture was stirred for 20 hours and the solvent was removed under reduced pressure to give compound **2** as an oil (0.38 g, 70% yield).

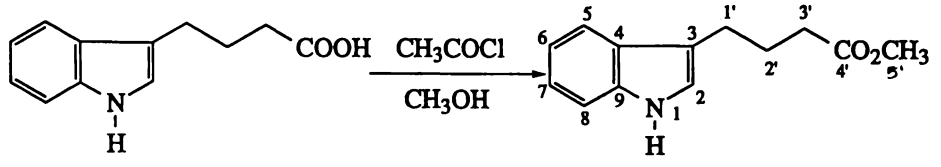

1 **2**

2 NMR: δ ^{1}H; 8.09 (sb, 1H, 1), 7.66 (d, 7.5 Hz, 1H, 5), 7.36 (d, 6.9 Hz, 1H, 8), 7.20 (m, 2H, 6, 7), 6.96 (s, 1H, 2), 3.71 (s, 3H, 5'), 2.85 (t, 7.8 Hz, 2H, 1'), 2.44 (t, 7.5 Hz, 2H, 3'), 2.10 (m, 2H, 2')

δ ^{13}C; 174.5 (4'), 136.5 (9), 127.5 (4), 122.0 (7), 121.7 (2), 119.3 (5, 6), 119.0 (5, 6), 115.5 (3) 111.3 (8), 51.6 (5'), 33.8 (3'), 25.5 (2'), 24.6 (1')

GC–MS: R_T 18.90 min; 217 (M^+, 20), 186 (7), 156 (3), 143 (19), 130 (100), 155 (4), 103 (9), 89 (2), 77 (11), 65 (3), 51 (4)

mp: 66-68°C (purple crystal)

Generation of 4-(3-Indolyl)butanol (3)

To compound **2** (1.0 g, 5×10^{-3} mol) in diethyl ether (100 ml) was added lithium aluminium hydride (0.76 g, 2.0×10^{-2} mol). The mixture was gently refluxed for two hours and then quenched with 10% ammonium chloride. The diethyl ether layer was retained, dried ($MgSO_4$), and the solvent was removed under reduced pressure to give compound (**3**) as a clear viscous oil (0.62 g, 66% yield). Attempts to recrystallise (**3**) from $CHCl_3$–petroleum sprirt (bp 60-80°C) were unsuccessful.

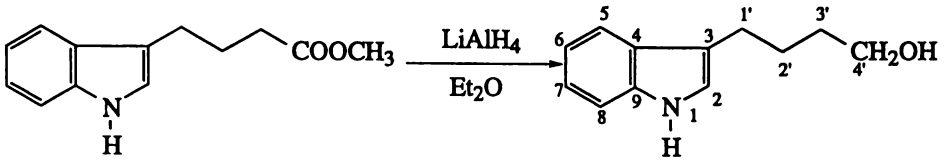

2 3

3 NMR: δ ^{1}H; 8.08 (sb, 1H, 1), 7.66 (dd, 7.8, 0.6 Hz, 1H, 5), 7.34 (dd, 7.8, 0.6 Hz, 1H, 8), 7.21 (m, 2H, 6, 7), 6.90 (d, 0.9 Hz, 1H, 2), 3.67 (t, 6.6 Hz, 2H, 4'), 2.82 (t, 7.2 Hz, 2H, 1'), 1.94 (sb, 1H, OH), 1.81 (m, 2H, 2', 3'), 1.28 (m, 2H, 2', 3')

δ ^{13}C; 136.5 (9), 127.6 (4), 121.9 (7) 121.5 (2), 119.1 (5, 6), 119.0 (5, 6), 116.4 (3), 111.3 (8), 62.9 (4'), 32.7 (3'), 26.4 (2'), 25.0 (1')

GC–MS: R_T 18.87 min; 189 (M^+, 19), 170 (1), 143 (4), 130 (100), 117 (4), 103 (9), 89 (2), 77 (10)

ESI–MS: positive ion, cone voltage 20 V, *m/z* 190, $[M+H]^+$

Generation of 1-Bromo-4-(3-indolyl)butane (4)

Compound **3** (0.052 g, 2.7×10^{-4} mol) was dissolved in diethyl ether (2 ml) with stirring CBr_4 (0.182 g, 5.5×11^{-4} mol) and triphenylphosphine (Ph_3P) (0.144 g, 5.5×10^{-4} mol) were added, and the mixture refluxed for three hours. The solvent was removed under reduced pressure and the mixture separated using preparatory silica plates (PLC) to give compound **4** (0.03 g, 41% yield).

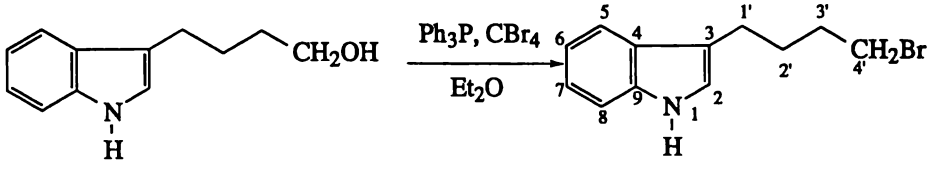

3 4

4 NMR: δ ^{1}H; 7.95 (sb, 1H, 1), 7.61 (d, 7.5, 1H, 5), 7.36 (d, 8.1 Hz, 1H, 8), 7.18 (m, 2H, 6, 7), 6.98 (s, 1H, 2), 3.45 (t, 6.3 Hz, 2H, 4'), 2.81 (t, 6.6 Hz, 2H, 1'), 1.96 (m, 2H, 2', 3'), 1.90 (m, 2H, 2', 3')

δ ^{13}C; 134.2 (9), 125.2 (4), 119.7 (7), 119.0 (2), 117.0 (5), 116.6 (6), 113.8 (3), 108.9 (8), 31.7 (4'), 30.4 (3'), 26.4 (2'), 22.1 (1')

ESI–MS: negative ion, cone voltage 20 V, *m/z* 330, 332, 334 $[M+Br]^-$

PLC: R_f 0.43 CH_3OH–CH_2Cl_2 (1:24)

Attempted Generation of Diethyl 4-(3-indolyl)butylphosphonate

To metallic sodium (0.001 g, 5.3 × 10^{-5} mol) in THF (5 ml) at reflux, was added DEP (0.007 ml, 5.3 × 10^{-5} mol) dropwise from a syringe, and the mixture refluxed for an additional three hours. To the refluxing DEP mixture compound **4** (0.013 g, 5.3 × 10^{-5} mol) in THF (5 ml) was added dropwise and the mixture refluxed a further four hours. The reaction was quenched with ethanol (2 ml), water (40 ml), and the ethanol was removed under reduced pressure. The aqueous phase was extracted with diethyl ether (20 ml), dried ($MgSO_4$) and the diethyl ether was removed under reduced pressure. NMR (^{1}H, ^{31}P and ^{13}C) showed that the desired compound had not been formed.

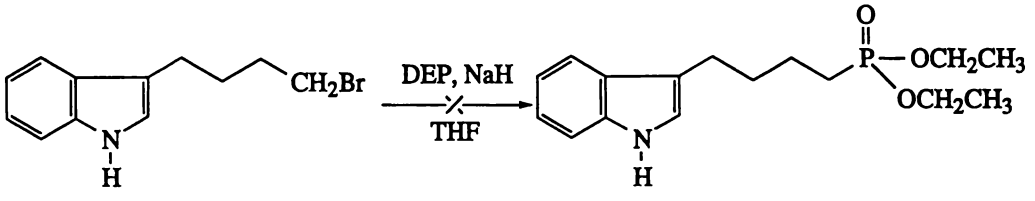

4

Generation of Diethyl 4-butylphosphonate (**4a**)

To metallic sodium (0.01 g, 5.0 × 10^{-3} mol) in THF (15 ml) at reflux, was added DEP (0.64 ml, 5.0 × 10^{-3} mol) dropwise from a syringe, and the mixture refluxed for an additional three hours. To the refluxing DEP mixture butyl bromide (0.54 ml, 5.0 × 10^{-3} mol) in THF (5 ml) was added dropwise and the mixture refluxed a further four hours. The reaction was quenched with ethanol (2 ml), water (40 ml), and the ethanol removed under reduced pressure. The aqueous phase was extracted with diethyl ether (20 ml), dried ($MgSO_4$), and the diethyl ether removed under reduced pressure, giving compound **4a** as a yellow oil in varying yield (10-30%).

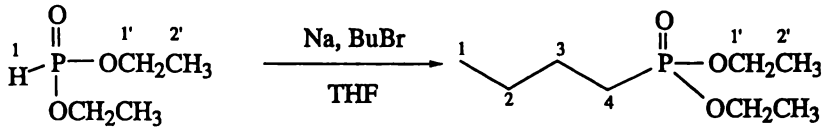

4b **4a**

4a NMR: δ ^{1}H; 4.03 (m, 4H, 1'), 1.61 (m, 2H, 4), 1.53 (m, 2H, 3), 1.35 (m, 2H, 2), 1.26 (t, 8.4 Hz, 6H, 2'), 0.86 (t, 7.2 Hz, 3H, 1)

δ ^{13}C; 61.4 (d, 6.3 Hz, 1'), 30.0 (d, 140.4 Hz, 4), 24.4 (d, 3.8 Hz, 3), 23.7 (d, 17.3 Hz, 2), 16.4 (d, 5.7 Hz, 2'), 13.5 (1)

δ ^{31}P; 33.4

4b NMR: ^{1}H; 6.37 (d, 692.1 Hz, 1), 4.99 (m, 1'), 1.32 (t, 7.2 Hz, 2')

^{13}C; 61.8 (d, 9.0 Hz, 2'), 16.3 (d, 9.75 Hz, 1')

δ ^{31}P; 8.0

2.3.2.2 ATTEMPTED GENERATION OF 4-AMINOPHENYLMETHANOL

Lithium aluminium hydride (0.83 g, 2.2×10^{-4} mol) was added to 4-aminobenzoic acid (0.1 g, 7.3×10^{-4} mol) in diethyl ether (10 ml). The reaction mixture was stirred under reflux for a further two hours, the reaction was quenched (20 ml 0.1 M NH_4Cl), extracted into ethyl acetate (20 ml) and washed with water (2×40 ml). The ethyl acetate layer was retained, dried ($MgSO_4$), and the solvent was removed under reduced pressure to give compound **6** (0.03 g, yield 35%).

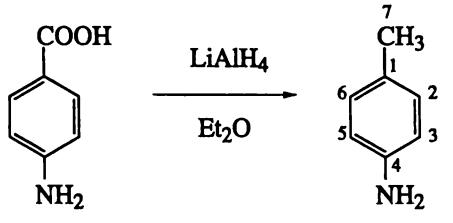

6

6 NMR: δ ^{1}H; 6.99 (d, 8.4 Hz, 2H, Ar), 6.63 (d, 8.4 Hz, 2H, Ar), 3.45 (sb, 2H, NH_2), 2.27 (s, 3H, 7)

δ ^{13}C; 143.9 (4), 129.8 (2, 6), 128.9 (1), 115.4 (3, 5), 20.5 (7)

DEPT^{135}; 129.8 (C-H), 115.4 (C-H), 20.5 (CH_3)

Generation of Methyl 4-Aminobenzoate (7)

To 4-Aminobenzoic acid (0.10 g, 7.3×10^{-4} mol) in methanol (20 ml) was added acetyl chloride (0.83 g, 2.2×10^{-2} mol) and the reaction stirred for 20 hours. The reaction mixture was adjusted to pH 8 (saturated sodium bicarbonate) and extracted into ethyl acetate. The ethyl acetate layer was retained, dried ($MgSO_4$), and the solvent was removed under reduced pressure to give compound **7** (0.09 g, yield 78%).

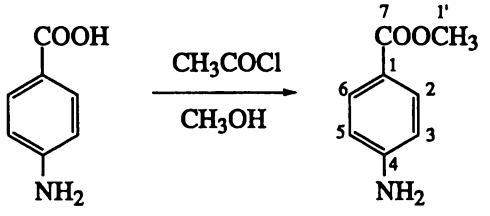

7

7 NMR: δ ^{1}H; 7.83 (d, 2H, 8.7 Hz, Ar), 6.62 (d, 2H, 9.0 Hz, Ar), 3.94 (sb, 2H, NH_2), 3.92 (s, 3H, 1')

δ ^{13}C; 167.3 (7), 151.0 (4), 131.6 (2, 6) 119.6 (1), 113.8 (3, 5), 51.6 (1')

Attempted Generation of 4-Aminobenzyl Alcohol

Compound **7** (0.05 g, 3.6×10^{-4} mol) dissolved in diethyl ether (20 ml) was refluxed with lithium aluminium hydride (0.05 g, 1.4×10^{-3} mol) for two hours. The reaction mixture was quenched with 10% ammonium chloride (20 ml), and extracted with ethyl acetate. The ethyl acetate layer was retained, dried ($MgSO_4$), and the solvent was removed under reduced pressure to give compound **6** (0.02 g, 40% yield), with ^{1}H and ^{13}C NMR as described previously.

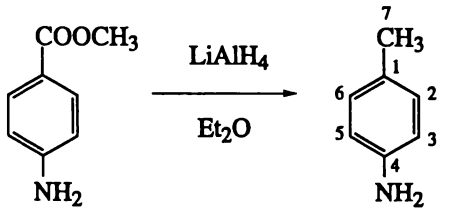

6

Generation of Diethyl 4-Nitrobenzylphosphonate

To a stirred mixture of sodium (0.053 g, 2.3×10^{-3} mol) in THF (10 ml) was added DEP **4d** (0.298 ml, 2.3×10^{-3} mol) dropwise. The mixture was gently refluxed for a further 30 minutes, at which time compound **8** (0.5 g, 2.3×10^{-3} mol) in THF (5 ml) was added and the reaction mix stirred a further five hours. The reaction was quenched in ethanol (5 ml), water (40 ml) and extracted with diethyl ether (30 ml). The diethyl ether layer was retained, dried ($MgSO_4$), and the solvent removed under reduced pressure. The resulting oil was separated using PLC to give compound **9** (0.01g, 2% yield).

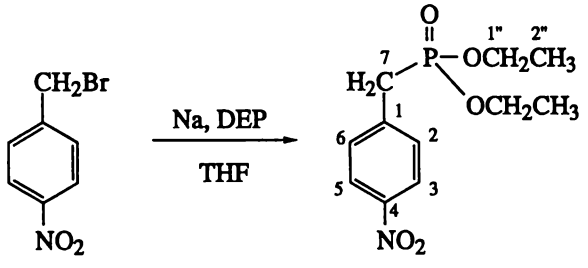

8 9

9 NMR: δ ^{1}H; 8.13 (d, 2H, 8.6 Hz, Ar), 7.27 (d, 2H, 8.8 Hz, Ar), 4.05 (m, 4H, 1"), 3.24 (d, 2H, 22.2 Hz, 7), 1.26 (t, 6H, 7.8 Hz, 2")

δ ^{31}P; 24.9

GC–MS: R_T 18.1 min; *m/z* 273 (M^+, 16), 217 (33), 187 (21), 137 (38), 109 (100), 89 (83), 69 (33)

PLC: R_f 0.07 diethyl ether–petroleum spirit (60:40)

Attempted generation of 4-Aminobenzylphosphonate

To a dressler bottle containing (4-nitro)benzyl bromide (0.01 g, 3.7×10^{-5} mol) in methanol (50 ml) was added Pd/C (0.01 g) and the mixture was bubbled with hydrogen for five hours. The reaction mixture was filtered (Whatman 2) and the solvent was removed under reduced pressure, however, the desired (4-amino)benzyl bromide was not detected by ^{1}H, or ^{13}C NMR.

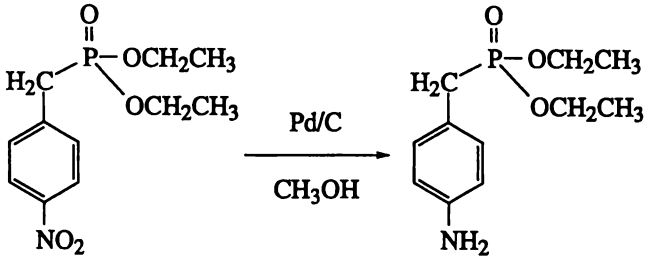

9

2.3.2.3 THE 4-HYDROXY BENZALDEHYDE SYSTEM

Generation of 4-Benzoyloxybenzaldehyde (11)

To a stirred solution of compound **10** (Fluka) (0.50 g, 4.1×10^{-3} mol) in pyridine (3 ml) was added benzoyl chloride (0.71 ml, 4.5×10^{-3} mol). The mixture was stirred for a further sixteen hours. The solution was adjusted to pH 2 (2 M HCl), extracted into ethyl acetate (30 ml), neutralised (saturated sodium bicarbonate 2×30 ml) and washed with water (2×30 ml). The ethyl acetate layer was retained, dried ($MgSO_4$), and the solvent was removed under reduced pressure to give compound **11** as a yellow oil (0.88 g, 95% yield).

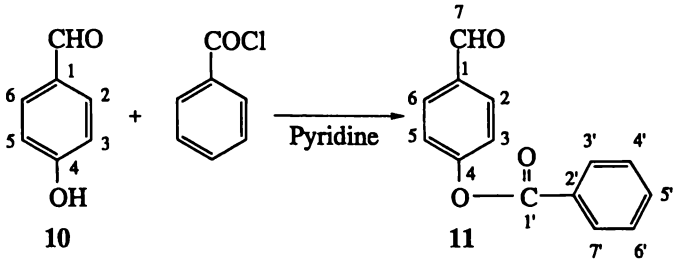

10 **11**

10 NMR: δ ^{1}H; 9.86 (s, 1H, 7), 7.84 (d, 8.7 Hz, 2H, Ar), 7.01 (d, 8.4 Hz, 2H, Ar), 2.58 (s, OH)

δ ^{13}C; 194.9 (7), 167.2 (4), 136.0 (2, 6), 132.4 (1), 119.8 (3, 5)

11 NMR: δ ^{1}H; 9.93 (s, 1H, 7), 8.14 (d, 7.5 Hz, 2H, Ar, Ar'), 7.88 (d, 6.6 Hz, 2H, Ar, Ar'), 7.59 (m, 1H, 5'), 7.45 (m, 2H, Ar), 7.35 (d, 7.5 Hz, 2H, Ar, Ar')

δ ^{13}C; 190.9 (7), 164.4 (1'), 155.7 (4), 134.1 (1), 134.1 (5'), 131.2 (2, 6)*, 130.3 (3', 7')*, 129.0 (2'), 128.8 (4', 6')*, 122.6 (3, 5)

*Tentative assignments

GC–MS: R_T 17.8 min; *m/z* 226 (M^+, 4), 197 (4), 168 (4), 141 (4), 105 (100), 77 (91), 51 (39)

mp: 78-79°C recrystallised from $CHCl_3$–petroleum spirit (bp 30-40°C)

Attempted Generation of 4-Benzoyloxybenzyl Alcohol

Compound **11** (0.36 g, 1.6×10^{-3} mol) in ethanol (EtOH) (10 ml) was stirred with sodium borohydride (Ajax) (0.12 g, 3.2×10^{-3} mol) for 30 minutes. The reaction mixture was quenched in ammonium chloride, adjusted to pH 8 (saturated sodium bicarbonate) and extracted into ethyl acetate (30 ml). The ethyl acetate layer was retained, dried ($MgSO_4$), and the solvent was removed under reduced pressure. The reaction was not further purified. The identity of compound **12** (ca 70% yield) was confirmed by GC–MS and NMR.

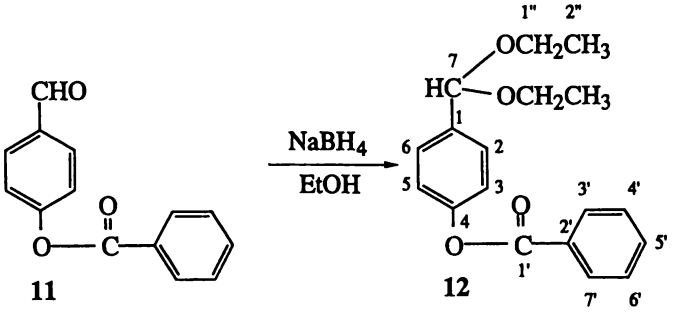

12 NMR: δ ^{1}H; 8.21 (d, 7.2 Hz, 2H, Ar, Ar'), 7.55 (m, 2H, Ar, Ar'), 7.50 (m, 2H, Ar, Ar'), 7.36 (m, 1H, 5'), 7.32 (d, 6.9 Hz, 2H, Ar, Ar'), 5.55 (s, 1H, 7), 3.60 (m, 4H, 1''), 1.27 (t, 6.9 Hz, 2H, 2'')

δ ^{13}C; 165.5 (1'), 156.8 (4), 151.0 (7), 138.9 (1), 136.9 (5'), 129.6 (2, 6)*, 129.5 (2'), 128.5 (3', 7')*, 128.1 (4', 6')*, 121.5 (3, 5), 61.2 (1''), 15.3 (2'')

*Tentative assignments

GC–MS: R_T 20.3 min; *m/z* 300 (M^+, 4), 255 (79), 225 (4), 153 (4), 122 (13), 105 (100), 77 (50)

Generation of 4-Benzoyloxybenzyl Alcohol (**13**)

Compound **11** (0.87 g, 3.8×10^{-3} mol) was dissolved in THF–H_2O (10 ml, 9:1) and stirred with sodium borohydride ($NaBH_4$) (0.28 g, 7.7×10^{-3} mol) for 30 minutes. The reaction mixture was quenched in ammonium chloride (0.1 M, 20 ml) and extracted into ethyl acetate (30 ml). The ethyl acetate layer was washed with; 2 M HCl (2 × 20 ml), saturated sodium bicarbonate (2 × 20 ml) and water (2 × 20 ml). The ethyl acetate layer was retained, dried ($MgSO_4$), and the solvent was removed under reduced pressure to give compound **13** as an oil, (0.55 g, 64 % yield).

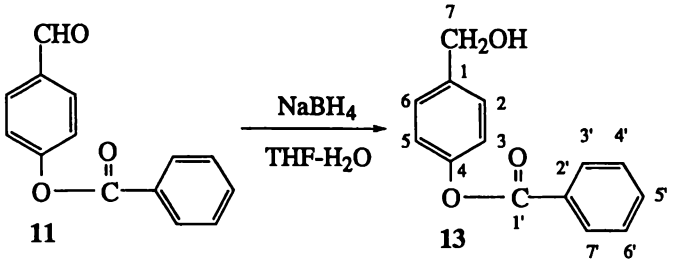

13 NMR; δ ^{1}H 8.20 (d, 7.2 Hz, 2H, Ar, Ar'), 7.65 (m, 1H, 5'), 7.51 (m, 2H, Ar, Ar'), 7.38 (d, 8.4 Hz, 2H, Ar, Ar'), 7.19 (d, 8.4 Hz, 2H, Ar, Ar'), 4.62 (s, 2H, 7), 3.28 (sb, 1H, OH)

δ ^{13}C; 165.5 (1'), 150.2 (4) 138.9 (1) 133.8 (5'), 130.3 (3', 7')*, 129.5 (2'), 128.7 (4', 6')*, 128.2 (2, 6)*, 121.8 (3, 5)*, 64.4 (7)

*Tentative assignments

GC–MS: R_T 18.5 min; *m/z* 228 (M^+, 4), 197 (1), 169 (1), 152 (1), 105 (100), 77 (46), 51 (17)

Generation of 4-Benzoyloxybenzyl chloride (**14a**)

Compound **13** (0.39 g, 1.7×10^{-3} mol) in pyridine (3 ml) was stirred with thionyl chloride ($SOCl_2$) (1.01 ml, 8.5×10^{-3} mol) for four hours at which time toluene (2×5 ml) was added and the pyridine removed by azeotropic distillation under reduced pressure. The reaction mixture was extracted into diethyl ether (30 ml) and washed twice with; 2 M HCl (2×20 ml), saturated sodium bicarbonate (2×20 ml), and water (2×20 ml). The diethyl ether layer was retained, dried ($MgSO_4$), and the solvent was removed under reduced pressure to give compound **14** as an oil (0.13 g, 30% yield).

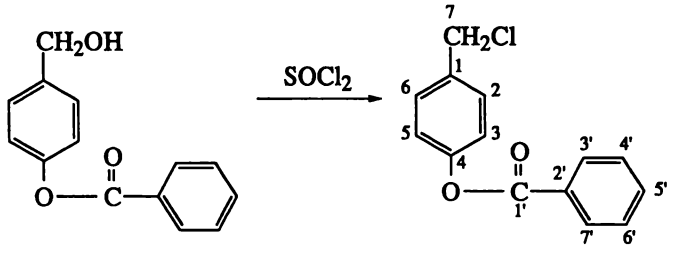

13 **14a**

14a NMR: δ ^{1}H; 8.20 (d, 7.8 Hz, 2H, Ar, Ar'), 7.65 (m, 1H, 5'), 7.52 (m, 2H, Ar, Ar'), 7.46 (d, 8.7 Hz, 2H, Ar, Ar'), 7.23 (d, 8.1 Hz, 2H, Ar, Ar'), 4.61 (s, 2H, 7)

δ ^{13}C; 165.1 (1'), 151.0 (4) 135.2 (1) 133.8 (5'), 130.3 (2, 6), 129.9 (3', 7'), 129.5 (2'), 128.7 (4', 6'), 122.1 (3, 5), 45.7 (7)

GC–MS: R_T 18.4 min; *m/z* 246, 247, 248, 249 (M^+, 4), 211 (4), 181 (1), 141 (1), 105 (100), 77 (75), 51 (29)

Generation of 4-Benzoyloxybenzyl bromide (**14b**)

To compound **13** (0.56 g, 2.4×10^{-3} mol) in diethyl ether (30 ml) was added CBr_4 (1.62 g, 4.8×10^{-3} mol), triphenylphosphine (1.25 g, 4.8×10^{-3} mol) and the mixture refluxed for

two hours. The reaction mixture was extracted into diethyl ether, dried ($MgSO_4$), and the solvent was removed under reduced pressure. Purification was conducted using PLC to give compound **15** as an oil (0.16 g, yield 23%).

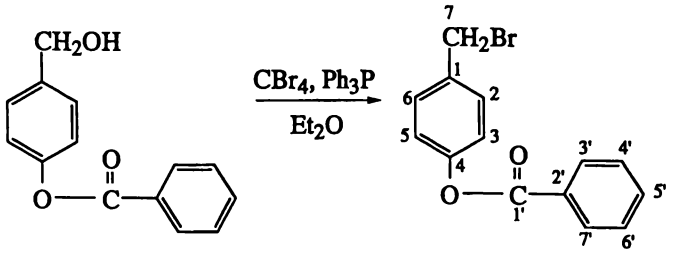

13 **14b**

14b NMR: δ ^{1}H; 8.22 (d, 7.2 Hz, 2H, Ar, Ar'), 7.66 (m, 1H, 5'), 7.55 (m, Ar, Ar'), 7.46 (d, 8.7 Hz, 2H, Ar, Ar'), 7.22 (d, 8.7 Hz, 2H, Ar, Ar'), 4.52 (s, 2H, 7)

δ ^{13}C; 165.0 (1'), 151.0 (4), 135.5 (1), 133.8 (5') 130.4 (2, 6)*, 130.4 (3', 7')*, 129.5 (2'), 128.7 (4', 6')*, 122.2 (3, 5), 32.9 (7)

*Tentative assignments

GC–MS: R_T 4.8 min; *m/z* 211 (M^+-Br, 13), 105 (100), 77 (39), 51 (22)

PLC: R_f 0.86 diethyl ether.

Attempted Generation of Diethyl 4-Benzoyloxybenzylphosphonate

This attempted preparation was carried out using both compound **14a** (data listed first) and **14b** (data listed second). To a stirred mixture of sodium (0.011, 0.010 g , 4.9/ 4.5 × 10^{-4} mol) in diethyl ether (10 ml), was added DEP (0.109/ 0.120 g, 4.4/ 4.1 × 10^{-4} mol) dropwise. The mixture was gently refluxed for half an hour, at which time compound **14a** (0.109, 4.4 × 10^{-4} mol) or **14b** (0.120 g, 4.1 × 10^{-4} mol) in dry THF (5 ml) was added dropwise from syringe and the mixture refluxed a further 4.5 hours. The reaction was quenched in ethanol (5 ml), water (40 ml), and then extracted with diethyl ether (30 ml). The diethyl ether layer was retained, dried ($MgSO_4$), and the solvent was removed under

reduced pressure. NMR analysis showed that the desired diethyl 4-benzoyloxybenzylphosphonate was not formed.

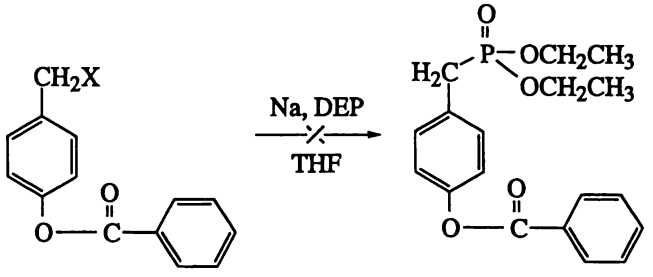

14a, 14b

X = Cl, Br respectively

2.3.2.4 THE ANISALCOHOL SYSTEM

Generation of 4-Methoxybenzylchloride (15)

Thionyl chloride (20 ml, 2.7 × 10^{-1} mol) was added dropwise from a glass syringe to compound **15** (10.1 ml, 7.9 × 10^{-2} mol) and the reaction mixture refluxed for one hour. The reaction mixture was then distilled under vacuum. The unreacted alcohol distilled first and crystallised on the condenser. This was removed by dissolution into methanol. The second fraction to distil was the desired chloride-**16** as a colourless oil (7.18 g, 58% yield).

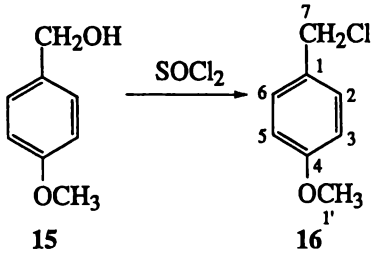

15 **16**

15 NMR: δ ^{1}H; 7.20 (d, 8.7 Hz, 2H, Ar), 6.84 (d, 8.7 Hz, 2H, Ar), 4.47 (s, 2H, 7), 3.92 (sb, 1H, OH), 3.73 (s, 3H, 1')

δ ^{13}C; 158.6 (4), 133.0 (1), 128.2 (2, 6), 113.5 (3, 5), 63.9 (7), 54.8 (1')

16 NMR: δ ^{1}H; 7.35 (d, 8.7 Hz, 2H, Ar), 6.94 (d, 8.7 Hz, 2H, Ar), 4.61 (s, 2H, 7), 3.81 (s, 3H, 1')

δ ^{13}C; 159.5 (4), 129.9 (2, 6), 129.5 (1) 113.9 (3, 5), 55.0 (1'), 46.1 (7).

bp: 73°C (1 mmHg)

Generation of Diethyl 4-Methoxybenzylphosphonate (**17**)

To a stirred mixture of sodium (0.51 g, 2.2 $\times 10^{-2}$ mol) in diethyl ether (10 ml), DEP (2.95 ml, 2.0 $\times$ 10^{-2} mol) was added dropwise and refluxed for half an hour, at which time, compound **16** (3.2 g, 2.0 $\times 10^{-2}$ mol) in dry THF (5 ml) was added dropwise from syringe and the mixture refluxed a further 4.5 hours. This reaction gave ca. 40% compound **17** (^{31}P NMR). Refluxing the DEP reaction mixture in triethyl phosphite (TEP) (10 ml, 5.8 $\times$ 10^{-2} mol) under a nitrogen atmosphere for 17 hours gave ca. 100% compound **17**. Compound **17** was purified by vacuum distillation to remove unreacted TEP (26-32°C at 1 mmHg) leaving compound **17** as an oil (4.59 g, 89% yield).

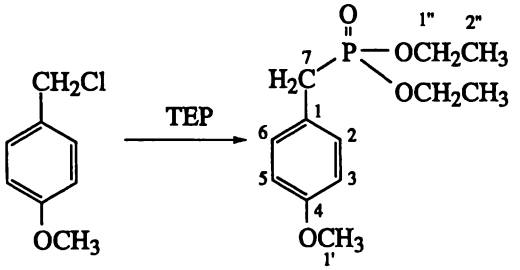

16 **17**

17 NMR: δ ^{1}H; 7.19 (dd, 8.1, 2.6 Hz, 2H, Ar), 6.82 (d, 8.1 Hz, 2H, Ar), 3.98 (m, 4H, 1"), 3.76 (s, 3H, 1'), 3.07 (d, 21.0 Hz, 2H, 7), 1.22 (t, 6.9 Hz, 6H, 2")

δ ^{13}C; 158.5 (4), 130.7 (d, 6.3 Hz, 2, 6), 123.4 (d, 9.1 Hz, 1), 113.9 (3, 5), 61.9 (d, 5.1 Hz, 1"), 55.1 (1'), 32.7 (d, 139.0 Hz, 7), 16.3 (d, 5.4 Hz, 2").

δ ^{31}P; 27.6 (m)

GC–MS: 16.50 min, 258 (M^+, 6), 230 (2), 215 (1), 121 (100), 91 (6), 77 (11), 65 (6), 51 (6).

ESI–MS: positive ion, cone voltage 20 V, *m/z* 259 $[M+H]^+$, 276 $[M+NH_4]^+$

Generation of Ethyl (4-Methoxybenzyl)phosphonylchloride (**18**)

To compound **17** (0.70 g, 2.7×10^{-3} mol) in chloroform ($CHCl_3$) (10 ml), phosphorus pentachloride (0.96 g, 4.6×10^{-3} mol) was added with vigorous stirring and the mixture gently refluxed for four hours. The reaction mix was poured onto water (100 ml), neutralised (saturated sodium bicarbonate, 2×20 ml) and extracted with chloroform (30 ml). The chloroform layer was retained, dried ($MgSO_4$), and the solvent removed to give compound **18** as an oil (0.60 g, 89% yield). Concern with the possible hydrolysis of compound **18** with the aqueous workup was investigated using ^{31}P NMR but appeared to be negligible for the time scale of the extraction.

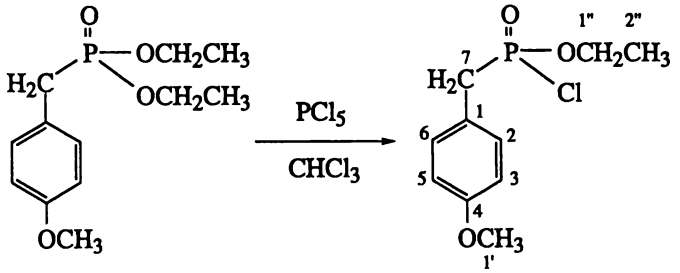

17 **18**

18 NMR: δ ^1H; 7.16 (m, 2H, Ar), 6.80 (m, 2H, Ar), 4.16 (m, 2H, 1"), 3.70 (s, 3H, 1'), 3.41 (d, 18.0 Hz, 2H, 7), 1.20 (m, 3H, 2")

δ ^{13}C; 159.2 (4), 131.2 (d, 7.5 Hz, 2, 6), 121.1 (10.8 Hz, 1), 114.2 (3, 5), 63.8 (d, 8.6 Hz, 1"), 55.1 (1'), 40.2 (d, 121.1 Hz, 7), 15.9 (d, 6.9 Hz, 2")

δ ^{31}P; 40.3 (m)

GC–MS: R_T 4.52 min; *m/z* 248. 249, 250, 251 (M^+, 8), 220 (1), 169 (1), 135 (1), 121 (100), 78 (8), 51 (5)

Attempted Generation of 4-Nitrophenyl Ethyl (4-Methoxybenzyl)phosphonamide

To a mixture of 4-nitroaniline (0.67 g, 2.7×10^{-3} mol) and potassium tert-butoxide ($KOBu^t$) (0.33 g, 3×10^{-3} mol) in DMSO (2 ml) under a nitrogen atmosphere was added compound **18** in DMSO (2 ml) and the mixture was refluxed for four hours. The reaction mixture was poured onto water (100 ml) and extracted with ethyl acetate (30 ml). The ethyl acetate layer was washed with 2 M HCl (2×20 ml), saturated sodium bicarbonate (2×20 ml) and water (2×20 ml). The ethyl acetate layer was retained, dried ($MgSO_4$), and the solvent was removed under reduced pressure. NMR showed the reaction did not proceed with the phosphorus mono acid ethyl ester of compound **18** and 4-nitroaniline recovered.

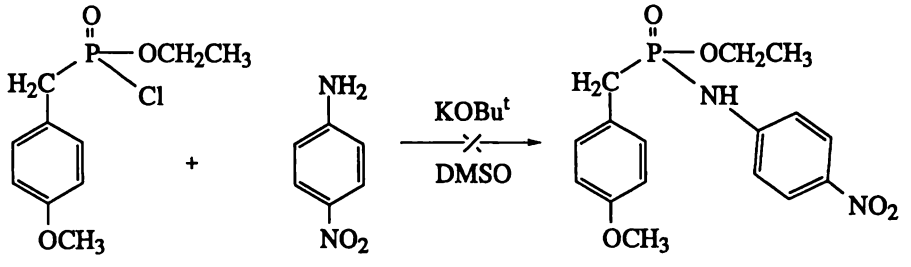

18

2.3.2.5 THE BENZYL PROTECTED SYSTEM

Generation of 4-Benzyloxybenzaldehyde (**19**)

To stirring solution of compound **10** (10.40 g, 8.5×10^{-2} mol) in acetone (100 ml), finely ground potassium carbonate (11.83 g, 8.6×10^{-3} mol) and potassium iodide (1.41 g, 8.5×10^{-3} mol) were added. Benzyl chloride (10 ml, 8.7×10^{-2} mol) was slowly added from a glass syringe, the mixture was stirred for seventeen hours in a flask fitted with a $CaCl_2$ drying tube. The acetone was removed under reduced pressure. The resulting solid was resuspended in diethyl ether–water (50:50 ml) and both layers were decanted from the brown material. The diethyl ether layer was washed with water (4×20 ml). The diethyl

ether layer was retained, dried ($MgSO_4$), and the solvent was removed under reduced pressure to give compound **19** as a purple crystalline material (15.86 g, yield 87%).

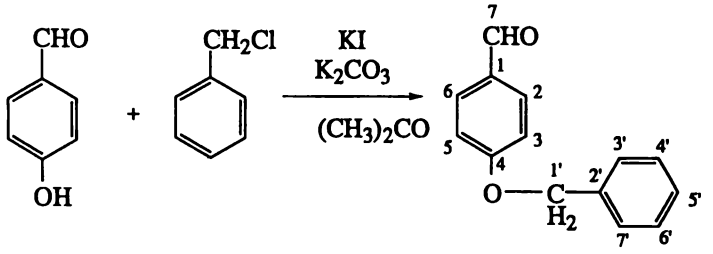

10 **19**

19 NMR: δ ^{1}H; 9.88 (s, 1H, 7), 7.84 (d, 9.0 Hz, 2H, 2, 6), 7.41 (m, 5H, Ar'), 7.08 (d, 8.7 Hz, 2H, 3, 5), 5.14 (s, 2H, 1')

δ ^{13}C; 190.8 (7), 163.8 (4), 136.1 (2') 132.1 (2, 6), 130.2 (1), 128.8 (3', 7'), 128.4 (5'), 127.6 (4', 6'), 115.2 (3, 5), 70.3 (1')

GC–MS: R_T 16.2 min; *m/z* 212 (M^+, 4), 165 (1), 152 (1), 120 (1), 91 (100), 65 (17)

mp: 68-70°C (purple powder)

Generation of 4-Benzyloxybenzyl alcohol (**20**)

Compound **19** (14.88 g, 7.0×10^{-2} mol) in THF–H_2O (25:25 ml) was stirred with sodium borohydride (5.20 g, 1.4×10^{-1} mol) for 30 minutes under a condenser (due to heat evolution). The THF was removed under reduced pressure and the reaction mixture extracted with diethyl ether (40 ml), washed HCl (2 M, 2 × 20 ml), saturated sodium bicarbonate (2 × 20 ml), and water (2 × 20 ml). The diethyl ether layer was retained, dried ($MgSO_4$), and the solvent was removed under reduced pressure to give compound **20** as a yellow powder (9.38 g, 63% yield).

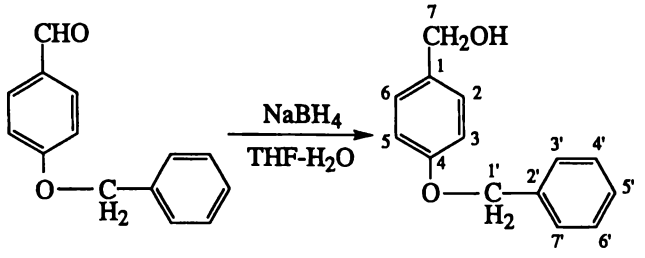

19 **20**

20 NMR: δ ^{1}H; 7.35 (m, 7H, Ar, Ar'), 6.97 (d, 8.7 Hz, 2H, Ar), 5.07 (s, 2H, 1'), 4.61 (s, 2H, 7), 1.69 (sb, 1H, OH)

δ ^{13}C; 158.5 (4), 137.0 (2'), 133.5 (1) 128.7 (3', 7')*, 128.6 (2, 6)*, 128.0 (5'), 127.5 (4', 6'), 115.0 (3, 5), 70.1 (1'), 65.1 (7)

*Tentative assignment

GC–MS: R_T 16.7 min; *m/z* 214 (M^+, 8), 183 (1), 152 (1), 122 (1), 91 (100), 65 (8)

Generation of 4-Benzyloxybenzylchloride (**21**)

Thionyl chloride (20 ml, 2.7×10^{-1} mol) was added to compound **20** (9.38 g, 4.5×10^{-2} mol) and stirred for one hour. The unreacted thionyl chloride was removed under reduced pressure. The chlorinated compound was redissolved in diethyl ether (30 ml), washed with saturated sodium bicarbonate (2 × 20 ml), and water (2 × 20 ml). The diethyl ether layer was retained, dried ($MgSO_4$), and the solvent was removed under reduced pressure to give compound **21** as an oil (7.08 g, 67% yield).

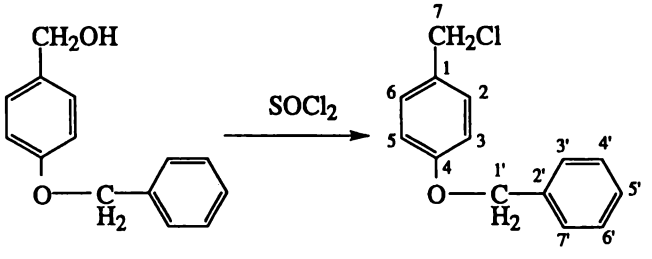

20 **21**

21 NMR; δ ^{1}H: 7.48 (m, 5H, Ar'), 7.40 (d, 8.4 Hz, 2H, Ar), 7.08 (d, 8.7 Hz, 2H, Ar), 5.14 (s, 2H, 1'), 4.65 (s, 2H, 7).

δ ^{13}C; 159.1 (4), 137.0 (2'), 130.3 (2, 6), 130.3 (1), 128.9 (3', 7'), 128.3 (5'), 127.7 (4', 6'), 115.3 (3, 5), 70.2 (1'), 49.5 (7).

GC–MS: R_T 5.7 min; *m/z* 232, 233, 234, 235 (M^+, 5), 197 (3), 165 (1), 141 (1), 106 (1), 91 (100), 65 (20)

Generation of Diethyl 4-Benzyloxybenzylphosphonate (22)

To compound **21** (7.08 g, 3×10^{-2} mol) under a nitrogen atmosphere was added TEP (16 ml, 4.2×10^{-1} mol) and the mixture refluxed for 22 hours. The product was separated from the excess TEP (26-32°C at 1 mmHg) via vacuum distillation to give compound **22** as a yellow oil (9.02 g, 90% yield).

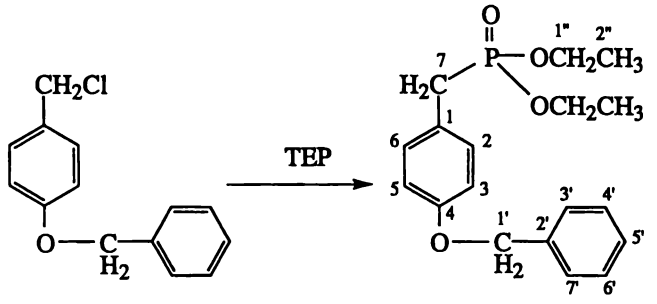

21 **22**

22 NMR: δ ^{1}H; 7.37 (m, 5H, Ar'), 7.20 (d, 6.7 Hz, 2H, Ar), 6.92 (d, 7.9 Hz, 2H, Ar), 5.04 (s, 2H, 1'), 4.00 (m, 4H, 1''), 3.08 (d, 21.1 Hz, 2H, 7), 1.23 (t, 6.9 Hz, 6H, 2'')

δ ^{13}C; 157.6 (d, 2.9 Hz, 4), 136.8 (2'), 130.6 (d, 6.5 Hz, 2, 6), 128.4 (3', 7'), 127.7 (5'), 127.3 (4', 6'), 123.6 (d, 9.3 Hz, 1), 114.8 (d, 1.6 Hz, 3, 5), 69.8 (1'), 61.9 (d, 6.9 Hz, 1''), 32.1 (d, 139.0 Hz, 7), 16.2 (d, 5.9 Hz, 2'')

δ ^{31}P; 27.5 (m)

Generation of Ethyl 4-Benzyloxybenzylphosphonylchloride (23)

To compound **22** (0.50 g, 1.5×10^{-3} mol) in chloroform (10 ml) was added PCl_5 (1.15 g, 5.5 $\times$ 10^{-3} mol) and the solution vigorously stirred for half an hour at which time the chloroform was removed under reduced pressure. The progress of the reaction was

monitored using ^{31}P NMR. Compound **23** was obtained (100% yield) and used in the subsequent synthetic step.

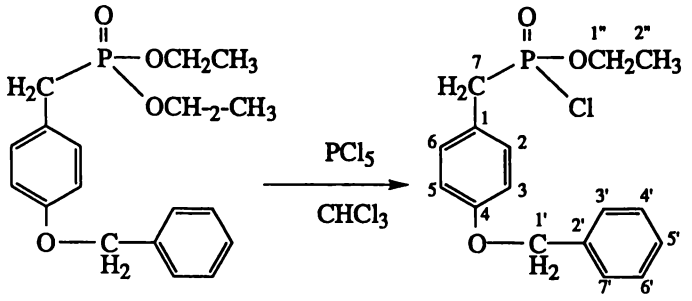

22 **23**

23 NMR: δ ^{1}H; 7.33 (m, 5H, Ar'), 7.19 (m, 2H, Ar), 6.94 (d, 8.0 Hz, 2H, Ar), 5.03 (s, 2H, 1'), 4.21 (m, 2H, 1"), 3.45 (d, 19.9 Hz, 2H, 7), 1.32 (t, 7.1 Hz, 2H, 2")

δ ^{13}C; 158.5 (d, 4.3 Hz, 4), 136.9 (2'), 131.3 (d, 7.5 Hz, 2, 6), 128.7 (3', 7'), 128.0 (5'), 127.52 (4', 6'), 121.5 (d, 10.8 Hz, 1), 115.2 (d, 3.5 Hz, 3, 5), 70.1 (1'), 63.8 (d, 8.6 Hz, 1"), 40.3 (d, 121.2 Hz, 7), 16.0 (d, 7.1 Hz, 2")

Note that the ^{13}C ($PO\underline{C}H_2\underline{C}H_3$) signals are half the intensity of the diester starting compound.

δ ^{31}P; 40.1 (m)

Attempted Generation of 4-Nitrophenyl Ethyl 4-Benzyloxybenzylphosphonamide

To stirred tert-butanol (5 ml, 5.3×10^{-2} mol) was added finely divided sodium (1.34 g, 5.8×10^{-2} mol) and the mixture refluxed for 30 minutes. The sodium tertiary butoxide ($NaOBu^{t}$) was syringed from the residual sodium and added to 4-nitroaniline (0.12 g, 8.7×10^{-4} mol) in THF (5 ml) and stirred for 30 minutes. This mixture was added to compound (**23**) and refluxed for four hours. The excess sodium was quenched with 95% ethanol (10 ml), poured onto water (100 ml), and extracted with diethyl ether (30 ml). The diethyl ether layer was retained, dried ($MgSO_4$), and solvent was removed under reduced pressure.

NMR and ESI–MS analysis showed that the 4-nitrophenyl ethyl 4-benzyloxybenzylphospho–4-nitroanilide had not been formed, with only the phosphorus mono acid ethyl ester of **23** and 4-nitroaniline being detected.

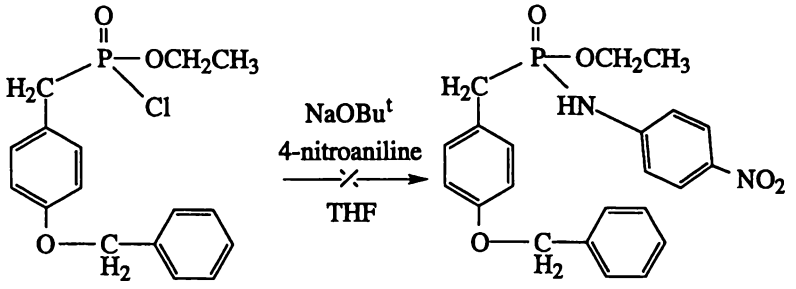

23

2.3.2.6 METHYL ETHANOATE PROTECTED SYSTEM

Generation of Methyl 2'-(4-Formylphenoxy)ethanoate (**24**)

To stirred compound **10** (1.26 g, 1.03×10^{-2} mol) dissolved in acetone (15 ml) were added finely ground potassium carbonate (1.43 g, 1.03×10^{-2} mol) and potassium iodide (0.17 g, 1.00×10^{-3}). To this solution methyl bromoacetate (1 ml, 1.06×10^{-2} mol) was added dropwise from a glass syringe and the mixture refluxed overnight. The reaction mixture was extracted into diethyl ether (20 ml) and washed with water (2×20 ml). The diethyl ether layer was retained, dried ($MgSO_4$), and the solvent was removed under reduced pressure to give compound **24** as a yellow oil (1.78 g, 89% yield).

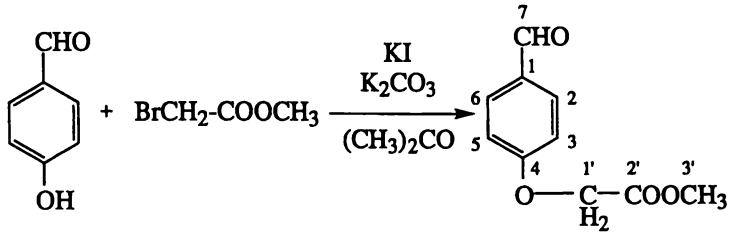

10 **24**

24 NMR: δ ^{1}H; 9.82 (s, 1H, 7), 7.78 (d, 8.9 Hz, 2H, Ar), 6.95 (d, 8.7 Hz, 2H, Ar), 4.67 (s, 2H, 1'), 3.75 (s, 3H, 3')

δ ^{13}C; 190.7 (7), 168.5 (2'), 162.6 (4), 132.0 (2, 6), 130.8 (1), 114.9 (3, 5), 65.1 (1'), 52.4 (3')

GC–MS: R_T 13.5 min; *m/z* 194 (M^+, 100), 165 (1), 149 (1), 135 (54), 105 (50), 77 (58), 51 (42)

mp: 32-38°C (colourless crystals)

Generation of Ethyl 2'-(4-Hydroxymethyl)ethanoate (**25**)

Compound **24** (0.20 g, 1.02 $\times 10^{-3}$ mol) in 100% ethanol (20 ml) was stirred with $NaBH_4$ (0.08 g, 2.0 $\times$ 10^{-3} mol) for half an hour. The ethanol was removed under reduced pressure and the remaining material redissolved in water (50 ml) and diethyl ether (30 ml). The diethyl ether layer was retained, dried ($MgSO_4$), and the solvent was removed under reduced pressure to give **25** as a colourless oil (0.09 g, yield 43%).

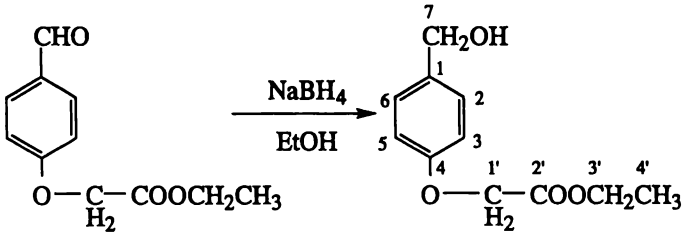

24 **25**

25 NMR: δ ^{1}H; 7.19 (d, 8.7 Hz, 2H, Ar), 6.83 (d, 9.0 Hz, 2H, Ar), 4.55 (s, 2H, 1'), 4.51 (s, 2H, 7), 4.21 (q, 6.9 Hz, 2H, 3'), 2.86 (sb, 1H, OH), 1.25 (t, 7.2 Hz, 3H, 4')

δ ^{13}C; 169.1 (2'), 157.3 (4), 130.4 (1), 128.6 (2, 6), 114.7 (3, 5), 65.4 (1'), 64.5 (7), 61.5 (3'), 14.2 (4')

GC–MS: R_T 14.3 min; *m/z* 210 (M^+, 58), 191 (8), 168 (8), 137 (29), 123 (67), 107 (100), 89 (25), 77 (42)

Preparation of Ethyl 2'-(4-Chloromethylphenoxy)ethanoate (**26**)

To stirred thionyl chloride (0.5 ml, 8.20 $\times$ 10^{-2} mol) at 0°C (ice–water slush bath) was added compound **25** (0.09 g, 4.30 $\times$ 10^{-4} mol) from a glass syringe and the mixture was

stirred for half an hour. Excess thionyl chloride was removed under reduced pressure to give compound **26** as an oil (0.10 g, 98% yield).

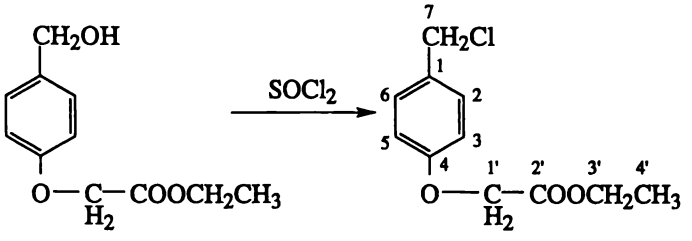

25 **26**

26 NMR: δ ^{1}H 7.30 (d, 8.7 Hz, 2H, Ar), 6.89 (d, 8.7 Hz, 2H, Ar), 4.66 (s, 2H, 1'), 4.54 (s, 2H, 7), 4.25 (q, 6.9 Hz, 2H, 3'), 1.28 (t, 7.2 Hz, 3H, 4')

δ ^{13}C; 168.7 (2'), 157.9 (4), 130.4 (1), 130.2 (2, 6), 114.9 (3, 5), 65.5 (1'), 61.5 (3'), 46.1 (7), 14.2 (4')

Formation of Diethyl 2'-(4-Phosphonatomethylphenoxy)ethylethanoate (27)

To compound **26** (0.10 g, 4.4×10^{-4} mol) under a nitrogen atmosphere was added TEP (2 ml, 1.1×10^{-2} mol) via syringe and the reaction mixture refluxed for 22 hours. Excess TEP was separated from the product via vacuum distillation (26-32°C 1 mmHg) to give compound **27** as a colourless oil (0.12 g, 85% yield).

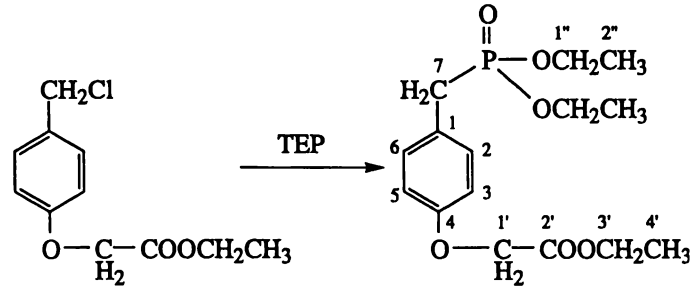

26 **27**

27 NMR; δ ^{1}H 7.13 (d, 8.5 Hz, 2H, Ar), 6.76 (d, 8.2 Hz, 2H, Ar), 4.50 (s, 2H, 1'), 4.16 (q, 7.1 Hz, 2H, 3'), 3.91 (m, 4H, 1"), 2.99 (d, 21.3 Hz, 2H, 7), 1.19 (m, 9H, 4', 2")

δ ^{13}C; 168.8 (2'), 156.9 (d, 3.6 Hz, 4), 130.8 (d, 6.5 Hz, 2, 6), 124.7 (d, 9.3 Hz, 1), 114.8 (d, 2.1 Hz, 3, 5), 65.5 (1'), 62.0 (d, 6.7 Hz, 1''), 61.3 (3'), 32.7 (d, 139.2 Hz, 7), 16.4 (d, 5.7 Hz, 2''), 14.1 (4')

δ ^{31}P; 27.2

GC–MS: R_T 18.8 min; *m/z* 330 (M^+, 42), 257 (4), 193 (100), 165 (8), 135 (4), 107 (21), 59 (13)

EI–MS: 330.1232 (M^+, 14; calc 330.1219 for $C_{15}H_{23}O_6P$), 316 (11), 139 (100), 179 (92), 125 (21), 107 (22), 90 (15), 45 (17)

Generation of Ethyl 2'-(4-Chlorophosphonatomethylphenoxy)ethylethanoate (28)

To compound **27** (0.14 g, 4.2 × 10^{-4} mol) in $CHCl_3$ (0.4 ml) was added phosphorus pentachloride (0.15 g, 7.2 × 10^{-4} mol) and the reaction stirred for half an hour. The chloroform was removed under reduced pressure and the reaction progress checked using ^{31}P NMR. Compound **28** was used immediately for the subsequent synthetic step.

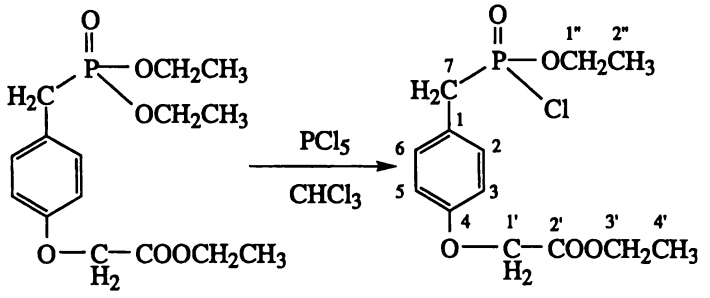

27 **28**

28 NMR; δ ^{1}H 7.19 (m, 2H, Ar), 6.85 (d, 8.1 Hz, 2H, Ar), 4.57 (s, 2H, 1'), 4.22 (t, 6.6 Hz, 2H, 3'), 4.01 (m, 2H, 1''), 3.44 (d, 19.8 Hz, 2H, 7), 1.28 (m, 6H, 4', 2'')

δ ^{13}C; 168.8 (2'), 157.5 (4), 131.3 (d, 7.5 Hz, 2, 6), 122.4 (d, 10.5 Hz, 1), 115.1 (3, 5), 65.5 (1'), 63.8 (d, 8.6 Hz, 1''), 61.4 (3'), 39.7 (d, 121.5 Hz, 7), 15.9 (d, 6.9 Hz, 2''), 14.2 (4').

A drop in intensity of signals associated with $POCH_2CH_3$ was noted in both ^{1}H and ^{13}C NMR.

$\delta^{31}P$; 40.1 (m)

Attempted generation of 4-Benzylamino Ethyl 2'-(4-Phosphonamidomethylphenoxy)ethylethanoate

To compound **28** (0.25 g, 2.3×10^{-3} mol) in chloroform (2.5 ml) was added benzylamine (0.25 g, 2.3×10^{-3} mol) and the reaction mixture stirred for four hours. The reaction mixture was washed with HCl (0.02 M, 4×50 ml), water (2×20 ml), saturated bicarbonate (2×20 ml), and water (2×50 ml). The chloroform layer was retained, dried ($MgSO_4$), and the solvent was removed under reduced pressure. NMR and ESI–MS analysis showed that the desired product was not formed with benzylamine and the phosphorus mono acid ethyl ester of **28** detected.

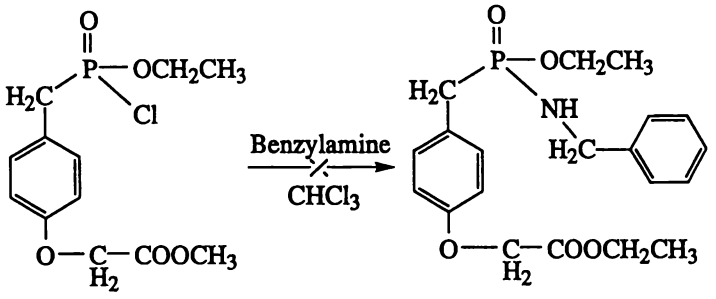

28

2.3.2.7 SUCCESSFUL GENERATION OF A TETRAHEDRAL PHOSPHORUS TRANSITION–STATE EMULATOR

Generation of Diethyl (4-Amidotrifluoroacetyl)benzylphosphonate (**30**)

To stirred diethyl 4-aminobenzylphosphonate-**29** (Aldrich) (1.0 g, 4.1×10^{-3} mol) in pyridine (5 ml) was added trifluoroacetic anhydride (TFAA) (5.0 ml, 3.5×10^{-2} mol) dropwise via syringe and the reaction stirred for fifteen hours. The reaction mixture was extracted with ethyl acetate (30 ml), washed with water (2×50 ml), 5% sulfuric acid (2×50 ml), water (2×50 ml), saturated sodium bicarbonate (2×50 ml), and water (2×50 ml).

The ethyl acetate layer was retained, dried ($MgSO_4$), and the solvent was removed under reduced pressure to give a yellow–orange crystalline material with varying yield over 20 preparations (70-90%).

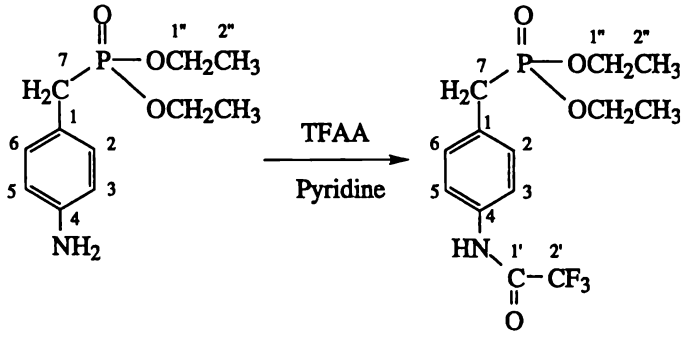

29 **30**

29 NMR: δ ^{1}H; 7.07 (d, 8.4 Hz, 2H, Ar), 6.62 (d, 8.4 Hz, 2H, Ar), 3.98 (m, 4H, 1"), 3.39 (sb, 2H, NH_2), 3.02 (d, 21.9 Hz, 2H, 7), 1.23 (t, 6.9 Hz, 6H, 2")

δ ^{13}C; 145.3 (4), 130.6 (d, 6.6 Hz, 2, 6), 121.1 (d, 8.4 Hz, 1), 115.3 (d, 2.3 Hz, 3, 5), 62.0 (d, 6.7 Hz, 1"), 32.8 (d, 139.2 Hz, 7), 16.4 (d, 6.1 Hz, 2")

δ ^{31}P; 27.9 (m)

30 NMR: δ ^{1}H; 10.53 (s, 1H, NH), 7.49 (d, 8.2 Hz, 2H, Ar), 7.11 (dd, 8.2, 2.6 Hz, 2H, Ar), 3.96 (m, 4H, 1"), 3.06 (d, 21.6 Hz, 2H, 7), 1.20 (t, 7.0 Hz, 6H, 2")

δ ^{13}C; 156.4 (37.6 Hz, 1'), 135.5 (d, 3.8 Hz, 4), 130.2 (d, 6.5 Hz, 2, 6), 128.1 (d, 8.9 Hz, 1), 121.3 (d, 2.1 Hz, 3, 5), 116.1 (q, 288.4 Hz, 2'), 62.4 (d, 7.1 Hz, 1"), 32.9 (d, 139.5 Hz, 7), 16.2 (d, 5.7 Hz, 2")

δ ^{31}P; 26.8 (m)

δ ^{19}F; -76.41 (s)

GC–MS: R_T 19.5 min; *m/z* 339 (M^+, 63), 311 (21), 283 (8), 229 (4), 214 (25), 202 (100), 185 (17), 107 (42), 78 (17)

mp: 140-144°C (orange crystals)

Generation of Ethyl (4-Amidotrifluoroacetyl)benzylphosphonylchloride (31)

To compound **30** (1.00 g, 3.0×10^{-3} mol) in $CHCl_3$ (2.5 ml), was added PCl_5 (0.68 g, 3.3×10^{-3} mol) and the reaction mixture stirred for one hour. The $CHCl_3$ was removed under reduced pressure. Formation of compound **31** was checked via ^{31}P NMR and **31** was used immediately for subsequent synthetic steps.

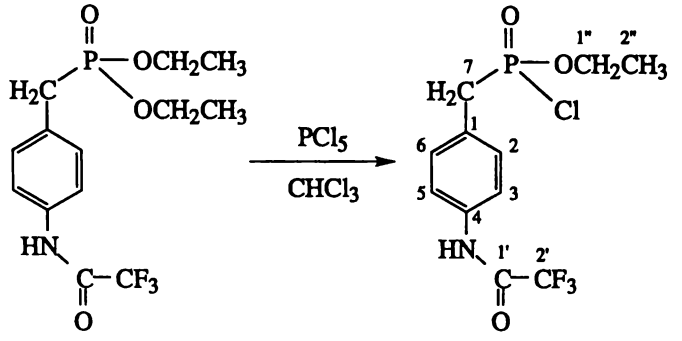

30 **31**

31 NMR: δ ^1H; 9.84 (s, 1H, NH), 7.49 (d, 8.1 Hz, 2H, Ar), 7.15 (dd, 8.0 , 2.7 Hz, 2H, Ar), 4.17 (m, 2H, 1"), 3.44 (m, 2H, 7, higher order splitting), 1.26 (t, 7.0 Hz, 3H, 2")

δ ^{13}C; 155.3 (q, 37.6 Hz, 1'), 135.9 (d, 4.8 Hz, 4), 130.6 (d, 7.5 Hz, 2, 6), 126.3 (d, 10.6 Hz, 1), 121.2 (d, 3.3 Hz, 3, 5), 115.9 (q, 288.4 Hz, 2'), 64.1 (d, 8.7 Hz, 1"), 40.2 (d, 121.3 Hz, 7), 15.7 (d, 6.8 Hz, 2")

δ ^{31}P: 39.3 (m)

δ ^{19}F: -76.42 (s)

Attempted Generation of Ethyl (4-Amidotrifluoroacetyl)benzylphospho-4-nitroanilide

To compound **31** (0.10 g, 3.0×10^{-4} mol) dissolved in DMSO (0.4 ml) under a nitrogen atmosphere was added 4-nitroaniline (0.04 g, 3.0×10^{-4} mol) pre-equilibrated (one hour) with potassium tert-butoxide (1.7 g, 1.5×10^{-3} mol) in DMSO (1 ml) and the reaction refluxed for 20 hours. The reaction mixture was extracted with chloroform (30 ml) washed

with HCl (2M, 2 × 40 ml), saturated sodium bicarbonate (2 × 40 ml) and water (2 × 40 ml). The chloroform layer was retained, dried ($MgSO_4$), and the solvent was removed under reduced pressure. NMR, GC–MS and ESI–MS showed that the desired product was not formed, with only 4-nitroaniline and the phosphorus mono acid diethyl ester of **31** being detected.

Generation of Ethyl (4-Amidotrifluoroacetyl)benzylphosphobenzamide (32)

To compound **31** (0.68 g, 5.0×10^{-4} mol) in chloroform (0.2 ml) was added benzylamine (0.16 g, 2.5×10^{-3} mol) and the reaction mixture stirred overnight. The reaction mixture was extracted with chloroform (30 ml) washed with HCl (2M, 2 × 40 ml), saturated sodium bicarbonate (2 × 40 ml) and water (2 × 40 ml). The chloroform layer was retained, dried ($MgSO_4$), and the solvent was removed under reduced pressure. The resulting material was separated on a silica column to give compound **32** as an oil (0.08 g, 40% yield).

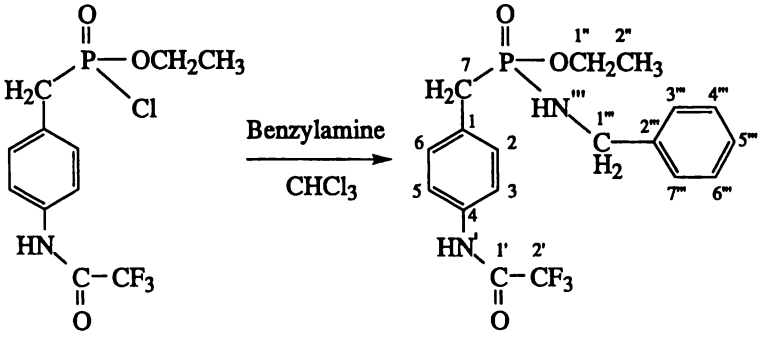

31 **32**

32 NMR: δ ^{1}H (400 MHz); 7.50 (d, 8.1 Hz, 2H, 3, 5), 7.28 (m, 5H, Ar'''), 7.09 (dd, 8.4, 2.4 Hz, 2H, 2, 6), 5.27 (s, 1H, NH'), 4.05 (m, 2H, 1'''), 4.00 (m, 2H, 1''), 3.11 (m, 2H, 7), 2.86 (m, 1H, NH'''), 1.25 (t, 7.2 Hz, 3H, 2'')

δ ^{13}C (400 MHz); 155.4 (q, 37.8 Hz, 1'), 139.4 (d, 5.4 Hz, 2'''), 135.3 (4), 130.4 (d, 6.3 Hz, 2, 6), 129.1 (d, 8.5 Hz, 1), 128.8 (4''', 6'''), 127.6 (5'''), 127.3 (3''', 7'''), 121.3 (3, 5), 116.1 (q, 288.5 Hz, 2'), 60.5 (d, 6.9 Hz, 1''), 45.1 (1'''), 34.8 (d, 126.8 Hz, 7), 16.3 (d, 6.6 Hz, 2'')

δ ^{31}P; 30.0 (m)

GC–MS: R_T 25.4 min; *m/z* 400 (M^+, 50), 3.7 (18), 202 (14), 185 (6), 132 (9), 106 (100), 85 (46), 77 (10)

ESI–MS: positive ion, cone voltage 20 V, *m/z* +20 V, 401 $[M+H]^+$, 418 $[M+NH_4]^+$

EI–MS: *m/x* 400.113686; 400 (M^+, 39; calc 400.1141 for $C_{13}H_{17}F_3NO_4P$), 371 (17), 202 (34), 185 (14), 132 (14), 106 (100), 91(81), 78 (14)

TLC: R_f 0.25 CH_3OH– CH_2Cl_2 (5:95)

mp: 130-131°C (white powder, recrystallised from $CHCl_3$–petroleum spirit (bp 60-80°C))

Table 2.9 HSQC NMR correlations for compound **32**

^1H signal (δ)	Correlated ^{13}C signal (δ)	Assignment
1.25	16.3	2"
3.11	34.8	7
4.00	60.5	1"
4.05	45.1	1'''
7.09	130.4	2, 6
7.24	127.3	3''', 7'''
7.29	127.6	5'''
7.33	128.8	4''', 6'''
7.50	121.3	3, 5

Table 2.10 HMBC NMR correlations for compound **32**

^1H signal (δ)	Correlated ^{13}C signal (δ)
1.25	60.5
3.11	129.1
4.05	128.8, 139.4
7.09	34.8, 121.3, 130.4, 135.3
7.24	45.1, 127.6

7.29	128.8, 139.4
7.33	127.6, 128.8, 139.4
7.50	121.3, 129.1, 135.3

Generation of Ethyl (4-Aminobenzylphosphobenzamide (33)

Compound **32** (0.026 g, 6.5×10^{-5} mol) was dissolved in ethanol (2 ml) and stirred with sodium borohydride (0.021 g, 5.7×10^{-4} mol) for one hour. The reaction mixture was extracted with ethyl acetate (60 ml), washed with HCl (2M, 2×20 ml), saturated sodium bicarbonate (2×20 ml), and water (2×20 ml). The ethyl acetate layer was retained, dried ($MgSO_4$), and the solvent was removed under reduced pressure. The resulting material was separated via flash chromatography to give compound **33** as an oil (0.014 g, 71 % yield).

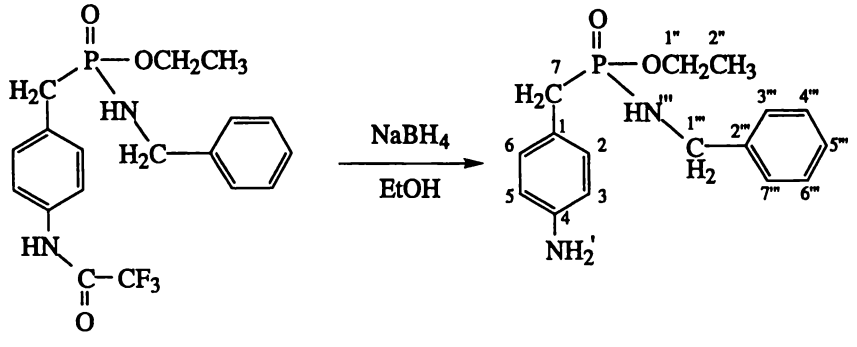

32 **33**

33 NMR: δ ^{1}H; 7.26 (m, 5 H, Ar'''), 6.99 (d, 8.1 Hz, 2H, Ar), 6.59 (d, 8.1 Hz, 2H, Ar), 4.02 (m, 4H, 1'', 1'''), 3.64 (sb, 2H, NH_2'), 3.03 (d, 20.1 Hz, 2H, 7), 2.70 (m, 1H, NH'''), 1.24 (t, 7.0 Hz, 3H, 2'')

δ ^{13}C; 145.2 (4), 140.0 (2'''), 130.6 (d, 6.3 Hz, 2, 6), 128.6 (4''', 6'''), 127.3 (3''', 7'''), 127.3 (5'''), 121.9 (1), 115.4 (3, 5), 60.2 (d, 6.9 Hz, 1''), 45.1 (1'''), 34.6 (d, 126.6 Hz, 7), 16.4 (d, 6.3 Hz, 2'')

δ ^{31}P; 31.0 (m).

ESI–MS: positive ion, cone voltage 20 V, 305 $[M+H]^+$, 322 $[M+NH_4]^+$

HR–MS (EI): elemental composition, expected (M^+) 400.114182, found (M^+) 400.113686; 400 (M^+, 39), 371 (17), 202 (34), 185 (14), 132 (14), 106 (100), 91 (81), 78 (14)

TLC: R_F 0.3 CH_3OH –Ethyl Acetate (5:95)

mp: 130-131°C (white powder recrystallised from $CHCl_3$–petroleum spirit 60-80°C)

Generation of Ethyl (4-Aminosuccinyl)benzylphosphobenzamide (**34**)

To compound **33** (0.014 g, 4.6×10^{-5} mol) in Et_3N (0.5 ml) and CH_2Cl_2 (0.5 ml) was added succinic anhydride (0.14 g, 1.4×10^{-4} mol) and the resulting mixture stirred for one hour. Solvents were removed under reduced pressure. The reaction mixture was extracted into ethyl acetate (30 ml), water added (50 ml) and the pH adjusted to 4 (2 M HCl). The ethyl acetate layer was kept, dried ($MgSO_4$), and solvent removed under reduced pressure. The resulting material was separated using flash column chromatography to give compound **34** (0.02 g, yield 90%).

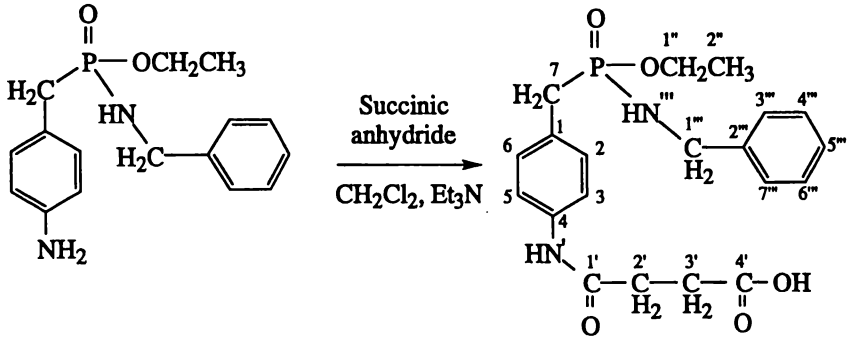

33 **34**

34 NMR: δ ^{1}H; 8.76 (s, 1H, NH'), 7.35 (d, 7.4 Hz, 2 H, Ar), 7.26 (m, 5H, Ar'''), 7.04 (d, 6.9 Hz, 2H, Ar), 4.00 (m, 1'', 1'''), 3.90 (m, 1'', 1'''), 3.70 (sb, 1H, NH''')*, 3.05 (dd, 21.0, 7.8 Hz, 2H, 7), 2.58 (m, 4H, 2', 3'), 1.20 (t, 3H, 6.9 Hz, 2''). *Tentative assignment.

$\delta^{13}C$; 176.1 (4'), 171.1 (1'), 139.5 (2'''), 137.1 (4), 130.3 (2, 6), 128.7 (4''', 6'''), 127.4 (5'''), 127.2 (3''', 7'''), 121.2 (1), 120.2 (3, 5), 60.7 (d, 7.0 Hz, 1''), 44.9 (1'''), 33.7 (d, 125.6 Hz, 7), 31.9 (2', 3'), 29.7 (2', 3'), 16.2 (d, 6.6 Hz, 2'').

The ^1H signal at 4.00 and 3.90 overlap and have an integration of ca 4H

^{31}P-^{13}C coupling was lost due to poor signal to noise in this compound.

$\delta^{31}P$; 32.7 (m).

ESI–MS: positive ion, cone voltage 20 V, *m/z* 422 $[M+NH_4]^+$, negative ion, 20 V, *m/z* 403 $[M-H^+]^-$

TLC: R_F 0.09 ethyl acetate–petroleum spirit (70:30)

Attempted Generation of 4-(Aminosuccinyl)benzylphosphonicbenzamide

To compound **34** (0.017 g, 4.3×10^{-5} mol) in CH_3CN–pyridine (1:1 ml) was added to trimethylsilyl chloride (0.027 ml, 2.1×10^{-4} mol) and the reaction mixture refluxed for four hours. NMR and ESI–MS showed that compound **34a** had not been formed.

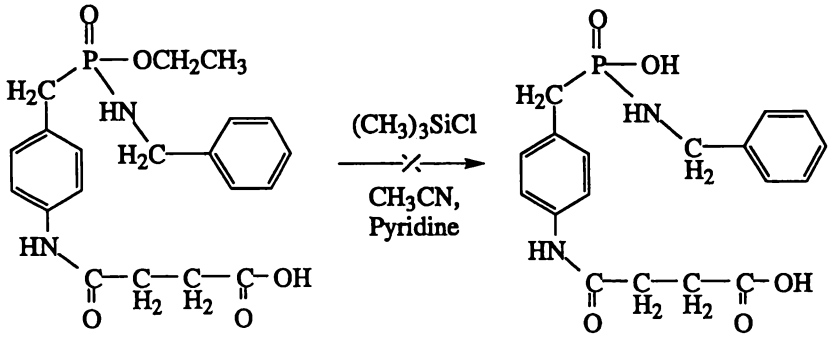

34 **34a**

Generation of 4-Nitrophenyl Ethyl (4-Trifluoroacetamido)benzyl–phosphonate (35)

To 4-nitrophenol (under a nitrogen atmosphere) (Riedel de Hann) (0.64 g, 4.6×10^{-3} mol) pre-equilibrated (30 min) in Et_3N (4 ml) was added a solution of compound **31** (1.32 g, 4.2 $\times 10^{-3}$ mol) in CH_2Cl_2 (9 ml) and the reaction mixture stirred for 17 hours. The reaction mixture was extracted with CH_2Cl_2 (16 ml). The CH_2Cl_2 layer was washed with; distilled water (2 × 40 ml), saturated bicarbonate (2 × 40 ml), and distilled water (2 × 40 ml). The CH_2Cl_2 layer was retained, dried ($MgSO_4$), and the solvent was removed under reduced

pressure. The resulting material was separated using flash chromatography to give compound **35** in varying yield (22-40%) over 20 preparations. One variation of this method involved preincubation of the Et_3N with compound **31** but contrary to work by Hirschmann *et al.*, (1997) this decreased the yield of **35**.

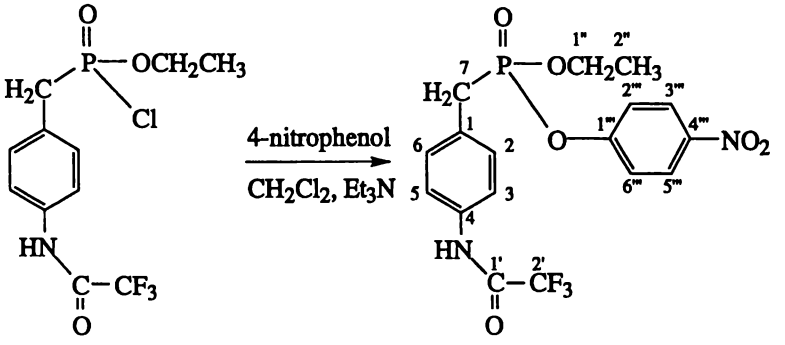

31 **35**

35 NMR: δ ^{1}H; 8.06 (d, 9.0 Hz, 2H, Ar, Ar'), 7.48 (d, 9.0 Hz, 2H, Ar, Ar'), 7.14 (m, 4H, Ar, Ar'), 4.11 (m, 2H, 1''), 3.33 (d, 21.7 Hz, 2H, 7), 1.22 (t, 7.1 Hz, 3H, 2'')

δ ^{13}C; 155.4 (m, 1'), 155.3 (1'''), 144.6 (4'''), 135.6 (d, 3.8 Hz, 4), 130.4 (d, 6.9 Hz, 2, 6), 127.2 (9.7 Hz, 1), 125.5 (3''', 5'''), 121.3 (d, 2.3 Hz, 3, 5), 121.0 (d, 4.5 Hz, 2''', 6'''), 115.9 (m, 2'), 63.9 (d, 7.5 Hz, 1''), 33.1 (d, 139.4 Hz, 7), 16.1 (d, 5.6 Hz, 2'')

δ ^{31}P; 24.3 (m)

δ ^{19}F; -76.39 (s)

GC–MS: R_T 27.9 min; *m/z* 432 (M^+, 86), 103 (5), 363 (29), 335 (10), 277 (3), 202 (100), 154 (4), 132 (22), 107 (44), 78 (10), 51 (3)

ESI–MS: positive ion, cone voltage 20 V, *m/z* 433 $[M+H]^+$, 450 $[M+NH_4]^+$

TLC: R_F 0.17 Ethyl acetate–petroleum spirit (70:30)

mp: 122°C (pale yellow crystal)

Crystal structure of 4-Nitrophenyl Ethyl (4-Trifluoroacetamido)benzylphosphonate (35)

Vapour diffusion recrystallisation of compound **35** from $CHCl_3$ and petroleum spirit (bp 30-40°C) at room temperature gave pale yellow tablets. Preliminary precession photography (Cu-K_α λ = 1.5418 Å) suggested monoclinic symmetry with systematic absences appropriate for the $P2_1/c$ space group. As no structure was reported in Cambridge Crystallographic database a full structural study was conducted.

Intensity data were collected at the Auckland University Crystallographic Unit on a Siemens SMART CCD diffractometer at -70°C with monochromated Mo- K_α radiation (0.7107Å). The data collection nominally covered over a hemisphere of reciprocal space, by a combination of three sets of exposures; each set had a different angle for the crystal and each exposure covered 0.3° in ω. The crystal to detector distance was 5.0 cm and the data sets were corrected empirically for absorption using SADABS (Blessing 1995).

Crystal Data

Formula	$C17H_{16}F_3N2O6P$
Molecular weight	432.9
Crystal class	Monoclinic; space group $P2_1/c$
Unit cell dimensions	a=7.8227(2) Å
	b=11.0942(1) Å β= 90.583(1)°
	c=22.4217(6) Å
Unit cell volume	1947.05(7) $Å^3$
Density calculated	1.475 g cm^{-3}
Z	4
F(000)	888
μ(Mo-$K\alpha$)	0.206 mm^{-1}
$T_{max,min}$	0.9934, 0.9566

A total of 11212 reflections were collected in the range of $1.82° \leq \theta \leq 26.39°$ corresponding to 3917 unique reflections (R_{int}=0.0577) of these 1898 had $I \geq 2\sigma(I)$.

Solution and refinement

The structure did not solve with the standard direct methods option so this problem was overcome using automatic interpretation of the Patterson map (SHELXS-96) to locate part of the structure about the phosphorus atom. The full structure was routinely developed.

All non hydrogen atoms are anisotropic, hydrogen atoms are in calculated positions with the exceptions of H(3) on the N(3) which were located as the highest peak in a penultimate difference map and was included with a fixed temperature factor but free coordinates. The refinement converged with $R_1 = 0.0599$, (2σ data), $R_1 = 0.1398$, $wR_2 = 0.1118$ and a GoF = 1.007 for all data. No parameter shifted more than 0.015 σ in the final cycle. The residual features were +0.289 e $Å^{-3}$ and -0.405 e $Å^{-3}$. A compilation of the phosphorus bond lengths and angles of interest are presented in tables 2.4 and 2.5 respectively.

Table 2.11 Thermal parameters for compound **35**

Atom	U11	U22	U33	U23	U13	U12
P(1)	0.0452(6)	0.0373(4)	0.0434(6)	0.0018(4)	-0.0120(5)	0.0036(4)
O(1)	0.0448(15)	0.0367(10)	0.0448(14)	0.0009(9)	-0.0104(12)	0.0023(9)
O(2)	0.0734(19)	0.0487(12)	0.0447(15)	0.0041(11)	-0.0181(13)	0.0054(12)
O(32)	0.128(3)	0.0415(13)	0.099(2)	0.0143(13)	-0.0546(19)	-0.0132(15)
O(41)	0.0398(15)	0.0424(11)	0.0575(15)	0.0082(10)	-0.0030(12)	0.0021(10)
O(42)	0.0514(19)	0.0730(16)	0.087(2)	0.0175(16)	-0.0191(17)	-0.0020(13)
O(43)	0.0511(17)	0.0532(14)	0.105(2)	0.0131(14)	0.0141(16)	0.0153(12)
F(1)	0.144(3)	0.0989(18)	0.191(3)	-0.0410(19)	-0.112(3)	0.0602(18)
F(2)	0.135(3)	0.190(3)	0.0578(18)	0.0369(17)	-0.0154(18)	-0.042(2)
F(3)	0.1025(19)	0.0634(13)	0.0692(15)	0.0082(10)	-0.0409(14)	-0.0158(12)
N(3)	0.0392(18)	0.0324(13)	0.0449(18)	0.0009(13)	-0.0059(15)	-0.0032(13)
N(4)	0.031(2)	0.0513(18)	0.086(3)	0.0168(18)	0.008(2)	-0.0018(15)
C(21)	0.103(4)	0.060(2)	0.043(2)	0.0051(18)	-0.010(2)	-0.010(2)
C(22)	0.126(5)	0.116(4)	0.076(3)	-0.003(3)	-0.036(3)	-0.036(3)
C(30)	0.036(2)	0.0347(15)	0.057(2)	-0.0019(14)	-0.0129(18)	0.0041(14)
C(31)	0.031(2)	0.0330(15)	0.045(2)	-0.0057(14)	-0.0080(17)	0.0078(14)
C(32)	0.035(2)	0.0305(15)	0.045(2)	-0.0016(14)	-0.0023(17)	0.0058(14)
C(33)	0.031(2)	0.0316(15)	0.043(2)	-0.0036(14)	-0.0056(17)	0.0007(13)
C(34)	0.030(2)	0.0318(15)	0.0367(19)	-0.0044(13)	-0.0037(16)	0.0046(14)
C(35)	0.034(2)	0.0359(16)	0.044(2)	0.0009(14)	0.0018(17)	0.0014(14)
C(36)	0.031(2)	0.0364(16)	0.054(2)	-0.0023(15)	-0.0011(18)	-0.0030(14)
C(37)	0.063(3)	0.0399(18)	0.054(2)	-0.0002(17)	-0.018(2)	0.0017(17)
C(38)	0.085(3)	0.052(2)	0.058(3)	0.0072(19)	-0.016(3)	0.001(2)
C(41)	0.035(2)	0.0349(16)	0.048(2)	0.0069(15)	0.0004(18)	-0.0003(15)
C(42)	0.053(3)	0.0523(19)	0.047(2)	-0.0058(16)	0.002(2)	-0.0007(18)
C(43)	0.045(2)	0.0492(19)	0.061(3)	-0.0050(18)	0.001(2)	0.0088(17)
C(44)	0.024(2)	0.0409(17)	0.064(3)	0.0117(17)	0.0014(19)	0.0001(15)
C(45)	0.033(2)	0.0481(18)	0.051(2)	-0.0004(16)	-0.0022(19)	-0.0058(16)
C(46)	0.038(2)	0.0392(16)	0.054(2)	-0.0025(16)	0.0000(18)	0.0030(16)

Table 2.12 Final positional and thermal parameters of calculated atoms for compound **35**

Atom	X	Y	Z	U_{eq}
P(1)	0.1714(1)	0.0956(1)	0.8980(1)	0.042(1)
O(1)	0.2039(3)	0.2186(2)	0.8773(1)	0.042(1)
O(2)	0.2321(3)	0.0645(2)	0.9626(1)	0.056(1)
O(32)	-0.0855(4)	0.1625(2)	0.6013(1)	0.090(1)
O(41)	-0.0290(3)	0.0647(2)	0.8987(1)	0.047(1)
O(42)	-0.5662(3)	0.3333(2)	0.7389(1)	0.071(1)
O(43)	-0.5582(3)	0.4530(2)	0.8156(1)	0.070(1)
F(1)	-0.3804(4)	0.1050(2)	0.5429(2)	0.145(1)
F(2)	-0.1792(4)	0.0396(3)	0.4932(1)	0.128(1)
F(3)	-0.3204(3)	-0.0787(2)	0.5461(1)	0.079(1)
N(3)	-0.0881(3)	-0.0351(2)	0.6307(1)	0.039(1)
N(4)	-0.5163(4)	0.3600(3)	0.7891(2)	0.056(1)
C(21)	0.1984(6)	0.1459(3)	1.0124(2)	0.069(1)
C(22)	0.3408(6)	0.1414(4)	1.0551(2)	0.106(2)
C(30)	0.2652(4)	-0.0214(2)	0.8544(1)	0.043(1)
C(31)	0.1843(4)	-0.0279(2)	0.7934(1)	0.036(1)
C(32)	0.0743(4)	-0.1222(2)	0.7782(1)	0.037(1)
C(33)	-0.0120(4)	-0.1231(2)	0.7250(1)	0.035(1)
C(34)	0.0089(4)	-0.0299(2)	0.6843(1)	0.033(1)
C(35)	0.1222(4)	0.0616(2)	0.6974(1)	0.038(1)
C(36)	0.2079(4)	0.0625(2)	0.7513(2)	0.041(1)
C(37)	-0.1320(5)	0.0591(3)	0.5962(2)	0.052(1)
C(38)	-0.2572(6)	0.0300(3)	0.5461(2)	0.065(1)
C(41)	-0.1533(4)	0.1371(2)	0.8719(2)	0.039(1)
C(42)	-0.2107(4)	0.2374(3)	0.9017(2)	0.051(1)
C(43)	-0.3328(5)	0.3106(3)	0.8746(2)	0.052(1)
C(44)	-0.3939(4)	0.2795(3)	0.8196(2)	0.043(1)
C(45)	-0.3412(4)	0.1770(3)	0.7902(2)	0.044(1)
C(46)	-0.2195(4)	0.1046(3)	0.8174(2)	0.044(1)

Table 2.13 Bond angles for compound **35**, esd's in parenthesis

Bond	Angle (°)	Bond	Angle (°)
O(1)-P(1)-O(2)	116.66(12)	C(34)-C(35)-C(36)	119.9(3)
O(1)-P(1)-O(41)	112.01(11)	C(35)-C(36)-C(31)	121.6(3)
O(2)-P(1)-O(41)	103.41(12)	O(32)-C(37)-N(3)	127.6(3)
O(1)-P(1)-C(30)	115.42(14)	O(32)-C(37)-C(38)	117.6(3)
O(2)-P(1)-C(30)	102.99(13)	N(3)-C(37)-C(38)	114.8(3)
O(41)-P(1)-C(30)	104.93(13)	F(1)-C(38)-F(3)	108.4(4)
C(21)-O(2)-P(1)	121.1(2)	F(1)-C(38)-F(2)	104.4(3)
C(41)-O(41)-P(1)	123.4(2)	F(3)-C(38)-F(2)	104.4(3)
C(37)-N(3)-C(34)	126.0(3)	F(1)-C(38)-C(37)	112.6(3)
O(42)-N(4)-O(43)	124.0(3)	F(3)-C(38)-C(37)	116.0(3)
O(42)-N(4)-C(44)	118.7(3)	F(2)-C(38)-C(37)	110.0(4)
O(43)-N(4)-C(44)	117.3(3)	C(46)-C(41)-C(42)	121.6(3)
O(2)-C(21)-C(22)	109.7(3)	C(46)-C(41)-O(41)	119.3(3)
C(31)-C(30)-P(1)	111.2(2)	C(42)-C(41)-O(41)	119.1(3)
C(36)-C(31)-C(32)	117.4(3)	C(41)-C(42)-C(43)	119.1(3)
C(36)-C(31)-C(30)	121.7(3)	C(44)-C(43)-C(42)	118.8(3)
C(32)-C(31)-C(30)	120.8(3)	C(43)-C(44)-C(45)	122.5(3)
C(33)-C(32)-C(31)	121.2(3)	C(43)-C(44)-N(4)	119.2(3)
C(32)-C(33)-C(34)	120.5(3)	C(45)-C(44)-N(4)	118.3(3)
C(35)-C(34)-C(33)	119.3(3)	C(44)-C(45)-C(46)	118.4(3)
C(35)-C(34)-N(3)	123.2(3)	C(41)-C(46)-C(45)	119.5(3)
C(33)-C(34)-N(3)	117.5(3)		

Table 2.14 Bond length data for compound **35**, esd's in parenthesis

Bond	Length(Å)	Bond	Length(Å)
P(1)-O(1)	1.465(2)	C(21)-C(22)	1.463(5)
P(1)-O(2)	1.558(2)	C(30)-C(31)	1.503(4)
P(1)-O(41)	1.606(2)	C(31)-C(36)	1.391(4)
P(1)-C(30)	1.787(3)	C(31)-C(32)	1.395(4)
O(2)-C(21)	1.462(4)	C(32)-C(33)	1.364(4)
O(32)-C(37)	1.208(3)	C(33)-C(34)	1.390(4)
O(41)-C(41)	1.394(4)	C(34)-C(35)	1.377(4)
O(42)-N(4)	1.225(4)	C(35)-C(36)	1.378(4)
O(43)-N(4)	1.236(3)	C(37)-C(38)	1.519(5)
F(1)-C(38)	1.275(4)	C(41)-C(46)	1.371(4)
F(2)-C(38)	1.343(4)	C(41)-C(42)	1.376(4)
F(3)-C(38)	1.304(4)	C(42)-C(43)	1.390(4)
N(3)-C(37)	1.342(4)	C(43)-C(44)	1.363(5)
N(3)-C(34)	1.417(4)	C(44)-C(45)	1.380(4)
N(4)-C(44)	1.472(4)	C(45)-C(46)	1.383(4)

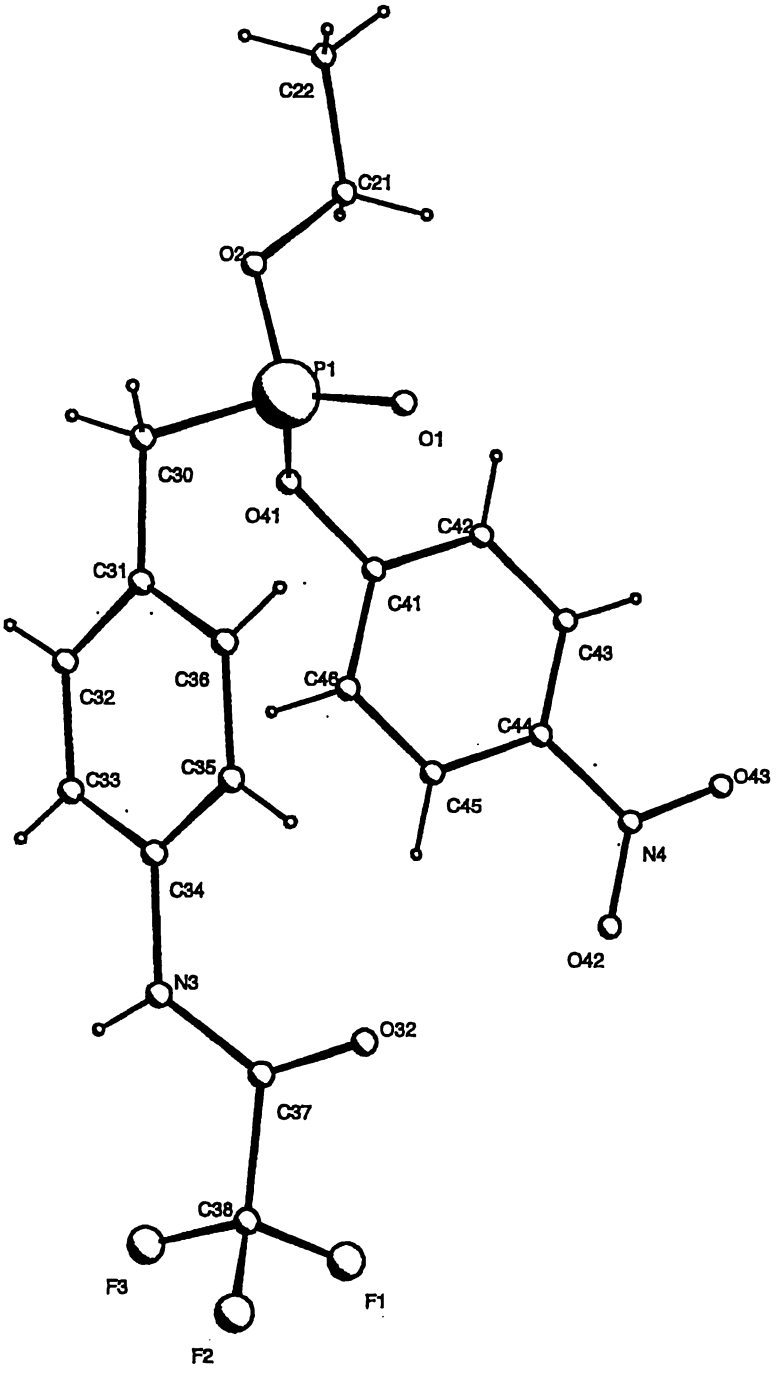

Figure 2. 22 Crystal structure of compound 35.

Generation of 4-Nitrophenyl Ethyl (4-Amino)benzylphosphonate (**36**)

To stirring compound **35** (0.96 g, 2.2×10^{-3} mol) in ethanol (20 ml) was added sodium borohydride (0.42 g, 1.1×10^{-3} mol). After 40 minutes the reaction mixture was poured onto saturated saline (200 ml) and extracted into ethyl acetate (3×30 ml). The ethyl acetate layers were combined, dried ($MgSO_4$) and the solvent was removed under reduced pressure. The resulting material was separated via flash column chromatography to give compound **36** in varying yield (18-42%) over twenty preparations.

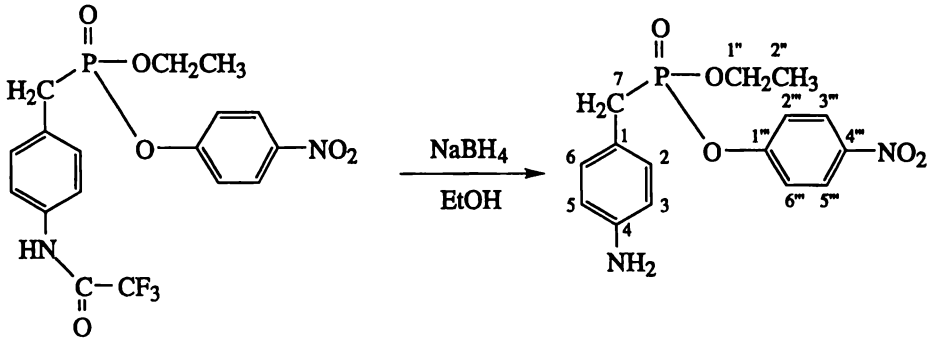

35 **36**

36 NMR: δ ^{1}H; 8.14 (d, 9.1 Hz, 2H, Ar, Ar'), 7.19 (dd, 9.3 Hz, 0.9 Hz, 2H, Ar, Ar'), 7.05 (dd, 8.3, 2.5 Hz, 2H, Ar, Ar'), 6.60 (d, 8.1, 2H, Ar, Ar'), 4.11 (m, 2H, 1''), 3.66 (sb, 2H, NH_2), 3.24 (d, 20.9 Hz, 2H, 7), 1.24 (t, 7.1 Hz, 3H, 2'')

δ ^{13}C; 155.9 (d, 8.6 Hz, 1'''), 146.2 (d, 3.0 Hz, 4), 144.3 (4'''), 130.7 (d, 6.7 Hz, 2, 6), 125.47 (3''', 5'''), 121.0 (d, 4.5 Hz, 2''', 6'''), 118.7 (d, 9.8 Hz, 1), 115.3 (d, 2.4 Hz, 3, 5), 63.5 (d, 7.3 Hz, 1''), 32.9 (d, 139.4 Hz, 7), 16.3 (d, 5.9 Hz, 2'').

^{31}P; 25.6 (m)

ESI–MS:positive ion, cone voltage 20 V, *m/z* 337 $[M+H]^+$, 354 $[M+NH_4]^+$

EI–MS: *m/z* 336.0875 (M^+, 100; calc 336.0877 for $C_{15}H_{17}NO_5P$), 134 (15), 106 (15), 77 (21), 39 (11)

TLC: R_f 0.16 ethyl acetate–petroleum spirit (70:30)

Generation of 4-Nitrophenyl Ethyl (4-Amidosuccinic)benzylphosphonate (37)

To stirring compound **36** (0.13 g, 1.0×10^{-4} mol) in CH_2Cl_2–Et_3N (2 ml:2 ml) was added succinic anhydride (0.12 g, 1.2×10^{-3} mol) and the mixture stirred for one hour. The solvents were removed under reduced pressure. The reaction mixture was redissolved in HCl (0.1 M, 100 ml) and extracted with ethyl acetate (4 × 30 ml). The ethyl acetate layer was dried ($MgSO_4$), and removed under reduced pressure. The resulting material was separated using flash column chromatography. Toluene (3 × 5 ml) was added to remove the residual acetic acid from the chromatographic separation via azeotrope under reduced pressure to give compound **37** in varying yield (30-50%) over 20 preparations.

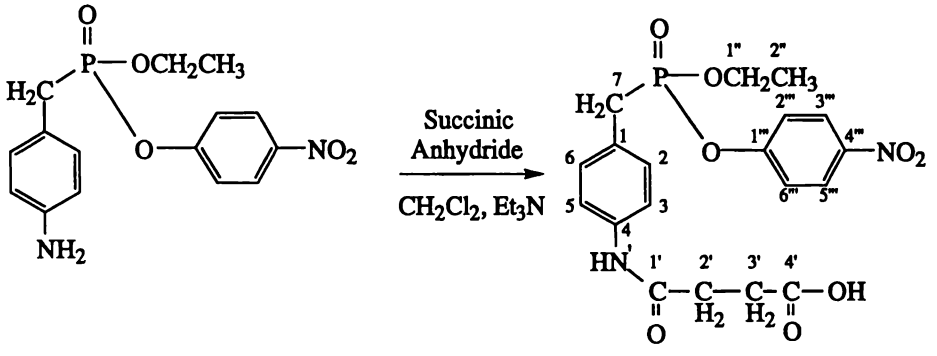

36 **37**

37 NMR: δ ^{1}H (400 MHz); 8.87 (s, 1H, NH'), 8.54 (sb, 1H, 4'), 8.07 (d, 9.1 Hz, 2H, 3''', 5'''), 7.39 (d, 8.2 Hz, 2H, 3, 5), 7.15 (d, 9.1 Hz, 2H, 2''', 6'''), 7.12 (d, 8.5 Hz, 2H, 2, 6), 4.08 (m, 2H, 1''), 3.29 (d, 21.2 Hz, 2H, 7), 2.59 (m, 2H, 3'), 2.54 (m, 2H, 2'), 1.19 (t, 7.1 Hz, 3H, 2'')

δ ^{13}C (400 MHz); 176.3 (4'), 171.1 (1'), 155.4 (d, 8.9 Hz, 1'''), 144.6 (4'''), 137.7 (d, 3.4 Hz, 4), 130.4 (d, 6.5 Hz, 2, 6), 125.6 (3'', 5'''), 125.1 (d, 9.7 Hz, 1), 121.1 (d, 4.4 Hz, 2''', 6'''), 120.4 (3, 5), 64.1 (d, 7.3 Hz, 1''), 33.0 (d, 139.5 Hz, 7), 31.6 (2'), 29.4 (3'), 16.3 (d, 5.7 Hz, 2'')

COSY assignment enables differentiation of 2' and 3' environments

δ ^{31}P; 25.2 (m)

2' and 3' assignment supported by COSY and ROESY data

ESI–MS:+20 V $[M+NH_4^+]$ = 454., -20 V $[M-H^+]$ = 435.

EI–MS: *m/z* 418.0927 (M^+-H_2O, 8; calc 418.0926 for $C_{19}H_{19}N_2O_7P$), 188 (44), 139 (100), 109 (35), 93 (20), 81 (16), 65 (69)

TLC: R_f 0.27 acetic acid– CH_3OH –ethyl acetate (1:5:94).

Table 2. 15 HSQC NMR correlation for compound **37**

^1H signal, (δ)	Correlates to ^{13}C signal(δ)	Assignment
1.19	16.3	2"
2.54	31.6	2'
2.59	29.4	3'
3.29	33.0	7
4.08	64.1	1"
7.12	130.4	2, 6
7.15	121.1	2"', 6"'
7.39	120.4	3, 5
8.07	125.6	3"', 5"'

Table 2. 16 HMBC NMR correlation for compound **37**

^1H signal, (δ)	Correlates to ^{13}C signal/s (δ)
1.19	64.1
2.54	29.4, 171.1, 176.3
2.59	31.6, 171.1, 176.3
3.29	125.1, 130.4
7.12	33.0, 130.4, 137.7
7.15	121.1, 144.6, 155.4
7.39	120.4, 125.1, 137.7
8.07	125.6, 144.6, 155.4
8.87	120.4, 171.1

Table 2.17 COSY NMR correlation for compound **37**

^1H (δ)	Correlates to ^1H (δ)
1.19	4.08
3.29	7.12
4.08	1.19
7.12	3.29, 7.39
7.15	8.07
7.39	7.12, 8.87
8.07	7.15
8.54	2.59
8.87	7.12, 7.39

Table 2. 18 NOESY NMR correlation for compound **37**

^1H	Correlates to ^1H
1.19	4.08, 7.12, 7.39
2.54	7.12, 7.39, 8.54, 8.87
3.29	7.12, 7.39, 8.87
4.08	1.19, 7.12, 7.39
7.12	1.19, 2.54, 3.29, 4.08, 7.39, 8.87
7.15	8.07
7.39	1.19, 2.54, 3.29, 4.08, 7.12, 8.87
8.07	7.15
8.54	2.54, 2.59
8.87	2.54, 3.29, 7.12, 7.39, 8.54

Table 2.19 DEPT[135] NMR for compound **37**

Carbon	Type
130.4	C-H
125.6	C-H
121.1	C-H
120.4	C-H
64.1	CH_2
33.0	CH_2
31.6,	CH_2
29.4	CH_2
16.3	CH_3

Generation of 4-Nitrophenyl (4-Amidosuccinic)benzylphosphonic Ester (**38**)

To compound **37** (0.10 g, 2.3 x 10^{-4} N) in d_5-pyridine (0.5 ml) and CD_3CN (0.5 ml) in an NMR tube was added trimethylsilyl bromide (Fluka) (0.6 ml, 4.5 × 10^{-3} mol). The reaction was monitored by NMR and typically found to be complete in 10 minutes (dependent on dryness of solvents). The reaction mix was poured onto water and washed with ethyl acetate (2 × 40 ml). The aqueous phase was retained and dried for 20 hours under reduced pressure. The resulting material was separated on a flash column to give compound **38** in varying yield (20-40%) over 20 preparations.

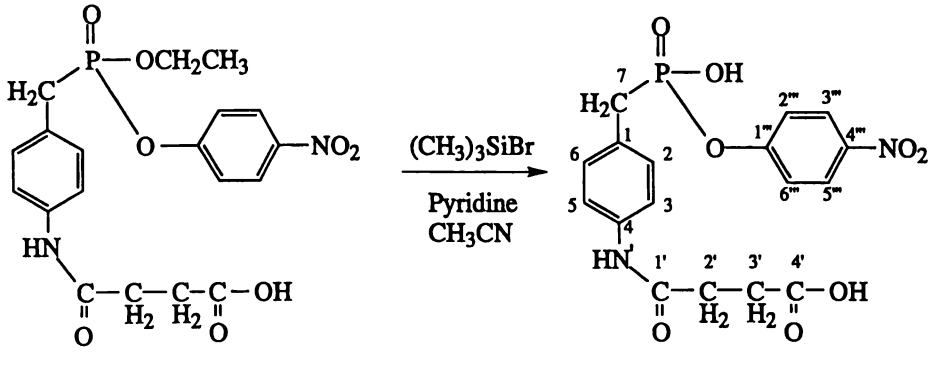

37 **38**

38 NMR: δ ^{1}H; (d_6–DMSO, 400 MHz) 10.02 (s, 1H, NH'), 8.31 (m, 2H, 3''', 5'''), 7.58 (d, 8.3 Hz, 3, 5), 7.43 (d, 8.5 Hz, 2H, 2''', 6'''), 7.31 (dd, 8.6, 2.4 Hz, 2H, 2, 6), 3.33 (d, 20.4 Hz, 2H, 7), 2.63 (s, 2H, 2', 3'), 2.61 (s, 2H, 2', 3')

δ ^{13}C; (d_6–DMSO, 400 MHz) 173.5 (4'), 169.8 (1'), 156.0 (d, 7.0 Hz, 1'''), 142.8 (4'''), 137.3 (4), 129.7 (d, 6.5 Hz, 2, 6), 127.0 (d, 9.0 Hz, 1), 125.2 (3''', 5'''), 120.7 (d, 4.5 Hz, 2''', 6'''), 118.6 (3, 5), 33.5 (d, 135.1 Hz, 7), 30.7 (2', 3'), 28.8 (2', 3').

δ ^{31}P; (D_2O) 21.2 (t).

ESI–MS: negative ion, cone voltage 20 V, *m/z* 407 $[M\text{-}H^+]^-$

LSIM–MS (negative mode): *m/z* 407.0644; 407 ($M\text{-}H^+$, 11; calc 407.0667 for $C_{17}H_{16}N_2O_8P$), 390 (32), 382 (13), 372 (9), 368 (100), 350 (10)

TLC: R_f 0.12 CH_3OH –CH_2Cl_2 (30:70)

LR–MS (FAB, positive mode): 413 ($M\text{-}H_2O\text{+}Na^+$, 9), 329 (21), 280 (7), 176 (100), 125 (5), 80 (64), 55 (5), 23 (33)

Table 2. 20 DEPT^{135} NMR for compound **38**

Carbon (δ)	Type
129.7	C-H
125.2	C-H
120.7	C-H
118.6	C-H
33.5	CH_2
30.7	CH_2
28.8	CH_2

Table 2. 21 ROESY NMR correlation for compound **38**

^{1}H (δ)	Correlates to ^{1}H (δ)
3.33	7.31
7.43	8.31
7.58	10.02

Table 2. 22 HMBC NMR correlation for compound **38**

^{1}H signal, (δ)	Correlates to ^{13}C signal/s (δ)
2.61	30.7, 173.5
2.63	28.8, 169.8, 173.5
3.33	127.0, 129.7
7.31	33.5, 129.7, 137.3
7.43	120.7, 142.8, 156.0
7.58	118.6, 127.0
8.31	125.2, 142.8, 156.0
10.02	118.6, 169.8

Table 2. 23 HSQC NMR correlation for compound **38**

^{1}H signal, (δ)	Correlates to ^{13}C signal (δ)	Assignment
2.61	28.8	2', 3'
2.63	30.7	2', 3'
3.33	33.5	7
7.31	129.7	2, 6
7.43	120.7	2''', 6'''
7.58	118.6	3, 5
8.31	125.2	3''', 5'''

Table 2. 24 COSY NMR correlation for compound **38**

^{1}H (δ)	Correlates to ^{1}H (δ)
7.31	7.58
7.43	8.31
7.58	7.31
8.31	7.43

2.3.2.8 SUBSTRATE PRODUCTION

Generation of PhenylAceto 4-Nitroanilide (39)

To phenylacetic acid (Aldrich) (1.0 g, 7.3×10^{-3} mol) was added thionyl chloride (5 ml, 2.2×10^{-1} mol) and the mixture stirred for one hour. The thionyl chloride was removed under reduced pressure and the resulting material dissolved in pyridine (3 ml) to this was added 4-nitroaniline (0.91g 6.6×10^{-3} mol) and the reaction mixture stirred for seventeen hours. The reaction mixture was extracted with ethyl acetate (30 ml). The ethyl acetate layer was retained, dried ($MgSO_4$), and the solvent was removed under reduced pressure. The resulting material was separated using a flash column to give compound **39** (0.45 g, 24% yield).

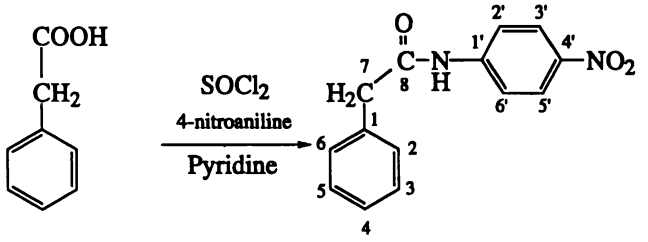

39

39 NMR: δ ^{1}H; 8.15 (d, 9.0 Hz, 2H, 2', 6'), 7.61 (d, 8.4 Hz, 2H, 3', 5'), 7.39 (m, 5H, Ar), 3.78 (s, 2H, 7)

δ ^{13}C; 169.6 (8), 143.7 (1'), 143.5 (4'), 133.6 (1), 129.5 (3, 5), 129.5 (2, 6), 128.1 (4), 125.1 (3', 5'), 119.2 (2', 6'), 44.9 (7).

GC–MS: R_T 22.6 min; *m/z* 256 (M^+, 9), 165 (1), 138 (3), 118 (37), 91 (100), 76 (4), 65 (19), 51 (4)

mp: 124-128°C (yellow crystal)

Generation of 4-NitroPhenyl Toluate (40)

To phenylacetic acid (1.0 g, 7.3×10^{-3} mol) was added thionyl choloride (5 ml, 2.2×10^{-1} mol) and the mixture stirred for one hour. The excess thionyl chloride was removed under reduced pressure and the resulting material was dissolved in chloroform (2 ml) and chilled in a 1,2 Dichloroethane/ $N_{2\,(l)}$ slush bath (@ -32°C). To the cooled solution was added

dropwise from a syringe a solution of 4-nitrophenol (0.92 g, 6.6×10^{-3} mol) in pyridine (3 ml). The reaction mixture was allowed to come to room temperature over one and a half hours with stirring. The reaction mixture was extracted with chloroform (30 ml). The chloroform layer was washed with water (2 × 40 ml), 2 M HCl (2 × 40 ml), saturated bicarbonate (2 × 40 ml), and water (2 × 40 ml). The chloroform was layer was retained, dried ($MgSO_4$), and the solvent removed under reduced pressure. The resulting material was separated using flash column chromatography to give compound **40** (0.41 g, 22% yield).

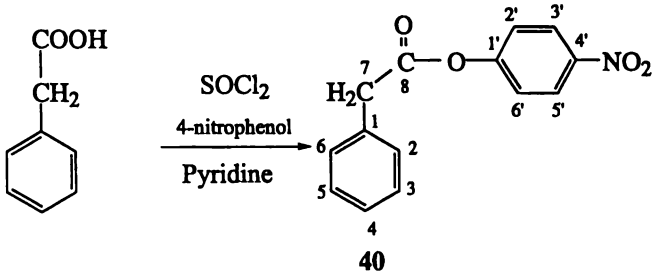

40

40 NMR: δ ^{1}H; 8.25 (d, 9.3 Hz, 2H, Ar'), 7.38 (m, 5H, Ar), 7.26 (d, 9.0 Hz, 2H, Ar'), 3.90 (s, 2H, 7)

δ ^{13}C; 169.1 (8), 155.5 (1'), 145.4 (4'), 132.7 (1), 129.3 (3, 5), 129.0 (4), 127.7 (2, 6), 125.2 (3', 5'), 122.4 (2', 6'), 41.4 (7).

GC–MS: R_T 20.2 min; *m/z* 257 (M^+, 1),181 (1), 165 (1), 153 (1), 139 (14), 118 (15), 91 (100), 75 (2), 65 (13), 51 (3)

TLC: R_f 0.60 CH_2Cl_2

mp: 118-122°C (yellow solid)

'Chaos is found in greatest abundance wherever order is being sought.
It always defeats order because it is better organised.'

Terry Pratchett.

CHAPTER THREE

ATTEMPTED PRODUCTION OF CATALYTIC POLYCLONAL ANTIBODIES

3.1 INTRODUCTION - THE IMMUNE RESPONSE

Having successfully generated a tetrahedral phosphorus transition–state emulation compound **38** suitable for ester and amide hydrolysis, the next step was to generate and characterise polyclonal antibodies to this material. However, small molecules do not generally elicit an immune response as, although they will bind to B cells, they are too small to contain determinants necessary to simultaneously bind the MHC II protein and the T cell. To overcome this problem small molecules (haptens) are conjugated to carriers such as proteins to effectively increase their size and ensure an immune response is obtained (see Chapter One).

Once conjugated to a protein the hapten serves as an epitope for binding to antibody present on the B cells, while the carrier protein enables the MHC II protein to bind the fragment for presentation. Generally the hapten is conjugated to a soluble carrier protein such as bovine serum albumin (BSA) or keyhole limpet haemocyanin (KLH), this is usually achieved with a bifunctional coupling agent. There are many methods available for linking hapten to protein including glutaraldehyde, N-hydroxysuccinimides and carbodiimides (Hermanson *et al.*, 1992, 1996).

As the first step of the antibody response to challenge is the engulfing of the foreign antigen by antigen–presenting cells (APC's), it is desirable to use sites of injection known to give

good response. Antigen can be administered by subcutaneous, intradermal, intramuscular, intraperitoneal, or intravenous injection.

Subcutaneous (SC) injection can include particulate material and adjuvant, which drains into the local lymphatic system to concentrate antigen at the local lymph nodes. Rabbits are usually given SC injection (up to 800 µl) on the back while mice (50-100 µl) are injected at the back of the neck or on one or both sides of the groin. Large injections of Freunds complete adjuvant should not be given at any one site as this may lead to site reactions or granuloma formation (Harlow *et al*, 1988).

Intramuscular (IM) injection is the method commonly used for slow release of antigen. The inoculum is deposited directly into the muscle tissue, with the antigen seen as it drains into nearby interstitial space, on the way to local lymph nodes. This method is not usually used on mice due to the practical problems associated with the muscle size but is both adjuvant– and particulate material–compatible (Harlow *et al*, 1988).

Intravenous (IV) injection is usually used for secondary (or later) boosts and is seldom used for primary injection. The antigen is rapidly delivered and processed. This method carries serious risk to animal welfare from pulmonary embolism, anaphylactic shock and toxicity of material present in the inoculum. IV injection is not suitable for inocula which include Freunds adjuvant, particulate material or detergents (Harlow *et al*, 1988).

Intraperitoneal (IP) injection describes direct injection into the peritoneal cavity and is highly appropriate for use with mice, with the antigen draining into the thoracic lymph ducts and then to the vena cava. IP injection is suitable for both particulate material and adjuvant, however, repeated use of Freunds complete adjuvant may cause granulomas (Harlow *et al*, 1988).

Adjuvants are non–specific stimulants of the immune system and, although not always required, judicious use of an adjuvant induces a strong antibody response to soluble antigens. One common component of most adjuvants is the use of a compound to form a localised deposit. To achieve this some adjuvants prepare the immunogen as a water-in-oil emulsion, others adsorb or trap the immunogen within aluminium hydroxide. The second component is a substance that stimulates the immune system by triggering of lymphokines which cause inflammation at the site of injection. Bacteria are usually the agents used for immune stimulation with heat killed *Mycobacterium tuberculosis* being used in the commercial preparations of Freunds complete adjuvant (Harlow *et al*, 1988). Recent concern with animal welfare issues due to adjuvant use has led to investigation of a number of new generation adjuvants which include the commercially available GERBU™ and Ribi™ which use less–toxic, immunogenic portions of bacterial material.

The immune system can be further manipulated by altering animal species and immunisation protocol. Commonly used laboratory animals are rabbits, mice, rats, hamsters and guinea pigs, the ideal choice depending on the application for which the antibody is required. For production of polyclonal antibodies the smaller animals are not usually used as the volumes of sera obtained can only be small (Harlow *et al*, 1988).

Different animals immunised with the same antigen will respond by producing a different spectrum of antibodies; using a large number of animals will make it more likely that antibodies with the desired properties will be obtained.

The dose required depends on many factors, but for a pure soluble protein antigen a dose of 50-100 mg in adjuvant at each immunisation is typical for a rabbit with mice requiring 0.5-1.0 mg in adjuvant. A delay of 2-3 weeks following primary injection is common (although much greater intervals can occur), with mice and rabbits remaining 'primed' for at least one year. Response to the second injection causes exponential antigen–specific B cell proliferation and antibody production reaches peak levels in 10-14 days but typically high

levels persist for 2-4 weeks. Subsequent injections follow the same response but the nature and quality of antibody binding alters due to the maturation process (Harlow *et al*, 1988).

Test bleeds are usually performed from mice tails, rabbit ears and sheep neck veins as these methods cause low animal stress. Small samples are collected until antibodies with the desired properties are detected at acceptable levels but once a good antibody titre is obtained regular boosts and bleeds are performed as required (Harlow *et al*, 1988).

Antibody cleanup is greatly aided by bacterial wall proteins such as protein A and G. Why proteins A and G bind to the Fc portion of the antibody is yet to be answered but biochemists have made great use of this phenomenon (Hermanson *et al.*, 1992). The difference in affinity of antibody binding between protein A and G means their use is complimentary in many situations. The binding of protein A and G is such that it leaves the antibody binding site free and lowering of pH disrupts the protein–antibody interaction. Usually cleanup of sera involves protein A or G (as a column material) binding of antibody, washing away of undesired material, followed by antibody elution at a lowered pH.

While there are a large number of immunological techniques that can be used for characterisation of antibodies only two were used in this study, the antibody titration enzyme linked immunosorbent assay (ELISA) and the competitive ELISA.

With the antibody titration ELISA (Fig. 3.1) the protein-hapten conjugate is coated to the solid phase plate, and non–specific binding sites blocked with an appropriate protein. Serum containing antibody is then applied and incubated; after unbound antibody is removed by washing an appropriate second antibody (anti-species antibody coupled to enzyme) is then applied which binds to the bound antibodies of the serum solution (which in turn are bound to the protein antigen conjugate). The plate is then washed to remove non-bound second antibody and incubated with a suitable substrate. The second antibody is linked to an enzyme so that a coloured substrate is formed when second antibody is

present and is detected spectrophotometrically. With appropriate dilutions it is possible to interpolate the concentration of antibody required for half maximal absorbance (I_{50}).

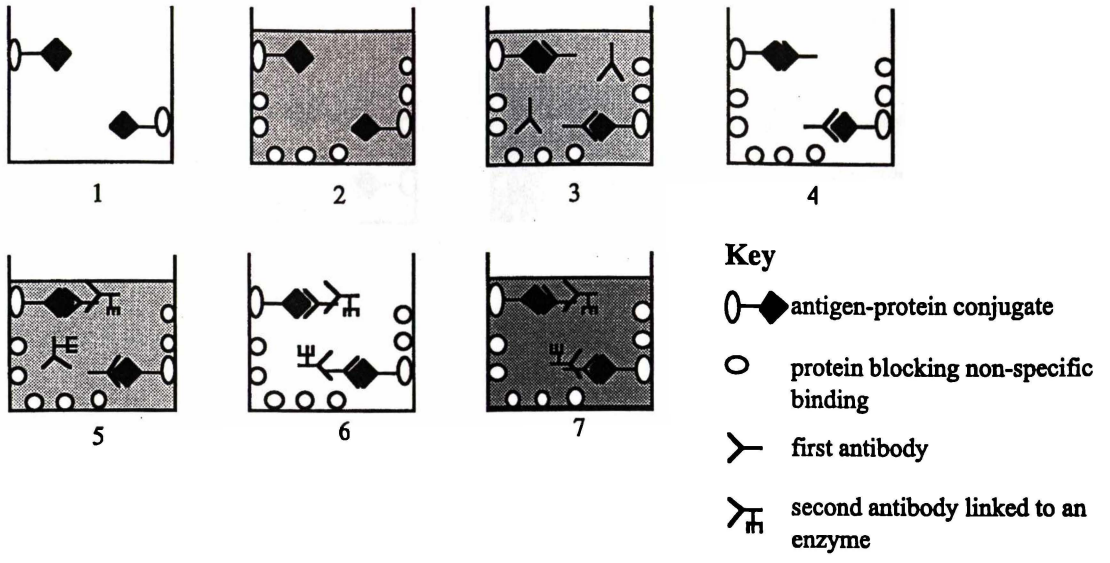

Figure 3. 1 Titration ELISA. 1) solid phase is coated with antigen-protein conjugate, 2) non-specific binding sites on the solid phase are blocked with protein, 3) serum containing antibody is incubated, 4) serum is removed leaving antibody with specific binding to the antigen, 5) second antibody (linked to an enzyme) is incubated, 6) second antibody solution is removed, 7) incubation with substrate which is converted to a coloured product by the enzyme; colour is detected spectrophotometrically.

Competitive ELISA is performed following an antibody titration as it makes use of the I_{50} value to ensure appropriate concentrations of antibodies and antigens. The competitive assay (Fig 3.2) involves attachment of the protein conjugate to a solid phase plate along with protein blocking; subsequently antigen is incubated with sera (containing antibody) at concentrations such that the free antigen competes with the solid phase protein–antigen conjugate for antibody binding, some of the sera antibody will not bind to the plate as it is bound to free antigen so that when the plate is washed the unbound antibody is removed. The second antibody (anti-species antibody with linked enzyme) is applied and washed to remove non–bound second antibody. Incubation of the plate with enzyme substrate gives a coloured product detected spectrophotometrically. An inverse relationship is obtained for this experiment with larger amounts of free antigen giving a lower absorbance.

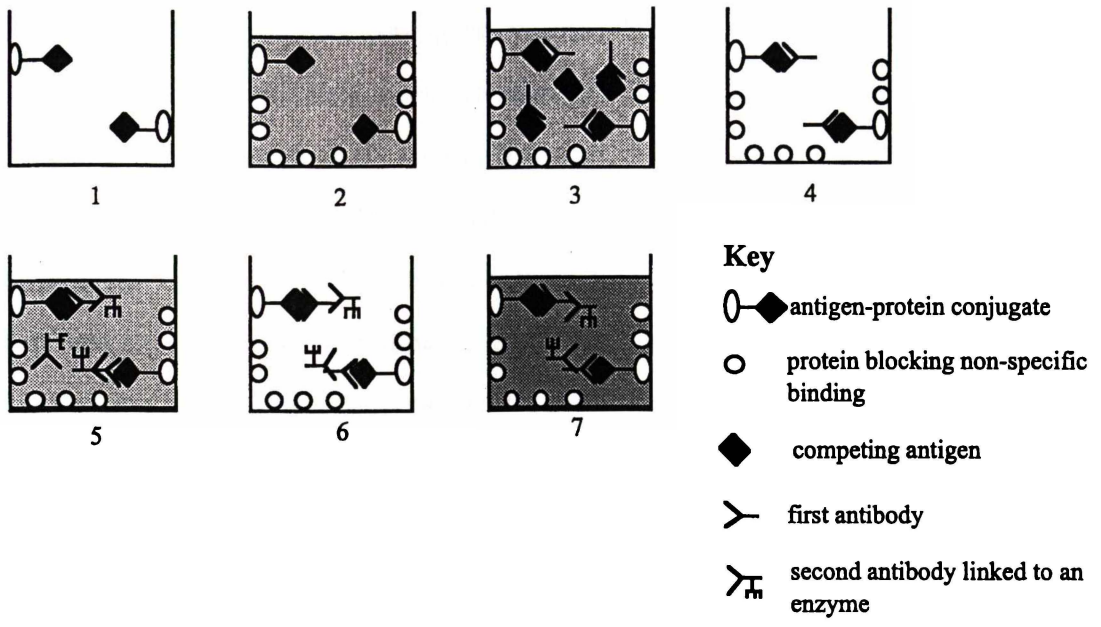

Figure 3. 2 Competitive ELISA. 1) solid phase is coated with antigen-protein conjugate, 2) non-specific binding sites on the solid phase are blocked with protein, 3) serum containing antibody is incubated in the presence of competing antigen, 4) serum is removed leaving antibody with specific binding to the antigen, 5) second antibody (linked to an enzyme) is incubated, 6) second antibody solution is removed body, 7) incubation with substrate which is converted to a coloured product by the enzyme; colour is detected spectrophotometrically.

3.2 DISCUSSION

3.2.1 CONJUGATION

Compound **38** was conjugated to three proteins, BSA, KLH and thyroglobulin (THY), using the succinic moiety. The major difficulty with characterisation was the small amount of material that was produced, for this reason characterisation was focussed predominantly on the BSA conjugate because more of this material was synthesised.

The conjugation reaction was monitored by TLC. For all proteins, a decrease in compound **38** with time was observed, which is consistent with conjugation occurring. The ideal technique for conjugate characterisation was expected to be ESI–MS as the binding of the hapten to the carrier protein should produce an easily detectable change in the mass to charge ratio (*m/z*).

Characterisation of protein conjugates via ESI–MS using spectra deconvolution has been reported and showed clear mass to charge ratio differences noted on hapten–protein conjugation (Adamczyk *et al.*, 1996). However, deconvoluted spectra of unconjugated BSA (Fig 3.4) and the BSA-**38** (Fig 3.5) conjugated material were compared there was no clear differences in *m/z*. The literature contains few methods for characterisation of hapten conjugation unless radiolabelling is available, most workers simply assume that the conjugation has occurred eg (Jones *et al.*, 1998; Pallavi *et al.*, 1997). Due to the expense, time and effort involved in immunisation and subsequent bleeding and sera characterisation, this lack of conjugate characterisation is surprising.

With the failure of the ESI-MS technique isoelectric focussing (IEF) was trialed. It was hoped that the change in charge ratio could be detected as not only is the phosphorus hapten negatively charged but the binding of the carboxyllic acid of the succinic linker arm to amines present on the protein further increases the net negative charge on the protein. What is evident from the IEF gel (Fig 3.6) is that the conjugated material has a band at the same isoelectric point (IEP) as the BSA and another band further toward the anode as would be expected for a net gain in negative charge. This, along with no suggestion of crosslinking from the SDS PAGE gel (Fig 3.6), provides good proof that conjugation has occurred for BSA and by inference the other proteins. Attempts at ^{31}P, ^{13}C and ^{1}H NMR were unsuccessful due to the small amounts of material available.

On the evidence obtained from the loss of the compound **38** on TLC and the production of a more negatively charged protein product (IEF), the conjugation was deemed to have been successful and the three protein conjugates were used for immunisation.

3.2.2 IMMUNE SERA CHARACTERISATION

3.3.2.2 ESTER AND AMIDE HYDROLYSIS

The sera of the various animals, collected at Bleed 1, were investigated for their ability to catalyse hydrolysis of substrates **39** and **40**. Although elevated levels of ester-**40**

hydrolysis relative to appropriate NIS control was noted for all mice immunised with conjugate-**38** (Fig. 3.8-3.11), no detectable hydrolysis of amide-**39** was observed in any of the hyper–immune sera (Bleed 1) when compared to the appropriate NIS, even after seven days at 20°C. Sheep immunised with conjugate-**38** showed lower levels of ester-**39** hydrolysis than the sheep NIS (Fig. 3.12). The rabbit antibodies, however, gave a large difference (2 orders of magnitude) between ester hydrolysis for the hyper immune rabbit compared to the rabbit NIS (Fig. 3.13). Unlike the mice, it was possible to obtain large enough amounts of sera for separation and characterisation of this hydrolytic element. With the high levels of ester hydrolysis, the question that needed to be answered was whether the catalysis was due to the presence of catalytic antibody.

The immune rabbit was bled (Bleed 2) and sera again found to have high levels of esterase activity (Fig. 3.14). It was decided to separate the antibody fraction from the rest of the protein material and ascertain which serum fraction was responsible for the catalysis, to confirm the presence of a catalytic antibody.

Protein G was used to separate the antibody fraction from the rest of the protein material. The isocratic elution system gave two protein–containing fractions, the elution time for the antibody fraction suggesting that the intermediate gradient steps were unnecessary. The later eluting antibody fraction was found to contain no esterolytic activity, with activity found in the unbound fraction I (Fig. 3.14). However, sodium dodecyl sulphate polyacrylamide gel electrophoresis (SDS-PAGE, results not shown) showed antibodies were still present in the first column fraction and it was possible that this material was responsible for the esterolytic activity. Further investigation was conducted.

A crude fractionation of immune rabbit serum (Bleed 2) was obtained by ammonium sulphate precipitation and the salt removed by dialysis. Both precipitate and dialysed solution showed high esterase activity. SDS-PAGE (Fig. 3.7) suggested that a reasonable separation of antibody from other sera proteins had occurred. The dialysed precipitated material was loaded onto a protein A column and separated; again two fractions were

prepared, unbound protein eluted in running buffer as fraction I prior to elution of the antibody fraction II at lower pH. Antibody fraction (II) contained no esterase activity, while activity was found in fraction I (Fig. 3.15). The SDS-PAGE showed high levels of antibody was still present in fraction I (Fig. 3.7), however, as ester hydrolysis was not obtainded from the antibody fractions of either protein A or G columns it must be assumed that this activity is due to some other serum component.

An extensive review of the literature indicated that over ten non–specific arylesterases have been noted in rabbit serum (Pilz *et al.*, 1968) and it was decided not to further characterise the esterase(s) present. Later esterase activity work indicated a drop in rabbit esterase activity (Bleed 3) suggesting that the activity observed fluctuates for unknown reasons and it was chance that the first two rabbit bleeds had such high levels of esterase activity (Fig. 3.16). One possible explanation for the higher levels of esterase activity detected for immunised animals was that the conjugate may have been binding to a repressor for the arylesterase activity, however, the high levels of esterase activity in the sheep NIS and the low levels of the later rabbit bleed suggest that the phenomenon was due to fluctuations in background esterase levels. Another indication which suggested that esterase activity was not due to the presence of a catalytic antibody was the very high rate of catalysis compared to that found in similar systems (Gallacher *et al.*, 1992). This is an example of one of the problems associated with characterisation of polyclonal sera. Of concern is that even if a catalytic antibody esterase had been generated capable of hydrolysing compound **40** it would not have been detectable with such a large enzyme background.

3.3.2.1 ELISA ANTIBODY TITRATIONS

The stability of the conjugate material when used as a plater coater in alkaline conditions was investigated by comparing a neutral coating buffer with an alkaline carbonate buffer, however, the alkaline carbonate coating buffer gave better binding of conjugate to the ELISA plate and was used for all subsequent experiments (Table 3.4). As three protein conjugates of compound **38** had been prepared initial experiments were aimed at determining which of the protein conjugates were good plate coaters.

The BSA-**38** conjugate was found to be a poor plate coater, binding poorly to anti-KLH-**38** rabbit and anti-THY-**38** sheep antibodies (Table 3.5). KLH-**38** as plate coater bound mouse anti–BSA-**38** and anti–THY-**38** well, however all sheep anti–THY-**38** sera bound minimally (Table 3.6). When THY-**38** was used as a plate coater it was found to bind mouse anti-BSA-**38** well, binding anti-KLH-**38** and GERBU anti-KLH-**38** antibodies to a lesser extent, and sheep anti-KLH-**38** antibodies poorly (Table 3.7). Anti–hapten reaction was determined on alternative conjugates to those used for immunisation to avoid protein recognition, for example the anti-BSA-**38** antibodies gave very good binding to the BSA-**38** plate coater (Table 3.5). This is probably due to the presence of antibodies recognising the conjugate protein. The good binding of anti–BSA-**38** antibodies from mice (numbers 5, 20, 30) to both THY-**38** and KLH-**38** plate coaters was promising; the similar levels of binding on two different plate coaters suggested that a specific binding interaction to the antigen hapten moiety was being observed. The data from the ELISA experiments were processed to give an antibody binding curve from which the percentage of maximum binding could be calculated. The 20% (I_{20}) and 80% (I_{80}) values of maximum binding were interpolated to give the 'working range' concentrations of antibody (I_{20}-I_{80}). The example (Fig 3.3) shows how the working range antibody concentrations (I_{20}, I_{50} and I_{80}) were calculated for binding of mouse anti-BSA-**38** antibodies to KLH-**38** plate coater (Bleed 1). A large I_{50} value indicated that this sera warranted further investigation using the competitive ELISA.

The ability of compound **38** to compete with plate–coated hapten–protein conjugate for antibody binding sites was investigated for the mice sera with highest antibody titre values. Unfortunately, no competition was detected when **38** was incubated with hyper–immune sera containing the antibodies (Table 3.8). Further, competitive binding of compound **40** with sera of the highest antibody titre values also showed no competition although an increase in yellow coloration was noted (Table 3.9). Lack of competition suggested that the interactions observed could be due to non–specific antibody interaction with plate coater. To investigate this theory non-immune sera (NIS) were included in the investigation of the second bleed to give an indication of background binding interactions of the various sera.

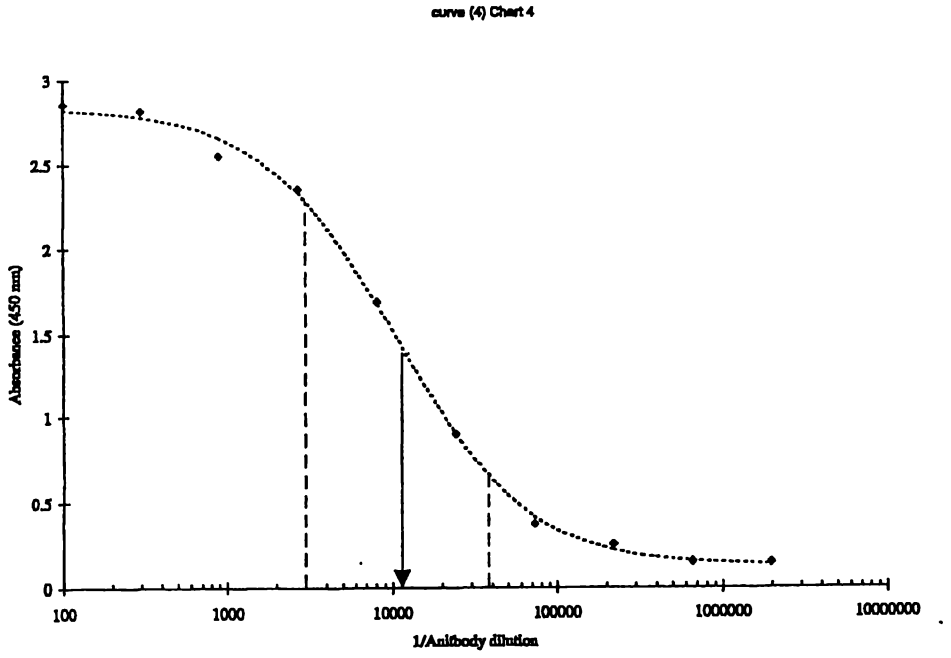

Figure 3. 3 ELISA titration of mouse 30 anti-BSA-**38** with KLH-**38** plate coater. The left broken line indicates the I_{80} value, the middle arrowed line indicates the I_{50} value, and the right broken line indicates the I_{20} value.

The second bleed (Bleed 2) gave ELISA titration results (Table 3.12-3.14) similar to those found for ELISA titration of Bleed 1. Some sera showed improved affinity for plate coated antigen (anti BSA-**38** mouse 6, THY-**38** coater) while others lost affinity (anti BSA-**38** mouse 30, THY-**38** coater). Again it was found that the antibodies with the best I_{50} values gave no response in the competitive assay (Table 3.10, 3.11). To further investigate antibody binding an ELISA plate was divided and coated half with KLH-**38** and half with unconjugated KLH; an antibody titration assay was run and, while binding was detectable for the KLH alone, it was found to be minimal compared to that for KLH-**38** (Table 3.13).

These data suggest that antibodies were generated to conjugate-**38**, however, they seemed to require the presence of a protein environment for recognition even if this was not the protein that the animals were immunised with. Conjugation of compound **38** to the protein would seem to have altered local chemical environmental properties such that the antibodies generated bind only this modified form of **38** and are not capable of binding the unmodified compound **38**. It has been previously noted that antibodies can be generated to particular

hapten conjugate and will give good antibody titres yet do not have the ability to bind the 'free' form of the hapten (Garthwaite, I. 1998, pers. comm.

3.3 EXPERIMENTAL

3.3.1 MATERIALS AND METHODS

3.3.1.1 REAGENTS AND SOLVENTS

All chemical reagents were obtained from BDH and were AnalAR grade unless otherwise noted. Dimethyl formamide (DMF) was dried by distillation and stored over 4Å molecular sieve. Water used was Milli Q (MQ). Measurement of pH was conducted using pH strips (BDH) or a Mettler Toledo 345 pH meter and 420 KCl electrode calibrated with standards (Orion).

3.3.1.2 CONJUGATION—SYNTHESIS OF HAPTEN PROTEIN CONJUGATE

Solution 1 composed of; 1-Ethyl-3-(3-dimethylamino-propyl)carbodiimide hydrochloride (EDC, Sigma), N-Hydroxy succinimide (NHS, Sigma) and compound **38** dissolved in DMF (1 ml) and stirred for 2 hours in a reactivial™ (Table 3.1).

Table 3.1 Conjugation Solution 1

Compound	Mr	Mole	Mole Ratio	Weight (mg)
EDC	192	2.6×10^{-5}	1.1	5
NHS	115	1.2×10^{-4}	5.0	14
Compound **38**	408	2.5×10^{-5}	1.0	10

Solution 1 was added to three different protein solutions BSA (Sigma A7-888, 3 ml of 10 mg ml^{-1} in 0.1 M $NaHCO_3$), THY (Serva 36488) and KLH (Boehringer GmbH-1376420) protein solutions (1 ml of 10 mg ml^{-1} in 0.1 M $NaHCO_3$) and stirred for 2 hours and the disappearance of compound **38** monitored by UV (TLC, R_f 0.5 methanol–$CHCl_2$ (70:30)). After two hours the three protein solutions were dialysed against phosphate buffered saline (1 × PBS, see ELISA) in dialysis tubing (12-14 kDa, molecular weight cut off, MWCO).

Following dialysis the protein solutions were made to a convenient volume, and aliqoted to vials: BSA (3 mg), THY (1 mg) and KLH (1 mg), and rapidly frozen with liquid nitrogen before lyophylisation. Conjugates were stored at -20°C until required.

3.3.1.3 CHARACTERISATION OF THE CONJUGATE

ESI–MS was used to characterise the conjugation reaction. Care was taken to ensure that both protein and protein conjugate were in the same environmental conditions (eg concentration, buffer molarity and pH) prior to loading to the ESI-MS so as to ensure that any change in *m/z* was not due to an artefact of the solution conditions but solely to conjugation. To this end both BSA and BSA-**38** were extensively dialysed with H_2O–CH_3OH–98% formic acid (50:50:2). The ESI-MS was analysed in the same solution using positive ion mode with a cone voltage of 45 V.

Isoelectric focusing was conducted using standard methods and is described later in this chapter under Gel Electrophoresis.

3.3.1.4 INJECTION AND BLEEDING OF ANIMALS

Immunogens were prepared for primary injection by resuspending in H_2O to give a conjugate concentration of 1 mg ml^{-1}. The resuspended conjugate[1] was added dropwise from a 3 ml syringe to a capped vial of the vortexing Freunds complete adjuvant (FCA, 2 ml) and the emulsion was thrice mixed by draw and expellation through a 18 g syringe needle. Subsequent boosts were prepared in the same manner except that Freunds incomplete adjuvant (FIA) was used in place of FCA. KLH-**38** (1 mg) was added to GERBU adjuvant (3 ml,) and stored at -20°C between inoculations.

Mice were injected IP at two sites (50 µl) with sheep injected IM at two sites (250 µl) and the rabbit injected SC at two sites (250 µl) (Table 3.2). Care was taken to monitor all animals for granuloma formulation especially the rabbit as granuloma tend to form more readily in this species (Garthwaite, I. 1998, pers. comm.).

[1] It should be noted that the immunogens were effectively in 1 × PBS due to residual buffer salts.

Table 3. 2 Description of conjugate and routes of injection for various species

Immunogen	Injection route	Species and amount injected
KLH-38	IP	4 mice @100 µl
	IM	2 Sheep @ 500 µl
KLH-38 GERBU	IP	4 mice @100 µl
	SC	1 Rabbit @500 µl
THY-38	IP	4 mice @100 µl
	IM	2 Sheep @ 500 µl
BSA-38	IP	4 mice @100 µl

Blood was collected at regular intervals (Table 3.3) from animals by standard procedures: mice via a puncture of the tail vein ca 100 µl, sheep via jugular vein into evacuated tubes ca 10 ml, and rabbit via a small cut in the marginal ear vein ca. 5 ml. With the exception of the immune rabbit (ca 12 ml) bulk bleeds were not conducted as no suitable antibodies were detected.

3.3.1.5 GEL ELECTROPHORESIS

12.5 % Homogenous SDS PAGE and IEF separations and silver staining were conducted on the PhastSystem™ using the standard methods (Pharmacia, 1987). Sigma SDS-7 standards used for SDS PAGE and Pharmacia IEF pH 3-10 calibration kit, 17-0471-01 for the IEF. Gels were left to air dry and photographed. In practice the working concentration range for silver staining was found to be 1–100 µg ml^{-1}.

Table 3. 3 Regime for injection and bleeding of animals

Immunogen	Species and ID	Immunisation 2	Immunisation 3	Immunisation 4	Immunisation 5	Bleed 1	Bleed 2	Bleed 3
KLH-**38**	Mouse NT, 3, 52, 56/60	4 Weeks	8 Weeks	12 Weeks		10 Weeks	14 Weeks	
KLH-**38** GERBU	Mouse NT, 1, 2, 3	4 Weeks	8 Weeks	12 Weeks		10 Weeks	14 Weeks	
KLH-**38** GERBU	Immune rabbit	2 Weeks	2 Weeks	2 Weeks	2 Weeks	4 Weeks	6 Weeks	8 Weeks
THY-**38**	Mouse 5, 6, 20, 60	4 Weeks	8 Weeks	12 Weeks		10 Weeks	14 Weeks	
BSA-**38**	Mouse 5, 6, 20, 30	4 Weeks	8 Weeks	12 Weeks		10 Weeks	14 Weeks	
KLH-**38**	Sheep 5819, 5820	4 Weeks	8 Weeks	12 Weeks		10 Weeks	14 Weeks	
THY-**38**	Sheep 5821, 5822	4 Weeks	8 Weeks	12 Weeks		10 Weeks	14 Weeks	

3.3.1.6 PURIFICATION OF SERA

Clotting

Sheep and rabbit sera were left to clot at room temperature for four hours then centrifuged (30 minutes @ 3000 g); working volumes were diluted with 0.02% thiomersal–PBS (1:100) and stored at 4°C. Mouse sera were left to clot and working sera diluted with 0.02% thiomersal–PBS (1:100) and stored at 4°C.

Column Separation

Rabbit serum was purified on the Protein A (Sigma Fastflow, 10 cm × 1 cm) and Protein G (Pharmacia Sepharose, 10 cm × 1 cm) columns; the sera were left to clot and centrifuged as previously described. Protein material was detected at 280 nm using a UV detector and the Bradford protein assay (see Sera Characterisation).

The sera purification methodology was adapted from the general outlines of Hermanson *et al.* (1992): sera was diluted (1:1) in phosphate buffer (0.2 M pH 8.0) filtered (0.2 μm, Supor Acrodisc 32, Gelman Sciences) and loaded onto the protein G column. Unbound protein was washed off the column with phosphate buffer and the bound antibody eluted with an isocratic stepped gradient system @ 2 ml min^{-1}; 45 min, 100% A, 27 min, 40% A, 33 min, 30 % A, and eluted with 18 min, 100% B, where solution A was phosphate buffer (0.2 M pH 8.0) and solution B was a citrate buffer (0.2 M citrate–sodium citrate pH 2.0).

The first protein material (fraction I) eluted at 2-5 minutes and the antibody material (fraction II) at 41-44 minutes using the protein G column. Both fractions were adjusted to pH 7.2 with concentrated NaOH or HCl as appropriate and made to 25 ml with 0.02% thiomersal–PBS. The diluted solutions were found to be too dilute for the esterase activity assay so both fractions were concentrated using ultrafiltration (UF) membranes (Amicon, 12-14 kD MWCO) to a volume of 5 ml. The esterase activity of the solutions was then assayed.

SDS PAGE of the two column protein G fractions I, II indicated that fraction I still contained large quantities of IgG and significant quantities of unknown sera proteins were present in fraction II which should have only contained IgG material (results not shown). It was for this reason that a more rigorous cleanup of immune rabbit sera was conducted.

The IgG fraction of immune rabbit sera was purified using an ammonium sulphate precipitation step followed by a protein A column separation. Saturated ammonium sulphate (0.5 ml, pH 7.0) was added dropwise to immune rabbit sera (2 ml, Bleed 2) and stirred for 30 minutes. Following centrifugation (20 min @ 3000 g), saturated ammonium sulphate (1.5 ml) was added dropwise to the stirring supernatent and the solution left at 4°C for four hours before centrifugation (30 min @ 3000 g). The antibody–containing precipitate (redissolved in H_2O (500 µl)) and supernatent were kept and both solutions dialysed (12-14 kD, MWCO).

The dialysed antibody fraction was separated on a protein A column by diluting (1:1) with phosphate buffer (0.2 M pH 8.0), filtering (0.2 µm Supor Acrodisc) and loading onto the column. Unbound protein was washed off the column with phosphate buffer and the bound antibody eluted with an isocratic stepped gradient @ 2 ml min^{-1}; 50 min, 100% A, 45 min, 100% B, where solution A was a glycine buffer (1.5 M, 3.0 M NaCl pH 8.9) and solution B a citrate buffer (0.1 M citrate–sodium citrate pH 4.0).

The first fraction (I) collected contained unbound protein and eluted after 2-8 minutes. The antibody material (fraction II) eluted at 21-25 minutes. Both the protein A fractions were adjusted to pH 7.2 with concentrated NaOH or HCl as appropriate and made to 40 ml with 0.02% thiomersal–PBS. The diluted fractions were found to be too dilute for the esterase activity assay so both fractions were concentrated using UF membranes (Amicon, 12-14 kD MWCO) to a volume of 1 ml. Again the rabbit sera purified with protein A showed esterase activity in fraction I but not in the antibody material (fraction II). SDS PAGE

indicated that the protein A fraction I contained a number of sera proteins with a small amount of IgG while fraction II contained just antibody (Fig. 3.7).

3.3.1.7 SERA CHARACTERISATION

Bradford Protein Assay

Coomassie Brilliant Blue G (B-0070, 50 mg) was dissolved in 95% ethanol (25 ml), to this was added 85% orthophosphoric acid (50 ml) dropwise from a burette over one hour. The brown-red solution was then made to 500 ml with H_2O to give a blue-brown solution (Bradford 1976). The solution was gravity filtered to give a brown-red solution which was stored in a darkened container.

Amide and Ester Assays

The spectral characteristics of 4-nitroaniline and 4-nitrophenol were examined using a Varian DMS 200 UV-VIS spectrophotometer and were found to have maximum absorptions at 382 and 400 nm respectively. The other cleavage product phenylacetic acid and parent compounds **39** and **40** were found to have no appreciable absorption in the region of interest (340-480 nm).

All solutions were preincubated (25°C), the assay solution was 0.02% thiomersal–PBS (160 µl) and, immediately prior to assay, 1 mg of either amide-**39** or ester-**40** was freshly dissolved in CH_3CN (1 ml) and 20 µl added to each well. The assay was conducted in duplicate and commenced on addition of diluted sera (20 µl, 1:200 PBS 0.02 % thiomersal) to each well. The negative control and the NIS had all the components of the assay except that in place of the immunised sera they contained 0.02% thiomersal–PBS and species–appropriate NIS respectively. The assay was conducted using a Biorad model 3550 Microplate reader monitoring absorbance at 405 nm and the kinetic data recorded using Microplate Manager 4.0 software (Biorad).

General ELISA method

- A solution of conjugate (1 mg ml^{-1}) was prepared in PBS (described below). Aliquots (55 µl) of this solution were used to prepare plate coater at 2.5 µg ml^{-1} by dilution in bicarbonate buffer (22 ml). This was coated onto microtitre well plates (50 µl, per well) (NUNC Immunoplate I, Denmark). The plate was tapped to mix, covered to minimise evaporation, and left overnight at room temperature (RT).

- The plate was washed once in PBS.

- The plate was then blocked with blocking buffer (described below), 300 µl to each well for one hour.

- The plate was washed once in PBS and used immediately, or 300 µl PBS was added for storage at 4°C (plates were used within two days over which time no loss of coater binding ability was noted).

- To each well, 50 µl of competitor (usually compound **38**) in PBS–CH_3OH (9:1) and 50 µl antibody at appropriate dilution in Blocking Buffer (as determined by the ELISA titration) was added. For ELISA titrations 50 µl of PBS was added in place of competitor. The plate was incubated for two hours.

- The plate was washed twice with PBS–Tween (described below) and then twice with PBS.

- To each well was added 100 µl of an appropriate second antibody–HRP (horse raddish peroxidase) conjugate (in coating buffer @ 1/3000 final dilution); sheep anti–mouse IgG, donkey anti-sheep IgG or goat anti-rabbit IgG (all obtained from Silenus laboratories, Australia).

- The plate was washed twice in PBS–Tween and then twice with PBS.

- To each well was added 100µl of Substrate Solution (made just prior to use). The plate was agitated at RT until colour developed (ca 15 minutes).

- The enzyme reaction was stoped by addition of 50 µl of H_2SO_4 (2 M) to each well.

- Absorbance was read at 450 nm.

Buffers

Coating Buffer (0.05 M Bicarbonate)

2.15 g $Na_2CO_3.2H_2O$, 1.47 g $NaHCO_3$ made to 500 ml with water and pH adjusted to 9.6.

Phosphate Buffered Saline (PBS) 10 × Stock

$NaH_2PO_4.2H_2O$ (2.897 g) and Na_2HPO_4 anhydrous (11.938 g) were made to 800 ml (H_2O), pH adjusted to 7.4 and the NaCl (87.660 g) added and made to one litre, if necessary the pH was adjusted to 7.2-7.6. Stock was diluted 1/10 and made fresh each day to give 0.01 M phosphate and 0.15 M NaCl.

PBS–Tween

Tween-20 was suspended at 0.05% in PBS (0.5 ml l^{-1})

1% OVA-Blocking buffer

OVA (3g) was dissolved in PBS (300 ml), used for plate blocking and all antibody dilutions.

Substrate Solution

Substrate Solution consisted of : 110 µl TMB (3,3',5,5'-tetramethylbenzidine, 10 mg in 1 ml DMSO, stored in dark at RT), 11 ml sodium acetate buffer 0.1 M. pH 5, and 165 µl of H_2O_2 solution (38 µl H_2O_2 (30%) made to 2.5 ml with H_2O).

3.3.2 RESULTS.

3.3.2.1 ESI–MS OF PROTEIN CONJUGATE

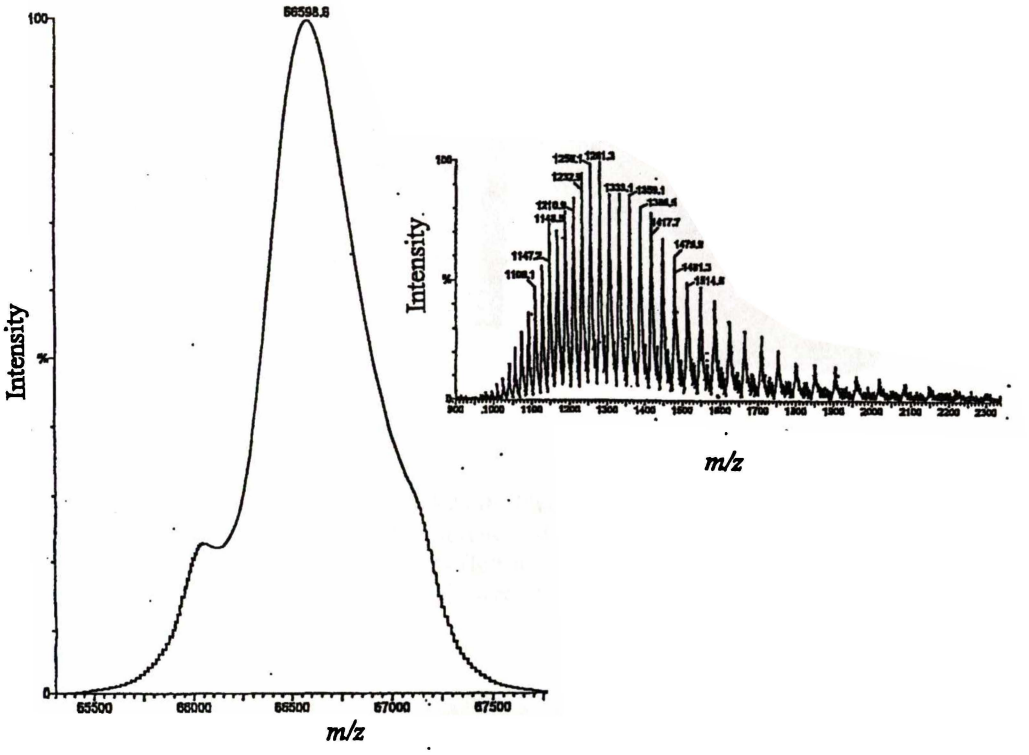

Figure 3. 4 The ESI–MS of BSA, deconvoluted (left) and complex spectra (right).

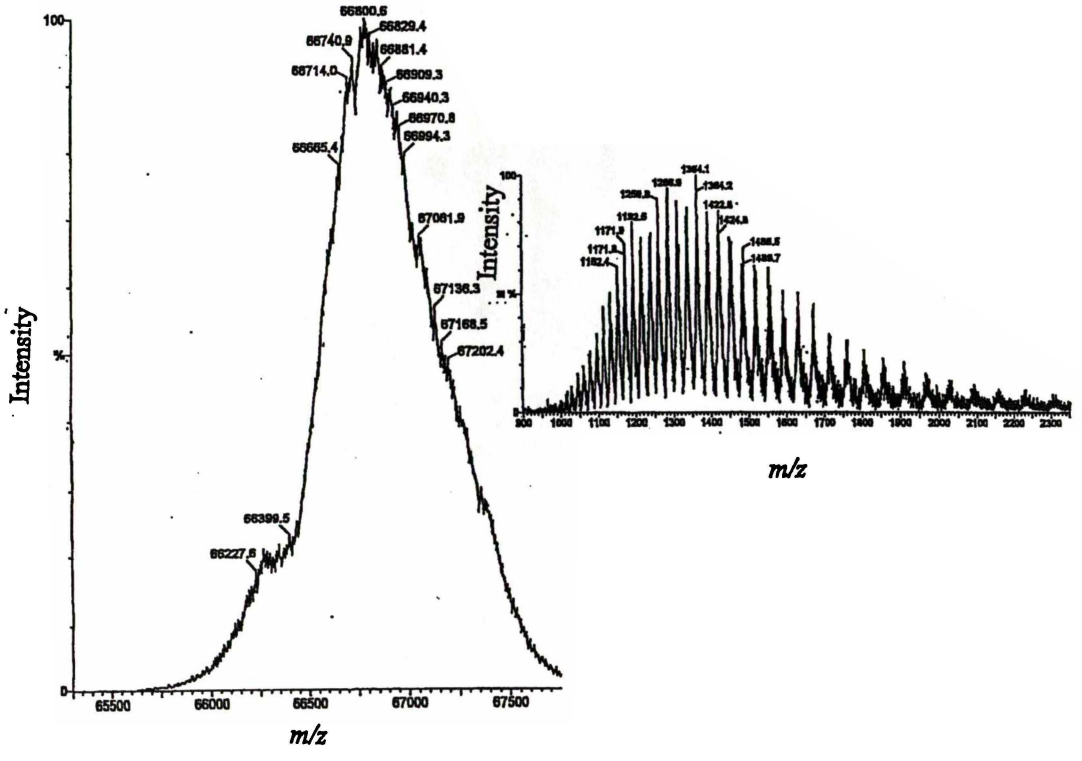

Figure 3. 5 The ESI–MS of BSA-38 conjugate, deconvoluted (left) and complex spectra (right)..

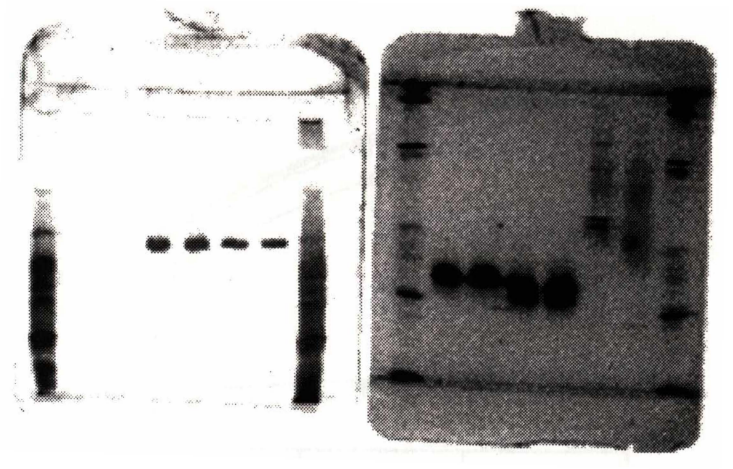

Figure 3. 6 12.5% Homogenous SDS PAGE PhastGel (left gel), lane contents (left to right), SDS-7 standards, THY (not detected), THY-**38** (not detected), BSA-**38**, BSA-**38**, BSA, BSA, standards. PhastGel IEF 3-10 standards (right gel), lane contents (left to right), standards, BSA, BSA, BSA-**38**, BSA-**38**, THY, THY-**38**, IEF 3-10 standards. Both PhastGels were run under standard conditions.

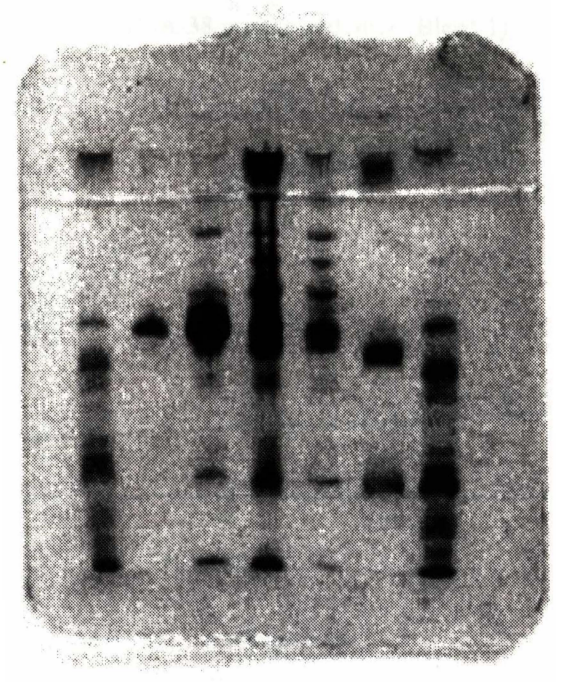

Figure 3. 7 Homogenous SDS PAGE PhastGel, lane contents (left to right), SDS-7 standards, protein A column fraction II, protein A column fraction I, dialysed ammonium sulphate precipitate (Bleed 2), immune rabbit (Bleed 2), immune rabbit (Bleed 1), SDS-7 standards.

3.3.2.2 ESTER AND AMIDE HYDROLYSIS ASSAY.

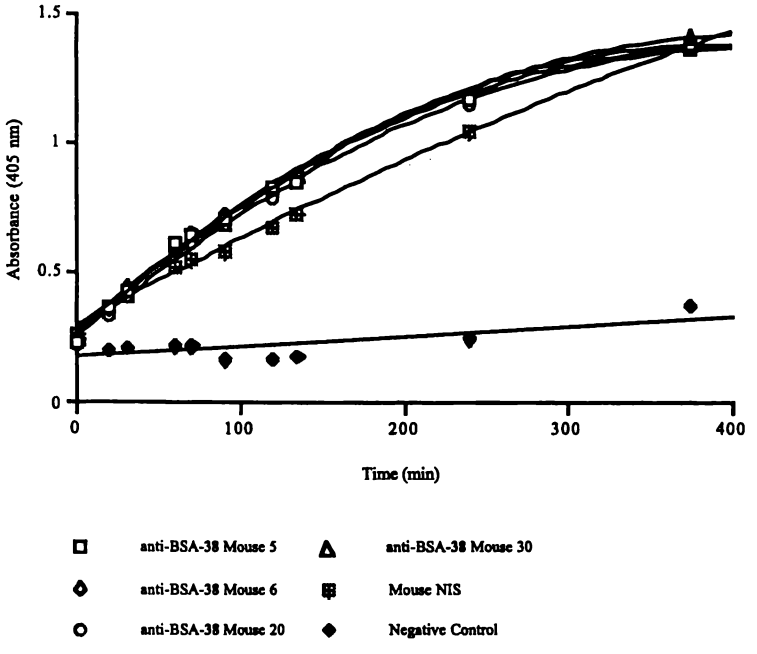

Figure 3. 8 Hydrolysis of Ester **40** by BSA-**38** immunised mice (Bleed 1),

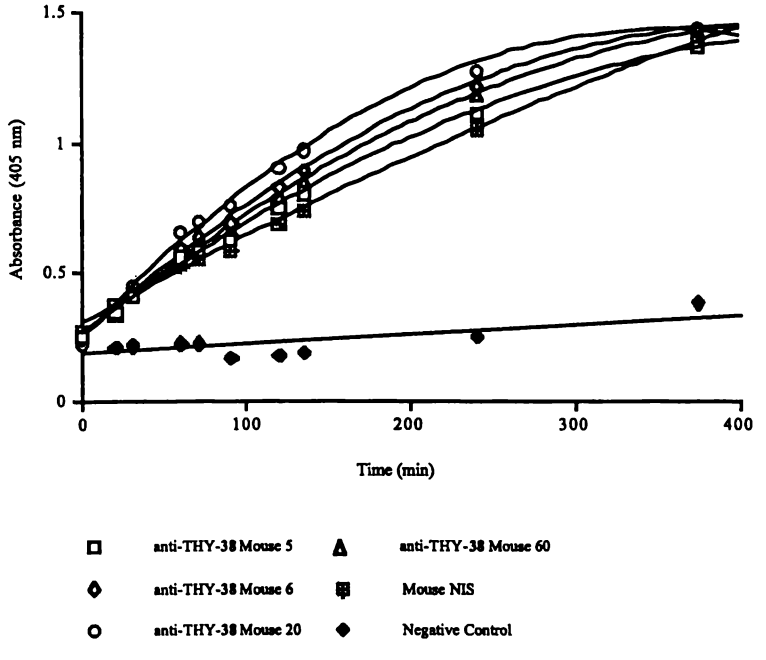

Figure 3. 9 Hydrolysis of Ester-**40** by THY-**38** immunised mice (Bleed 1)

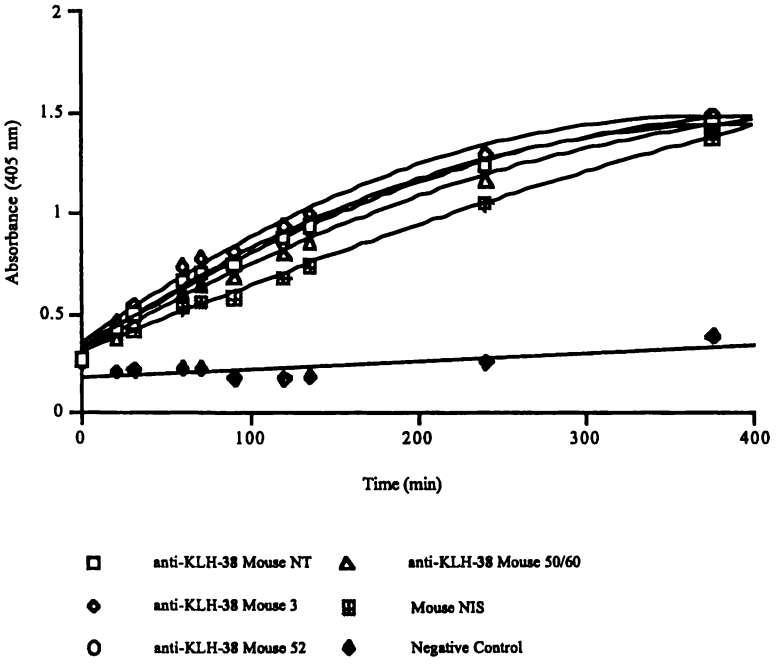

Figure 3. 10 Hydrolysis of Ester-40 by KLH-38 immunised mice (Bleed 1)

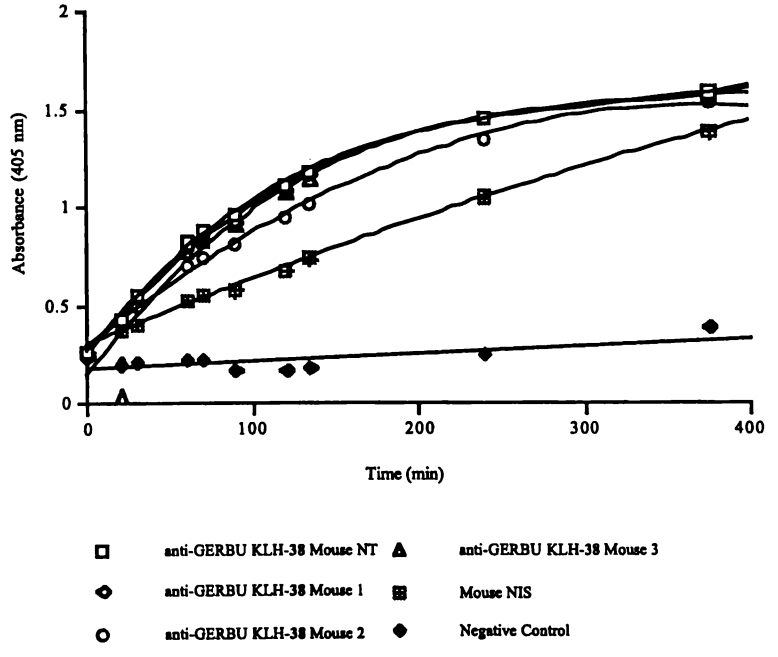

Figure 3. 11 Hydrolysis of Ester-40 by GERBU KLH-38 immunised mice (Bleed)

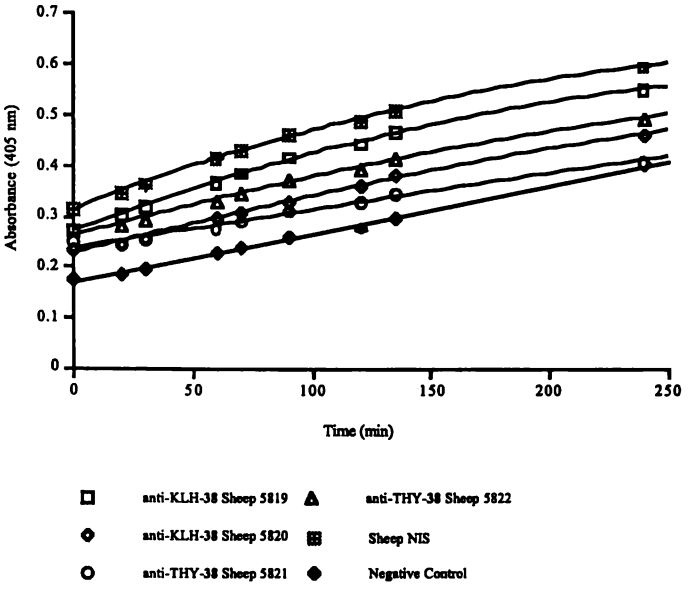

Figure 3. 12 Hydrolysis of Ester-**40** by THY-**38** immunised sheep (Bleed 1)

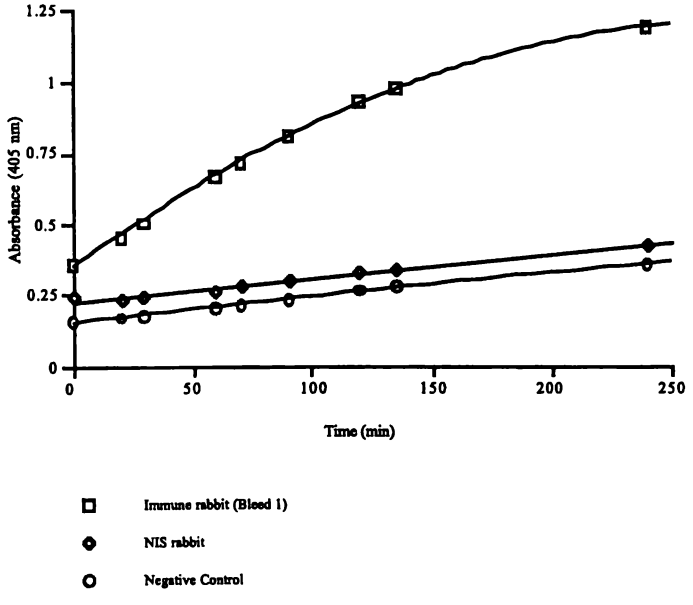

Figure 3. 13 Hydrolysis of Ester-**40** by GERBU KLH-**38** immune rabbit (Bleed 1). Non–immune rabbit sera was GERBU immunised with OVA-MicrosystinLR conjugate ie an irrelevant hyperimmune control.

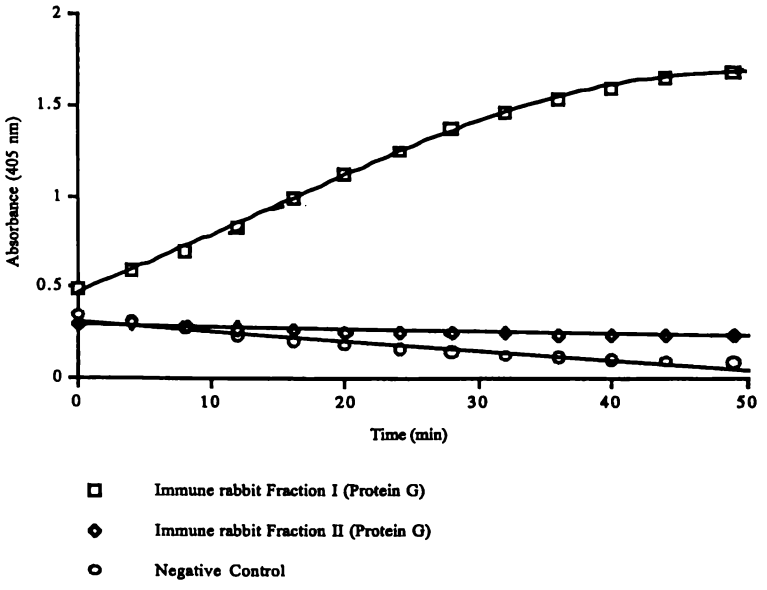

Figure 3. 14 Hydrolysis of Ester-40 by GERBU KLH-38 immune rabbit (Bleed 2) anti–sera was fractionated using Protein G.

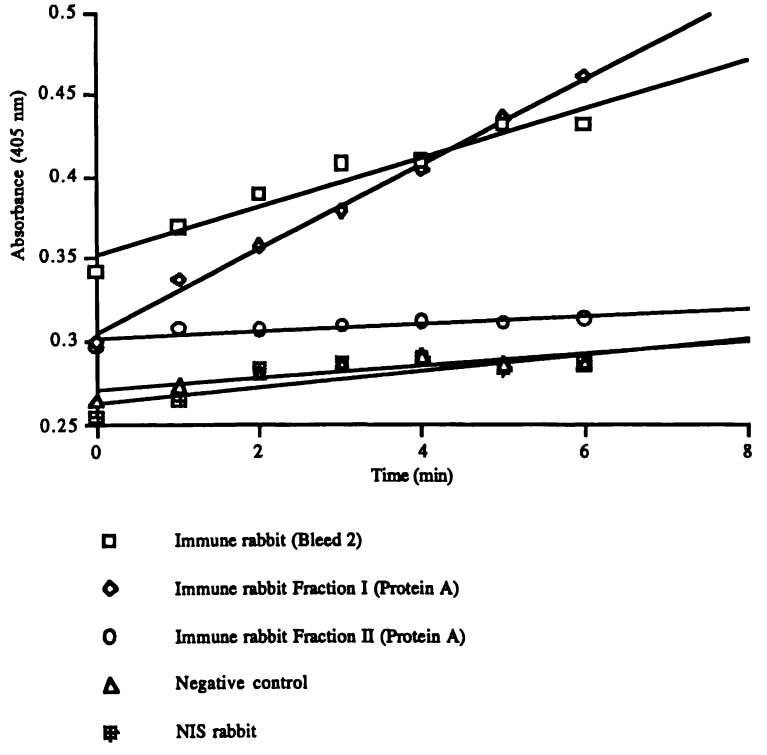

Figure 3. 15 Hydrolysis of Ester-40 by GERBU KLH-38 immune rabbit (Bleed 2) anti–sera was fractionated using Protein A.

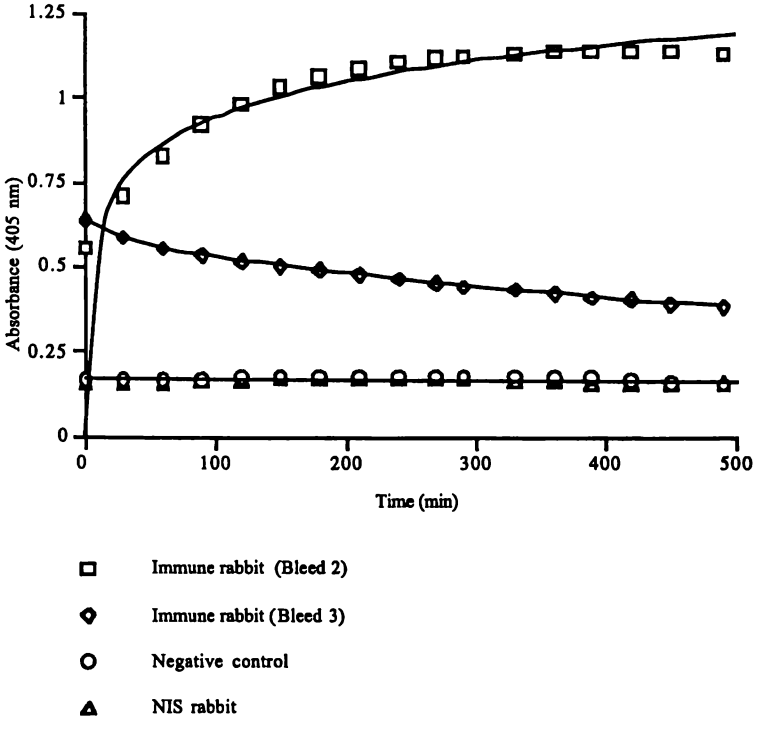

Figure 3. 16 Hydrolysis of Ester-**40** by GERBU KLH-(**38**) immunised immune rabbit (Bleed 2 and 3)

3.3.2.3 ELISA TITRATION AND COMPETITION FOR BLEED 1 AND BLEED 2

See series of Tables 3.4-3.14 on subsequent pages.

Table 3. 4 ELISA Titration (Bleed 1) using a 0.1 M phsophate coating buffer.

BSA-38 coater	I_{20}	I_{50}	I_{80}
Mouse 20 BSA-38	10056	2224	10231
Mouse 30 BSA-38	513	2250	12123
Sheep 5821 THY-38	242	89	2
Sheep 5822 THY-38	261	64	8

Table 3. 5 ELISA Titration (Bleed 1).

BSA-38 coater	I_{20}	I_{50}	I_{80}
Mouse 5 BSA-38	261001	76737	22501
Mouse 6 BSA-38	260374	85068	27793
Mouse 20 BSA-38	402348	108580	29302
Mouse 30 BSA-38	746760	156875	33083
Sheep 5821 THY-38	9654	2792	807
Sheep 5822 THY-38	4495	1381	424
NIS (sheep) THY-38	4491	1266	357
Immune rabbit KLH-38 GERBU	119	21	3

Table 3. 6 ELISA Titration (Bleed 1).

KLH-38 coater	I_{20}	I_{50}	I_{80}
Mouse 5 BSA-38	18811	5100	1383
Mouse 6 BSA-38	11291	3107	855
Mouse 20 BSA-38	17152	6307	2319
Mouse 30 BSA-38	37744	10652	2426
Mouse 5 THY-38	23233	5760	1428
Mouse 6 THY-38	10802	2325	590
Mouse 20 THY-38	10839	2251	467
Mouse 60 THY-38	3811	991	258
Sheep 5821 THY-38	2242	558	139
Sheep 5822 THY-38	2529	702	195

Table 3. 7 ELISA Titration (Bleed 1).

THY-38 coater	I_{20}	I_{50}	I_{80}
Mouse 5 BSA-38	17549	5114	1491
Mouse 6 BSA-38	10658	2798	734
Mouse 20 BSA-38	19151	6515	2217
Mouse 30 BSA-38	33480	10475	3277
Mouse NT KLH-38	1011	239	57
Mouse 3 KLH-38	649	198	61
Mouse 52 KLH-38	1008	267	71
Mouse 50/ 60 KLH-38	255	52	11
Mouse NT KLH-38 GERBU	5312	1363	350
Mouse 1 KLH-38 GERBU	4475	776	135
Mouse 2 KLH-38 GERBU	1388	284	58
Mouse 3 KLH-38 GERBU	4279	1165	317
Sheep 5819 KLH-38	90	18	4
Sheep 5820 KLH-38	89	18	4

Table 3. 8 ELISA Competition (Bleed 1).

KLH-**38** coater **38** as a competitor	I_{20}	I_{50}	I_{80}
Mouse 5 BSA-**38**	----	No competition	----
Mouse 20 BSA-**38**	----	No competition	----
Mouse 30 BSA-**38**	----	No competition	----
Mouse 5 THY-**38**	----	No competition	----

Table 3. 9 ELISA Competition (Bleed 1).

KLH-**38** coater **40** as a competitor	I_{20}	I_{50}	I_{80}
Mouse 5 BSA-**38**	----	No competition	----
Mouse 20 BSA-**38**	----	No competition	----
Mouse 30 BSA-**38**	----	No competition	----
Mouse 5 THY-**38**	----	No competition	----

Table 3. 10 ELISA Competition (Bleed 2).

THY-(**38**) coater **38** as competitor	I_{20}	I_{50}	I_{80}
Mouse 5 BSA-**38**	--	No competition	--
Mouse 6 BSA-**38**	--	No competition	--
Mouse 20 BSA-**38**	--	No competition	--
NIS	--	No competition	--

Table 3. 11 ELISA Competition (Bleed 2)

KLH-**38** coater **38** as a competitor	I_{20}	I_{50}	I_{80}
Mouse 5 BSA-**38**	--	No competition	--
Mouse 6 BSA-**38**	--	No competition	--
Mouse 20 BSA-**38**	--	No competition	--
NIS (mouse)	--	No competition	--
Mouse 5 THY-**38**	--	No competition	--
Mouse 6 THY-**38**	--	No competition	--
Mouse 20 THY-**38**	--	No competition	--
NIS	--	No competition	--

Table 3. 12 ELISA Titration of (Bleed 2).

KLH-**38** coater	I_{20}	I_{50}	I_{80}
Mouse 5 THY-**38**	22286	6100	1669
Mouse 6 THY-**38**	2591	994	381
Mouse 20 THY-**38**	2154	631	185
Mouse 60 THY-**38**	452	121	33
NIS (mouse)	4546	1188	310
Sheep 5821 THY-**38**	7248	3073	1303
Sheep 5822 THY-**38**	10688	3688	1273
NIS (sheep)	------	No binding	------

Table 3. 13 ELISA Titration (Bleed 2)

KLH-38 coater	I_{20}	I_{50}	I_{80}
Mouse 5 BSA-38	3485	881	223
Mouse 6 BSA-38	16233	5671	1981
NIS (mouse)	377	97	25
KLH coater	I_{20}	I_{50}	I_{80}
Mouse 5 BSA-38	153	33	7
Mouse 6 BSA-38	575	118	24
NIS (mouse)	39	9	2

Table 3. 14 ELISA Titration (Bleed 2)

THY-38 coater	I_{20}	I_{50}	I_{80}
Mouse 5 BSA-38	7181	7288	679
Mouse 6 BSA-38	34703	8568	2116
Mouse 20 BSA-38	8075	3004	1117
Mouse 30 BSA-38	6439	2876	1192
NIS (mouse)	7673	2678	935
Mouse NT KLH-38	1563	210	28
Mouse 3 KLH -38	682	168	42
Mouse 52 KLH -38	797	184	42
Mouse 56/60 KLH -38	331	65	13
NIS (mouse)	155	41	11
THY-38 coater	I_{20}	I_{50}	I_{80}
Mouse NT KLH-38 GERBU	4151	803	155
Mouse 1 KLH-38 GERBU	902	105	12
Mouse 2 KLH-38 GERBU	398	92	21
Mouse 3 KLH-38 GERBU	7251	1806	450
NIS (mouse)	310	77	19
Sheep 5819 KLH-38	4041	1024	259
Sheep 5820 KLH-38	1691	309	56
NIS (sheep)	--------	No binding	--------
immune rabbit KLH-38 GERBU	8	20	223
immune rabbit KLH-38 GERBU	25	103	1062
immune rabbit KLH-38 GERBU Dialysed ab precipitate	125	1021	7622
immune rabbit KLH-38 GERBU Fraction I Protein A	--------	No binding	--------
immune rabbit KLH-38 GERBU Fraction II Protein A	172	1052	8623
NIS (rabbit)	82	204	509

'Picture yourself on a train in a station,
with plasticine porters with looking glass ties
suddenly someone is there at the turnstile,
the girl with the kaleidoscope eyes.'

J. Lennon and P. McCartney
Lucy In the Sky With Diamonds
phonogram 1974

CHAPTER FOUR

CHARACTERISATION OF ERGOT ALKALOIDS IN *ACNATHERUM INEBRIANS*

4.1 INTRODUCTION

Due to the problems encountered with generation of a catalytic antibody, it was decided to investigate some of the chemistry associated with the other area of interest of this project, the ergot alkaloids. The interaction between humans and ergot alkaloids has a rich and eventful history (see Chapter One), but while most of mankind no longer suffers directly from the effects of ergot alkaloids (with the possible exceptions of medicinal and recreational use) the same cannot be said for grazing livestock.

While large numbers of ergot alkaloids have been identified, it is not unreasonable to assume that many unknown ergot alkaloids, with detrimental or beneficial biological properties toward both humans and livestock, are as yet undiscovered. The knowledge gained from the study of ergot alkaloids in a particular grass–endophyte relationship is of importance for the screening of potential grazing grasses in breeding programs, as well as contributing to the understanding of the symbiosis.

One grass–endophyte interaction, associated with production of ergot alkaloids, that has not been extensively studied is that between *Achnatherum inebrians* (drunken horse grass, DHG) and an unclassified *Neotyphodium*-like endophyte (Bruehl *et al.*, 1994; Miles *et al.*, 1996a). What is particularly interesting in this grass–endophyte relationship is the presence of very high levels of ergot alkaloids. Endophyte–infected DHG contained up to 2500 mg kg^{-1} ergonovine, however, none of these compounds were detected in the

endophyte–free DHG (Miles *et al.*, 1996a). For this reason only endophyte–infected DHG was used in the present study and all subsequent mention of DHG refers to the endophyte–infected grass. Other grass–endophyte interactions produce much lower levels of ergot alkaloids, for example endophyte–infected tall fescue seed contains ergonovine at levels below 3 mg kg^{-1} (Yates, 1989). It has been reported that livestock grazing DHG suffer adverse effects, with sheep showing lacrymation, excessive salivation, muscle spasm, panting, and shedding of hooves and tail, with severely affected animals typically dying within 24 hours (Miles *et al.*, 1996a).

Interest in DHG stems from its potential as a stock fodder (at least in the endophyte–free form) and Chinese concern at the grass spreading into grazing land (Miles *et al.*, 1996a). The high levels of ergot alkaloids in DHG potentially make isolation and identification of new compounds easier than in other endophyte–infected grasses.

As previous investigation of DHG compounds (Miles *et al.*, 1996a) successfully applied reverse phase high performance liquid chromatography (RP HPLC) with UV and fluorescence detection systems, it was decided that this approach would be used for separation and characterisation of extracted ergot alkaloids.

4.2 DISCUSSION

4.2.1 PRELIMINARY STUDIES

With the limited amount of endophyte–infected DHG material available preliminary studies were carried out on a small scale. DHG was extracted with methanol and the filtrate analysed with an analytical RP HPLC system similar to that described by Miles *et al.* (1996a). This system used an NH_4OAc–buffered gradient system (henceforth referred to as system I). When system I was used for analysis of ergonovine and lysergic acid amide retention times were inconsistent and not in agreement with those previously described (Fig. 4.1). Alternative gradient systems were therefore investigated.

The second system (system II) developed used the same buffer system as system I but with a different gradient, this was found to give good separation and acceptable run times (Fig. 4.1). However, in order to obtain consistent retention times, it was necessary to use regular equilibration and elution cycles. This phenomenon has been previously noted for lysergic acid amides (Lane, G. 1998, pers. comm.).

Extracted DHG material was fractionated by RP HPLC using system II and the fractions were analysed by positive mode ESI–MS. In the fraction consistent with ergonovine an ion was detected corresponding to ergonovine $[M+H^+]$.

To avoid lengthy equilibration times a buffered isocratic RP HPLC system was developed. This system (system III) used the same components as system I and gave a chromatogram similar to gradient system II (Fig 4.2). System III, however, required little pre–equilibration time.

Using system III it was possible to determine which of the available DHG material contained ergot alkaloids in significant amounts. It was found that DHG stem/leaf and flowerhead stem/leaf (Table 4.1) material contained high levels of ergonovine, while levels in the whole grass and root fractions were about an order of magnitude lower. This is in agreement with previous work (Miles *et al.*, 1996a).

Table 4. 1 Levels of ergonovine detected in different portions of DHG

DHG plant portion	Amount of material available (g)	Concentration of ergonovine detected (mg kg^{-1})
stem/leaf	35	400
flowerhead stem/leaf	20	400
root	90	55
whole grass	90	66

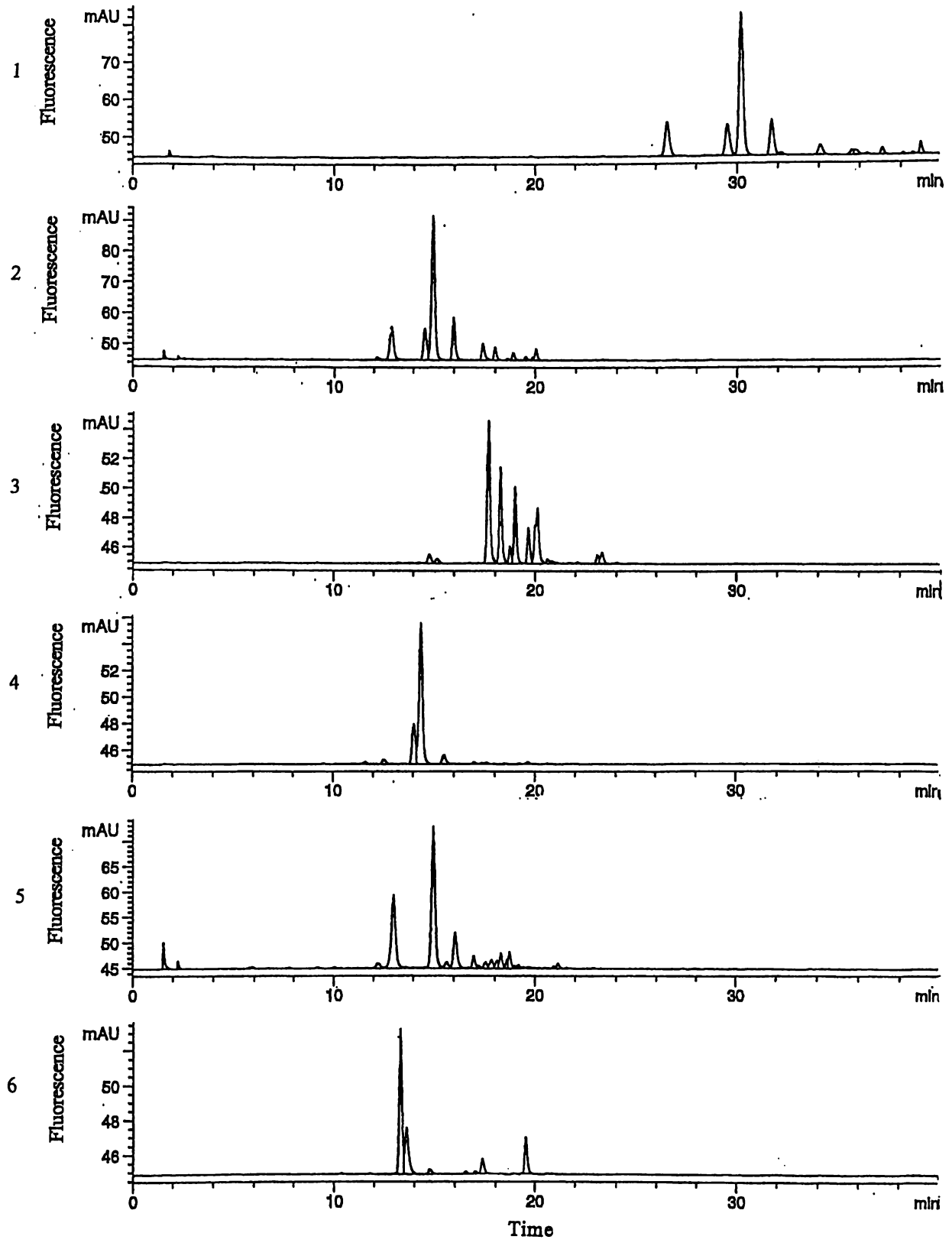

Figure 4. 1 Fluorescence (excitation 310 nm, emission 427 nm) chromatograms obtained from the analytical RP HPLC of the preliminary DHG extract: 1) gradient system I, 2) gradient system II, 3) gradient system II; first fraction from silica flash column 4) gradient system II; second fraction from silica flash column, 5) gradient system II; third fraction from silica flash column, 6) gradient system II; fourth fraction from silica flash column.

Although the level of ergonovine from the extracted DHG was approximately 400 mg kg^{-1}, the levels of unknown ergot alkaloids were approximately 10-100 fold lower (assuming a similar fluorescence response). This level of ergot alkaloid extracted from the DHG in the preliminary extraction studies suggested that if the same extraction efficiency could be achieved on a larger scale then sufficient amounts of the unknown compounds could be obtained for NMR analysis.

The possibility of separating DHG extract using a silica gel flash column was investigated. The flash column gave good separation and conveniently removed undesired non–ergot alkaloid polar material (Fig 4.1). However, concern with possible loss of ergot alkaloids meant that reverse phase flash column was used instead of silica for the large scale extraction of the DHG material.

4.2.2 LARGE SCALE DHG EXTRACTION

The DHG material from stem/leaf and flowerhead stem/leaf were combined and repeatedly extracted with methanol until only low levels of ergot alkaloids were detectable using analytical RP HPLC and system III (Table 4.4). The estimated amount of ergonovine extracted from the DHG was 1090 mg kg^{-1} of DHG material, with approximately 80% being extracted in the first two extractions. The levels of the unknown ergot alkaloids were 10–100 fold less abundant than ergonovine (assuming a similar fluorescence response).

A portion of this extract was fractionated using RP HPLC system III and examined by ELISA (Fig. 4.2). The polyclonal antibodies used for the ELISA were generated against a lysergol conjugate and they recognise a wide range of lysergyl derivatives (Table 4.2). While the ability of these antibodies to bind the different lysergic acid amides would be affected by the side chains at the C–8 position the effect would be expected to be small with the non–specific recognition of the polyclonal sera (Table 4.2). It was expected that the ELISA would enable detection of ergot alkaloid structures lacking the conjugated ring system responsible for fluorescence since such compounds would still possess the basic

ergolene–like structure which the antibody recognises (Table 4.2). The ELISA data corresponded well with the RP HPLC fluorescence spectra, suggesting that the fluorescent DHG compounds all possessed the ergolene moiety and that (at least for the extracted and RP HPLC compatible compounds) there were no non–conjugated structures in the DHG extract investigated (Fig 4.2).

Table 4. 2 Cross reactivity of ergot alkaloids to BSA-lysergol conjugate (2.5 mg ml^{-1}) as determined by competitive ELISA using polyclonal OVA-lysergol immune sheep sera at a 1/70000 dilution (Garthwaite, I. 1998, unpublished data)

Alkaloid	Percentage cross reactivity[1]
Lysergol	100
Lysergic acid	2.7
Lysergic acid amide	15.4
Ergovaline	0.3
Festuclavine	34.6
Di-hydro-ergonovine	4.2
Ergonovine maleate	12.9
Ergonovine	22.3
α-Ergocyphine	1.3
2-Bromo α-ergocryptine	0.2
Ergotamine tartrate	1.5

[1] Relative to lysergol response

The remaining DHG extract was then separated on a preparative RP flash column. Analysis using analytical RP HPLC and system III indicated most of the non–ergot alkaloid material had been removed. However, separation of individual ergot alkaloids was not achieved. Removal of the non–ergot alkaloid material was expected to improve the resolution attainable on the preparative RP flash column, so the separation was repeated. However, resolution of individual ergot alkaloids was again not achieved.

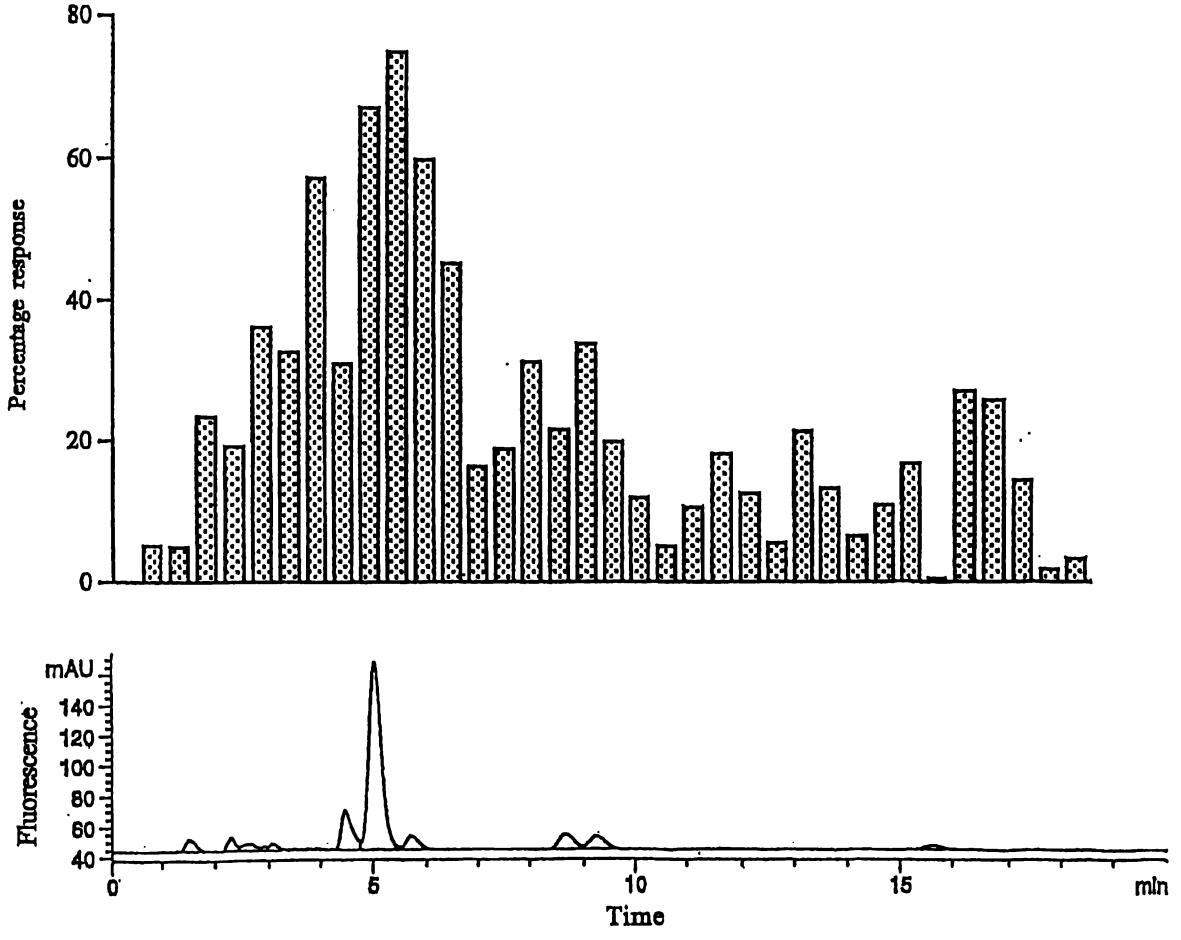

Figure 4. 2 ELISA response (top), to DHG large scale extract fractionated using analytical RP HPLC and system III, relative to the response obtained for the first HPLC fraction (fractions were diluted 1/100). The fluorescence trace for the HPLC fractionation (bottom).

The possibility that ergot alkaloids extracted from the DHG might epimerise on concentration with buffer salts when solvent was removed under reduced pressure led to the development of system IV. System IV again used the same components described for system I but had a ten–fold decrease in NH_4OAc concentration. This system gave very similar retention time in both analytical and preparative systems when compared to system III (compare Fig 4.2 bottom, and 4.3 top).

The partially purified ergot alkaloids from the preparative RP flash column were then separated on the preparative RP HPLC using system IV. This allowed separation of ergonovine from the two later eluting ergot alkaloids. The two later eluting ergot alkaloids were not separated, however, due to extensive tailing of the ergonovine peak.

The first of the two ergot alkaloid fractions eluting after ergonovine on the preparative HPLC setup was further separated using the semi–preparative RP HPLC system. This gave a compound of ca 80% purity which was identified as **41.** Comparison of the retention time and absorbance of **41** with an authentic standard of *iso*–lysergic acid amide showed good agreement (Fig. 4.4). However, despite being freeze dried and stored at -20°C in a darkened container, **41** was found to isomerise with time (Fig. 4.3). Isomerisation of **41** at the C–8 position is characteristic of the lysergic acid amides and has been noted previously (Miles *et al.*, 1996a). The structure of compound **41** was investigated using one– and two–dimensional NMR experiments. Assignment of NMR spectra was aided by comparison with previously published lysergyl chemical shifts (Bach *et al.*, 1974; Breitmaier *et al.*, 1987; Cvak *et. al.*, 1997). Due to the small amount of **41** isolated the time taken for the ^{13}C experiment became prohibitive, however, non-protonated ^{13}C environments were assigned using the HMBC experiment. ESI–MS of **41** in positive ion mode gave an ion *m/z* 268.8 $[M+H^+]$, while the negative ion mode gave an ion *m/z* 267.4 $[M^-]$. Both of these data support (within experimental error of the technique) a compound with an exact mass of 267.1 consistent with **41**. EI–MS data was also consistent with **41**.

The RP HPLC retention time, mass spectrometry, UV, fluorescent and NMR spectroscopy conclusively prove that **41** is *iso*–lysergic acid amide.

The second fraction eluting after ergonovine on the preparative RP HPLC was separated on the analytical RP HPLC column using preparative system IV. This enabled separation of compound **42**. Compound **42** was identified as ergonovinine by comparison of its retention time and absorbance spectra with those of authentic ergonovinine (Fig. 4.4). However, with time, despite freeze drying and storage in a darkened container, compound **42** was found to isomerise (Fig. 4.3).

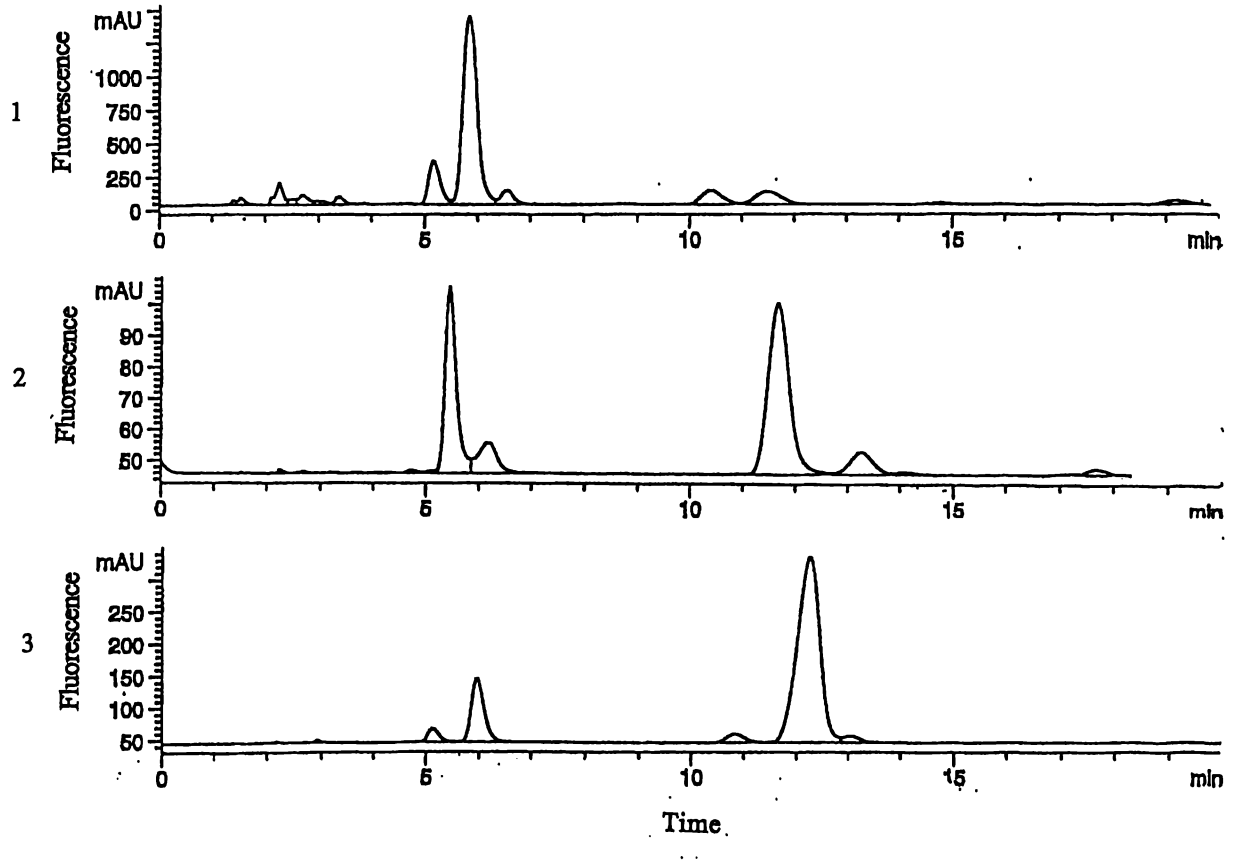

Figure 4. 3 Fluorescence (excitation 310, emission 427 nm) chromatograms obtained from the analytical RP HPLC of various DHG material from the large scale extract separated using isocratic system (IV): 1) large extract just after extraction, 2) *iso*–lysergic acid (**41**) (3 weeks @ -20°C) at 11.5 minutes, the small peak at 5 minutes is lysergic acid amide the peaks at 6 and 13 min are ergonovine and ergonovinine respectively, 3) ergonovinine (**42**) (3 weeks @ -20°C) at 12.5 min, the peak at 5 min is lysergic acid amide the peak at 6 min is ergonovine, the peak at 11 min is lysergic acid amide and the peak at 13 min is unidentified.

Comparison of the retention time of compound **42** with the original fluorescent trace obtained just subsequent to extraction revealed no peak of a similar retention time (Fig. 4.3). This evidence, along with the amount of compound **42** extracted relative to compound **41**, suggested that the ergonovinine isolated from DHG probably resulted from the isomerisation of ergonovine during the separation process (Fig. 4.3). Compound **42** was analysed using positive ion ESI–MS and gave the species *m/z* 326.7 [$M+H^+$]. The ESI–MS was consistent (within experimental error of the technique) with **42**. The NMR assignment of **42** was conducted in a similar manner to that of **41**. To further characterise **42** the NMR solvent was changed to d_6–DMSO in an attempt to obtain NOE correlations of ergolene resonances to the amide side chain at the C–8 position. The NMR solvent d_6–DMSO was used because it does not exchange with the N-H environments (at least not on the time scale for the NMR experiments), thereby enabling detection of through space NOE interactions between the ergolene moiety and the amide side chain. Attempts to establish stereochemical configuration using H-8 as a stereochemical reference were frustrated by the lack of ROESY correlation to C-5. The NOE data shows correlation of the proton of NH' to H-9 of the ergolene moiety suggesting a through space distance of 2.5 Å or less. This data establishes that the amide side chain is connected to the ergolene portion of the molecule. The RP HPLC retention time, mass spectrometry, UV, fluorescent and NMR spectroscopy conclusively prove that **42** is ergonovinine.

While the study of the DHG material resulted in isolation and characterisation of compounds **41** and **42**, the lack of resolution obtained using the preparative RP HPLC system was disappointing. The buffer system or separation properties of the ergot alkaloids did not behave in the same manner as expected from the analytical scale RP HPLC. Preliminary work with these ergot alkaloids suggested that silica could be a very useful method for separation of these compounds. Although not attempted (due to the limited amount of material available) it may be possible to use silica for a 'crude cleanup' of grass extract.

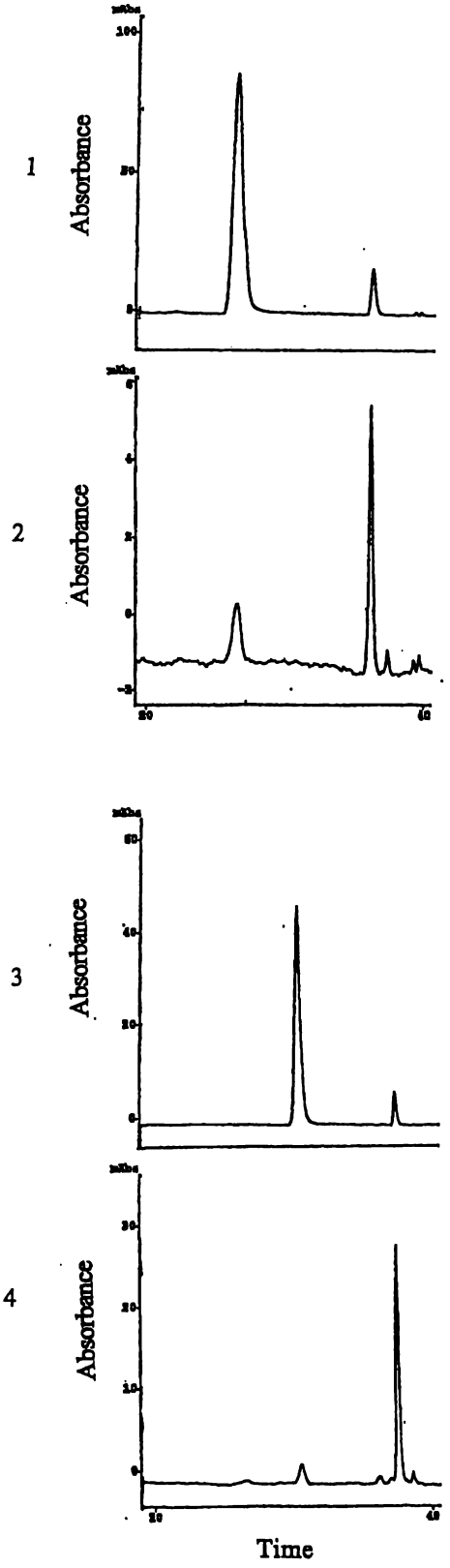

Figure 4. 4 Absorbance trace (312 nm) of: 1) isomerised lysergic acid amide (large peak at 26.8 min is lysergic acid, small peak at 36.3 min is *iso*–lysergic acid amide), 2) compound **41** (small peak 26.5 is lysergic acid amide, the large peak 36.1 min is iso–lysergic acid amide), 3) isomerised ergonovine (large peak at 30.9 min is ergonovine, small peak at 37.6 min is ergonovinine, 4) and compound **42** (small peak 30.7 min is ergonovine the large peak at 37.4 min is ergonovinine). This work was conducted by G. Lane the equipment and separation conditions are described in the experimental section (system V).

It may even be possible to separate the ergot alkaloids on silica using a solvent system similar to that investigated in the preliminary work of this study. This could be a very convenient and cost effective method for investigation of these compounds.

4.3 EXPERIMENTAL

4.3.1 MATERIALS AND METHODS

4.3.1.1 REAGENTS AND SOLVENTS

Ergonovine was obtained from Sigma and lysergic acid amide was a gift from M. Flieger and V. Kren of the Czechoslovak Academy of Sciences, Prague, Czech Republic. Reagents used were obtained from BDH and were LR grade or better. All solvents were HPLC ChromAR grade (Mallinkrodt) and Milli Q water was used. The endophyte infected DHG material was sourced from Xinjiang province, People's Republic of China (Miles *et al.*, 1996a). Seedlings were grown in a glasshouse (15-30°C) until harvest at 15 weeks. Plants were harvested and freeze dried following division into stem/leaf, flowerhead stem/leaf, root and whole grass (gift from G. Lane Grasslands Palmerston North, New Zealand). The freeze dried DHG material was stored at 4°C.

4.3.3.2 CHROMATOGRAPHY

Silica Flash Column

Silica column and TLC were conducted as described in Chapter 2. The DHG extract was separated using CH_3OH–$CHCl_3$ (1:9) with ca 10 ml fractions collected. Fractions were analysed by analytical HPLC (system II) and fractions containing similar ergot alkaloids were pooled to give four crude fractions.

Reverse Phase Flash Column

The RP (C_{18}) was prepared as described by Evans *et al.* (1980) and a flash preparative column (ca 3 × 20 cm) was formed from this material by slurry packing with the eluent

(CH_3OH was added to the RP material to help slurry formation). The column was eluted at approximately 2 ml min^{-1}, and 5-10 ml fractions were collected.

The DHG extract material was dissolved in 80% A, 20% B, (where solvent A was NH_4OAc (0.1 M) and solvent B was CH_3CN–NH_4OAc (0.1 M) (3:1)), filtered (Whatman 2) and loaded to the top of the column. Negligible flow rates were achieved as the extract precipitated, blocking the top of the column. This problem was remedied by removing both the soluble material and the solid material from the top of the column. The column material was filtered to remove precipitated compounds, repacked, washed and re-equilibrated. Although the solvent soluble material contained reasonable levels of ergot alkaloid the recovered precipitate contained the majority (analytical RP HPLC system III).

The material that had precipitated on the column was filtered twice (Whatman 2), dissolved in 80% A, 20% B, and separated on the regenerated preparative RP flash column (Table 4.3). This procedure was repeated for the solvent soluble material. Both preparative RP flash column runs were monitored by analytical RP HPLC (system III). Fractions containing the same compounds were combined to give three fractions, one of which was found to contain the majority of the ergot alkaloid material.

Table 4. 3 Separation conditions for the preparative RP flash column

Volume (ml)	A%	B%
100	80	20
100	75	25
100	70	30
100	50	50
200	CH_3OH	

4.3.3.3 RP HPLC

Analytical Setup

Ergonovine and lysergic acid amide standards were dissolved and diluted in CH_3OH such that 0.8 µg (10 µl) was loaded to the RP HPLC system. DHG samples were filtered through tissue paper and 20 µl applied.

The analytical RP HPLC system used a Phenomenex Prodigy column (ODS 3, 100A, 150 mm × 4.6 mm, 5 µm) and a Perkin Elmer Binary LC pump. Ergot alkaloids were detected with a Waters 470 Scanning Fluorescence detector (excitation 310 nm, emission detection at 427 nm), Perkin-Elmer LC–85B spectrophotometric detector (312 nm), and a Hewlett–Packard 1040M SERIES II diode array UV detector (220-320 nm). Elution using systems I-IV were conducted at 1 ml min^{-1}.

System I

System I was a gradient system as described by Miles *et al.* (1996a): 0 min, 95% A, 5% B; 30 min, 75% B, 25% B; 60 min, 0% A, 100% B; where solvent A was NH_4OAc (0.1 M), and solvent B was CH_3CN–NH_4OAc (0.1 M) (3:1).

System II

0 min, 85% A, 15% B;10 min, 75% A, 25% B; 30 min, 0% A, 100% B; 5 min, 85% A, 15% B; 10 min, 85% A, 15% B; where solvent A was NH_4OAc (0.1 M), and solvent B was CH_3CN–NH_4OAc (0.1 M) (3:1).

System III

75% A , 25% B, where A was NH_4OAc (0.1 M), and solvent B was CH_3CN–NH_4OAc (0.1 M) (3:1).

System IV

75% A, 25% B; where solvent A was NH_4OAc (0.01 M), and solvent B was CH_3CN–NH_4OAc (0.01 M) (3:1).

System IV Preparative Scale

As described for system IV with the exception that 50 µl of concentrated sample and a flow rate of 2 ml min^{-1} was used.

System V- Analytical Setup used by G. Lane (Grasslands Palmerston North, New Zealand)

Compound **41** and **42** were sent for analysis by G. Lane. The analytical setup used by G. Lane for separation of DHG material was as follows: Phenomenex Prodigy column (ODS 3, 100A, 150 mm × 4.6 mm, 5 µm), a Shimadzu LC101AD chromatograph, Shimadzu 10AD pump, SPD–M10A diode array UV detector (200-350 nm), and RF10A fluorimeter (excitation 310 nm, emission 410 nm). System V was used at a rate of 1 ml min^{-1}.

System V was the analytical RP HPLC setup (G. Lane) with the following gradient: 0 min, 95% A, 5% B, 30 min, 75% A, 25% B; 60 min, 0% A, 100% B; solvent A was NH_4OAc (0.1 M), and solvent B was CH_3CN–NH_4OAc (0.1 M) (3:1).

Preparative Setup

The standards (ergonovine and lysergic acid amide, 10 µl, 0.8 µg) or filtered (through tissue paper) DHG samples (20-200 µl) were loaded to the preparative RP HPLC column. The preparative RP HPLC system consisted of a Zorbax column (ODS 21.2 mm × 25 cm, 7 µm), Waters 600 pump and controller, Waters 486 tunable UV absorbance detection system (312 nm), and a Waters 470 Scanning Fluorescence detector (excitation at 310 nm and emission detection at 427 nm). Elution was conducted using system IV at 20 ml min^{-1}.

Semipreparative HPLC

Semipreparative HPLC purification of the ergot alkaloids was performed on a RCM-100 radial compression system (Waters) fitted with a 8 mm × 10 cm, 5 μm C18 Radial–Pak cartridge (Waters). Eluting compounds were detected with a Perkin-Elmer LC–85B spectrophotmetric detector (312 nm) and a Waters 470 scanning fluorescence detector (excitation at 310 nm, emission detection at 427 nm). System VI with a flow rate of 2-3 ml min^{-1} was used. During separation the cartridge back pressure continued to rise steadily such that it was necessary to lower the flow rate to reduce backpressure to within the cartridge limits.

System VI

System VI consisted of an isocratic elution: 40% A, 60% B; where solvent A was NH_4OAc (0.01 M), and solvent B was CH_3CN–NH_4OAc (0.01 M) (3:1).

4.3.3.4 NMR

The conditions and abbreviations used for the NMR experiments are as described in Chapter 2. For the case of the ergot alkaloids, however, all experiments were conducted in a CD_3OD solution (unless otherwise noted) with a Brucker DRX-400 spectrometer fitted with a 5 mm dual $^{13}C/^{1}H$ probehead or a 5 mm inverse $^{1}H/^{13}C$ probehead.

4.3.3.5 MASS SPECTROMETRY

The facilities and conditions used for ESI–MS and EI–MS of compound (**41**) and (**42**) were as described in Chapter Two.

4.3.4 SEPARATION OF DHG ERGOT ALKALOIDS

4.3.4.1 PRELIMINARY STUDIES

Due to the limited amount of DHG material available (Table 4.1) a small scale extractions was conducted. This was performed by suspending finely ground freeze dried DHG (50 mg) in methanol (1ml), the suspension was stirred for 20 hours using a reactivial™. The

resulting methanolic extract was filtered through tissue paper and analysed using one of the various analytical HPLC systems.

Fractions (1 ml) from the analytical RP HPLC gradient system II were concentrated to dryness using a centrifugal evaporator for ESI–MS analysis, the only ion detected was ergonovine [$M+H^+$] with an analytical RP HPLC retention time of 15 minutes.

The levels of ergonovine in the four different plant portions (stem/leaf, flowerhead stem/leaf, root and whole grass) of DHG were investigated using system III (Table 4.1).

4.3.4.2 LARGE SCALE ISOLATION AND CHARACTERISATION OF ERGOT ALKALOIDS FROM DRUNKEN HORSE GRASS

The large scale extraction was performed by suspending (in a 1 l Schott bottle) finely ground freeze dried DHG material (55 g, of flowerhead + stem/leaf and stem/leaf), in methanol and stirring vigorously for a 56 hour period. Methanol was decanted and replaced at various intervals to give six separate methanol extracts. Extractions were conducted sequentially until such a time that ca 1/30 th of the original ergonovine material was extracted (as determined via analytical RP HPLC using system III. The six extracts were combined, filtered (Whatman 2), and the methanol removed under reduced pressure.

ELISA of Large DHG Extract

The large DHG extract was also analysed using an ELISA assay (as described generally in Chapter 3). The DHG material was fractionated (0.5 ml) using the analytical RP HPLC and system III. A competitive assay was run using a BSA-lysergol plate coater and polyclonal lysergol binding antibodies (Garthwaite *et. al.,* 1994). The HPLC fractions (diluted 1/100) were then used in competition with the plate–coated lysergol–BSA and free lysergol binding antibody (Fig 4.3).

The remaining large scale extract was separated using a preparative RP flash column. Two further filtration steps (Whatman 2) were required before column precipitation of the ergot alkaloid material was avoided.

Table 4. 4 Times and volumes used for the large scale extraction of DHG material.

Extract	Time (hours)	Volume CH_3OH (l)	Converted height (cm)	Amount of ergonovine (mg)
1	4	0.5	11.5	24.2
2	20	1.0	6.5	27.4
3	4	0.5	2	4.2
4	4	0.5	1.5	3.2
5	4	0.5	1	2.1
6	20	1.0	0.4	1.7

The amount of ergonovine is estimated by comparison of the peak height of the sample versus that of ergonovine standard (0.0008 mg, peak height 9.5 cm). The volume from which the sample is taken must also be taken into account. For example a 20 µl aliquot from extract 1 (total volume 0.5 l) was found to have a peak height of 11.5 cm via RP HPLC using system II. This gives ((11.5 × 0.0008)/ 9.5 (× 25000) which means 24.2 mg of ergonovine was present in extract 1.

The ergot alkaloid material resulting from the preparative RP flash column was separated using preparative RP HPLC. However, initial separation of the ergot alkaloid standards could not be detected using the preparative RP HPLC and the same isocratic elution as analytical system IV. To rectify this problem a fluorescence detector was used. The addition of the fluorimeter did not solve the detection problem, with high levels of standard giving no detectable signal. This evidence suggested that the column was faulty. To investigate this possibility, the analytical RP HPLC column was connected to the preparative RP HPLC setup. When the ergot alkaloid standards were separated using this setup the expected retention times were obtained, confirming that the preparative column was faulty. The RP preparative column was opened and found to have considerable dead volume at the head. Following repacking of the preparative RP HPLC column the ergot alkaloid standards gave consistent retention times, peak shape and no baseline roll.

Using the rejuvenated column the DHG material was separated using the preparative RP HPLC setup using the same isocratic elution as described for the analytical system IV. The DHG was fractionated and similar material combined and the solvent removed under reduced pressure.

The first eluting peak after ergonovine from the preparative scale RP HPLC was separated using semipreparative HPLC over five repetitions with fractions containing similar material combined. The solvent was removed under reduced pressure and residual material freeze dried to give **41**.

The back pressure problems with the semipreparative HPLC meant that this system could no longer be used. Therefore the second eluting peak after ergonovine from the preparative scale RP HPLC was separated using the analytical RP HPLC column and the preparative scale system IV. The separation was repeated six times with like fractions combined and solvent removed under reduced pressure and residual material freeze dried to give **42**.

4.3.5 RESULTS

4.3.5.1 *ISO*–LYSERGIC ACID AMIDE(**41**) (Fig. 4.5)

NMR: (CD_3OD, 400 MHz) δ ^1H; 7.39 (dd, 1.7, 0.5 Hz, 1H, 14), 7.29 (m, 2H, 12, 13), 7.15 (m, 1H, 2). 6.71 (d, 1.4 Hz, 1H, 9), 6.63 (impurity), 3.77 (dd, 3.7, 1.4 Hz, 1H, 4), 3.67 (m, impurity), 3.43 (d, 2.8 Hz, 2H, 5, 7), 3.32 (m, 1H, 8), 2.99 (dd, 3.0, 1.0 Hz, 1H, 7), 2.89 (m, 1H, 4), 2.83 (s, 3H, N-CH_3)

δ ^{13}C; 124.0 (13), 120.4 (2), 112.9 (12), 111.5 (14), 64.8 (5), 56.0 (7), 44.0 (8, N-CH_3), 28.6 (4)

Table 4. 5 HSQC NMR correlation observed for compound **41**

^{1}H signal (δ)	Correlates to ^{13}C signal (δ)	Assignment
2.89, 3.77	28.6	4
2.83	44.0	$N\text{-}CH_3$
2.99, 3.43	56.0	7
6.71	118.9	9
7.15	120.4	2
7.29	112.9	12
7.29	124.0	13
7.39	111.5	14

Table 4. 6 COSY NMR correlation observed for compound **41**

^{1}H	^{1}H
2.89	3.43, 3.77
2.99	3.43, 3.32
3.32	2.99, 3.43
3.43	2.83, 2.99, 3.32, 3.77
3.77	2.89, 3.43
6.71	3.32
7.15	2.89
7.29	7.39

Table 4. 7 HMBC NMR correlation observed for compound **41**

2.83	56.0, 64.8
3.43	44.0, 64.8, 118.9, 179.2
3.77	64.8, 110.8, 128.1, 138.9
6.71	44.0

^{1}H	^{13}C
7.15	110.8, 127.7, 136.2
7.29	128.1, 136.2
7.39	112.9

Table 4. 8 Assignments for compound **41**

Assignment	^{1}H	^{13}C
2	7.15	120.4
3		110.8[1]
4	2.89, 3.77	28.6
5	3.43	64.8
N-CH_3	2.83	44.0
7	2.99, 3.43	56.0
8	3.32	44.0
9	6.71	118.9
10		138.9[1]
11		128.1[1]
12	7.29	112.9
13	7.29	124.0
14	7.39	111.5
15		136.2[1]
16		127.7[1]
1'		179.2[1]

[1]These assignments were made using HMBC data.

Analysis of compound (**41**) using system V showed a peak (ca 20%) at 26.5 min (lysergic acid amide) and a peak (ca 80%) at 36.07 min (*iso*–lysergic acid amide), these data agree well with the epimerised lysergic acid amide standard which shows a large peak at 26.8 min (lysergic acid amide) and a small peak at 36.4 min (*iso*–lysergic acid amide). The UV data

for (**41**) shows a peak at 238 and 312 nm with a trough 272 nm. The *iso*–lysergic acid amide standard shows a peak at 237 and 312 nm, and a trough at 271 nm.

EI–MS: *m/z* 267.1368 (M^+, 100; calc 267.1371 for $C_{16}H_{16}N_2O_2$), 221 (50), 207 (64), 196 (44), 181 (56), 167 (24), 154 (32), 127 (13), 111 (14), 72 (31), 59 (48)

ESI–MS: positive ion mode, 20 V, *m/z* 268.8, [$M+H^+$], negative ion mode, cone voltage 40 V, *m/z* 267.4, [$M-H^+$], 249.2 [$M-NH_4^+$]

4.3.5.2 ERGONOVININE (**42**) (Fig. 4.6)

NMR: δ ^1H (CD_3OD, 400 MHz) 7.39 (m, 1H, 14), 7.28 (m, 2H, 12, 13), 7.15 (m, 1H, 2), 6.70 (d, 5.7 Hz, 1H, 9), 4.09 (m, 1H, 3'), 3.77 (m, 1H, 4), 3.64 (m, 2H, 4'), 3.49 (impurity), 3.42 (d, 9.4 Hz, 1H, 5), 3.38 (m, 1H, 7), 3.30 (m, 1H, 8), 2.98 (m, 2H, 4, 7), 2.81 (s, 3H, N-CH_3), 1.48 (impurity), 1.35 (d, 9.3 Hz, 3H, 5')

δ ^{13}C 176.6 (1'), 139.2 (10), 136.0 (15), 129.1 (11), 128.0 (16), 124.0 (13), 120.4 (2), 119.1 (9), 112.9 (12), 111.5 (14), 110.8 (3), 66.3 (4'), 64.6 (5), 56.0 (7), 48.5 (3'), 44.6 (8), 43.8 (N-CH_3), 28.6 (4), 17.7 (5')

Table 4. 9 COSY NMR correlation observed for compound **42**

^1H	^1H
3.30	2.98
3.38	2.81, 2.98, 3.30
3.42	2.92, 3.77
3.64	4.09
3.77	2.92, 3.42, 6.70
4.09	1.35, 3.64
6.70	3.30
7.15	2.92
7.39	7.28

Table 4. 10 HSQC NMR correlation observed for compound **42**

^{1}H (δ)	Correlates to ^{13}C (δ)	Assignment
1.35	17.7	5'
2.81	43.8	N-CH_3
2.92, 3.77	28.6	4
2.98, 3.38	56.0	7
3.30	44.6	8
3.42	64.6	5
3.64	66.3	4'
4.09	48.5	3'
6.70	119.1	9
7.15	120.4	2
7.28	112.9	12
7.28	124.0	13
7.39	111.5	14

Table 4. 11 HMBC NMR correlation observed for compound **42**

^{1}H	^{13}C
1.35	48.5, 66.3
2.92	64.6, 110.8
2.98	43.8, 64.6, 119.1, 176.6
3.30 and 3.38	44.6, 64.6, 119.1, 176.6
3.77	64.6, 110.8, 119.1, 128.0, 136.0
4.09	17.7, 66.3, 176.6
6.70	44.6, 56.0, 64.6, 129.1
6.92	120.1 (impurity)
7.15	110.8, 128.0, 136.0
7.28	111.5, 129.1, 136.0

^{1}H	^{13}C
7.37	120.1 (impurity)
7.39	112.9, 128.0, 136.0

δ ^{1}H (d_6–DMSO, 400 MHz) 10.78 (s, 1H, NH), 8.03 (d, 4.6 Hz, 1H, 'NH), 7.28 (m, 1H, 14), 7.15 (m, 3H, 2, 12, 13), 6.55 (m, 1H, 9), 3.83 (m, 1H, 3'), 3.53 (m, 1H, 4), 3.29 (m, 2H, 4',7), 2.76 (impurity), 2.65 (m, 1H, 4), 2.54 (s, 3H, NCH_3), 2.42 (impurity), 1.30 (impurity), 1.12 (s, 3H, 5')

Table 4. 12 HSQC (d_6–DMSO) NMR correlation observed for compound **42**

^{1}H (δ)	Correlates to ^{13}C (δ)	Assignment
1.12	17.4	5'
2.54	43.0	N-CH_3
2.65, 3.53	26.9	4
2.69, 3.13	54.0	7
3.09	42.7	8
3.15	62.0	5
3.29, 3.39	64.3	4'
3.83	46.2	3'
6.55	119.0	9
7.12	119.2	2
7.15	110.9	12
7.15	122.1	13
7.28	109.6	14

Table 4. 13 COSY (d_6–DMSO) NMR correlation observed for compound **42**

^{1}H (δ)	Correlates to ^{1}H (δ)
1.12	3.83
3.83	1.12
7.12	10.78
7.15	7.28
7.28	7.15
8.03	3.83
10.78	7.12

Table 4. 14 HMBC (d_6–DMSO) NMR correlation observed for compound **42**

^{1}H	^{13}C
1.12	46.2, 64.3
2.54	54.0, 62.0
2.65	62.0, 109.1
3.13, 3.15	119.0, 62.0, 171.8
3.29	17.4
3.39	17.4
3.53	62.0, 109.1, 119.0, 126.0, 135.9
7.12	109.1
7.15	126.0, 133.8
7.15	127.8, 133.8
7.28	110.9

Table 4. 15 ROESY (d_6–DMSO) NMR correlation observed for compound **42**

^1H	^1H
3.13	2.69
3.83	1.12, 3.29
7.12	2.65, 3.15, 3.53
7.15	6.55, 7.28
8.03	1.12, 3.09, 3.83, 6.55
10.78	7.12, 7.28

Table 4. 16 NOE (d_6–DMSO) NMR correlation observed for compound **42**

^1H	^1H
3.39	-----
6.55	3.09, 7.15, 8.03
8.03	1.12, 3.09, 3.83, 6.55
10.78	7.12, 7.28

Table 4. 17 Assignments for compound **42** (d_6–DMSO)

Assignment	^1H	^{13}C
N-H	10.78[1]	
2	7.12	119.2[2]
3		109.1[2]
4	2.65, 3.53	26.9
5	3.15	62.0
N-CH_3	2.54	43.0
7	2.69, 3.13	54.0
8	3.09	42.7
9	6.55	119.0

Assignment	^{1}H	^{13}C
10		135.9[2]
11		127.8[2]
12	7.15	110.9
13	7.15	122.1
14	7.28	109.6
15		133.8[2]
16		126.0[2]
1'		171.8[2]
NH'	8.03[1]	
3'	3.83	46.2
4'	3.29, 3.39	64.3
5'	1.12	17.4

[1]These assignments were made using COSY and ROESY.
[2]These assignments were made using HMBC data.

Analysis of compound (**42**) using system V gave a peak (ca 10%) at 30.7 min (ergonovine) and a peak (ca 90%) at 37.4 min (ergonovinine), these data agree well with the epimerised ergonovinine standard which shows a large peak at 30.9 min (ergonovine) and a small peak at 37.6 min (ergonovinine). The UV data for (**42**) shows a peaks at 236 and 312 nm with a trough 271 nm. The ergonovinine standard shows a peak at 236 and 312 nm, and a trough at 272 nm.

EI–MS: *m/z* 325.1796 (M^+, 54; calc 325.1790 for $C_{19}H_{23}N_3O_2$), 307 (30), 264 (16), 249 (10), 221 (82), 206 (23), 196 (100), 181 (33), 167 (20), 154 (26), 127 (8), 112 (21), 73 (19), 60 (30)

ESI–MS:positive ion mode, cone voltage 20 V, *m/z* 326.7, $[M+H^+]$

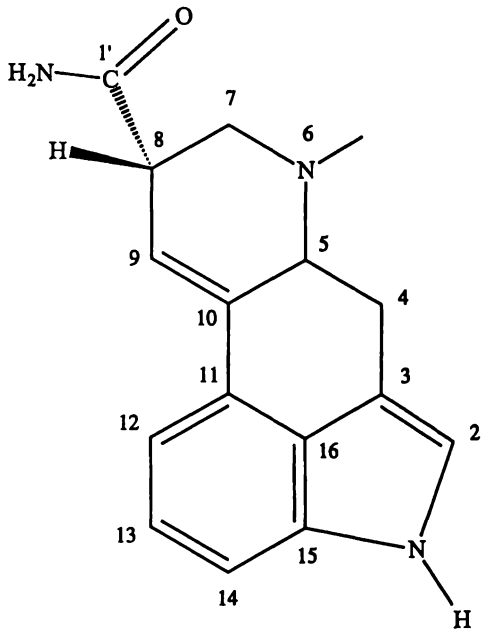

Figure 4. 5 Compound **41**, *iso*–lyergic acid amide.

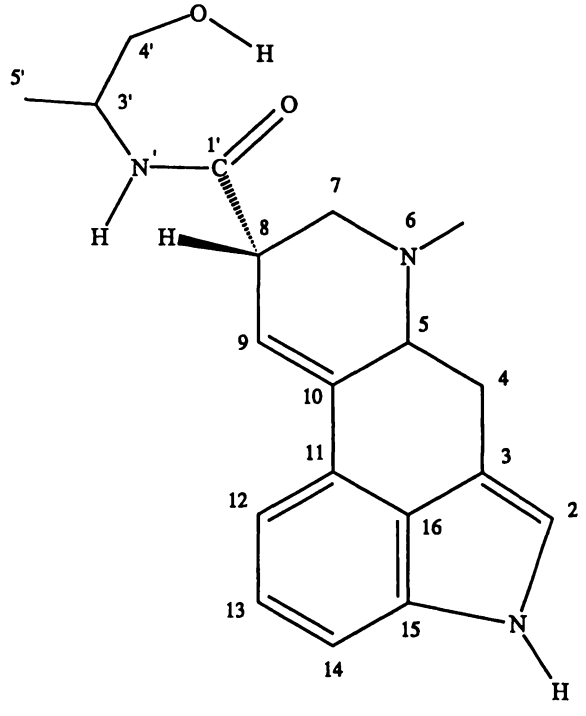

Figure 4. 6 Compound **42**, ergonovinine.

There and back again.

Bilbo Baggins

CHAPTER FIVE

SUMMARY

Despite the large number of documented catalytic antibodies, there exist few examples where catalytic antibodies have been used to solve practical problems. One area where practical applications have proved to be successful is in organic synthesis. Multi–gram synthetic manipulations have been achieved (Reymond *et al.*, 1994) and in one case a system has been designed using a catalytic antibody that could be scaled up for industrial application (Shevlin *et al.*, 1994). Medicinal applications of catalytic antibodies are also being investigated, both for improved human (Wentworth *et al.*, 1996) and animal welfare (Gallacher *et al.*, 1993). While work with medical applications continues, efforts to create catalytic antibody vaccines have yet to be successful. Indeed, the work conducted in this thesis highlights a number of problems associated with generating a hydrolytic polyclonal vaccine versus ergopeptine alkaloids.

The production of catalytic antibodies capable of hydrolysing ergopeptines was an ambitious target. It was postulated that one could generate a catalytic antibody capable of hydrolysing a 4-nitroanilide–lysergyl compound **C** (Fig 2.1) using a tetrahedral phosphorus emulator transition–state emulator, but only because 4-nitroanilide moiety provides a good leaving group. It was initially thought that the 4-nitroanilides were used in transition–state analogues as they provide a good immune response and a suitable spectroscopic label (for monitoring of substrate hydrolysis), however, it is the leaving group properties that are most important for substrate hydrolysis. The 4-nitroanilide moiety can be readily protonated, unlike the cyclic tripeptide of the naturally occurring toxin, whereas the ability to protonate the cyclic tripeptide moiety is expected be the rate limiting factor for an ergopeptine. Traditionally 4-nitroanilide/phenol groups have been used for generation of

catalytic antibodies as they provide a system which is likely to succeed because they posses:

- a known immunogenic moiety,
- an easily detectable substrate label,
- a good leaving group,
- and the transition–state can be emulated using a tetrahedral phosphorus compound.

In hindsight, catalytic antibodies (if they had been generated using our model system) that could hydrolyse the lysergyl 4-nitroanilide–/phenol system would not be expected to catalyse ergopeptine hydrolysis, as the two processes are limited by different transition states, as indicated by Blackburn *et al.* (1993). The hydrolysis of the ergopeptine compounds would require the design of a new transition–state emulator. Design of this transition–state is expected to be a challenge as non–stabilised aliphatic amides have yet to be hydrolysed by catalytic antibodies elicited by introduced transition–state emulators. The difficulties experienced with antibody hydrolysis of aliphatic non stabilised amide are thought to be due to use of poor transition–state models, however, investigation of better amide transition–state models is ongoing (Blackburn *et al.*, 1993; Grynszpan *et al.*, 1998). Reports of highly efficient auto-antibody hydrolysis of the VIP peptide (Paul *et al.*, 1989), (Paul *et al.*, 1990) would seem to indicate that antibody acceleration of amide hydrolysis is not only possible but can be highly efficient. Application of information gained from further mechanistic study of these auto–antibodies and peptidase enzymes should enable new rational approaches to transition–state design for peptide hydrolysing antibodies.

A more immediately suitable candidate for the production of a catalytic antibody vaccine would be the zearalenone (ZEN) (Fig. 5.1) family of toxins. These toxins are produced by a *Fusarium* species, which grow on pasture and grain and are associated with animal infertility (Smith *et al.* 1990). ZEN contains a cyclic ester, which is a possible site for catalytic antibody hydrolysis. The hydrolysis products, of which, would not be expected to be oestrogenic or to cause significant product–inhibition of the catalytic antibody. In

addition, ester hydrolysis is generally a more energetically favourable reaction than amide hydrolysis (Blackburn *et al.*, 1993). One suitable transition–state emulator would be a tetrahedral phosphorus at the 12' position, although the generation of such a compound could prove to be synthetically challenging. Coupling of such an emulator through the 6' position to a protein by standard procedures should have the advantage of generating antibodies capable of hydrolysing α– and β–zearalenol, the major mammalian metabolites of ZEN (Miles *et al.*, 1996).

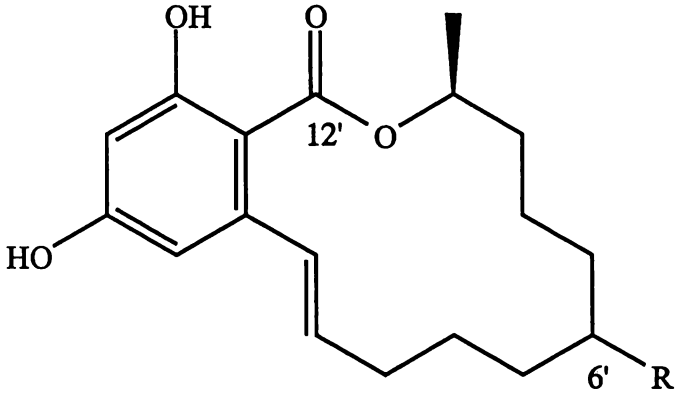

Figure 5. 1 Zearalenone and zearalenol, possess a potential site (at 12') for an esterolytic catalytic antibody, R = OH zearalenol, or R = O zearalenone.

The inability to produce 4-nitroaniline or 4-nitrophenol amide– or ester–hydrolysing catalytic antibodies in this study appears to be due to the requirement of the conjugated environment for binding of antibody to hapten (antibodies require both the protein and hapten of the conjugate for recognition). This is suggested by the good binding of the antibodies (of some sera) to the hapten conjugate in the antibody titration and the inability of non–conjugated hapten **38** to compete with this interaction in the competitive ELISA. Variation of the tether length (ie the length of the attachment between the protein and antigen) could have been investigated to avoid the difficulties experienced.

Another problem with the polyclonal sera generated was the high levels of background, non-specific, esterase activity detected for compound **40**. This has been an area of concern noted by other workers with extensive characterisation being necessary to rule out enzyme

contamination (Gallacher *et al.*, 1991). Screening of pre–immune sera for esterolytic activity prior to generation of a transition–state emulator and immunisation would have proved, in hindsight, to be a sensible approach.

With the lack of knowledge on how to produce a transition–state emulator for aliphatic amide hydrolysis, and the problems with characterisation and screening of polyclonal sera, the successful generation of an ergopeptine hydrolysing antibody is not anticipated in the near future.

Characterisation of the ergot alkaloids from naturally occurring grass–endophye symbiosis may reveal new compounds with interesting biological properties and although compounds **41** and **42** have been previously identified in DHG they had not been isolated or characterised from this material. The levels of **42** were found to increase during purification. This was unexpected. The change in level of **42** during the purification regime is thought to be due to epimerisation of ergonovine at the C-8 position. This epimerisation highlights one of the difficulties associated with the isolation of naturally occurring compounds. The characterised compound is sometimes the result of the purification process. Clearly careful choice of purification conditions is critical for isolation of the lysergic acid amides to avoid epimerisation.

The problems of grass–endophyte toxin production will continue to be a concern for grazing livestock in the future. Selection of novel endophytes and the genetic manipulation of grass–endophyte association are in progress (Garthwaite, 1997), however this process is time consuming and far from trivial. The bio–synthetic pathways of the grass–endophyte are, as yet, not understood. In addition the beneficial traits that the endophyte confers to the grass may prove difficult to separate from the less desirable effects on grazing stock.

With the inability (at least in the near future) to remove the undesirable toxins from the grass–endophyte symbiosis at a genetic level, it is necessary to remove the toxins in some

other manner. The removal of toxicity is beginning to be addressed by workers investigating the use of ergotamine–protein conjugates to induce antibodies to bind ergopeptine alkaloids. These workers observed short term increases in weight gain in animals suffering from 'fescue toxicosis' when immunised with these conjugates (Rice *et al.*, 1998). This technique is however, limited by the stoichiometry of antibody–toxin binding. In this type of situation, a catalytic antibody vaccine is an attractive solution, providing a suitable transition–state emulator can be produced and the problems associated with generation and characterisation of polyclonal sera can be solved.

REFERENCES

Ada, G. L.; Nossal, G. (1987). The Clonal-Selection Theory. *Scientific American* **257**(2): 50-57.

Adamczyk, M.; Gebler, J. C.; Mattingly, P. G. (1996). Characterisation of Protein-Hapten Conjugate. Electrospray Mass Spectrometry of BSA-Hapten Conjugates. *Bioconjugate Chemistry* **7**: 475-481.

Amit, A. G.; Poljak, R. J.; Phillips, S. E. V. (1986). Three-Dimensional Structure of an Antigen-Antibody Complex at 2.8 Å Resolution. *Science* **233**: 747-753.,

Ashley, J. A.; Lo, C. H. L.; McElhaney, G. P.; Wirsching, P.; Janda, K. D. (1993). A Catalytic Antibody Model for Plp-Dependent Decarboxylases. *Journal of the American Chemical Society* **115**(6): 2515-2516.

Bach, N. J.; Boaz, H. E.; Kornfeld, E. C.; Chang, C.-J.; Folss, H. G.; Hagaman, E. W.; Wenkert, E. (1974). Nuclear Magnetic Resonance Spectral Analysis of Ergot Alkaloids. *Journal of Organic Chemistry* **39**(9): 1272-1276.

Bacon, C. W. (1995). Toxic Endophyte-Infected Tall Fescue and Range Grasses: Historic Prespectives. *Journal of Animal Science* **73**: 861-870.

Bacon, C. W.; Porter, J. K.; Robbins, J. D.; Luttrell, E. S. (1977). *Epichloe typhina* from Toxic Tall Fescue Grasses. *Applied and Environmental Microbiology* **34**(5): 576-581.

Baldwin, J. E. (1982). Rules fo Ring Closure: Applications to Intramolecular Aldol Condensations in Polyketonic Substrates. *Tetrahedron* **38**(19): 2939-2947.

Ball, D. M.; Pederson, J. F.; Lacefield, G. D. (1993). The Tall-Fescue Endophyte. *American Scientist* **81**: 371-379.

Ball, J.-P.; Miles, C. O.; Prestidge, R. A. (1997). Ergopeptine Alkaloids and *Neotyphodium lollii* - Mediated Resistance in Perrenial Ryegrass Against Adult *Heteronychus arator* (Coleoptera: Scarabaeidae). *Plant Resistance* **90**(5): 1382-1391.

Bartlett, P.; Johnson, C. (1985). An Inhibitor of Chorismate Mutase Resembling the Transition-State Conformation. *Journal of the American Chemical Society* **107**: 7792-7793.

Beardall, J. M.; Miller, J. D. (1994). Diseases in Humans with Mycotoxins as Possible Causes. In: *Mycotoxins in grain - Compounds other than Aflatoxin.* Miller, J. D.; Trenholm, H. L. Eds. St Paul (USA), Eagan Press: 487-529.

Bellucci, C.; Gualtieri, F.; Chiarini, A. (1987). Negative Inotropic Activity of *para*-sustituted diethyl benzylphosphonates Related to Fostedil. *European Journal of Medicinal Chemistry* **22**: 473-477.

Benkovic, S. J.; Lerner, R. A.; Napper, A. D. (1988). Catalysis of a Stereospecific Bimolecular Amide Synthesis by an Antibody. *Proceedings Of the National Academy Of Science (USA)* **85**(15): 5355-5358.

Benkovic, S. J.; Adams, J. A.; Borders, C. L.; Janda, K. D.; Lerner, R. A. (1990). The Enzymic Nature of Antibody Catalysis - Development of Multistep Kinetic Processing. *Science* **250**(4984): 1135-1139.

Blackburn, G.; Deng, S. (1993). Catalytic Antibodies for the Hydrolysis of Unactivated Peptides. *Biochemical Society Transactions* **21**: 1102-1107.

Blessing, R. H. (1995). An Empiracal Correction for Absorption Anisotrophy. *Acta Crystallographica* **A51**: 33.

Bossier, J. R. (1978). General Pharmacology of Ergot Alkaloids. *Pharmacology* **16**: 12-26.

Bradford, M. M. (1976). A Rapid and Sensitive Method for Quantitation of Microgram Quantities of Protein Utilizing the Principle of Protein-Dye Binding. *Analytical Biochemistry* **72**: 248-254.

Braisted, A. C.; Schultz, P. G. (1990). An Antibody-Catalyzed Bimolecular Diels-Alder Reaction. *Journal of the American Chemical Society* **112**(7430-7431).

Braisted, A. C.; Schultz, P. G. (1994). An Antibody-Catalyzed Oxy-Cope Rearrangement. *Journal of the American Chemical Society* **116**(5): 2211-2212.

Branden, K.; Tooze, J. (1991). *Introduction to Protein Structure.* New York, Garland Publishing: 179-199.

Braun, S.; Kalinowski, H.-O.; Berger, S. (1996). *100 and More Basic NMR Experiments.* Weinheim, Germany, VCH.

Breitmaier, E.; Voelter, W., Eds. (1987). *Carbon-13 NMR Spectroscopy.* New York, VCH.

Brimfield, A.; Lenz, D.; Maxwell, D.; Broomfield, C. (1993). Catalytic Antibodies Hydrolysing Organophosphorus Esters. *Chemico-Biological Ineractions* **87**: 95-102.

Bruehl, G. W.; Kaiser, W. J.; Klein, R. E. (1994). An Endophyte of *Achnatherum inebrians*, an Intoxicating Grass of Northwest China. *Mycologia* **86**(6): 773-776.

Buckle, D. R.; Fenwick, A. E.; Outred, D. J.; Rockell, C. J. M. (1987). Synthesis of Aryloxy Analogues of Arachidoic Acid via Wittig and Palladium-catalysed Cross-coupling Reactions. *Journal of Chemical Research. Synopses.* **394-395**.

Bush, L. P.; Wilkinson, H. H.; Schardl, C. L. (1997). Bioprotective Alkaloids of Grass-endophyte symbiosis. *Plant Physiology* **114**: 1-7.

Campbell, A. P.; Tarasow, T. M.; Massefski, W.; Wright, P. E.; Hilvert, D. (1993). Binding of a High-Energy Substrate Conformer in Antibody Catalysis. *Proceedings of the National Academy of Science (USA)* **90**: 8663-8667.

Capra, J. D.; Edmundson, A. B. (1977). The Antibody Combining Site. *Scientific American* **236**: 50-59.

Chahn, T. C.; Rappocciolo, G.; Hewtson, J. F. (1990). Monoclonal Anti-Idiotype Induces Protection Against The Cytotoxicity of The Tricothecene Mycotoxin T-2. *The Journal of Immunology* **144**: 4721-4728.

Chanh, T. C.; Siwak, E. B.; Hewetson, J. F. (1991). Contemporary Issues In Toxicology. *Toxicology and Applied Pharmacology* **108**: 183-193.

Chook, Y. M.; Ke, H.; Lipscoomb, W. N. (1993). Crystal Structures of the Monofunctional Chorismate Mutase from *Bacillus subtilis* and its Complex with a Transition State Analogue. *Proceedings of the National Academy of Science (USA)* **90**: 8600-8603.

Christensen, M. J.; Leuchtmann, A.; Rowan, D. D.; Tapper, B. A. (1993). Taxonomy of *Acremonium* Endophytes of Tall Fescue (*Festuca arundinacea*), Meadow Fescue (*F. pratensis*) and Perrenial Ryegrass (*Lolium perenne*). *Mycological Research* **97**(9): 1083-1092.

Colman, P. M.; Laver, W. G.; Varghese, J. N.; Baker, A. T.; Tulloch, P. A.; Air, G. M.; Webster, R. G. (1987). Three-Dimensional Structure of a Complex of Antibody with Influenza Virus Neuraminidase. *Nature* **326**: 358-362.

Conover, L. H.; Tarbell, D. S. (1950). Hydrogenolysis of Certain Substituted Aromatic Acids and Carbonyl Compounds by Lithium Aluminium Hydride. *Journal of the American Chemical Society* **72**: 3586-3588.

Cravatt, B. F.; Ashely, J. A.; Janda, K. D.; Boger, D. L.; Lerner, R. A. (1994). Crossing Extreme Mechanistic Barriers by Antibody Catalysis: Syn Elimination of a Cis Olefin. *Journal of the American Chemical Society* **116**: 6013-6014.

Crowder, M.; Stewart, J.; Roberts, V.; Bender, C.; Tevelrakh, E.; Peisach, J.; Getzoff, E.; Gaffney, B.; Benkovic, S. (1995). Spectroscopic Studies on the Designed Metal-Binding Sites of the 43C9 Single Chain Antibody. *Journal of the American Chemical Society* **117**: 5627-5634.

Crumpton, M. J.; Wilkinson, J. M. (1963). Amino Acid Composition of Human and Rabbit γ-Globulins and the Fragments Produced by Reduction. *Biochemical Journal* **88**: 228-234.

Cunningham, I. J. (1948). Tall Fescue Grass is Poison For Cattle. *New Zealand Journal of Agriculture* **77**: 519.

Curley, K.; Pratt, R. (1997). Effectiveness of Tetrahedral Adducts as Transition-State Analogs and Inhibitors of the Class C β-Lactamase of *Enterobacter cloacae* P99. *Journal of the American Chemical Society* **119**: 1529-1538.

Cvak, L.; Jegorov, A.; Pakhomova, S.; Bohumil, K.; Sedmer, P.; Havlicek, V.; Minar, J. (1997). 8α-Hydroxy-α-Ergokryptine, An Ergot Alkaloid. *Phytochemistry* **44**: 365-369.

Dostrovsky, I.; Halmann, M. (1953). Kinetic Studies in the Phosphinyl Chloride and Phosphorochoridate Series. Part IV. General Discussion. *Journal of the Chemical Society*: 516-519.

Dugas, H. (1989). *Bioorganic Chemistry- A Chemical Approach to Enzyme Action*. 2nd Edition. New York, Springer-Verlag.

Edelman, G. M. (1973). Antibody Structure and Molecular Immunology. *Science* **180**: 830-840.

Evans, M. B.; Little, C. J.; Dale, A. D. (1980). The Preparation and Evaluation of Superior Bonded Phases for Reversed-Pase, HPLC. *Chromatographia* **13**(1): 5-10.

Fairclough, R., J.; Ronaldson, J. W.; Jonas, W. W.; Mortimer, P. H.; Erasmuson, A. G. (1984). Failure of Immunisation against Sporidesmin or a Structurally Related Compound to Protect Ewes Against Facial Eczema. *New Zealand Vetinary Journal* **32**: 101-104.

Fleischman, J. B.; Porter, R. R.; Press, E. M. (1963). The Arrangement of the Peptide Chains in γ-Globulin. *Biochemical Journal* **88**: 220-228.

Fletcher, L. R.; Harvey, I. C. (1981). An Association of a *Lolium* Endophyte with Ryegrass Staggers. *New Zealand Veterinary Journal* **29**: 185-186.

French, D.; Laskov, R.; Scharff, M. D. (1989). The Role of Somatic Hypermutation in the Generation of Antibody Diversity. *Science* **244**: 1152-1157.

Fresneda, P. M.; Molina, P. (1981). Synthesis of Diethyl Arylmethanephosphonates form Arylmethanamines. *Synthesis*(3): 222-223.

Friebolin, H. (1993). *Basic One- and Two-Dimensional NMR Spectroscopy*. Weinheim, Germany, VCH.

Fujii, I.; Tanaka, F.; Miyashita, H.; Tanimura, R.; Kinoshita, K. (1995). Correlation Between Antigen-Combining-Site Structures and Functions Within a Panel Of Catalytic Antibodies Generated Against a Single Transition State Analogue. *Journal of the American Chemical Society* **117**(23): 6199-6209.

Fujii, I.; Fukuyama, S.; Iwabuchi, Y.; Tanimura, R. (1998). Evolving Catalytic Antibodies in a Phage-Displayed Combinatorial Library. *Nature Biotechnology* **16**: 463-367.

Gadberry, M. S.; Denard, T. M.; Spiers, D. E.; Piper, E. L. (1997). Ovies Aries: a Model for Studying the Effects of Fescue Toxins on Animals Performance in a Heat-Stress Environment. *Proceedings of the Third International Symposium on Acremonium/Grass Interactions*. Bacon, C.W., Hill, N. S. Eds., New York, Plenum Press: 429-431.

Gallacher, G.; Jackson, S.; Searcey, M.; Badman, T.; Goel, R.; Topham, C.; Mellor, G.; Brocklehurst, K. (1991). A Polyclonal Antibody Preparation with Michaelian Catalytic Properties. *Journal of Biochemistry* **279**: 871-881.

Gallacher, G.; Searcey, M.; Jackson, C. S.; Brocklehurst, K. (1992). Polyclonal Antibody-Catalyzed Amide Hydrolysis. *Biochemical Journal* **284**(JUN): 675-680.

Gallacher, G.; Jackson, C.; Searcey, M.; Goel, R.; Mellor, G.; Smith, C.; Brocklehurst, K. (1993). Catalytic Antibody Activity Elicited by Active Immunisation. Evidence for Natural Variation Involving Preferential Stabilisation of the Transition State. *European Journal of Biochemistry* **214**: 197-207.

Gallagher, R. T.; Hawkes, A. D.; Steyn, P. S.; Veggaar, R. (1984). Tremorgenic Neurotoxins from Perennial Ryegrass causing Ryegrass Staggers Disorder of Livestock: Structure Elucidation of Lolitrem B. *Journal of the Chemical Society. Chemical Communications*: 614-616.

Gao, C.; Lavey, B.; Chih-Hung, L.; Datta, A.; Wentworth, P.; Janda, K. (1998). Direct Selection for Catalysis from Combinatorial Antibody Libraries Using a Boronic Acid Probe: Primary Amide Bond Hydrolysis. *Journal of the American Chemical Society* **120**(10): 2211-2217.

Garthwaite, I.; Sprosen, J.; Briggs, L.; Collin, R.; Towers, N. (1994). Food Quality on the Farm: Immunological Detection of Mycotoxins in New Zealand Pastoral Agriculture. *Food and Agricultural Immunology* **6**: 123-129.

Garthwaite, I. (1997). Cellular and Molecular Techniques for Characterising *Neotyphodium*/Grass Interactions. In: *Proceedings of the Third International Symposium on Acremonium/Grass Interactions.* Bacon, C.W., Hill, N. S. Eds., New York, Plenum Press: 361-436376.

Gibbs, R. A.; Benkovic, P. A.; Janda, K. D.; Lerner, R. A.; Benkovic, S. J. (1992). Substituent Effects on an Antibody-Catalyzed Hydrolysis of Phenyl-Esters - Further Evidence for an Acyl-Antibody Intermediate. *Journal of the American Chemical Society* **114**(9): 3528-3534.

Glenn, A. E.; Bacon, C. W.; Price, R.; Hanlin, R. T. (1996). Molecular Phlogeny of *Acremonium* and its Taxonomic Implications. *Mycologia* **88**(3): 369-383.

Gould, S.; Laufer, D. A. (1979). Carbon-13 Nuclear Magnetic Resonance Spectra of *p*-Aminobenzoic Acid Oligomers; Range Dependence of Additive Substituent Effects. *Journal of Magnetic Resonance Spectroscopy* **34**:37-55.

Gouverneur, V. E.; Houk, K. N.; Depascualteresa, B.; Beno, B.; Janda, K. D.; Lerner, R. A. (1993). Control of the Exo-Pathway and Endo-Pathway of the Diels-Alder Reaction by Antibody Catalysis. *Science* **262**(5131): 204-208.

Green, B. S.; Glikson, M. (1991). Towards Catalytic Antibodies for the Degradation of Toxic Agents. In : *Biotechnology: Bridging Research and Applications.* Kamely, D. Ed. Kluwar Academic Publications: 249-264.

Griffith, R. W.; Grauwiler, J.; Hodel, C.; Leist, K. H.; Matter, B. (1978). Ergot Alkaloids and Related Compounds. In: *Handbook of experimental pharmacology*. Berde, B.; Schild, H. O. Eds. Berlin, Springer-Verlag.

Grynszpan, F.; Keinan, E. (1998). Use of Antibodies to Dissect the Components of a Catalytic Event. The Cyclopropmone Hapten. *Chemical Communications*: 865-866.

Guo, J.; Huang, W.; Scanlan, T. (1994). Kinetic and Mechanistic Characterisation of an Efficient Hydrolytic Antibody: Evidence for the Formation of an Acyl Intermediate. *Journal of the American Chemical Society* **116**: 6062-6069.

Habib, F.; Shiriny, F. (1996). New Application of Tungsten Hexachloride (WCl_6) in Organic Synthesis. Halo-de-Hydroxylation and Dihalo-de-oxo-Bisubstitution Reactions. *Tetrahedron* **52**(47): 14929-14936.

Harger, M. J. P.; Smith, A. (1990). Migration of a Benzyl Group in the Loss-like Rearrangement of an *N*-Phosphinoyl-*O*-sulphonylhydrooxyamine. *Journal of the Chemical Society. Perkin transactions I*: 1447-1451.

Harlow, E. D.; Lane, D. (1988). *Antibodies- A Laboratory Manual*. New York, Cold Spring Harbor Laboratory.

Haynes, M. R.; Stura, E. A.; Hilvert, D.; Wilson, I. A. (1994). Routes to Catalysis: Structure of a Catalytic Antibody and Comparison with its Natural Counterpart. *Science* **263**: 646-652.

Hermanson, G. T.; Mallia, A. K.; Smith, P. K. (1992). *Immobilized Affinity Ligand Techniques*, Academic Press.

Hermanson, G. T. (1996). *Bioconjugate Techniques*. San Diego, California, Academic Press.

Hill, N. S.; Thompson, F. N.; Dawe, D. L.; Stuedemann, J. A. (1994). Antibody Binding of Circulating Ergot Alkaloids in Cattle Grazing Tall Fescue. *American Journal of Vetinary Research* **55**(3): 419-424.

Hillerns, F.; Rehder, D. (1991). Functionalized Oxovanadium Alkoxides - Potential Haptens. *Chemische Berichte* **124**: 2249-2254.

Hilvert, D.; Carpenter, S. H.; Nared, K. D.; Auditor, M. M. (1988). Catalysis of Concerted Reaction by Antibodies: The Claisen Rearrangement. *Proceedings of the National Academy of Science (USA)* **85**: 4953-4955.

Hilvert, D.; Hill, K. W.; Nared, K. N.; Auditor, M.-T. M. (1989). Antibody catalysis of a Diels-Alder Reaction. *Journal of the American Chemical Society* **111**: 9261-9262.

Hirschmann, R.; Smith, A. B.; Taylor, C. M.; Benkovic, P. A.; Taylor, S. D.; Yager, K. M.; Sprengeler, P. A.; Benkovic, S. J. (1994). Peptide Synthesis Catalyzed by an Antibody Containing a Binding-Site for Variable Amino-Acids. *Science* **265**: 234-237.

Hirschmann, R.; Yager, K. M.; Taylor, C. M.; Witherington, J.; Sprengeler, P. A.; Phillips, B. W.; Moore, W.; Smith III, A. B. (1997). Phosphonate Diester and Phosphonamide Synthesis. Reaction Coordinate Analysis by ^{31}P NMR Spectroscopy: Identification of Pyrophosphonate Anhydrides and Highly Reactive Phosphonylammonium Salts. *Journal of the American Chemical Society* **119**: 8177-8190.

Ho, T.; Olah, G. A. (1976). Cleavage of Esters and Ethers with Iodotrimethylsilane. *Angewandte Chemie International Edition (Eng)* **15**(12): 774-775.

Hooz, J.; Gilani, S. S. H. (1968). A Rapid Mild Procedure for the Preparation of Alkyl Chlorides and Bromides. *Canadian Journal of Chemistry* **46**: 86.

Hosangadi, B. D.; Dave, R. H. (1996). An Efficient General Method for Esterification of Aromatic Carboxylic Acids. *Tetrahedron Letters* **37**(35): 6375-6378.

Hoveland, C. S.; Haaland, R. L.; King, C. C.; Anthony, W. B.; Clark, E. M.; McGuire, J. A.; Smith, L. A.; Grimes, H. W.; Holliman, J. L. (1980). Associatin of *Epichloe Typhina* Fungus and Steer Performance on Tall Fescue Pasture. *Agronomy Journal* **72**: 1064-1065.

Hozumi, N.; Tonegawa, S. (1976). Evidence for Somatic Rearrangement of Immunoglobulin Genes Coding for Variable and Constant Regions. *Proceedings of the National Academy of Science (USA)* **73**(10): 3628-3632.

Hsieh, L. C.; Yonkovich, S.; Kochersperger, L.; Schultz, P. G. (1993). Controlling Chemical-Reactivity with Antibodies. *Science* **260**(5106): 337-339.

Hsieh, L.; Stephens, J.; Schultz, P. (1994). An Efficient Antibody-Catalyzed Oxygenation Reaction. *Jounal of the American Chemical Society* **116**: 2167-2168.

Hudson, R. F.; Keay, L. (1960). The Mechanism of Hydrolysis of Phosphonochloridates and Related Compounds. Part I. THe Effect of Substituents. *Journal of the Chemical Society*: 1859-1868.

Iverson, B. L.; Lerner, R. A. (1989). Sequence-Specific Peptide Cleavage Catalyzed by an Antibody. *Science* **243**(4895): 1184-1188.

Iverson, B. L. (1995). Consider Polyclonal Antibody Catalysts. *CHEMTECH* **June**: 17-21.

Jackson, D. Y.; Jacobs, J. W.; Sugasawara, R.; Schultz, P. G.; Reich, S. H.; Bartlett, P. A. (1988). An Antibody-Catalyzed Claisen Rearrangement. *Journal Of the American Chemical Society* **110**(14): 4841-4842.

Jackson, R. W.; Manske, R. H. (1930). The Synthesis of Indolyl-Butyric Acid and Some of its Derivatives. *Journal of the American Chemical Society* **52**: 5029-5035.

Jacobsen, J. R.; Schultz, P. G. (1994). Antibody Catalysis of Peptide Bond Formation. *Proceedings of the National Academy of Sciences (USA)* **91**: 5888-5892.

Jacobsen, J.; Cochran, A.; Stephans, J.; King, D.; Schultz, P. (1995). Mechanistic Studies of Antibody-Catalyzed Pyrimidine Dimer Photocleavage. *Journal of the American Chemical Society* **117**: 5453-5461.

Janda, K. D.; Lerner, R. A.; Tramontano, A. (1988). Antibody Catalysis of Bimolecular Amide Formation. *Journal Of the American Chemical Society* **110**(14): 4835-4837.

Janda, K. D.; Lerner, R. A.; Schloeder, D.; Benkovic, S. J. (1988a). Induction of an Antibody That Catalyzes the Hydrolysis of an Amide Bond. *Science* **241**(4870): 1188-1191.

Janda, K. D.; Shevlin, C. G.; Lerner, R. A. (1993). Antibody Catalysis of a Disfavored Chemical Transformation. *Science* **259**: 490-493.

Janjic, N.; Tramontano, A. (1989). Antibody-Catalyzed Redox Reaction. *Journal of the American Chemical Society* **111**: 9109-9110.

Jencks, W. P. (1969). *Catalysis in Chemistry and Enzymology*. New York, McGraw-Hill, Inc.

Jones, W. T.; Harvey, D.; Suttherland, P. W.; Reynolds, P. H. S. (1998). Production of Anti-idiotypic Monoclonal Antibodies that Mimic Phytotoxin Dothistromin. *Food and Agricultural Immunology* **10**: 67-78.

Joost, R. E. (1995). *Acremonium* in Fescue and Ryegrass: Boon or Bane? A review. *Journal of Animal Science* **73**: 881-888.

Jorge, A. L. J.; Kiyan, N. Z.; Miyata, Y.; Miller, J. (1981). Methanolysis (Solvolysis) and related Synthesis of 4'-Substituted 4-Benzoyloxybenzyl Chloride and Some Related Compounds: Comparisons with the Corresponding Benzoyl Compounds. *Journal of the Chemical Society. Perkin Transactions II.* **1**: 100-103.

Jung, M. E.; Lyster, M. A. (1976). Quantitative Dealkylation of Alkyl Esters via Treatment with Trimethylsilyl Iodide. A New Method for Ester Hydrolysis. *Journal of the American Chemical Society* **99**(3): 968-969.

Kagan, F.; Birrkenmeyer, R. D.; Strube, R. E. (1958). Nitrogen Mustard Derivative Containing the Phophonate Group. *Journal of the American Chemical Society* **81**: 3026-3031.

Kawashima, Y.; Sato, M.; Yamamoto, S.; Shimazaki, Y.; Chiba, Y.; Satake, M.; Iwata, C.; Hatayama, K. (1995). Structure-Activiy Relationship Study of TXA_2 Receptor Antagonists.4-[2-(4-Substituted Phenylsulfonylamino)ethylthio]phenoxyacetic Acids and Related Compounds. *Chemical and Pharmaceutical Bulletin* **43**(7): 1132-1136.

Keay, L. (1963). Reactions between Amines and Ethyl Methylphosphonochloridate. *Journal of Organic Chemistry* **28**: 329-331.

Kemp, D.; Cox, D.; Paul, K. (1975). The Physical Chemistry of Benzisoxazoles. IV. The Origins and Catalytic Nature of the Solvent Rate Acceleration for the Decarboxylation of 3-Carboxybenzisoxazoles. *Journal of the American Chemical Society* **97**(25): 7312-7318.

Kimball, J. W. (1986). *Introduction to Immunology*. New York, Macmillan Publishing Company.

Kirsch, J. F.; Clewell, W.; Simon, A. (1968). Multiple Structure-Reactivity Correlations. The Alkaline Hydrolyses of Acyl- and Aryl-Substituted Phenyl Benzoates. *Journal of Organic Chemistry* **33**: 123-132.

Kitazume, T.; Takeda, M. (1995). A Cyclisation Reaction Catalysed by Antibodies. *Journal Chemical Society Chemical Communications*: 39-40.

Kohen, F.; Kim, J. B.; Lindner, H. R.; Eshnar, Z.; Green, B. (1980). Monoclonal Immunoglobulin G Augments Hydrolysis of an Ester of the Homologous Hapten. *FEBS LETTERS* **111**(2): 427-431.

Komarov, I. V.; Kornilov, M. Y.; Turov, A. V.; Gorichko, M. V.; Popov, V. O.; Tolmachev, A. A.; Kirby, A. J. (1995). Phosphorylation Of 1,3-Di(N-Alkyl)Azoles By Phosphorus(V) Acid Chlorides - a Route to Potential Haptens Derived From Phosphinic Acids. *Tetrahedron* **51**(45): 12417-12424.

Kosolapoff, G. M. (1945). Isomerization of Alkylphosphites. III. The Synthesis of N-Alkylphosphonic Acids. *Journal of the American Chemical Society* **67**: 1180-1182.

Kraut, J. (1988). How Do Enzymes Work ? *Science* **242**: 533-540.

Krebs, J. F.; Siuzdak, G.; Dyson, H. J.; Stewart, J. D.; Benkovic, S. J. (1995). Detection of a Catalytic Antibody Species Acylated at the Active-Site by Electrospray Mass-Spectrometry. *Biochemistry (USA)* **34**(3): 720-723.

Lane, G. A.; Davies, O. J.-P.; Davidson, E.; Christensen, M. J.; Latch, G. C. M. (1997). Occurrence of Extreme Alkaloid Levels in Endophyte Infected Perennial Ryegrass, Tall Fescue and Meadow Fescue. In: *Proceedings of the Third International Symposium on*

Acremonium/Grass Interactions. Bacon, C.W., Hill, N. S. Eds., New York, Plenum Press: 433-436.

Latch, G. C. M.; Christensen, M. J.; Samuels, G. J. (1984). Five Endophytes of Lolium and Festuca in New Zealand. *Mycotaxon* **20**(2): 535-550.

Lee, A. Y.; Karplus, A.; Ganem, B.; Clardy, J. (1995). Atomic Structure of the Buried Catalytic Pocket of *Escherichia coli* Chorismate mutase. *Journal of the American Chemical Society* **117**: 3627-3628.

Lerner, R. A.; Benkovic, S. J. (1990). Observations in the Interface Between Immunology and Chemistry. *Chemtracts-Organic Chemistry* **3**: 1-36.

Lewis, C.; Kramer, T.; Robinson, S.; Hilvert, D. (1991). Medium Effects in Antibody-Catalyzed Reactions. *Science* **253**: 1019-1022.

Lewis, C.; Paneth, P.; O'Leary, M.; Hilvert, D. (1993). Carbon Kinetic Isotope Effects on the Spontaneous and Antibody-Catalysed Decarboxylation of 5-Nitro-3-Carboxybenzisoxazole. *Jounal of the Americal Chemical Society* **115**: 1410-1413.

Lewis, R. J.; Camilleri, P.; Kirby, A. J.; Marby, C. A. (1991). Structure Activity Studies on Amides Inhibiting Photosystem II. *ournal of the Chemical Society. Perkin Transactions 2*: 1625-1630.

Li, T. Y.; Janda, K. D.; Hilton, S.; Lerner, R. A. (1995). An Antibody-Catalyzed Nucleophilic-Substitution Reaction at a Primary Carbon That Appears to Proceed by an Ionization Mechanism. *Journal of the American Chemical Society* **117**(8): 2367-2368.

Li, W.-S.; Liu, L. K. (1989). A Convienient Oxidation of Benzylic Methyl, Methylene, and Methine Groups with Potassium Permanganate/Triethylamine Reagent. *Synthesis* **4**: 293-295.

Liotta, L. J.; Gibbs, R. A.; Taylor, S. D.; Benkovic, P. A.; Benkovic, S. J. (1995). Antibody-Catalyzed Rearrangement of a Peptide-Bond - Mechanistic and Kinetic Investigations. *Journal of the American Chemical Society* **117**(17): 4729-4741.

Ludger, E. (1977). ^{13}C NMR Spectroscopy of Diethyl Alkyl- and Benzyl-phosphonates. A study of Phosphorus-Carbon Spin-spin Coupling Constants over One to Seven bonds. *Organic Magnetic Resonance* **9**(1): 35-43.

Luo, G.; Ding, L.; Zhu, Z.; Gao, G.; Sun, Q.; Liu, Z.; Yang, T.; Shen, J. (1995). A New Strategy for Generating Selenium-containing Abzyme. Chemical Mutation of Monoclonal Antibodies with Substrate-binding Sites. *Annals New York Academy of Sciences* **750**: 277-283.

Maag, D. D.; Tobiska, J. W. (1956). Fescue Lameness in Cattle II. Ergot Alkaloids in Tall Fescue Grass. *American Journal of Vetinary Science*: 202-204.

MacDougald, O. A. (1990). Effects of Immunizing Gilts Against Zearalenone on Height of Vaginal Epithelium and Urinary Excretion of Zearalenon. *Journal of Animal Science* **68**: 3713-3718.

Mann, J. (1992). *Murder Magic and Medicene*. Suffolk, St. Edmundsbury Press.

March, J. (1992). *Advanced Organic Chemistry*. New York, John Wiley & Sons, Inc.

Mase, T.; Kiyoshi, M.; Tsuzuki, R.; Tomioka, K.; Hiromu, H. (1987). (Substituted Benzyl)thio Heterocyclic Compounds having a Leukotrene–antagonistic Activity. European patent application EP 214732 A2:1-97.

Martin, M. T.; Angeles, T. S.; Sugasawara, R.; Aman, N. I.; Napper, A. D.; Darsley, M. J.; Snachez, R. I.; Booth, P. T., R. C. (1994). Antibody-Catalyzes Hydrolysis of an Unsubstituted Amide. *Journal of the American Chemical Society* **115**: 6508-6512.

McLeod, D. A.; Brinkworth, R. I.; Ashley, J. A.; K.D., J.; Wirsching, P. (1991). Phosphonamidates and Phosphonamidate Esters as HIV-1 Protease Inhibitors. *Bioorganic and Medicinal Chemistry Letters* **1**(11): 653-658.

McKenna, C. E.; Higa, M. T.; Cheung, N. H.; McKenna, M.-C. (1977). The Facile Dealkylation of Phosphonic Acid Dialkyl Esters by Bromotrimethylsilane. *Tetrahedron Letters* **2**: 155-158.

Meekel, A. A. P.; Resmini, M.; Pandit, U. K. (1995). First Example of an Antibody-catalysed Hetero-Diels-Alder Reaction. *Journal of the Chemical Society. Chemical Communications*: 571-572.

Miles, C. O. (1983). Metal Hydride Reductions of some Phenolic Compounds. MSc Thesis, University of Waikato, New Zealand: 9-12.

Miles, C. O.; Erasmuson, A. F.; Wilkins, A. L.; Towers, N. R.; Smith, B. L.; Garthwaite, I.; Scahil, B. G.; Hansen, R. P. (1996). Ovine Metabolism of Zearalenone to α-Zearalanol (Zeranol). *Journal of Agricultural and Food Chemistry* **44**(10): 3244-3250.

Miles, C. O.; Lane, G. A.; di Menna, M. E.; Garthwaite, I.; Piper, E. L.; Ball, O. J.-P.; Latch, G. C. M.; Allen, J. M.; Hunt, M. B.; Bush, L. P., et al. (1996a). High Levels of Ergonovine and Lysergic Acid Amide in Toxic *Achnatherum inebrians* Accompany Infection by an *Acremonium*-like Endophytic fugus. *Journal of Agricultural Food Chemistry* **44**: 1285-1290.

Milstein, C. (1980). Monoclonal Antibodies. *Scientific American* **243**(4): 56-64.

Miyashita, H.; Hara, T.; Tanimura, R.; Fukuyama, S.; Cagnon, C.; Kohara, A.; Fujii, I. (1997). Site-Directed Mutagenesis of Active Site Contact Residues in a Hydrolytic Abzyme: Evidence for an Essential Histidine Involved in Transition State Stabilisation. *Journal of Molecular Biology* **267**: 1247-1257.

Monzingo, A.; Matthews, B. (1984). Binding of N-Carboxymethyl Dipeptide Inhibitors to Thermolysin Determined by X-ray Crystallography: A Novel Class of Transition-State Analogues for Zinc Peptidases. *Biochemistry* **23**: 5724-5729.

Morgan-Jones, G.; Gams, W. (1982). An Endophyte of *Festuca Arundinacea* and the Anamorph of *Epichloe Typhina*, New Taxa in one of two New Sections of *Acremonium*. *Mycotaxon* **15**: 311.318.

Morita, T.; Okamoto, Y.; Sakurai, H. (1978). A Convienient Dealkylation of Dialkyl Phosphonates by Chlorotrimethylsilane in the Presence of Sodium Iodide. *Tetrahedron Letters* **28**: 2523-2526.

Morrison, G. A.; Qureshi, M. I. (1972). One Step Conversion of a Styrene Derivative into a Benzoylolefin. *Tetrahedron* **28**: 4239-4242.

Mravec, D.; Kalamar, J. (1975). 4-Bromobenzonitrile Catalytic Hydrgoenation Under Pressure. *Chemical Abstracts* **82**: 86178.

Mucha, A.; Kafarski, P. (1994). The Preparation of Phosphono Peptides Containing a Phosphonamidate Bond. *Tetrahedron* **50**(44): 12743-12754.

Neill, J. C. (1941). The Endophytes of *Lolium* and *Festuca*. *The New Zealand Journal of Science and Technology* **23**: 185-193A.

Nisonoff, A. (1960). Properties of the Major Component of a Peptic Digest of Rabbit Antibody. *Science* **132**: 1770-1771.

Novotny, J. (1983). Molecular Anatomy of the Antibody Binding Site. *Journal of Biological Chemistry* **258**(23): 14433-14437.

Oliver, J. W. (1997). Physiological Manifestations of Endophyte Toxicosis in Ruminant and Laboratory Species. In: *Proceedings of the Third International Symposium on Acremonium/Grass Interactions*. Bacon, C.W., Hill, N. S. Eds., New York, Plenum Press: 311-346.

Pain, R. H. (1963). The Molecular Weights of Peptide Chains of γ-Globulin. *Biochemical Journal* **88**: 234-239.

Pallavi, R. M.; Ramana, D.; Sashidaar, R. B. (1997). Synthesis of the Antigen Bovine Serum Albumin-Ergosterol and its Immunocharacteriastion. *Food and Agricultural Immunology* **9**: 85-95.

Paul, S.; Volle, D. J.; Beach, C. M.; Johnson, D. R.; Powell, M. J.; Massey, R. J. (1989). Catalytic Hydrolysis of Vasoactive Intestinal Peptide by Human Autoantibody. *Science* **244**: 1158-1162.

Paul, S.; Volle, D. J.; Mei, S. (1990). Affinity Chromatography of Catalytic Autoantibody to Vasoactive Intestinal Peptide. *The Journal of Immunology* **145**(4): 1196-1199.

Pauling, L. (1940). A Theory of the Structure and Process of Formation of Antibodies. *Journal of the American Chemical Society*: 2643-2657.

Pauling, L. (1946). Molecular Architecture and Biological Reactions. *Chemical and Engineering News* **24**: 1375.

Pharmacia (1987). *Developement Technique. Silver Staining 210*, Pharmacia LKB Biotechnology AB, Sweden, Upsala.

Pharmacia (1987). *Homogeneous SDS 12.5% Separation Technique 111*, Pharmacia LKB Biotchnology AB, Sweden, Upsala.

Pharmacia (1987). *IEF 3-9 Separation Technique 100*, Pharmacia LKB Biotechnology AB, Sweden, Upsala.

Phillips, J. R.; Williams, D. J.; Slawin, A. M. Z.; Woollins, J. D. (1996). The Preparation Of Dialkylthiophosphonatoamines. X-Ray Structures Of $(EtO)_2PSNHC_6H_4NO_2$ and $[(EtO)_2PSNHC_6H_4NO_2]_2PdCl2$. *Polyhedron* **15**(21): 3725-3729.

Pilz, W.; Stelzl, E.; Johann, I. (1968). Untersuchungen uber esterspaltende Enzyme von Versuchstieren und Methoden zu ihrer routinemassigen Bestimmung, IV. In: *Enzymogia. Biolica et Clinica* **9**: 97-123.

Poljak, R. J.; Amzel, L. M.; Avey, H. P.; Chen, B. L.; Phizackerley, R. P.; Saul, F. (1975). Three-Dimensional Structure of the Fab' Fragment of a Human Immunoglobulin at 2.8 Å resolution. *Proceedings of the National Academy of Science (USA)* **70**(12): 3305-3310.

Pollack, S. J.; Jacobs, J. W.; Schultz, P. G. (1986). Selective Chemical Catalysis by an Antibody. *Science* **234**: 1570-1573.

Pollack, S. J.; Schultz, P. G.; Hsiun, P. (1989). Stereospecific Hydrolysis of Alkyl Esters by Antibodies. *Journal Of the American Chemical Society* **111**(15): 5961-5962.

Porter, R. (1959). The Hydrolysis of Rabbit γ-Globulin and Antibodies with Crystalline Papain. *Biochemical Journal* **73**: 119-126.

Porter, R. R. (1973). Structural Studies of Immunoglobulins. *Science* **180**: 713-716.

Pouchert, C. J.; Campbell, J. R. (1974). *The Aldrich Library of NMR Spectra.* Milwaukee (USA), Aldrich Chemical Company.

Prestidge, R. A.; Ball, O.J-P (1993). The Role of Endophytes In Alleviating Plant Biotic Stress In New Zealand. *Proceedings of the Second International Symposium on Acremonium/Grass Interactions*. Bacon, C.W., Hill, N. S. Eds., Plenary Press: 141-151.

Rabinowitz, R. (1963). The Reactions of Phosphonic Acid Esters with Acid Chlorides, A Very Mild Hydrolytic Route. *Journal of Organic Chemistry* **28**: 2975-2978.

Radzicka, A.; Wolfenden, R. (1995). A Proficient Enzyme. *Science* **267**: 90-93.

Ralph, W. (1990). Lupinosis: Tests and a Vaccine on the Way. *Rural Research* **146**: 4-7.

Ranadive, N. S.; Sehon, A. H. (1976). Antigenicity of 5-Hydroxyindole-3-Acetic Acid, A derivative of Serotonin. *Canadian Journal of Biochemistry* **45**: 1681-1688.

Raso, V.; Stoller, B. D. (1975). The Antibody-Enzyme Analogy. Comparison of Enzymes and Antibodies specific for Phosphopyridoxyltyrosine. *Biochemistry* **14**(3): 591-599.

Reymond, J. L.; Janda, K. D.; Lerner, R. A. (1991). Antibody Catalysis of Glycosidic Bond Hydrolysis. *Angewandte Chemie International Edition (Eng)* **30**(12): 1711-1713.

Reymond, J. L.; Reber, J. L.; Lerner, R. A. (1994). Enantioselective, Multigram-Scale Synthesis with a Catalytic Antibody. *Angewandte Chemie International Edition (Eng)* **33**(4): 475-477.

Reymond, J. L.; Janda, K. D.; Lerner, R. A. (1995). (S)-Selective Retroaldol Reaction and (R)-Selective β-elimination with an Aldolase Catalytic activity. *Angewandte Chemie International Edition (English)* **34**(20): 2285-2287.

Rice, R. L.; Blodgett, D. J.; Schurig, G. G.; Swecker, W. S.; Thatcher, C. D.; Eversole, D. E. (1998). Oral and Parenteral Vaccination of Mice with Protein-Ergotamine and Evaluation of Protection against Fescue Toxicosis. *Vetinary Immunology and Immunopathology* **61**: 305-316.

Rivero, I. A.; Somanathan, R.; Hellberg, L. H. (1993). Triphosgene/Triphenylphosphine: A Mild Reagent for the Conversion of Alcohols to Chlorides. *Synthetic Communications* **23**(5): 711-714.

Roberts, V.; Stewart, J.; Benkovic, S.; Getzoff, E. (1994). Catalytic Antibody Model and Mutagenesis Implicate Arginine in Transition-state Stabilisation. *Journal of Molecular Biology* **235**: 1098-1116.

Roitt, I. (1988). *Essential Immunology*. Carlton, Victoria, Blackwell Scientific Publications (Australia) Pty Ltd.

Rosenblum, J. S.; Lo, L. C.; Li, T. Y.; Janda, K. D.; Lerner, R. A. (1995). Antibody-Catalyzed Phosphate Triester Hydrolysis. *Angewandte Chemie. International Edition. (Eng)* **34**(20): 2275-2277.

Rowan, D. (1987). Detection of Ergopeptine Alkaloids in Endophyte-Infected Perrenial Ryegrass by Tandem Mass Spectrometry. *New Zealand Vetinary Journal* **35**: 197-190.

Rowan, D. D.; Latch, G. C. M. (1994). Utilization of Endophyte-Infected Perrenial Ryegrasses for Increased Insect Resistance. *Biotechnolgy of Endophytic Fungi of Grasses*. Bacon, C. W.; White, J. F. Boca Raton: 169-183

Scanlan, T. S.; Prudent, J. R.; Schultz, P. G. (1991). Antibody-Catalyzed Hydrolysis of Phosphate Monoesters. *Journal of the American Chemical Society* **113**(24): 9397-9398.

Schultz, P. G.; Jacobs, J. W. (1988). Catalytic Antibodies: Generation and Characterization. In: *Environmental Influences and Recognition in Enzyme Chemistry*. J. F. Liebman; A. Eds. Greenberg. New York, VCH: 303-335.

Scott, B.; Schardl, C. (1993). Fungal Symbionts of Grasses: Evolutionary Insights and Agricultural Potential. *Trends in Microbiloogy* **1**(5): 196-200.

Shapiro, B. L.; Mohrmann, L. E. (1977). NMR Spectral Data: A Compillation of Aromatic Proton Chemical Shifts in Mono- and Di-Substituted Benzenes. *Journal of Physical and Chemical Reference Data* **6**(3): 919-991.

Shchurov, D. V. (1997). Catalytic Antibodies. *Molecular Biology* **31**(1): 1-9.

Shevlin, C. G.; Hilton, S.; Janda, K. D. (1994). Automation of Antibody Catalysis - A Practical Methodology for the Use of Catalytic Antibodies in Organic-Synthesis. *Bioorganic & Medicinal Chemistry Letters* **4**(2): 297-302.

Shokat, K.; Uno, T.; Schultz, P. (1994). Mechanistic Studies of an Antibody-Catalyzed Elimination Reaction. *Journal of the American Chemical Society* **116**: 2261-2270.

Shreder, K.; Harriman, A.; Iverson, B. (1995). Polyclonal Antibodies Elicited via Immunization with a $Ru(bpy)_3^{2+}$-Methyl Viologen Conjugate: Is a Polyclonal Antibody Immune Response Always Heterogeneous. *Journal of the American Chemical Society* **117**: 2673-2674.

Siegel, M. R.; Latch, G. C. M.; Bush, L. P.; Fannin, F. F.; Rowan, D. D.; Tapper, B. A.; Bacon, C. W.; Johnson, M. C. (1990). Fungal Endophyte-Infected grasses: Alkaloids Accumulation and Aphid Response. *Journal of Chemical Ecology* **16**(2): 3301-3315.

Slade, C. J.; Vulfson, E. N. (1998). Induction Of Catalytic Activity In Proteins By Lyophilization In the Presence Of a Transition State Analogue. *Biotechnology & Bioengineering* **57**(2): 211-215.

Slobin, L. (1966). Preparation and some Properties of Antibodies with Specificity towards p-Nitrophenyl Esters. *Biochemistry* **5**(9): 2836-2844.

Smid, J.; Varma, A.; Shah, S. (1979). Decarboxylation of 6-Nitrobenzisoxazole-3-Carboxylate in Benzene Catalyzed by Crown Ethers and their Polymers. *Journal of the Americal Chemical Society* **101**(19): 5764-5769.

Smith, J. F.; di Menna, M. E.; McGowan, L. T. (1990). Reproductive Performance of Coopworth Ewes Following Oral Doses of Zearalenone Before and After Mating. Journal of Reproduction and Fertility **89**: 99-106.

Smith, J. F. (1992). Effect of Dose of Zearalenone on Plasma levels of FSH and Zearalenone in Ewes. *9th International Congress of Endocrinology*, Nice, France.

Steward, M. W. (1984). Antibodies: Their Structure and function. *Outline Studies in Biochemistry*. Brammer, W.J.; Edidin, M. Eds. New York, Chapman and Hall Ltd.

Stewart, J. D.; Roberts, V. A.; Thomas, N. R.; Getzoff, E. D.; Benkovic, S. J. (1994). Site-Directed Mutagenesis of a Catalytic Antibody - An Arginine and a Histidine Residue Play Key Roles. *Biochemistry* **33**(8): 1994-2003.

Still, W. C.; Kahn, M.; Mitra, A. (1978). Rapid Chromatographis Technique for Preparative Separations with Moderate Resolution. *Journal of Organic Chemistry* **14**: 2923-2925.

Strickland, J. R.; Oliver, J. W.; Cross, D. L. (1993). Fescue Toxicosis and its Impact on Animal Agriculture. *Vet. Human Toxicol* **35**: 454-469.

Stryer, S. (1988). *Biochemistry*. New York, W. H. Freeman and Company.

Suckling, C. J.; Tedford, M. C.; Bence, L. M.; Irvine, J. I.; Stimson, W. H. (1993). An Antibody with Dual Catalytic Activity. *Journal of the Chemical Society Perkin Transactions Part 1*: 1925-1929.

Suga, H.; Tanimoto, N.; Sinskey, A.; Masamune, S. (1994). Glycosidase Antibodies Induced to a Half-Chair Transition-State Analog. *Jounal of the American Chemical Society* **116**: 11197-11198.

Suga, H.; Ersoy, O.; Tsumuraya, T.; Lee, J.; Sinskey, A. J.; Masamune, S. (1994a). Esterolytic Antibodies Induced to Haptens with a 1,2-Amino Alcohol Functionality. *Journal of the American Chemical Society* **116**(2): 487-494.

Suga, H.; Ersoy, O.; Williams, S. F.; Tsumuraya, T.; Margolies, M. N.; Sinskey, A. J.; Masamune, S. (1994b). Catalytic Antibodies Generated via Heterologous Immunization. *Jounal of the American Chemical Society* **116**: 6025-6026.

Suvorov, N. N.; Eryshev, B. Y.; Dubinin, A. G. (1973). 3-Indolylalkyl bromides. *Chemical Abstracts* **79**: 391.

Suvorov, N. N.; Eryshev, B. Y.; Dubinin, A. G.; Buyanov, V. N. (1975). Indole derivatives. *Chamical Abstracts* **82**: 545.

Tanaka, F.; Kinoshita, K.; Tanimura, R.; Fujii, I. (1996). Relaxing Substrate Specificity In Antibody-Catalyzed Reactions - Enantioselective Hydrolysis Of N-Cbz-Amino Acid Esters. *Journal of the American Chemical Society* **118**(10): 2332-2339.

Tchani, G.; Baziard-Mouysset, G.; Younes, S.; Bellan, J.; Payard, M.; Stigliani, J. L.; Grassy, G.; Bonnafous, R.; Tisne-Versailles, J. (1992). Evaluation de l'activite inhibitrice calcique d'une serie de benzylphosphonates de diethyle. *European Journal of Medicinal Chemistry* **27**: 845-850.

Teraishi, K.; Saito, M.; Fujii, I.; Nakamura, H. (1992). Ab Initio Structural Comparison Between the Tetrahedral Intermediates and the Phosphorous-Containing Analogues in the Esterand Amide Hydrolysis. *Tetraheron Letters* **33**(47): 7153-7156.

Tfelt-Nansen, P.; Saxena, P. R.; Ferrari, M. D. (1995). Ergot Alkaloids. In: *Intoxications of the Nervous System. Part II.* de Wolff, F. A. Eds. Elsevier Science B. V. **21 (65):** 61-78.

Thomas, N. R. (1996). Catalytic Antibodies- Reaching Adolescence. *Natural Product Reports* **13**(6): 479-511.

Thorsett, E. D.; Haris, E. E.; Peterson, E. R.; Greenlee, W. J.; Pratchett, A. A.; Ulm, E. H.; Vassil, T. C. (1982). Phosphorus Containing Inhibitor of Angiotensin-Converting Enzyme. *Proceedings of the National Academy of Science(USA)* **79**: 2176-2180.

Tonegawa, S. (1983). Somatic Generation of Antibody Diversity. *Nature* **302**: 575-581.

Tramontano, A.; Janda, K. D.; Lerner, R. A. (1986). Catalytic Antibodies. *Science* **234**: 1566-1570.

Tramontano, A.; Janda, K. D.; Lerner, R. A. (1986a). Chemical Reactivity at an Antibody Binding Site elicited by Mechanistic Design of a Synthetic Antigen. *Proceedings of the National Academy of Science (USA)* **83**: 6736-6740.

Tubul, A.; Brun, P.; Michel, R.; Gharib, B.; De Reggi, M. (1994). Polyclonal Antibody-Catalysed Aldimine Formation. *Tetrahedron Letters* **35**(32): 5865-5868.

Ulrich, H. D.; Schultz, P. G. (1998). Analysis Of Hapten Binding and Catalytic Determinants In a Family Of Catalytic Antibodies. *Journal of Molecular Biology* **275**(1): 95-111.

van Nunen, J. L. M.; Folmer, B. F. B.; Nolte, R. J. M. (1997). Induction of Liquid Crystallinity by Host-Guest Interactions. *Journal of the American Chemical Society* **119**: 283-291.

Wade, H.; Scanlan, T. S. (1997). The Structural and Functional Basis of Antibody Catalysis. *Annual Review in Biophysics and Biomolecular structure* **26**: 461-493.

Wade, W. S.; Koh, J. S.; Han, N.; Hoekstra, D. M.; Lerner, R. A. (1993). Engineering Metal Coordination Sites into the Antibody Light-Chain. *Journal of the American Chemical Society* **115**(11): 4449-4456.

Wagner, J.; Lerner, R. A.; Barbas, C. F. (1995). Efficient Aldolase Catalytic Antibodies That Use the Enamine Mechanism of Natural Enzymes. *Science* **270**(5243): 1797-1800.

Wehry, E. L. Ed. (1976). *Modern Fluorescence Spectroscopy 2.* Plenum Press, New York.

Wentworth, P.; Datta, A.; Blakely, D.; Boyle, T.; Partridge, L. J.; Blackburn, M. (1996). Toward Antibody-Directed 'abzyme' Prodrug Therapy, ADAPT: Carbamate Prodrug Activation by a Catalytic Antibody and its *in vitro* Application to Human Tumour Cell Killing. *Proceedings of the National Academy of Science (USA)* **93**: 799-803.

Wirsching, P.; Ashley, J. A.; Lo, C. H. L.; Janda, K. D.; Lerner, R. A. (1995). Reactive Immunization. *Science* **270**(5243): 1775-1782.

Wolfenden, R. (1969). Transition State Analogues for Enzymatic Catalysis. *Nature* **233**: 704-705.

Wolfenden, R.; Frick, L., (1987). *Enzyme Mechanisms.* Page, M.I.; Williams, A. Eds. London, The Royal Society of Chemistry Burlington House:101.

Wong, C. H.; Whitesides, G. M. (1994). Enzymes in Synthetic Organic Chemistry. In: *Tetrahedron Organic Chemistry Series.* Baldwin, J. E.; Magnus, P. D Eds. New York, Elsevier Sciences Inc **12**: 19-22.

Wu, T. T.; Kabat, E. A. (1970). An Analysis of the Sequences of the Variable Regions of Bence Jones Proteins and Myeloma Light Chains and their Implications for Antiblody Complimentarity. *Journal of Experimentle Medicene* **132**: 211-250.

Yates, S.; Plattner, R.; Garner, G. (1985). Detection of Ergopeptine Alkaloids in Endophyte Infected, Toxic Ky-31 Tall Fescue by Mass Spectrometry/Mass Spectrometry. *Journal of Agricultural Food Chemistry* **33**: 719-722.

Yates, S. G.; Fenster, J. C.; Bartlet, R. J. (1989). Assay of Tall Fescue Seed Extracts, Fraction, and Alkaloids Using the Large Milkweed Bug. *Journal of Agricultural and Food Chemistry* **37**: 354-357.

Yli-Kauhaluoma, J. T.; Ashley, J. A.; Lo, C.; Tucker, L.; Wolfe, M. M.; Janda, K. D. (1995). Anti-Metallocene Antibodies: A New approach to Enantioselective Catalysis of the Diels-Alder Reaction. *Journal of the American Chemical Society* **117**: 7041-7047.

Yu, J. H.; Hsieh, L. C.; Kochersperger, L.; Yonkovich, S.; Stephans, J. C.; Gallop, M. A.; Schultz, P. G. (1994). Progress Toward an Antibody Glycosidase. *Angewandte Chemie International Edition (Eng)* **33**(3): 339-341.

Zhou, G. W.; Guo, J. C.; Huang, W.; Fletterick, R. J.; Scanlan, T. S. (1994). Crystal-Structure of a Catalytic Antibody with a Serine-Protease Active-Site. *Science* **265**(5175): 1059-1064.